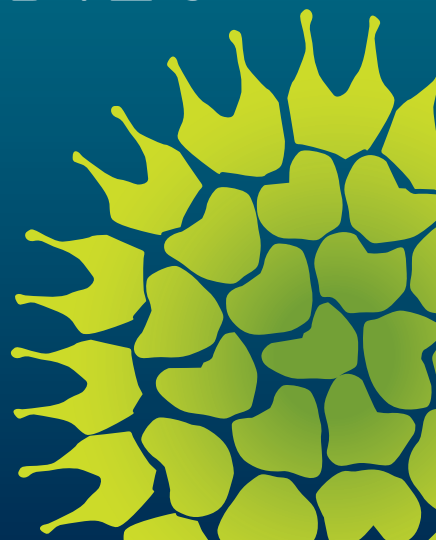


# SCENARIO STUDIES FOR ALGAE PRODUCTION

PETRONELLA MARGARETHA SLEGGERS





# **Scenario studies for algae production**

**Petronella Margaretha Slegers**

## **THESIS COMMITTEE**

### **Promotors**

Prof. Dr G. van Straten  
Emeritus Professor of Systems and Control  
Wageningen University

Prof. Dr R.H. Wijffels  
Professor of Bioprocess Engineering  
Wageningen University

### **Co-promotor**

Dr A.J.B. van Boxtel  
Associate professor, Biomass Refinery and Process Dynamics  
Wageningen University

### **Other members**

Prof. Dr E.J. van Henten, Wageningen University  
Dr E.J.A. Roebroek, LGem, Voorhout, the Netherlands  
Dr R. Suryo, ExxonMobil Research and Engineering, Fairfax, USA  
Prof. Dr A.P.C. Faaij, Utrecht University

This research was conducted under the auspices of the Graduate School VLAG (Advanced studies in Food Technology, Agrobiotechnology, Nutrition and Health Sciences).

# **Scenario studies for algae production**

**Petronella Margaretha Slegers**

## **Thesis**

Submitted in fulfilment of the requirements for the degree of doctor  
at Wageningen University

by the authority of the Rector Magnificus

Prof. Dr M.J. Kropff,

in the presence of the

Thesis Committee appointed by the Academic Board

to be defended in public

on Friday 21 March 2014

at 1.30 p.m. in the Aula.

P.M. Slegers  
Scenario studies for algae production  
224 pages

PhD thesis, Wageningen University, Wageningen, NL (2014)  
With references, with summaries in Dutch and English

ISBN 978-94-6173-858-5

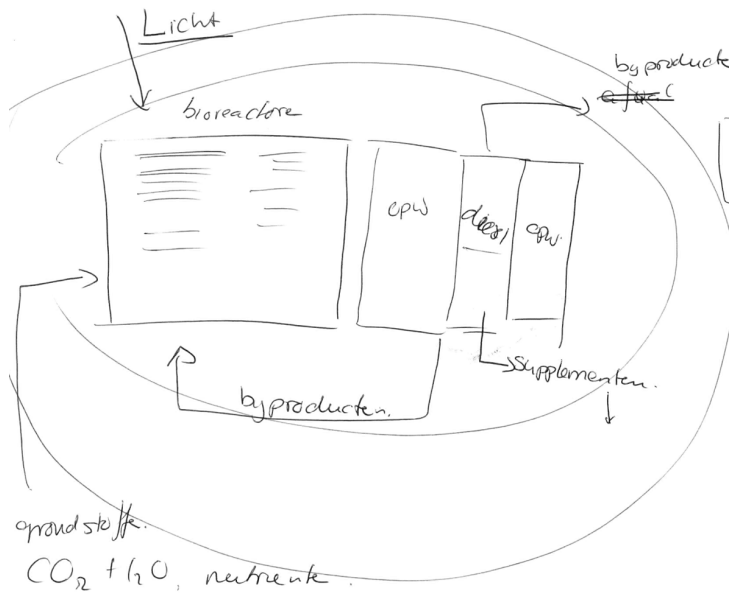
## TABLE OF CONTENTS

<b>Chapter 1</b>	Scenario studies for algae production: Introduction	7
<b>Chapter 2</b>	Design scenarios for flat panel photobioreactors	23
<b>Chapter 3</b>	Scenario analysis of large-scale algae production in tubular photobioreactors	49
<b>Chapter 4</b>	Scenario evaluation of open pond microalgae production	73
<b>Chapter 5</b>	Analysis of algae cultivation supply logistics	97
<b>Chapter 6</b>	A model-based combinatorial optimisation approach for energy-efficient processing of microalgae	123
<b>Chapter 7</b>	Food commodities from microalgae	153
<b>Chapter 8</b>	Scenario studies for algae production: Achievements, insights and new challenges	167
	References	193
	Summary	209
	Samenvatting	211
	Dankwoord	215
	About the author	218
	Publications	219
	Overview of completed training activities	221



# SCENARIO STUDIES FOR ALGAE PRODUCTION

## INTRODUCTION





## **TOWARDS A BIOBASED ECONOMY**

### **Current status**

The economy is changing from being fossil-based to renewable and biobased. This is supported by policy incentives like the 20-20-20 goals by the EU that aim for 20% increase in energy efficiency, 20% reduction of CO<sub>2</sub> emissions and 20% renewable energy by 2020 compared to the 1990 levels (European Union 17125/08). The biobased share of the economy was estimated to be around 5% for the EU in 2010 [1, 2], for Canada 6.4% and the US 8.45% [1].

In a biobased economy biomass is valorised and used for the sustainable production of food, feed, chemicals, fuels, power and heat (definition of IEA Bioenergy task 42 biorefinery). The use of agricultural raw materials for production of goods is not new; plant resources have been used a long time to produce energy, cloths, tools, shelter and medicines [3, 4]. However, this practise has declined since the industrial revolution through the use of fossil resources [3]. Currently, most applications of biomass are for food and feed [2]. Today's biofuel production in the EU is very limited, it is 1.6 million ton while 1702 million ton of fossil resources are consumed for energy [5].

A major step should be taken to increase the production of biobased energy and chemicals. There are possibilities to enhance the biobased economy using the advantages that biomass is geographically more evenly distributed [6] and has nearly closed carbon cycles.

### **Feedstocks in the biobased economy**

To realise a biobased economy it is important to combine various feedstocks, conversion techniques and production routes [7, 8]. Biorefineries are essential to achieve these goals. Ideally, biorefineries use one or several feedstocks to produce a spectrum of low and high value products, thereby balancing the production cost and life cycle impacts between the products. Figure 1 shows a network of possible biorefinery routes using various feedstocks and conversion processes to produce a wide variety of products.

The first generation of biobased feedstocks are wood, grasses and sugar, starch and oil crops. Second generation feedstocks include agricultural residues like straw and corn stover, by-products and waste streams such as sewage, manure and leftovers. These feedstocks offer many possibilities to locally produce energy, fuel and chemicals. Algae biomass is a third generation feedstock and the use of microalgae and macroalgae (sea weeds) for the production of biofuel, food, feed and chemicals is emerging [9-11].

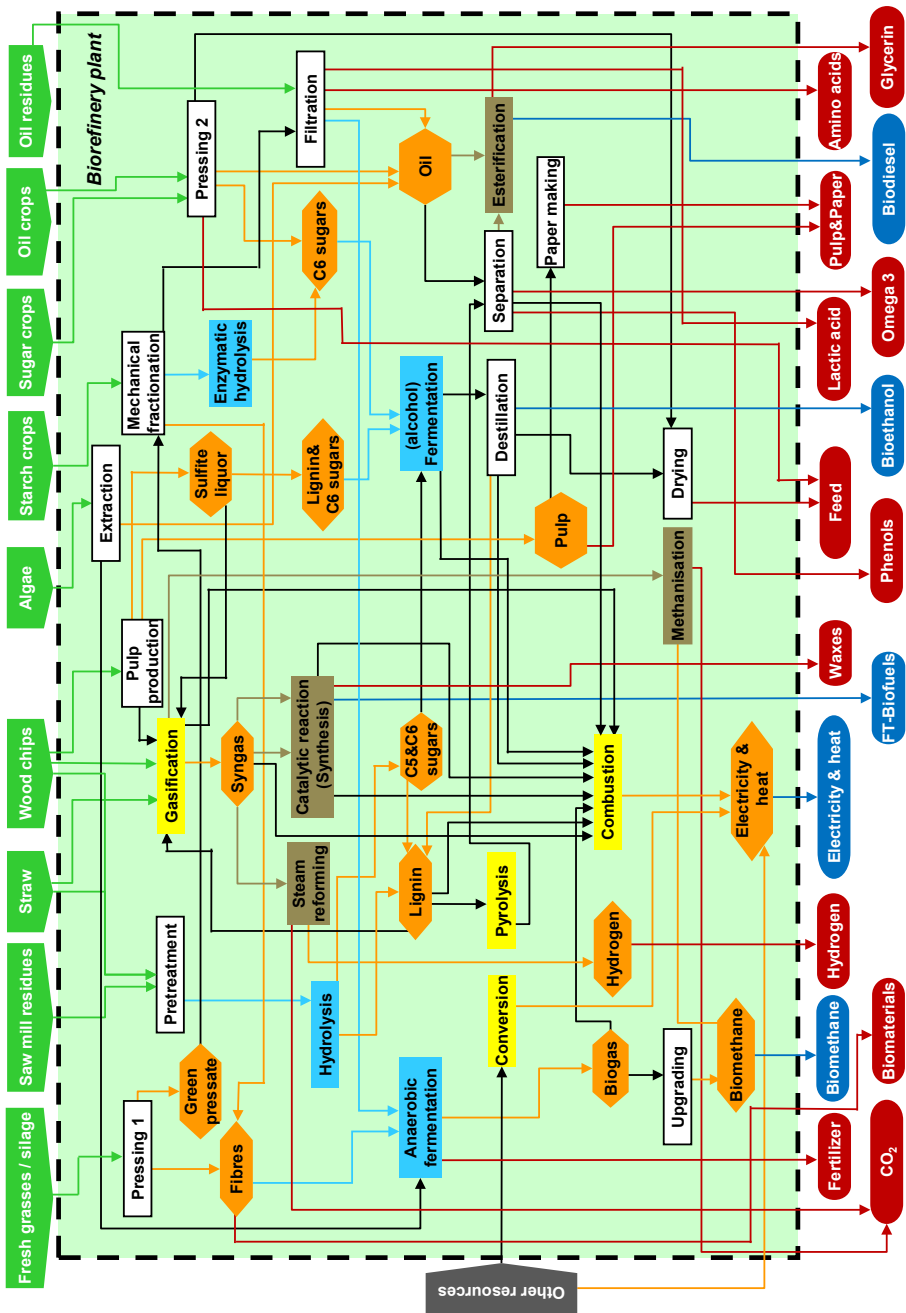


Figure 1. Overview of possible biorefinery feedstocks, conversion processes and products (Joanneum Research Forschungsgesellschaft mbH on behalf of IEA Bioenergy Task42, January 2013). FT-Biofuels are Fischer-Tropsch biofuels.

Especially microalgae get a lot of attention [12] for their high growth yields, low land requirement compared to other crops, the ability to grow on salt and waste water, and diversity of biomass content [13, 14].

### **Opportunities for algae biomass**

Algae biomass consists mainly of lipids, proteins, carbohydrates and pigments and the product range is very versatile [15, 16]. Figure 2 gives an overview of valuable components in algae as well as potential applications. These range from high value nutraceuticals, healthy food components and cosmetics to the lower value commodities biofuels, food, fertiliser and application in waste water treatment. Research on microalgae was initially focussed on food and feed applications [15, 17], but recently much attention is given to the ability to produce lipids for biofuel [13, 14, 18]. The wide product range makes algae biomass unique and enables a self-supporting biorefinery, where other feedstocks are unnecessary. In fact, to achieve a sustainable and economically feasible commercial algae production it is essential to apply the biorefinery principle [14].

### **Key elements in algae cultivation and processing**

There are many elements to consider in the algae production chain, like production and supply of resources; the algae cultivation process; the formation of algal product components; resource recycling; processing of biomass and the integration with biomass production; transport of algae biomass, products and waste streams; and the implications for economics, environment, community and society [13, 14, 19]. Most elements are connected to the algae biomass production step, which can be seen as a central element in the algae chain. Algae cultivation has received much attention in the past decade [12]. Still, most research is done on laboratory scale and is aimed at understanding the behaviour of single cells under controlled conditions. As a central element in the production chain, cultivation should also be studied in more detail under commercial or “large-scale” conditions.

### **Estimating algae productivity**

For commercial production algae are cultivated outdoors [20, 21], using the freely available sunlight. Hence, the knowledge on algae behaviour in lab-scale reactors should be transferred to the performance in larger reactor systems that have to deal with light and temperature variation at the production location.

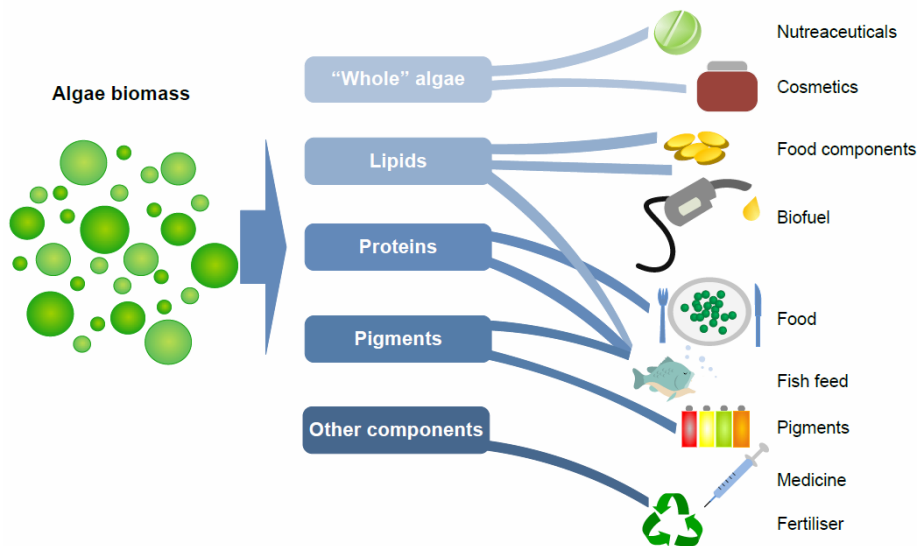


Figure 2. Refinery of microalgae into a wide variety of products.

### Growth affecting factors

Algae growth and thus biomass productivity depends on several factors. Algae need light and nutrients at a certain temperature to grow. High light intensities, high oxygen levels and non-optimal temperatures negatively affect growth. The magnitude of the effect of these factors depends on the algae species: some grow well at low temperatures and low light intensities (for example *Chlamydomonas nivalis*), while others are adapted to higher irradiance (e.g. *Chlorella sorokiniana*).



Figure 3. The four main reactor types, at AlgaePARC Wageningen UR. From left to right: raceway pond, horizontal tubes, vertically stacked horizontal tubes and flat panels. With permission of Wageningen UR.

Several reactor types and designs are available for algae production [22-24]. The four main types are shown in Figure 3. Light penetrates along the so-called “light path”, which is the depth or diameter of the reactor. The simplest reactor systems are raceway ponds. These open systems are usually 30 cm deep and are relatively easy to construct and operate. More advanced reactor are closed, in which case they are also known as “photobioreactors” (PBR). Flat panel PBRs are rectangular reactors with light paths

between 0.02-0.10 m. Tubular PBRs commonly have a light path of 0.06 m. The tubes can be placed horizontally next to each other, “horizontal” tubular PBR, and the horizontal tubes can be stacked vertically, resulting in a so-called “vertical” tubular PBR. Several variations of the main reactor designs are available in which benefits of various designs are combined (for example the designs made by Proviron<sup>®</sup>, Subitec<sup>®</sup> and Solix<sup>®</sup>).

The shape and dimensions determine the achievable algae productivity. When reactor systems are very thin it is possible that not all the light can be absorbed by the algae, thus leading to less optimal biomass productivities. When the systems are too deep algae mostly respire and the biomass concentration will decrease when not enough light is present to sustain the biomass. The optimal design therefore seeks for the best combination of reactor dimensions in relation to the local light conditions and growth properties of the algae species used.

### **Maximum algae production**

The maximum biomass production can be estimated using “photosynthetic efficiencies” (PE). The PE is the conversion efficiency of light energy into biomass. In a perfectly designed reactor using perfect algae a PE of 9% is achievable [11, 19]. Ranges of PEs have been found for various reactor designs using a variety of algae species [22, 25]. Average PEs have been presented for each reactor system, e.g. 1.5% for raceway ponds, 3% for horizontal tubes and 5% for flat panels [25]. Such PE values are often used to roughly estimate algae productivity [26, 27], but they do not involve differences in algae growth between species or varying production efficiencies due to varying solar angles.

### **Reported productivities**

Outdoor production of algae in experimental, pilot and commercial facilities is increasing. Table 1 gives an overview of reported areal algae productivities for one year in various reactor designs on several locations. The reported productivities are specific for the reactor designs, operating conditions, local weather conditions and algae species. These productivities cannot be simply extrapolated to other growth conditions. For example, the weather conditions in Tucson, USA [28] and in Perth, Australia [29] are comparable, but with similar light paths of the raceway ponds, completely different productivities are achieved as two different algae species are used. Table 1 also shows data for horizontal tubular systems. In the Netherlands 20 ton ha<sup>-1</sup> year<sup>-1</sup> is produced, while at Hawaii 55 ton ha<sup>-1</sup> year<sup>-1</sup> is achieved. Is the difference because of the light and climate conditions, algae species or reactor design?

Table 1. Overview of some reported outdoor culture productivities observed during one year of production. Four reactor systems are considered; raceway ponds, horizontal tubular and vertically stacked horizontal “vertical” tubular PBRs and flat panels. The areal productivity is based on one hectare ground surface area.

Reactor system	Location	Light path (m)	Algae species	Productivity (ton ha <sup>-1</sup> year <sup>-1</sup> )	Reference
Raceway pond	Hawaii	0.12	<i>Haematococcus pluvialis</i>	37.2	[30]
Raceway pond	Tucson, Arizona	0.08-0.20	<i>Nannochloropsis salina</i>	12.2-12.7	[28]
Raceway pond	La Jolla, California	0.28	<i>Phaeodactylum tricorutum</i>	59.1	[31]
Raceway pond	Poole, England	0.40	<i>Phaeodactylum tricorutum</i>	10.6-27.3	[32]
Raceway pond	Perth, Australia	0.16	<i>Pleurochrysis carterae</i>	60	[29]
Raceway pond	La Mancha, Mexico	0.1-0.25	<i>Spirulina platensis</i>	43.1	[33]
Raceway pond	Florence, Italy	0.035	<i>Spirulina platensis</i>	20.0	[34]
Raceway pond	Malaga, Spain	0.30	<i>Spirulina platensis</i>	23.6-30.0	[35]
Raceway pond	Australia		<i>Spirulina platensis</i>	91.0	[20]
Horizontal tubular	Hawaii	0.38	<i>Haematococcus pluvialis</i>	55.1	[30]
Horizontal tubular	Netherlands	0.03	<i>Nannochloropsis</i>	20.0	[36]
Horizontal tubular	Florence, Italy	0.06	<i>Spirulina platensis</i>	30.0	[34]
Horizontal tubular	Hawaii	0.41	<i>unknown</i>	47.5	[37]
Vertical tubular	Almeria, Spain	0.09	<i>Scenedesmus almeriensis</i>	95.8	[38]
Vertical tubular	Cadiz, Spain	0.30	<i>unknown</i>	73.0	[39]
Flat panel	Sede-Boquer, Israel	0.10	<i>Nannochloropsis</i>	22.1	[40]

### Research challenges in estimating large-scale productivity

The limited number of outdoor algae production systems makes it difficult to estimate large-scale algae productivity and to quantify the effect of various reactor designs, locations and algae species. Models are therefore indispensable in design situations to systematically compare microalgae productivity under a range of decision variables like weather, reactor design and operating conditions.

Models of outdoor algae production should consider weather conditions and solar angles. Quinn *et al* [41] developed a productivity model for a commercial reactor design and found a good fit between the model prediction and measurements. Growth is modelled using the expressions introduced by Geider *et al* [42] for carbon assimilation and include the effect of light and temperature on growth. However, it is unclear how the light entering the reactor is derived and therefore the model cannot be transferred to other reactor designs. Bosma *et al* [43] predict the volumetric algae production in a bubble column using a regression model for the growth equation. All light angles are used to derive the light path for Lambert-Beers law to predict the light gradient in the culture volume. Productivity is underestimated when assuming that algae grow with the local light intensities in the culture volume and is overestimated when the average light intensity is used to derive growth [43]. The regression-based growth equation

makes it difficult to apply the model to light and temperature conditions outside the employed range of conditions.

Pruvost *et al* [44] developed a model to study different harvesting regimes in ponds and flat panels and include also scattering by algae cells as described in [45, 46]. In addition, weather conditions are used and a two dimensional light path is applied to Lambert-Beers law.

A model for algae production in a horizontal tubular photobioreactor has been developed by Acien Fernández *et al* [47, 48]. Solar angles are used to calculate the full light path in Lambert-Beers law, which is coupled to a hyperbolic growth model [49] using the average light intensity in the tubular system. The predicted light intensities were compared with measurements [47] to find that the model overestimates the light intensities. Conversely, the model slightly underestimates algae productivity in Spain during spring [50] and summer [51].

The predictions of the models given above consider only one situation and one algae species and do not allow predicting productivity in various reactor designs. The challenge is therefore to develop a framework to predict the algae productivity for any location, reactor design (see Figure 3) and all weather conditions. The development and application of such a framework is part of this thesis.

## **Embedding algae cultivation**

Algae biorefinery is not only a matter of cultivation; it also relates to the availability of resources and energy used in transportation of resources. Likewise, the cultivation and processing of biomass are intertwined and choices made in one of these processes influence the other. Introducing new technologies such as algae biorefineries affects the current economy of the products and changes their sustainability indicators. This thesis also considers the logistics, processing of biomass to biodiesel and environmental impact of algae biorefineries.

### **Research challenges for logistics**

The current approach for selecting a production location is to first analyse the potential regions using geographical maps that indicate which areas are most suitable for production. Geoinformation science (GIS) studies have been performed to assess regions for algae production based on solar irradiation [19, 52], combined with land slopes [53] and even including proximity to CO<sub>2</sub> and water resources [54-57]. Algae cultivation requires CO<sub>2</sub>, water and nutrients as resources which need to be supplied

to algae plants, while algae biomass needs to be transported to biorefineries. Transport over long distances reduces the energy efficiency of algae cultivation systems. Feasible and favourable production locations are thus also determined by logistic aspects, such as infrastructure, resource supply and availability, and biomass transport.

The role of supply chain logistics in the choice for processing locations for forestry and lignocellulosic biorefineries has been analysed by scenario studies to show how the choice of production locations is affected by resource availability [58-60], changing prices [58-60] and increased demands [58, 61].

For algae systems the contribution of logistics has not yet been investigated. It is unknown how much energy is consumed during resource transport, which transport distances are feasible and which areas are the best for algae production within specific regions. These elements are tackled in this thesis. Hereby, the productivity at different locations is predicted using the productivity framework and these productivities are linked to a logistic allocation model to determine the logistic needs in these regions.

### **Research challenges of biobased algae processing**

Algae biomass is processed into biodiesel by harvesting, concentration, disruption, lipid extraction and conversion. Many of the available biorefinery processes are variations on existing techniques that have been used in bio and food processing. Well-known examples are centrifugation, filtration, mechanical disruption and hexane extraction. However, new techniques like bio-flocculation, pulsed electric field, ultrasound sedimentation and supercritical CO<sub>2</sub> extraction are being developed and show potential for energy-efficient processing of algae biomass to biodiesel [62, 63]. Also integrated processing techniques arise, such as microwave assisted extraction and conversion, and supercritical methanol extraction and conversion. These integrated techniques are usually specifically designed for algae processing and thereby reduce not only the number of process units, but also the overall energy consumption.

At this moment, several chain analyses on the energy requirements of algae processing are presented in the literature [63-69]. The general approach in these analyses is to use a known sequence of process units and fixed processing conditions. However, the process routes in these energy analyses are not optimised with respect to the choice of the processing unit and process conditions, while efficient processing of the biomass into the products is important to achieve a promising biorefinery chain design [14]. In addition, the choice of process units, design characteristics and process conditions for each step in the algae biorefinery chain affect the performance of successive processing steps [63, 70] and the energy consumption in the processing route [71, 72].

In this work a model-based combinatorial approach to analyse the processing of algae biomass is presented, in which process conditions are optimised. The approach is applied to the production of biodiesel to search for the best combination of process units, find the best process conditions and indicate bottlenecks for process design.

### **Research challenges for impacts of algae biorefinery chains**

Two of the essential criteria for the feasibility of algae biorefineries are the economic and sustainability impact. Economic impacts focus on cost estimates, cost targets and payback times (see [25, 65, 73, 74]), while sustainability is based on life cycle indicators. Both require estimates of the performance of the total chain, which can be derived from process models.

Studies as presented in Table 1 and on techno-economic and life cycle analysis [63, 69, 70, 75-79] focus on one location and a few alternative designs for cultivation and biomass processing. This limits the application of the results, as the performances cannot be extended to other system designs [63, 78, 79], locations or algae species [80] [81].

The effect of differences in productivity between locations, reactor designs and algae species on economic and sustainability impacts have not yet been demonstrated. In this thesis the environmental and economic impacts of food commodities production with algae are studied for two regions and with two algae species and four different reactor systems.

### **Other challenges for algae biorefineries**

The developing algae biorefinery chains have to compete with existing fully-developed fossil-based facilities that produce at low costs. Especially biobased energy and fuel production have difficulties to compete with cheap fossil fuel production [14, 25, 82]. This asks for strong tools such as predictive models which can assess the current status of algae biorefinery, explore the bottlenecks in knowledge and technology, and the limiting factors in production and indicate whether these issues can be overcome in different chain designs. In this thesis frameworks are being developed and applied to assess algae productivity, to analyse the logistic chain and the processing to biodiesel.

Biomass availability and supply is geographically spread, but there is a limit to the supply. Integrating process steps leads to the most effective use of the available biomass for the production of food, non-food and energy [3, 83]. Furthermore, the integration is essential to maximise economic potential and to simultaneously minimise the environmental impacts [83, 84]. Integration should be done on several levels; 1) use the interactions between resource supply, algae growth and processing in the process chain design, 2) combine the processing of biomass to several products,

and 3) consider various performance indicators. It is this integration that is studied and developed in this thesis, as explained in the next section.

## SCENARIO STUDIES FOR ALGAE PRODUCTION

In this thesis all mentioned elements for the algae biorefinery chain are assessed by scenario analysis. These elements are systematically studied using a model-based approach and include alternate choices for design and operation, environmental conditions and the performance of algae production, cultivation supply logistics and processing of biomass.

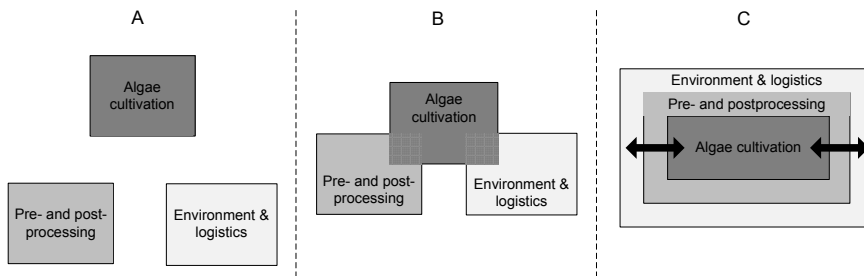


Figure 4. System division, A) the current approach where different system elements such as cultivation and processing are studied separately; B) design and analysis of system elements using information from other elements present as realized in this thesis; C) utopic systems analysis where the interactions between the different system elements are fully integrated.

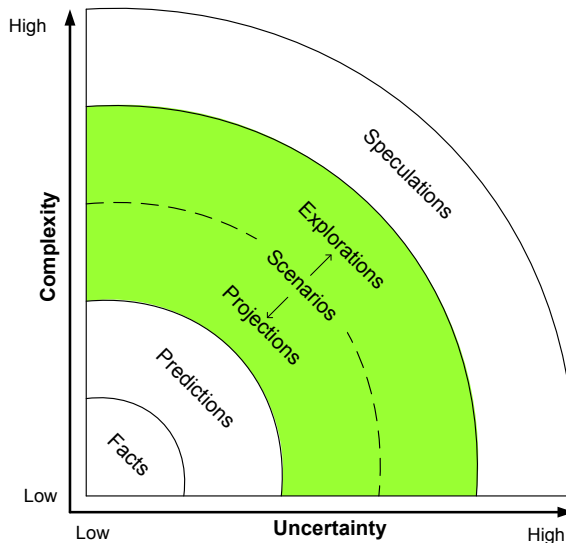


Figure 5. Scenarios help to explore complex systems under uncertainty (figure from [90])

## Integrating process chains

Often distinct elements of biorefineries are studied in detail, but the interaction between elements is limited. For example, the performance of algae cultivation is studied without connection with impact studies and processing in the biorefinery. Figure 4A shows this current approach where the elements of each study domain are separated from each other. Integration of all elements is important to achieve the utopic production process. Figure 4C shows this situation where all elements are fully integrated and studied simultaneously. Such analysis is not easy to perform because of the complexity, as all interactions and their effect on the performance indicators need to be included. In addition, when validation is not yet possible uncertainty arises in the models. Figure 4B shows the partial interaction as realised in this thesis. Scenario studies are applied to this situation to compare the performance of systems under varying conditions or foreseen scenarios.

## Scenario studies

Figure 5 illustrates the spectrum of techniques applied in systems analysis. The methods vary from fact statements to speculations and the choice depends on the level of uncertainty and complexity. Scenario studies are in the middle of this spectrum and are a valuable tool to manage with complex decisions in process and chain design, especially when uncertainty has to be coped with. Scenarios are often used to answer “what if” questions, but several definitions and uses are available (see Zhu *et al* and EEA [85, 86]). In summary, the results from scenario studies can point out bottlenecks that need to be solved to reach the desired goal [86, 87], help to explore and understand the effects of measures, technical developments or alternative designs [86-88] or indicate the consequences of uncertainty [89].

For algae production several scenarios are applicable. Firstly, “design scenarios” that indicate the effect of reactor type, specific design and algae species on e.g. biomass production. These design scenarios do not only comprise existing or specific reactor designs, but also consider wide ranges of relevant design variables. With such scenarios, designs can be compared, even if fully validated models have not yet been developed, so that the potential of new designs can be explored. Secondly, “location scenarios” to analyse the effect of location and regional conditions, such as weather or supply infrastructure, on the performance of reactor and chain design, various life cycle impacts and logistics. These scenarios are valuable to study the possibilities and constraints of a production process at various locations. Is a design flexible and can it deal with regional differences or are location specific designs or process units necessary? Lastly, we include “future scenarios”, which consider future possible situations for production cost, productivity or supply of resources.

Chapter 1	<b>Introduction</b>
Part 1: Algae production	
Chapter 2	<b>Design scenarios for flat panel photobioreactors</b>
Chapter 3	<b>Scenario analysis of large-scale algae production in tubular photobioreactors</b>
Chapter 4	<b>Scenario evaluation of open pond microalgae production</b>
Part 2: Extending the system	
Chapter 5	<b>Analysis of algae cultivation supply logistics</b>
Chapter 6	<b>A model-based combinatorial optimisation approach for energy-efficient processing of microalgae</b>
Part 3: Impacts	
Chapter 7	<b>Food commodities from microalgae</b>
Chapter 8	<b>Scenario studies for algae production: Achievement, insights and new challenges</b>

*Figure 6. Thesis outline.*

Typically these scenarios are used to answer ‘what if?’ questions. Based on current developments these future scenarios can be expected or are perhaps necessary to achieve the foreseen goals.

### **Thesis outline**

The thesis outline is shown in Figure 6. This thesis starts with the development of a productivity framework, which is described in part 1. Bio-physics-based models, first published by Ación Fernández *et al* [47, 48, 91], were expanded and integrated into a generic model framework. The uniform basis enables us to estimate biomass productivities around the world in various lay-outs and designs of reactors and for many algae species. The productivity framework is applied to predict the productivity under various conditions and optimise the design. First, flat panel systems are studied through design and location scenarios (Chapter 2). The framework is applied to horizontal and horizontally stacked “vertical” PBRs in Chapter 3. In Chapter 4 energy balances to predict the water temperature are added to the framework, which is applied to raceway ponds.

Part 2 of the thesis considers the link of cultivation with the logistic network and processing of biomass. Location and future scenarios are applied to quantitatively evaluate algae cultivation supply logistics in Chapter 5. In Chapter 6 an approach is presented to analyse a flexible network of process units. Here, not only the choice of processing units but also the process conditions are included in the optimisation routine, thereby exploring a wider range of feasible options for processing algae to biodiesel.

Part 3 concerns the implications of the productivity models on the system embedding. Chapter 7 illustrates the environmental and economic impact of location, reactor design and algae species on bulk production of food commodities through several scenarios.

A reflection on the applied approaches and an overview of the achievements and insights of this work are given in Chapter 8. In addition, the new horizons from this work are presented.

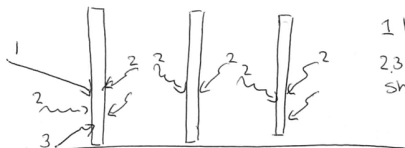


# DESIGN SCENARIOS FOR FLAT PANEL PHOTOBIOREACTORS

for front & back the scenarios

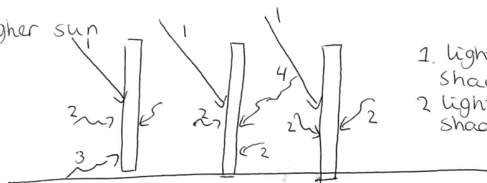
- 1 direct
- 2 diffuse
- 3 ground-reflected
- 4 panel reflected

1. Low sun



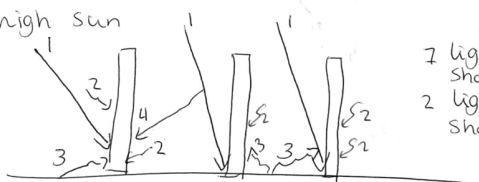
- 1 light = 1+2+3
- 2,3 light = 0
- shadow = 2 (all)

2 higher sun



- 1 light = 1+2+3
- Shadow = 2+4 (all back)
- 2 light = 1+2
- Shadow = 2

3. high sun



- tilt front > 0
- tilt back > 0
- 1 light = 1+2+3
- Shadow = 2+3+4
- 2 light = 1+2+3
- Shadow = ~~2+3~~ 0

THIS CHAPTER IS PUBLISHED AS:

P.M. SLEGGERS, R.H. WIJFFELS, G. VAN STRATEN, A.J.B. VAN BOXTEL  
 DESIGN SCENARIOS FOR FLAT PANEL PHOTOBIOREACTORS  
 JOURNAL OF APPLIED ENERGY (2011), 88(10): 3342-3353

## ABSTRACT

Evaluation of the potential of algae production for biofuel and other products at various locations throughout the world requires assessment of algae productivity under varying light conditions and different reactor layouts. A model was developed to predict algae biomass production in flat panel photobioreactors using the interaction between light and algae growth for the algae species *Phaeodactylum tricornutum* and *Thalassiosira pseudonana*. The effect of location, variable sunlight and reactor layout on biomass production in single standing and parallel positioned flat panels was considered. Three latitudes were studied representing the Netherlands, France and Algeria. In single standing reactors the highest yearly biomass production is achieved in Algeria. Biomass production fluctuates the most during the year in the Netherlands, while it is almost constant in Algeria. Several combinations of path lengths and biomass concentrations can result in the same optimal biomass production. The productivity in parallel placed flat panels is strongly influenced by shading and diffuse light penetration between the panels. Panel orientation has a large effect on productivity and at higher latitudes the difference between north–south and east–west orientation may go up to 50%.

Keywords: *microalgae, flat panel photobioreactor, modelling, large-scale cultivation, scenario studies*

## INTRODUCTION

The role of algae in the production of biochemicals and biofuels is emerging. Large-scale production facilities are necessary to fulfill the expected future demands for biodiesel and biochemicals produced by algae. With this development the challenge arises for efficient design of large-scale production facilities. The design of such large-scale systems is not straightforward. Biomass productivity and economic feasibility are related to the type of reactor, the cultivation location, the production scale, substrates and operating conditions [13, 25]. Co-production of chemicals and fuels will lead to a feasible biofuel production process [14]. Scenario studies that use model approaches help to design optimal large and complex integrated systems [92].

Large-scale production of biodiesel and biochemicals by algae is nowadays critically reviewed in life cycle assessment (LCA) studies [70, 79, 93, 94]. The outcome of the LCAs is ambiguous, because of the many uncertainties in the production system. Kadam [94] indicates that drying of biomass consumes more energy than cultivation of algae. However, energy consumption can be reduced by using alternative drying techniques. Conversely according to Stephenson *et al* [79] cultivation of algae uses most energy in the biofuel production process. They consider low energy consuming harvesting techniques such as flocculation. LCA results are strongly influenced by assumptions regarding yearly areal productivity [79, 93] and composition of the algae mass [70].

A major problem in current design studies and LCA studies is the lack of specific information and argumentation of the information together with large uncertainties in the assumptions. For example, Wijffels *et al* [14] use an algae productivity in photobioreactors (PBR) between 40-80 ton ha<sup>-1</sup> year<sup>-1</sup>. Campbell *et al* [93] use a biomass productivity of 110 ton ha<sup>-1</sup> year<sup>-1</sup> in open ponds as a starting point. Then to compensate for uncertainties a productivity of only 25% of the mentioned value is used in the final evaluation. Both the results of Campbell *et al* and Wijffels *et al* depend on estimates. Another limitation of using generic data for algae cultivation is that the designs used in the studies are based on experimental work which is not necessarily performed under practical conditions. Most experimental studies concern only the effect of a few decision variables at a time. So the outcome of the studies does not reflect the practical possible performance. Finally, most laboratory and pilot plant studies have been performed under controlled light conditions. Translation of these results to large-scale production units under variable light conditions is another challenge.

Predictive models will improve the insight in biomass production using large-scale unit designs and LCA studies. Moreover it provides an opportunity for optimisation and hence a better position to judge the feasibility of proposed algae plants for a specific location. In this work we developed and used a predictive model for flat panel reactors. Algae biomass production in both single and parallel placed PBRs was predicted under a range of weather conditions.

## METHODOLOGY

### Calculation overview

Algal growth is related to the light pattern inside a temperature controlled and in continuous mode operated flat panel PBR. The light pattern is influenced by the diurnal cycle, seasonal differences in light intensity and the spatial light distribution caused by obstruction of the sky dome by the panels. An extensive description of the predictive model for single and parallel flat panel PBRs can be found in Appendix A and B.

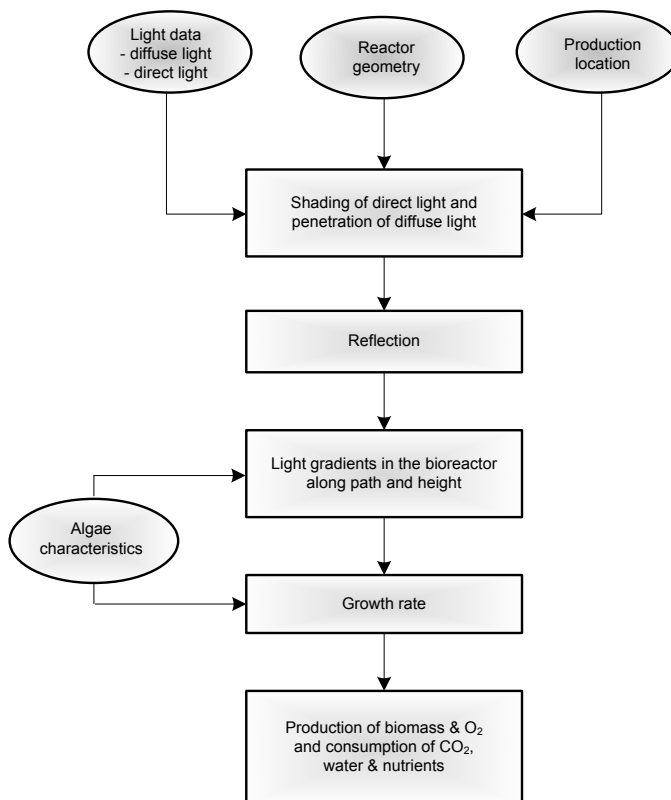


Figure 1. Calculation scheme

To make reliable estimations of the daily and/or yearly biomass productivity, the following aspects are taken into account: 1) the latitude of the PBR; 2) the reactor orientation (for example a vertical flat panel PBR orientated to north-south); 3) the light variation during the day, caused by the diurnal cycle; 4) seasonal variations in light intensity; 5) the influence of neighbouring panels on the light input, e.g. shadow effects; 6) reflection of light by the reactor walls and ground surface; 7) the light gradient in the reactor caused by light absorption by algae; 8) the algae species used; 9) the growth of algae according to the light gradient and 10) dark respiration. In addition, the need for oxygen removal and supply of water, CO<sub>2</sub> and nutrients (i.e. phosphorus and nitrogen) are computed.

Figure 1 shows the calculation scheme to calculate biomass production in flat panel PBRs from weather data. The reactor geometry is used to convert weather data on direct and diffuse light to the light falling on the reactor surface. For parallel positioned panels the effect of shading and penetration of diffuse light is taken into account as well. After calculation of light reflection, the light gradients in the reactor volume are calculated. Biomass production and substrate consumption are related to this light pattern.

## Data

To obtain realistic estimations of biomass production weather radiation data of the World Radiation Monitoring Centre (WMRC) are used as input for the calculations [95-97]. Two algae species are considered in the scenario studies: *Thalassiosira pseudonana* and *Phaeodactylum tricornutum*. These species differ in maximum specific growth rate and light absorption characteristics. Relevant parameter values are listed in Appendix C, Table C.1 and Table C.2.

## Decision variables

Algae biomass production in flat panel PBRs is influenced by several decision variables. An overview of the decision variables is given in Table 1. Some of them are fixed in this study, i.e. reactor type, operating temperature and substrates used. Others, like latitude, algae species, reactor configuration, light path, distance between panels and biomass concentration are varied to quantify their effect on the biomass production. The decision variables have a range of values. Table 2 gives standard values to determine biomass production during one year. Several sensitivity analyses are performed to quantify the effect of the decision variables on yearly algae biomass production. The analyses are divided in two groups. The first group considered single flat panel reactors; so shading of the reactor and the penetration of diffuse light between the

panels are excluded. The second group deals with parallel flat panel reactors that affect each other.

Table 1. Overview of decision variables involved in algae growth.

Decision variable	Value
Cultivation location	51.97° N, 4.93° E (Netherlands); 44.08° N, 5.06° E (France); 22.78° N, 5.51° E (Algeria)
Algae species	<i>Phaeodactylum tricornutum</i> <i>Thalassiosira pseudonana</i>
Biomass concentration	1 - 5 kg m <sup>-3</sup> ( <i>T. pseudonana</i> ) 2.5 - 13 kg m <sup>-3</sup> ( <i>P. tricornutum</i> )
Reactor type	Flat panel PBR
Distance between panels	0.01 - 1 m
Light path	0.005 – 0.10 m
Reactor configuration	Vertical reactor walls, orientation varying north-south to east-west
Operating conditions	Optimal, ideally mixed
Substrate	Nitric and phosphoric acid, water, CO <sub>2</sub> , minerals
Temperature	Optimal: 18°C ( <i>T. pseudonana</i> ) [98] 23°C ( <i>P. tricornutum</i> ) [98]
Two sided illuminated, total surface area: 2 m <sup>2</sup>	

Table 2. Overview of standard values used in simulations.

Decision variable	<i>T. pseudonana</i>	<i>P. tricornutum</i>
Biomass concentration (kg m <sup>-3</sup> )	10	1
Light path (m)	0.03	0.02
Orientation of walls	North-south	North-south
Reference	[99]	[100]

## SIMULATION RESULTS AND DISCUSSION

### Single flat panel reactors

#### Yearly variation of biomass production

Daily biomass production for a full year in the Netherlands, France and Algeria is given in Figure 3. The main walls of the vertical flat panel reactor were orientated towards north and south. A biomass concentration of 10 kg m<sup>-3</sup> and light path of 0.03 m were used (see Table 2). The graphs in Figure 3 show differences between the yearly production patterns for the three latitudes. Large fluctuations in daily biomass production occurred through the year for the Netherlands and France. In contrast, production was almost constant through the year for Algeria.

Some days did not result in effective biomass production in the Netherlands and France

because of the low light intensities at those days. This phenomenon is more common for winter days in the Netherlands than for France. The low light intensities during winter create large dark zones in the PBR and biomass is lost due to dark respiration. Maintaining a constant reactor temperature has a considerable effect on the energy requirement of the production system; in Algeria the system has to be cooled, while in the Netherlands heating is required. This energy consumption will be considered in future work.

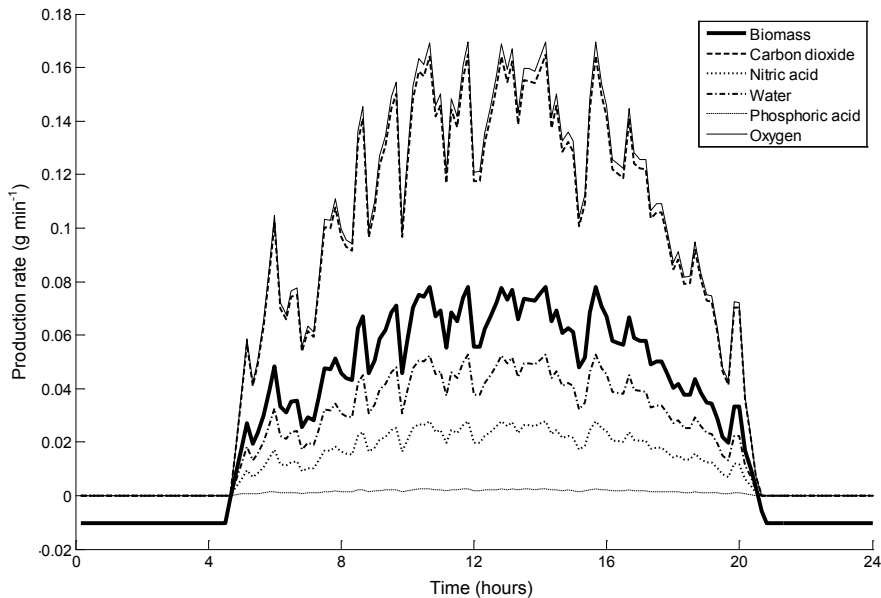


Figure 2. Daily variation of substrate and product flows for cultivation of *P. tricornutum* in the Netherlands on June 4. Consumption of  $\text{CO}_2$ , nitric acid, water and phosphoric acid are printed positive.

Remarkable is that the maximum achieved daily biomass production was higher in the Netherlands ( $50 \text{ g day}^{-1} \text{ panel}^{-1}$ ) than in Algeria ( $40 \text{ g day}^{-1} \text{ panel}^{-1}$ ). This is related to the difference in day length between the countries. In summer the reactor receives light for more than 16 hours in the Netherlands compared to 13 hours in Algeria. The higher latitude of the Netherlands is then more favourable for growth in a vertical flat panel. More light falls on the reactor surface due to the lower solar elevation compared to Algeria. Yet, Table 3 shows that the highest yearly biomass production is predicted for Algeria ( $12.1 \text{ kg panel}^{-1} \text{ year}^{-1}$ ). Yearly biomass production in the Netherlands is about 25% lower than in Algeria.

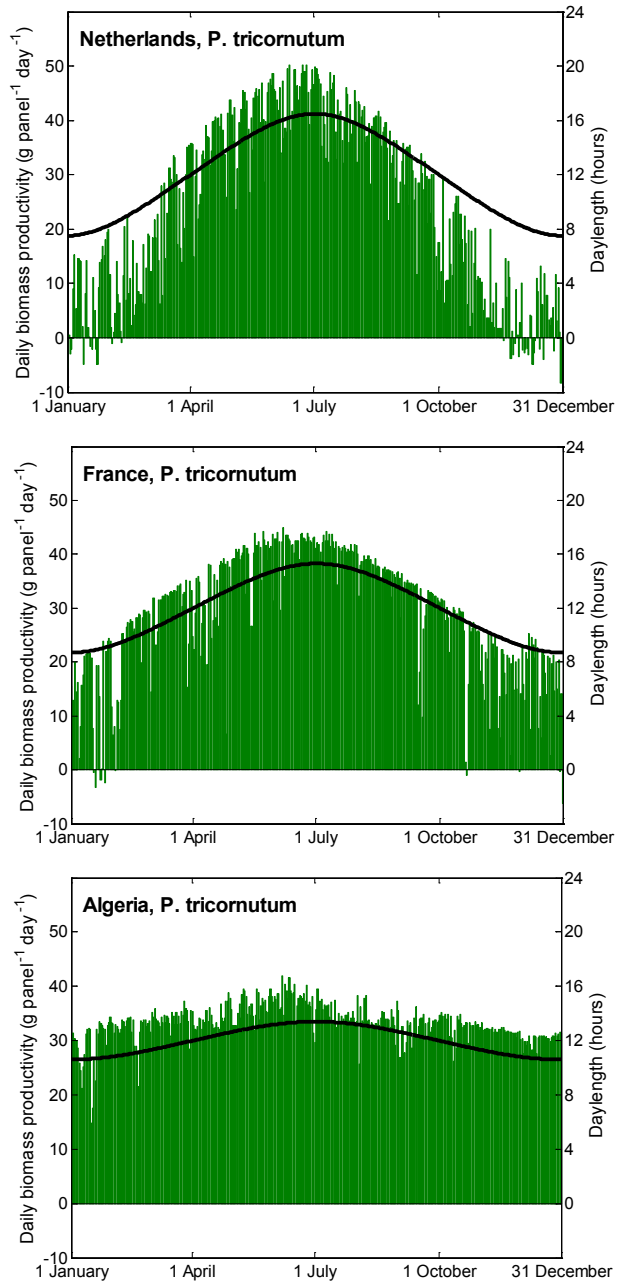


Figure 3. Daily algae biomass production for *P. tricornutum* and day length during one year. The left y-axes give the daily biomass production in  $\text{g panel}^{-1} \text{day}^{-1}$  is given, the right y-axes the day length in hours.

As the light path and biomass concentration were fixed in these calculations they do not constitute the optimal combination. Higher productivities are possible, as is shown in the next sections.

Similar results were found for the algae species *T. pseudonana* using the parameter values of Table 2, however the achieved biomass production was much lower (Table 3). The lower biomass levels are partly results of the lower biomass concentration used (see Table 2). Remarkable is that for *T. pseudonana* production is possible throughout the year in the Netherlands, while it is not for *P. tricornutum*. This is result of the relative high effect of the maintenance rate on growth of *P. tricornutum* (3.6%) compared to *T. pseudonana* (1.5%).

Table 3. Yearly biomass production ( $\text{kg panel}^{-1} \text{ year}^{-1}$ )<sup>a</sup> on three locations, based on reference values for biomass concentration and light path.

	<i>T. pseudonana</i>	<i>P. tricornutum</i>
Netherlands	5.3	8.8
France	6.1	10.6
Algeria	6.7	12.1

<sup>a</sup> Since it is not meaningful to express biomass production in a single panel per ground surface, the biomass production is expressed per panel.

Biomass production is accompanied by substrate consumption and oxygen production. Figure 2 shows the variation of these variables during a representative summer day in the Netherlands. During night there is an overall decrease of biomass because sunlight is absent and biomass is lost due to dark respiration. A small overestimation in biomass production is made since the biomass concentration is assumed to stay constant during the day. Substrate consumption and oxygen production during the night are not considered. In the light period substrate consumption and oxygen production closely followed the pattern of biomass production. Reaction stoichiometry links the different mass flows. Therefore, similar patterns were visible for production on other days or other locations. The ratio however was slightly different if another algae species is used.

Figure 2 shows that substrate demand peaks can be expected. In the design of large-scale cultivation units it is important to consider the technical possibilities of balancing the substrate supply with the demand of the algae.

### Effect of decision variables on biomass production

Following the work of Meiser *et al* [100] and Shen *et al* [99], the biomass concentration in the previous section was set to  $10 \text{ kg m}^{-3}$  for *P. tricornutum* and to  $1 \text{ kg m}^{-3}$  for *T. pseudonana* and a light path of 0.03 m and 0.02 m were used respectively.

Sensitivity analyses have been performed to quantify the effect of light path, biomass concentration, surface angle and surface azimuth angle on yearly biomass production. During these analyses one or two decision variable are varied at a time.

The different locations show similar patterns for yearly biomass production under variation of decision variables (results not shown). As expected there are different optima in cultivation conditions for the two algae species (Figure 4). *P. tricornutum* can be cultured at high biomass concentrations (10-13 kg m<sup>-3</sup>) and long light paths, while a very short light path is required for *T. pseudonana* at high cell densities. Although longer light paths give a lower volumetric productivity, a high volumetric productivity does not necessarily coincide with the highest yearly yield. Furthermore, a long light path is attractive for construction and operation.

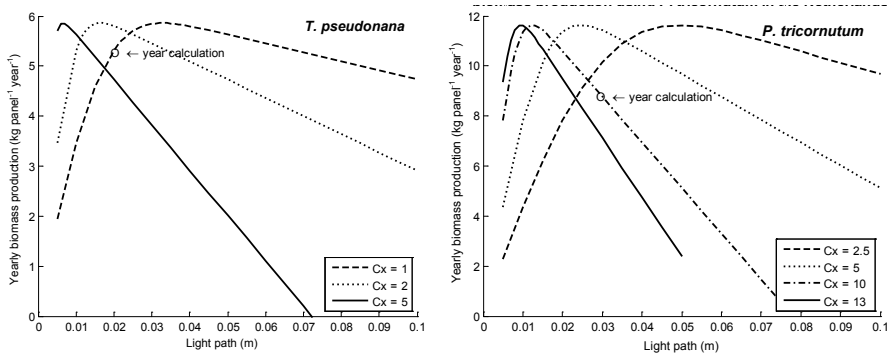


Figure 4. Effect of light path and biomass concentration on yearly biomass production using *T. pseudonana* (left) and *P. tricornutum* (right) in the Netherlands. Yearly biomass production using literature values for biomass concentration and light path (based on [99] and [100]) are indicated with a circle.

The highest annual biomass production is achieved with *P. tricornutum* (about 12 kg panel<sup>-1</sup> year<sup>-1</sup>). The same optimal biomass production level can be reached using several combinations of light path and biomass concentration. This effect has been shown before by Hu *et al* [101]. The optimum is achieved if all light is consumed in conjunction with a low dark respiration level. Thus, the optimal combination of biomass concentration and light path is achieved by low concentration and long light paths or by high cell densities and short light paths. Remarkable are the different shapes of the curves. Low biomass concentrations result in broad optima, while narrow optima are present at high biomass concentrations. Productivities at the left side of the optima are lower because not enough light energy is available for optimal growth. At

the right side of the optimum they are lower because dark zones exist and energy is required for dark respiration. Dark respiration is linked to the biomass concentration, therefore yearly biomass production decreases faster for dense cell cultures.

In a system with short light path small deviations in the biomass concentration have a strong influence on the yearly biomass production. Controlling the biomass concentration in a system with narrow production optima can be more critical than in a system with broad optima.

The sensitivity graphs in Figure 4 show also that the combination of light path and biomass concentration as used by Meiser *et al* [100] and Shen *et al* [99] can be further improved. For commercial algae production optimal growth conditions should be used, instead of commonly used values from literature. The results show that optimal conditions cannot be determined in a straightforward way. The modelling approach helps to make an optimal design for biomass production based on characteristics of the location and algae species used.

Biomass production can be further improved by optimising for the reactor surface angle and surface azimuth. A vertical reactor system results in the highest yearly biomass production for the three latitudes investigated (results not shown). These results are not in accordance with Hu and Richmond who found that each latitude has an optimal surface angle for PBRs facing south and north [102].

A reactor orientation towards east and west results in the highest biomass production (results not shown). This is independent of the algae species and latitude used. The difference between an orientation of north-south and east-west is below 5%.

### **Parallel flat panel reactors**

Biomass production in parallel positioned flat panel reactors is influenced by the same decision variables as single flat panels. In addition, shading effects occur and these have a considerable influence on the light pattern in the panels and thus on the biomass production (Appendix A.3). Besides, less diffuse sky light reaches the ground when panels are positioned closer to each other. In Figure 5 the effect of panel distance on diffuse light penetration between one meter high panels is shown. For a panel distance of one meter 30% of the diffuse sky light intercepted at the top of the reactor penetrates to the bottom of the reactor. For shorter panel distances less light reaches the bottom part of the panels.

Areal yearly biomass production was predicted for *P. tricornutum* using a biomass concentration of 2.5 kg m<sup>-3</sup> and light path of 0.05 m, i.e. optimum values from the

single panel system. Figure 6 shows the results of a sensitivity analysis on the distance between the reactor panels. The areal biomass production depends on the latitude; higher latitudes result in lower yearly areal biomass production. Biomass production per reactor panel decreases when the panels are positioned closer to each other. Still areal yearly biomass production increases due to the larger number of panels on a hectare. After a maximum yearly areal biomass production is achieved, areal production reduces as a result of biomass loss in the panels caused by large dark zones. Optimal biomass production is achieved using a panel distance between 20 and 40 cm. The optimal panel distance is specific for the location and algae species. The optimal panel distance for *T. pseudonana* ranges between 15 and 30 cm (results not shown). Optimal panel distances can be found for areal production, per panel most biomass is produced using single standing panels.

Yearly areal biomass production is significantly improved when the reactor orientation is changed from east-west to north-south (Figure 6). While the effect of orientation on a single flat panel reactor was found to be less than 5%, Figure 6 shows that the effect on parallel positioned flat panels is much larger (up to 50%). In addition it was found that the reactor orientation does not only influence the achieved biomass production, but also the optimal panel distance. This distance decreases when the orientation is changed to north-south. Similar results are found for *T. pseudonana*.

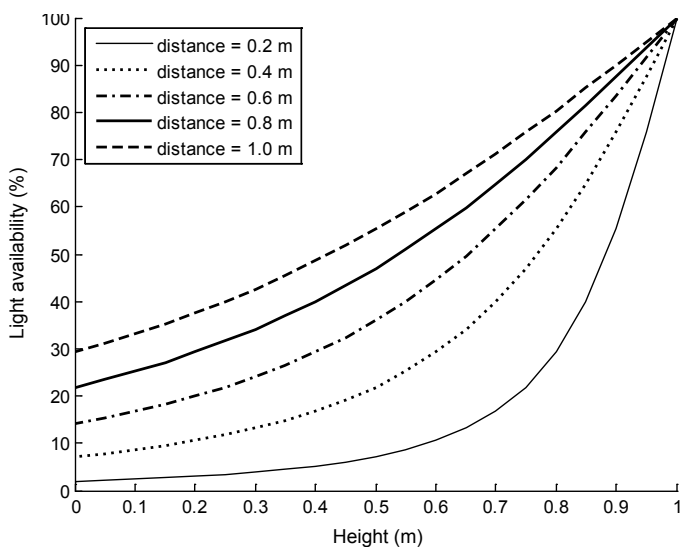


Figure 5. Light availability (%) at various heights within a panel as result of decreasing diffuse sky light availability towards the bottom of the parallel placed vertical flat panels. Height = 1 meter equals the top of the reactor panel, height = 0 meter the bottom.

One should keep in mind that in this sensitivity analysis the same biomass concentration and light path are used for all the panel distances. However, for each distance optimal light conditions are established by a different combination of biomass concentration and light path. As a result higher areal biomass production levels are possible and the optimal distance may change.

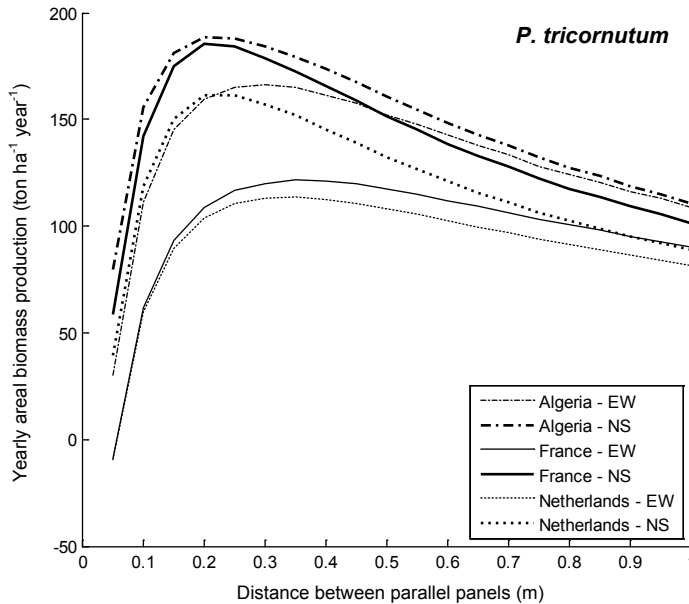


Figure 6. Effect of panel distance on areal yearly biomass production using *P. tricorutum* in the Netherlands, France and Algeria. The thin lines indicate that the reactor walls are orientated to the east and west. The fat lines represent panels with the walls orientated to the north and south.

## CONCLUSIONS

Prediction of biomass production in PBRs is the fundament for feasibility studies on large-scale algae production plants and LCAs. The productivity, however, varies between locations, reactor layout, algae species and the varying light input over the day and the year. In this work a model approach is presented and used to predict the yearly production of single and parallel placed flat plate PBRs.

Vertical placed and east-west orientated single panels produce the most biomass and productivity is correlated with the day length. A high volumetric productivity is not the goal to go for. The reactor layout must be such that the light is efficiently used by the algae and dark respiration is low. As a result, several combinations of path lengths

and biomass concentrations can yield the same optimal value for biomass productivity.

Shading and diffuse light penetration between parallel panels have a strong effect on the productivity in parallel placed flat panels. The productivity per panel decreases with a shorter distance between panels, but due to the higher number of panels the total areal productivity increases till a maximum value is achieved. For the considered algae species the optimal panel distances ranges between 0.2 m and 0.4 m.

The highest yearly areal biomass productivity decreases for higher latitudes. The orientation of parallel placed panels has a strong influence on productivity. For higher latitudes north-south oriented panels produce up to 50% more than east-west oriented panels.

For production of algae there are over 6 decision variables that affect productivity. In the design of large-scale production facilities it is difficult to investigate all these decision variables in experimental work. Experimental work reported in the literature is not necessarily performed under optimal conditions. A model approach is powerful to explore the sensitivity of productivity around the conditions reported in literature.

## **ACKNOWLEDGEMENT**

This work was performed in the cooperation framework of Wetsus, centre of excellence for sustainable water technology ([www.wetusus.nl](http://www.wetusus.nl)). Wetusus is co-funded by the Dutch Ministry of Economic Affairs and Ministry of Infrastructure and Environment, the European Union Regional Development Fund, the Province of Fryslân, and the Northern Netherlands Provinces. The authors like to thank the participants of the research theme Algae for the discussions and their financial support.

## APPENDIX A. LIGHT

### A.1 Solar incidence angle

Direct light on a flat panel reactor varies with the solar position. The solar incidence angle  $\theta$  ( $^\circ$ ) on a flat plate reactor depends on the solar declination  $\delta$  ( $^\circ$ ) which is angular position of the sun at solar noon with respect to the plane of the equator, the latitude of the reactor location  $\phi$  ( $^\circ$ ), the slope of the reactor with respect to the ground surface  $\beta$  ( $^\circ$ ), the surface azimuth angle between the normal of the reactor surface and south  $\gamma$  ( $^\circ$ ) and the solar hour angle  $\omega$  ( $^\circ$ ). Figure A.1 gives an overview of the parameters involved in the calculation of the solar incidence angle  $\theta$ :

$$\begin{aligned} \cos(\theta) = & \sin(\delta) \sin(\phi) \cos(\beta) \\ & - \sin(\delta) \cos(\phi) \sin(\beta) \cos(\gamma) \\ & + \cos(\delta) \cos(\phi) \cos(\beta) \cos(\omega) \\ & + \cos(\delta) \sin(\phi) \sin(\beta) \cos(\gamma) \cos(\omega) \\ & + \cos(\delta) \sin(\beta) \sin(\gamma) \sin(\omega) \end{aligned} \quad (\text{A.1})$$

The angles  $\beta$ ,  $\gamma$ ,  $\phi$  are fixed, the angle  $\omega$  depends on the solar hour and angle  $\delta$  on the day of the year.

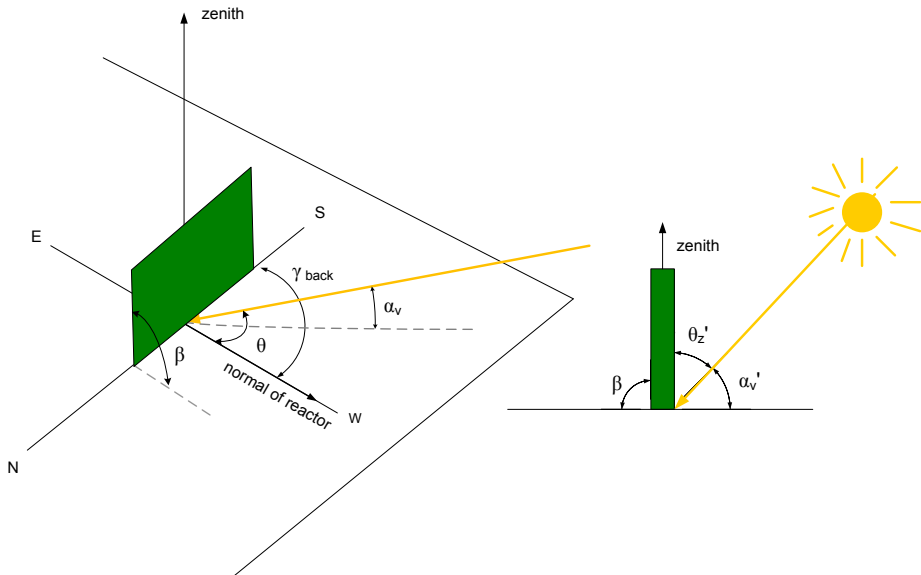


Figure A.1 Illustration of sunlight parameters; surface azimuth angle  $\gamma_{back}$ , the solar incidence angle  $\theta$ , the solar elevation  $\alpha_v$ , and the projected elevation  $\alpha_v'$ , solar incidence angle  $\theta$  and slope of the reactor surface  $\beta$ .

Since the sun illuminates two sides of a tilted flat panel PBR, the solar incidence angle is calculated from the reactor front and back side azimuths and surface angles

( $\gamma_{front}$  &  $\beta_{front}$  and  $\gamma_{back}$  &  $\beta_{back}$ )

$$\beta_{back} = 180 - \beta_{front} \quad (\text{A.2})$$

$$\gamma_{back} = \gamma_{front} + 180 \quad (\text{A.3})$$

The solar declination  $\delta$  for equation A.1 varies with the day number in the year  $N$

$$\delta = 23.45 \sin\left(\frac{360(284 + N)}{365}\right) \quad (\text{A.4})$$

and the solar hour angle, which is displacement of the sun from the local meridian  $\omega$  in equation A.1, is given by

$$\omega = 15(t_{solar} - 12) \quad (\text{A.5})$$

in which the solar time  $t_{solar}$  (h) depends on the actual time  $t$  (h), longitude of the reactor location  $\lambda$  ( $^{\circ}$ ), the meridian of the reactor location  $\kappa$  ( $^{\circ}$ ) and the equation of time  $e$  (see equations A.6-A.8):

$$\zeta = (N - 1) \frac{360}{365} \quad (\text{A.6})$$

$$e = 0.017 + 0.43 \cos(\zeta) - 7.35 \sin(\zeta) - 3.35 e^{-2} \cos(2\zeta) - 9.37 \sin(2\zeta) \quad (\text{A.7})$$

$$t_{solar} = t + \frac{4(\lambda - \kappa) + e}{60} \quad (\text{A.8})$$

The zenith angle  $\theta_z$  ( $^{\circ}$ ) and the solar elevation angle  $\alpha_v$  ( $^{\circ}$ ) in Figure A.1 are given by:

$$\cos(\theta_z) = \sin(\varphi) \sin(\delta) + \cos(\varphi) \cos(\delta) \cos(\omega) \quad (\text{A.9})$$

$$\alpha_v = 90 - \theta_z \quad (\text{A.10})$$

## A.2 Light input for single flat panels

Meteorological stations provide radiation data measured perpendicular to the earth surface. To convert horizontal light data to a tilted flat panel reactors geometric factors are used [103, 104]. A flat panel reactor has two geometric factors: one for the front side and one for the back side. The geometric factors for direct radiation are:

$$G_{direct,front}(t) = \frac{\cos(\theta(\beta_{front}, \gamma_{front}))}{\cos(\theta_z)} \quad (\text{A.11})$$

$$G_{direct,back}(t) = \frac{\cos(\theta(\beta_{back}, \gamma_{back}))}{\cos(\theta_z)} \quad (\text{A.12})$$

in which  $\theta$  the solar incidence angle and  $\theta_z$  the solar zenith angle. The surface angle  $\beta$  and surface azimuth angle  $\gamma$  differ for the two geometric factors (see Appendix A1).

The geometric factor for isotropic diffuse sky radiation is only a function of the surface angle of the reactor surface  $\beta$ :

$$G_{diffuse,front} = \frac{1 + \cos(\beta_{front})}{2} \quad (A.13)$$

$$G_{diffuse,back} = \frac{1 + \cos(\beta_{back})}{2} \quad (A.14)$$

The geometric factor for ground reflected diffuse radiation is influenced by the reflectivity  $\rho$  of the ground surface:

$$G_{reflect,front} = \rho \frac{1 - \cos(\beta_{front})}{2} \quad (A.15)$$

$$G_{reflect,back} = \rho \frac{1 - \cos(\beta_{back})}{2} \quad (A.16)$$

A flat panel PBR has two sides which are exposed to a different amount of light (Figure A.2).

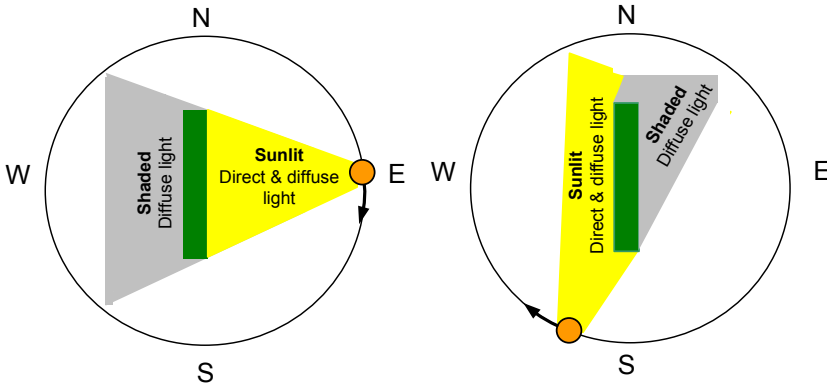


Figure A.2. Top view of illumination of vertical flat panel PBR walls orientated toward the east and west. On the left the situation early in the morning, on the right the situation after noon. The different illumination patterns are imposed by equation A.17 and A.18.

The total light input at each side of the tilted panel  $I_o$  ( $\text{J m}^{-2} \text{s}^{-1}$ ) at a moment is given by:

$$I_{o,front}(t) = (G_{direct,front}(t) + G_{reflect,front}) I_{hor,direct}(t) + (G_{diffuse,front}(t) + G_{reflect,front}) I_{hor,diffuse}(t) \quad (A.17)$$

$$I_{o,back}(t) = (G_{direct,back}(t) + G_{reflect,back}) I_{hor,direct}(t) + (G_{diffuse,back}(t) + G_{reflect,back}) I_{hor,diffuse}(t) \quad (A.18)$$

with the geometric factors as defined in equations A.11-A.16. Direct and diffuse radiation data,  $I_{hor,direct}$  and  $I_{hor,diffuse}$  obtained from meteorological stations (WRMC) are used [95-97]. Global and diffuse radiation data were measured on a horizontal surface. Direct radiation was recorded perpendicular to the direction of the sunrays. The interval time for the used measurements is one minute, but the data supplied by WRMC contain some gaps; these were searched and then filled manually. Gaps smaller than 10 measurements were filled with the average of the two neighbouring measurements. Otherwise the dataset of the whole day was replaced by the data of the neighbouring days. Ten minute average values are used in the simulations.

### A.3 Light input for parallel panels

For large-scale cultivation parallel positioned flat panels are used. Parallel placement causes shading and consequently part of the panels no longer receive direct sky light (Figure A.3). The shadow height on vertical reactor panels is given by:

$$h_{shadow}(t) = h - \tau \tan(90 - \theta'_z) \quad (A.19)$$

which is a function of the reactor height  $h$  (m), the distance between the reactor panels  $\tau$  (m) and the projected solar elevation which equals  $90 - \theta'_z$ . Deviations in the shade pattern at the beginning and end of a row of flat panel PBRs are neglected. For the simulations the flat panel is divided in two parts. The upper part receives direct and diffuse light, the lower part only diffuse light. The separation between upper and lower part varies with the solar position and is calculated every simulation step.

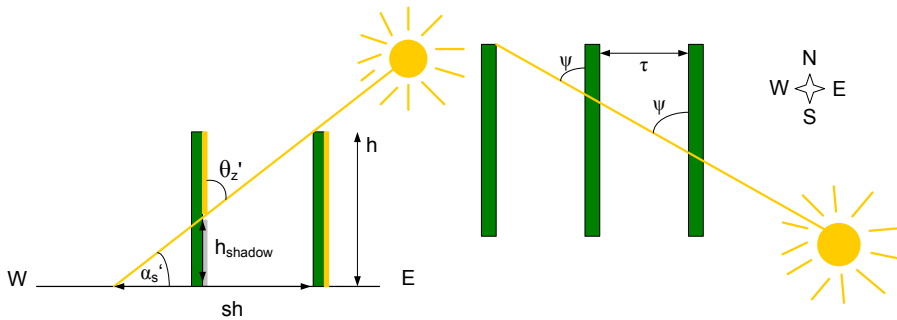


Figure A.3. Side view (upper) and top view (below) of parallel positioned flat panel PBRs. The shadow height  $h_{shadow}$  depends on the solar elevation  $\alpha_s'$ , the panel height  $h$ , the angle between the sunrays and the panel  $\psi$  and the distance  $\tau$ .

Parallel placement of panels influences the penetration of diffuse sky light into the space between panels; the light intensity decreases from top to the bottom. Similarities can be seen with the penetration of light in urban street canyons [105]. The geometric

factor for diffuse sky light at height  $y$  (m) measured from the top of the panel is given by:

$$G_{diffuse,front,parallel}(y) = \frac{1 + \cos(\beta_{front} + u)}{2} \quad (\text{A.20})$$

$$G_{diffuse,back,parallel}(y) = \frac{1 + \cos(\beta_{back} + u)}{2} \quad (\text{A.21})$$

In which

$$u = \tan^{-1}\left(\frac{y}{\tau}\right) \quad (\text{A.22})$$

The penetration of diffuse sky light is a function of the slope of the reactor surface  $\beta$ , the height  $y$  and the distance between the panels  $\tau$ .

The reactor panels at the border of the algae plant experience a different light pattern. We assume that this effect is negligible on large-scale. Therefore, all reactor panels are treated similarly in the calculations. Ground reflection is low for parallel placed panels and is therefore not taken into account. The total amount of light falling on each side of the tilted panel  $I_o$  ( $\text{J m}^{-2} \text{s}^{-1}$ ) at height  $y$  is given by:

$$I_{0,front}(y,t) = G_{direct,front}(t)I_{hor,direct}(t) + G_{diffuse,front,parallel}(y)I_{hor,diffuse}(t) \quad (\text{A.23})$$

$$I_{0,back}(y,t) = G_{direct,back}(t)I_{hor,direct}(t) + G_{diffuse,back,parallel}(y)I_{hor,diffuse}(t) \quad (\text{A.24})$$

with the geometric factors as defined in equations A.13, A.14, A.20 and A.21.

#### A.4 Light reflection at and transmission through the flat panel wall

Figure A.4 shows the different interfaces that the light encounters. For the flat panel reactor the first interface is between the air and the reactor wall. The second interface is between the reactor wall and the culture volume. The amount of reflected light on each interface is related to the differences in refractive indices and the angle of incidence [104]. The angle of refracted light follows from Snell's law. The angle of incidence for direct light equals the angle of solar elevation. The angle of incidence for incoming diffuse light is assumed to be  $60^\circ$  [103].

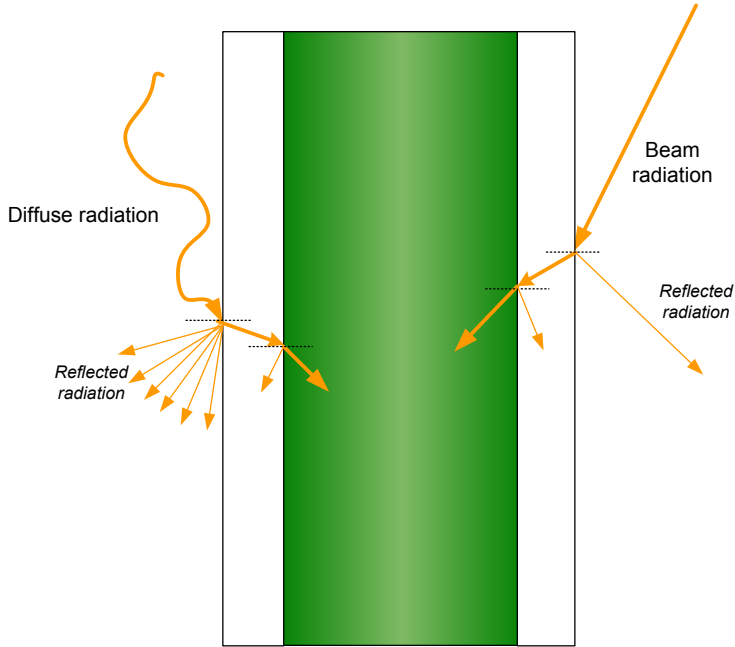


Figure A.4. Refraction of light through the reactor wall and the light losses due to reflection. Diffuse light is drawn with a curved line to indicate that it is scattered. Reflected diffuse light has any direction.

Light reflection by the flat panel walls follow from the Fresnel equations given in equations A.25 and A.26. The reflection of  $s$ -polarized light  $R_s$  is formulated by equation A.25, the reflection of  $p$ -polarized light  $R_p$  by equation A.26.

$$R_s = \left[ \frac{\eta_i \cos(\theta_i) - \eta_t \sqrt{1 - \left(\frac{\eta_i}{\eta_t} \sin(\theta_i)\right)^2}}{\eta_i \cos(\theta_i) + \eta_t \sqrt{1 - \left(\frac{\eta_i}{\eta_t} \sin(\theta_i)\right)^2}} \right]^2 \quad (\text{A.25})$$

$$R_p = \left[ \frac{\eta_i \sqrt{1 - \left(\frac{\eta_i}{\eta_t} \sin(\theta_i)\right)^2} - \eta_t \cos(\theta_i)}{\eta_i \sqrt{1 - \left(\frac{\eta_i}{\eta_t} \sin(\theta_i)\right)^2} + \eta_t \cos(\theta_i)} \right]^2 \quad (\text{A.26})$$

The angle of incidence  $\theta_i$  ( $^\circ$ ) and the refractive indices of the material before  $\eta_i$  and after the interface  $\eta_t$  are necessary to calculate the transmittance.

Normal sunlight is unpolarised, therefore the overall reflection coefficient  $R'$  equals the average of the reflection coefficients for  $s$ - and  $p$ -polarized light.

$$R' = \frac{R_p + R_s}{2} \quad (\text{A.27})$$

The light reflected within the reactor wall is completely transmitted to the air. The total light transmitted to the culture volume  $I_i$  ( $\text{J m}^{-2} \text{s}^{-1}$ ) is:

$$I_i(t) = I_0(t)(1 - R_1 - R_2 + R_1 R_2) T_m \quad (\text{A.28})$$

where  $I_0$  is the total light falling on the outside of the reactor wall (see equations A.17, A.18 and A.23, A.24). Additional light may be lost due to a low transparency of the wall material, indicated by  $T_m$ . The calculation is done for both sides of the reactor (so  $I_{o,front}$  and  $I_{o,back}$ ) and for parallel positioned panels for each height.  $R_1'$  and  $R_2'$  are the reflection coefficients for the air-reactor wall interface and the reactor wall-culture volume interface respectively.

## A.5 Light gradients in culture volume

Two light intensity gradients exist in the culture volume. First, as a function of height due to shading and the penetration of diffuse light between parallel positioned panels as a function of the height, and second in the liquid between the two reactor walls. The gradient as function of height is described by equations A.23 and A.24. The gradient between the two reactor walls runs from the reactor wall to the centre of the reactor and is caused by the absorption of light by the medium and the algae. Since light enters the culture volume from two sides the light level is the highest at the walls and decreases towards the centre of the liquid.

Only the photosynthetic active radiation (PAR) of the spectrum is absorbed by the algae ( $f_{PAR}$ ). The remaining part is considered heat energy. Algae use the photons for growth, therefore the light radiation  $I_{i,front}$  and  $I_{i,back}$  are converted into a photon flux density (PFD) using the conversion factor  $f_{PFD}$ :

$$I_{PFD}(t) = f_{PAR} f_{PFD} I_i(t) \quad (\text{A.29})$$

The Lambert-Beer law is used for the overall PFD gradient in the culture volume:

$$I_{PFD}(y, z, t) = I_{PFD,front}(y, t) e^{-(\epsilon + k_a C_x)z} + I_{PFD,back}(y, t) e^{-(\epsilon + k_a C_x)(d-z)} \quad (\text{A.30})$$

This expression gives the PFD ( $\mu\text{mol m}^{-2} \text{s}^{-1}$ ) at location  $z$  (m) in the reactor depth measured from the wall (referred to as depth  $z$ ) and height  $y$  at time  $t$ . The reactor depth ranges from  $0$  at the front side of the reactor panel to  $d$  at the back side of the

panel.  $I_{PFD,front}(y)$  is the PFD at the inside of the reactor walls at the front side of the panel at a certain height and  $I_{PFD,back}(y)$  the PFD at the back side of the panel at the same height. Local PFDs are influenced by the diffuse and direct sky light passing the reactor wall, the extinction coefficient of the medium  $\varepsilon$ , the spectrally averaged absorption coefficient  $k_a$  ( $\text{m}^2 \text{kg}^{-1}$ ) of the algae, the biomass concentration  $C_x$  ( $\text{kg m}^{-3}$ ) and the position in the reactor depth  $z$ . The absorption coefficient of the culture broth  $\varepsilon$  ( $\text{m}^{-1}$ ) was neglected. The algae are grown in a water-like solution which has a very low absorption coefficient compared to algae cells.

## APPENDIX B. ALGAE

### B.1. Algal productivity

The accumulation of algae biomass in the reactor as function of the path  $z$ , height of the panel  $y$  and time  $t$  is given by:

$$\frac{dC_x(y, z, t)}{dt} = (\mu(y, z, t) - D(t))C_x(y, z, t) \quad (\text{B.1})$$

The overall specific growth rate  $\mu$  ( $\text{s}^{-1}$ ) and biomass concentration  $C_x$  are a function of height  $y$ , depth  $z$  and time  $t$  as well. The biomass concentration is assumed to be constant in the panel. For constant production a “pseudo control law” can be applied in which the dilution rate is varied such that the biomass concentration remains constant in time. This leads to a small overestimation in biomass production during the night when biomass decreases due to dark respiration. The system is in steady-state and the biomass produced of  $1 \text{ m}^2$  is:

$$P(t) = \int_0^h \int_0^d \mu(y, z, t) C_x dz dy \quad (\text{B.2})$$

Hereby the production (kg) is obtained by integration for every position in reactor height  $h$  and reactor depth  $d$ . Areal production ( $\text{kg ha}^{-1}$ ) is expressed per hectare of ground area:

$$P_{areal}(t) = N_{reactors} P(t) \quad (\text{B.3})$$

in which  $N_{reactors}$  is the number of panels on one hectare ground surface.

The year production ( $\text{kg ha}^{-1} \text{ year}^{-1}$ ) is the integral of the momentary production:

$$P_{areal} = N_{reactors} \int_0^{365} P(t) dt \quad (\text{B.4})$$

Any growth model can be used in the system. In the presented simulations the growth model of Geider *et al* based on pI-curves is applied [42]. The model considers photo-acclimation and is valid for an ideally mixed system at constant optimal temperature:

$$\mu(y, z, t) = P_m^c \left( 1 - \exp\left( \frac{-\alpha I_{PFDD}(y, z, t) \Theta_a(y, z, t)}{P_m^c} \right) \right) - r_m \quad (\text{B.5})$$

With  $P_m^c = \mu_{max} + r_m$

The overall specific growth rate  $\mu$  depends on the chlorophyll  $a$  and carbon ratio in the cell  $\Theta_a$  (g Chl  $a$  g<sup>-1</sup> C) and on the PFD  $I_{PFDD}$  experienced by the algae cell at height  $h$ , depth  $z$  and time  $t$  (see equation A.30). The cells adapt the ratio between chlorophyll  $a$  and carbon in their cells according to the light intensity. The overall specific growth rate  $\mu$  also depends on the maximum carbon specific rate of photosynthesis  $P_m^c$  (s<sup>-1</sup>), the functional cross section of the photosynthetic apparatus  $\alpha$  (g C (mol<sup>-1</sup> photons) m<sup>2</sup> g<sup>-1</sup> Chl  $a$ ) and the maintenance metabolic coefficient  $r_m$  (s<sup>-1</sup>). The maximum carbon specific rate of photosynthesis in turn depends on the maximum specific growth rate  $\mu_{max}$  and the maintenance metabolic coefficient  $r_m$ .

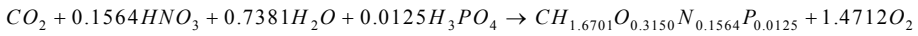
The chlorophyll  $a$ :carbon ratio is given by:

$$\Theta_a(y, z, t) = \Theta_{a,max} \frac{1}{1 + \frac{\Theta_{a,max} \alpha I_{PFDD}(y, z, t)}{2P_m^c}} \quad (\text{B.6})$$

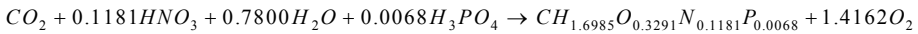
With  $\Theta_{a,max}$  the maximum chlorophyll  $a$ :carbon ratio.

## B.2. Substrate consumption and oxygen production

Stoichiometric factors are used to determine the substrate consumption rates and the oxygen production rate from the biomass production rate. The reaction stoichiometry is determined using the biochemical biomass composition (Table C.1), the average biochemical composition [106] and the molar composition of the substrates and products. The reaction stoichiometry for growth of *T. pseudonana* on nitric and phosphoric acid is:



and for growth of *P. tricornutum* on nitric and phosphoric acid:



## APPENDIX C. PARAMETERS

Table C.1: Overview of general model parameters.

Parameter	Value	Reference
$f_{PAR}$	0.43	
$f_{PFD}$ ( $\mu\text{mol J}^{-1}$ )	4.57	
$T_m$	1	
$\varepsilon$ ( $\text{m}^{-1}$ )	0	water
$\eta_{air}$	1.0008	
$\eta_{algaesolution}$	1.330	water
$\eta_{reactorwall}$	1.510	glass
$\theta_{i,diffuse}$ ( $^{\circ}$ )	60	[103]
$\rho$	0.5	white lining, [102]

Table C.2: Algae specific parameter values.

Parameter	<i>T. pseudonana</i>	<i>P. tricornutum</i>	Reference
$k_a$ ( $\text{m}^2 \text{kg}^{-1}$ )	269	75	[47, 107]
$r_m$ ( $\text{day}^{-1}$ )	0.05	0.05	[42]
$T_{opt}$ ( $^{\circ}\text{C}$ )	18	23	[98]
$\alpha$ ( $\text{g C mol}^{-1}$ photons $\text{m}^2 \text{g}^{-1}$ Chl <i>a</i> )	10	10	[42]
$\Theta_{a,max}$ ( $\text{g Chl } a \text{ g}^{-1} \text{ C}$ )	0.08	0.08	[42]
$\mu_{max}$ ( $\text{day}^{-1}$ )	3.29	1.40	[42]
Biochemical composition (carbohydrates : lipids : proteins)	14-20-33	11-20-56	[31, 108]
Average phosphorcarbon ratio	1:80	1:147	[109]

## APPENDIX D. GROUND REFLECTION

The ground reflected light input  $I_{reflect,front}$  ( $\text{W m}^{-2}$ ) for parallel panels is calculated by:

$$I_{reflect,front}(t) = G_{reflect,front} \left( I_{hor,diffuse}(t) f_{bottom} \frac{\tau}{h} + I_{hor,direct}(t) \frac{l_{shadow}}{h} \right) \quad (\text{D.1})$$

$$I_{reflect,back}(t) = G_{reflect,back} \left( I_{hor,diffuse}(t) f_{bottom} \frac{\tau}{h} + I_{hor,direct}(t) \frac{l_{shadow}}{h} \right) \quad (\text{D.2})$$

Where  $G_{reflect,front}$  (-) is the geometric factor for ground reflection at the front side of the system,  $I_{hor,diffuse}$  ( $\text{W m}^{-2}$ ) the diffuse light intensity on horizontal surface,  $I_{hor,direct}$  ( $\text{W m}^{-2}$ ) the direct light intensity on horizontal surface,  $f_{bottom}$  (-) the fraction of diffuse light reaching the ground surface between parallel panels,  $l_{shadow}$  (m) the shadow length,  $\tau$  (m) the distance between panels and  $h$  (m) the total height.

The geometric factor  $G_{groundreflected}$  is calculated by:

$$G_{groundreflected}(\beta, h') = \rho \frac{1 - \cos(\beta + u(h'))}{2} \quad (\text{D.3})$$

using the reflectivity of the ground  $\rho$  (-). The sky view angle  $u$  is a function of height  $h'$  (m) measured from bottom and the distance between the tubes  $\tau$ :

$$u(h) = \tan^{-1}\left(\frac{h'}{\tau}\right) \quad (\text{D.4})$$

$$l_{shadow} = \frac{h}{\tan(\lambda)} \quad (\text{D.5})$$

The factor of diffuse light reaching the bottom is calculated by:

$$f_{bottom} = \cos(\delta) \quad (\text{D.6})$$

$$\delta = \tan^{-1}\left(\frac{h}{0.5\tau}\right) \quad (\text{D.7})$$

The shadow length  $l_{shadow}$  is calculated by:

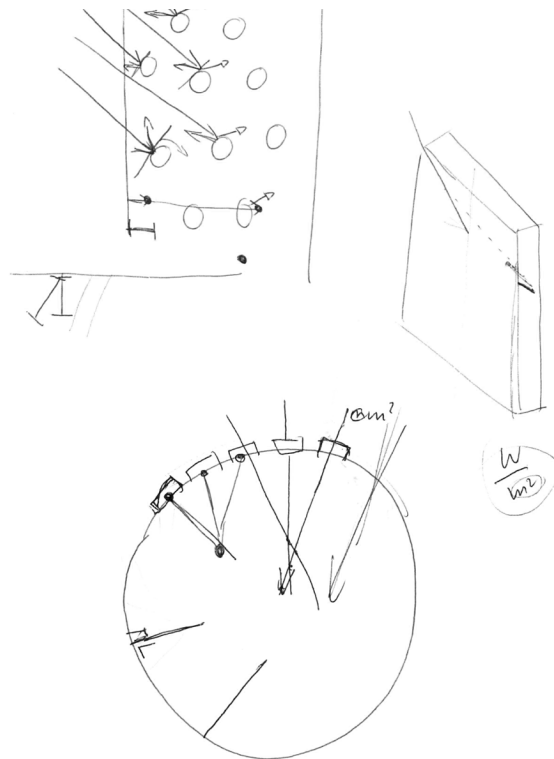
$$l_{shadow} = \frac{h}{\tan(\lambda)} \quad (\text{D.8})$$

with  $\lambda$  ( $^{\circ}$ ) the projection of  $\alpha_v$  on the plane perpendicular to the reactor surface.



# SCENARIO ANALYSIS OF LARGE-SCALE ALGAE PRODUCTION IN TUBULAR PHOTOBIOREACTORS

3



THIS CHAPTER IS PUBLISHED AS:

P.M. SLEGGERS, P.J.M. VAN BEVEREN, R.H. WIJFFELS, G. VAN STRATEN, A.J.B. VAN BOXTEL  
SCENARIO ANALYSIS OF LARGE SCALE ALGAE PRODUCTION IN TUBULAR PHOTOBIOREACTORS  
APPLIED ENERGY (2013),105: 395-406

## **ABSTRACT**

Microalgae productivity in tubular photobioreactors depends on algae species, location, tube diameter, biomass concentration, distance between tubes and for vertically stacked systems, the number of horizontal tubes per stack. A simulation model for horizontal and vertically stacked horizontal tubular reactors was made to quantify the effect of these decision variables on production yield. The model uses reactor dimensions, dynamic sunlight patterns over the day and year, and growth characteristics of algae species as inputs. Scenario studies were done to study the effect of decision variables on reactor performance in the Netherlands, France and Algeria. Results indicate that the areal biomass productivity in vertically stacked photobioreactors is 25%-70% higher than in plain horizontal systems. Reactor design is location specific because light conditions differ. In the Netherlands, the best horizontal distance between tubes is 0.05 m for horizontal and 0.25 m for vertical systems. For France and Algeria, the best horizontal distance between vertical systems is 0.20 m and 0.15 m respectively. System performance can be improved further by using light reflecting materials on the ground surface. Improving the transparency properties of tube material does not significantly affect areal productivity.

*Keywords: tubular photobioreactor, microalgae, scenario studies, large-scale production, models*

## INTRODUCTION

Microalgae are sunlight-driven cell factories that convert CO<sub>2</sub> and water into biomass containing lipids, proteins and carbohydrates. Microalgae have become an emerging source for the production of transport fuels, biochemicals and food products. Various production systems are used to cultivate algae on a large-scale: open systems such as raceway ponds, and closed systems like flat panel and tubular photobioreactors (PBRs). The maximum yield and production in closed systems is higher than in open raceway ponds [25]. It is expected that algae productivities between 40 and 80 tonnes of dry matter per hectare per year can be realised in closed systems [14]. Norsker *et al* [25] indicate that the production costs for tubular PBRs are in the same range as for raceway ponds. However, it is projected that the costs of algae production in closed systems will be lower than in open systems after optimisation of the system design [25]. Previous work showed that productivity depends on reactor technology, reactor design, algae species and production location and that there is room for optimisation of productivity [110, 111].

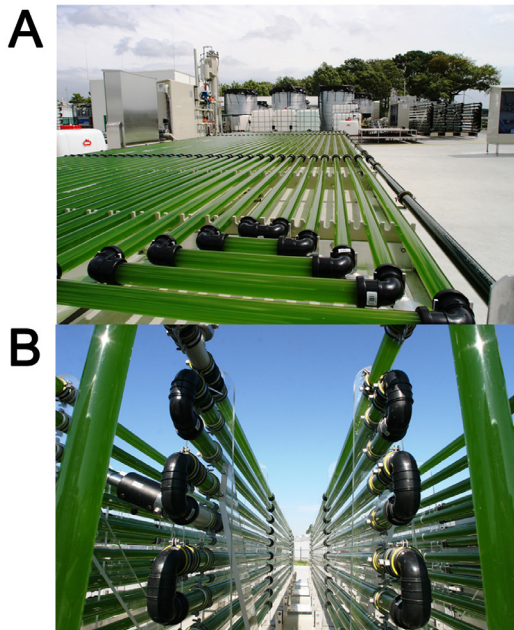


Figure 1. Tubular reactor systems at the AlgaePARC in Wageningen (the Netherlands); A) Horizontal, B) Vertical tubular PBRs (with permission of Wageningen UR).

Tubular PBRs are advantageous for scale up and high volumetric biomass productivities can be reached [112]. These systems consist of an array of straight horizontal transparent

tubes that are placed either next to each other, called "horizontal", or vertically stacked, referred to as "vertical" (Figure 1). Tubes are usually made out of glass or plastic and have a diameter of 0.1 meter or less. The high surface/volume ratio of tubes promotes high areal yields [23]. Cultivation medium is recirculated and turbulent conditions are needed to use the benefits of light/dark cycles [23]. Applicable tube length is limited due to oxygen accumulation in the tubes. To limit biomass losses through respiration in the dark zone biomass concentrations have to be adjusted to tube diameter and available light conditions [51].

Productivity data of commercially exploited tubular PBRs is limited and design and scaling rules are not yet available. To counteract the lack of information from experience, simulation models are a fast and cost-effective alternative to predict trends in reactor performance. Macroalgae cell cultivation in horizontal tubular reactor systems has been studied using light integration and Lambert-Beer's law [113]. A similar approach has been used for microalgae [47, 51], where the light path depends on the solar angle. However, using light integration to estimate algae growth leads to overestimation [43]. These models require extension and adjustments before they can be applied to detailed TE and LCA studies.

To explore the role of decision variables and weather conditions on algae growth, a new simulation tool for tubular PBRs has been developed based on the approach [110, 111] used for flat panels and open raceway ponds. The light modelling of flat panels was extended to predict microalgae productivity in large-scale parallel horizontal and vertically stacked tubular PBRs. In contrast to the approach of [47], local specific growth rates are based on the internal light profile and are then averaged to prevent overestimation that occurs with light integration. In addition, algae suspensions in closed systems are strongly scattering solutions with particles an order of magnitude larger than the wavelength. Therefore, the light path is taken perpendicular to the curved wall [114].

The simulation tool presented in this work allows to study the effect of decision variables, such as location, reactor orientation, algae species, biomass concentration and diameter of tubes on growth on biomass production.

## **TUBULAR PBR MODEL AND SIMULATION APPROACH**

Predictive models for raceway ponds and flat panel reactors have been developed [110, 111]. In raceway ponds, light homogeneously distributes over the reactor surface. In parallel placed flat panel PBRs a gradient is present from reactor top to

bottom for diffuse light. Tubular PBRs require extended light calculations as light enters the reactor walls at various angles. Figure 2 shows the calculation scheme to compute algae biomass production in a tubular PBR from weather data, reactor design properties, characteristics of algae species and location on earth (latitude) at any time during the year. To calculate the solar angles at a given time it is important to include the latitude. The model equations to describe light patterns on the tubular surface are given in the Appendix.

### Model overview

First, the amount of light reaching the tube walls is calculated, based on direct, diffuse and ground reflected light. The curved reactor surface and the effect of reactor orientation are taken into account. Parallel tubular PBRs are affected by shading and light penetration effects between the tubes [111]. Robinson *et al* [105] describe the canyon effect between buildings, where light penetration decreases from top to bottom. For large-scale algae cultivation systems this effect is related to the tube diameter, total reactor height, location and distance between tubes. Reflection light from the ground surface is added to the light input on the reactor surface. Location and time determine the solar angles and the light input on the reactor walls. Not all light falling on the reactor reaches the algae culture inside the tube; part is reflected due to differences in refractive indices of air and tube material. In addition, tube material absorbs some light. Reflection and absorption of light by the tube material are considered.

The PBR has an internal light gradient due to self-shading and light absorption by algae. Algae suspensions in tubular PBRs are strongly scattering media with particles in an order of magnitude larger than the wave length [114]. Therefore, scattered light mainly reflects and the light penetration can be described by taking the light path perpendicular to the curved wall in Lambert-Beer's law. The light path is calculated for every point in the cross section of the tube and every time step.

Algae growth is derived from local light intensities, called "growth integration", or using the average light intensity in the system, called "light integration". Growth integration assumes that algae grow using local light intensities they experience while light integration assumes that algae experience the average light intensity. In this work algae growth is described using growth integration, since light integration usually leads to overestimation of algae growth [43]. We assume an optimal, constant culture temperature and an ideally mixed system for biomass and nutrients. The biomass concentration inside the reactor is controlled and constant over time, which means in practice that the harvesting rate must equal the specific growth rate. Quantitative

relations for the inhibiting effect of oxygen on growth are limiting, therefore this effect is not considered. Besides, the negative effect of oxygen accumulation can be prevented if higher CO<sub>2</sub> concentrations are used [115]. Algae biomass production is estimated with the growth model of Geider *et al* [42], see also [111].

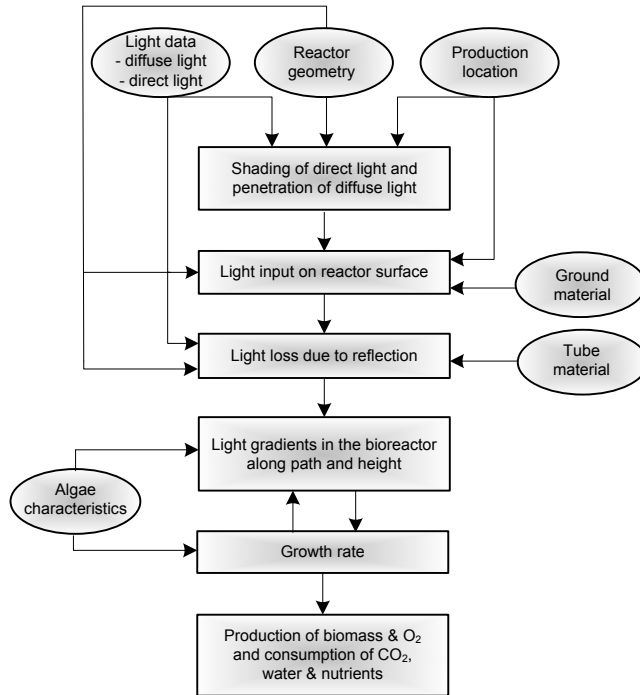


Figure 2. Calculation scheme to determine algae biomass productivity in tubular PBRs.  = Calculation and  = Input.

## Scenario studies

The effect of decision variables on algae productivity was quantified using scenarios. Table 1 gives an overview of the decision variables for production in tubes. Three locations, the Netherlands, France and Algeria were compared to demonstrate the influence of latitude and climate conditions on tubular PBR performance. Tubular PBR performance was expressed as ton dry biomass production per hectare of ground surface per year. Other variables like tube diameter, biomass concentration, algae species, tube material and ground reflectivity were varied to show their effect on production. Ranges were chosen such that effects of the parameter of interest are evident (Table 1). In all scenarios, the constant biomass concentration and horizontal distance between tubes resulting in the highest yearly areal biomass production were determined. These are referred to as “best” or “optimal”. All remaining operating

conditions (such as nutrient supply, oxygen removal and culture temperature) were taken to be non-limiting. Standard values for reactor design are also listed in Table 1. The algae species *Phaeodactylum tricornutum* and *Thalassiosira pseudonana* were considered in the simulations. They differ in maximum specific growth rate and light absorption coefficient. Parameter values for the algae species are given in the Appendix, Table A1.

Radiation data of the World Radiation Monitoring Centre [95-97] were employed to acquire estimations of biomass production. The data set contains light intensities for direct and diffuse light. The per-minute recorded data were averaged to ten-minute data to reduce computation time.

Table 1. Decision variables for horizontal and vertical tubular PBRs. Standard values for simulations are given as well.

Decision variable	Values used in scenario studies	Standard value
Cultivation location	51.97° N, 4.93° E (the Netherlands) 44.08° N, 5.06° E (France) 22.78° N, 5.51° E (Algeria)	
Algae species	<i>Phaeodactylum tricornutum</i> <i>Thalassiosira pseudonana</i>	
Biomass concentration	0.2 – 12 kg m <sup>-3</sup>	<sup>a</sup>
Distance between stacked tubes	0.01-0.06 m	0.01 m
Horizontal distance between tubes (horizontal configuration)	0.01-0.50 m	0.03 m
Horizontal distance between tubes (vertically stacked tubes)	0.10-0.75 m	<sup>a</sup>
Number of rows in vertical stack	1-25	9
Reflectivity ground material	0-1	0.5 (white lining)
Tube diameter	0.02-0.30 m	0.06 m
Tube material	Glass (refraction = 1.510, transmission = 1) PMMA (refraction = 1.540, transmission = 0.92) PVC (refraction = 1.491, transmission = 1) Perfect (100% transmittance)	Glass
Wall thickness		0.003 m

<sup>a</sup> Standard values for the horizontal distance between tubes and also for the biomass concentration depend on location, algae species and tube diameter.

## SIMULATION RESULTS AND DISCUSSION

### Light distribution and algae production

Light profiles in a tubular PBR are the key to algae growth. Figure 3 shows the light distribution in a single horizontal tube without shading by neighbouring tubes at three moments on 30 June 2009 using the algae species *P. tricornutum*.

The movement of the sun over the reactor is clearly visible from early in the morning to afternoon. The light distributions inside the tube arise from Lambert-Beer's law. Light intensities at the bottom are slightly increased, since light is reflected from the ground surface to the tubular PBR surface.

Biomass production is affected by this internal light profile. The impact depends on the growth characteristics of algae species used. For *P. tricornutum* maximum specific growth rates are reached above  $50 \text{ W m}^{-2}$ , so high specific growth rates are present even early in the morning and in the afternoon<sup>1</sup>.

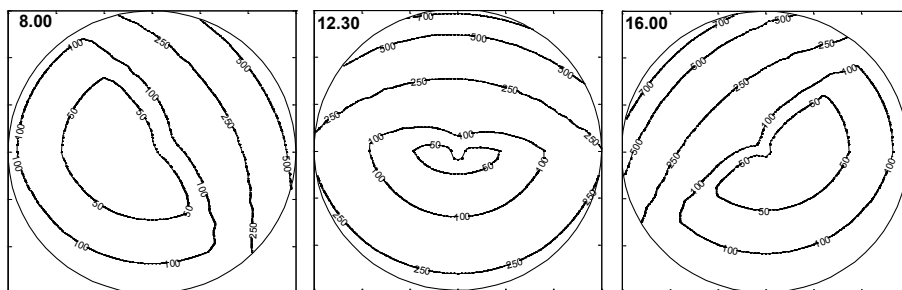


Figure 3. Cross-sectional light profile ( $\text{W m}^{-2}$ ) inside a single horizontal tube in the Netherlands at 8:00, 12:30 and 16:00 hours on a clear sky day (30 June 2009) as seen from south. Reactor is oriented on north-south line, tube diameter is 0.06 m and characteristics of the algae species *P. tricornutum* have been used with a biomass concentration of  $1 \text{ kg m}^{-3}$ .

Daily areal biomass production in horizontal and vertical tubular PBRs under standard conditions is shown in Figure 4. Settings for this condition are listed in Table 1 and the results for the best biomass concentrations and corresponding horizontal distances are presented in Figure 4. Local light intensities and the solar trajectory affect the patterns for biomass production. For the Netherlands, this results in a pattern with large day-to-day variations in biomass production, within a month. The behaviour for biomass production in France and Algeria is less erratic. Figure 4 shows that in France and the Netherlands some days have a negative daily biomass production. At these days, the solar input is not enough to sustain the culture as respiration is larger than growth. Similar trends were seen for open raceway ponds and vertical flat panels PBRs [110, 111]. The biggest difference is that the maximum daily areal biomass production for horizontal tubes is almost equal for the three locations. This results from the smaller culture volume in which dark zones can be prevented by adapting the biomass concentration. Adjustment of the biomass concentration ensures maximum specific growth rates during most of the day, thus reaching similar productivities at all three locations in summer. In vertical tubular PBRs, biomass production is affected more

<sup>1</sup> Light intensity at which maximum growth rates are achieved is derived from the growth curve as presented in Slegers *et al* [111] and the algae growth characteristics given in the Appendix, Table A1.

by the varying light levels during the year. The large culture volume and height of the system make it difficult to achieve comparable light conditions in the total reactor system for all locations.

As mentioned before, experimental data is limited and experiments often do not fully conform to assumptions made in modelling studies. In addition, experimental results may concern other algae species with different growth characteristics, thus making a full and direct comparison difficult. Still, a first step in model validation is to compare estimated productivities with experimental results to make sure the results are in the same order of magnitude. Productivities of 19.1-19.8 g m<sup>-2</sup> day<sup>-1</sup> have been reported for outdoor cultivation of *P. tricornutum* in a two layered tubular PBR in Spain using a constant optimal dilution rate during the year [50]. These productivities are similar to our estimates for algae growth in France during spring and lower than our estimates for Algeria. In earlier work by [48], maximum productivities of 14.1 and 16.8 g m<sup>-2</sup> day<sup>-1</sup> are given for algae growth in horizontal tubular PBRs in winter and summer respectively. These values have the same scale, although experimental productivities in winter and summer are slightly lower than our daily estimates for France.

### **Effect of reactor design**

Reactor design affects biomass production in tubular PBRs. Therefore, to predict the best possible productivity the biomass concentration and horizontal distance should be adapted to each situation. The vertical distance and number of vertical rows in a stack are also important to consider. Generally, higher areal algae productivities are reached in vertical systems [116]. Figure 5 illustrates that yearly areal yields in vertical tubular PBRs depend on both the number of rows and the vertical distance between tubes in a stack. A small vertical distance results in the best achievable yearly areal productivity. The increase in productivity by stacking tubes is limited due to shading of neighbouring tubes and the canyon effect [105]. The best constant biomass concentration and horizontal distance between tubes have to be adapted accordingly; high systems ask for lower biomass concentrations and large horizontal distances between the tubes. The highest yearly areal productivities are reached with about nine tubes in each stack (nine rows), which equals a total reactor system height of 0.62 m.

A few rows less or more results in a small decrease in areal productivity. This means that there is a limit to the positive effect of increasing the number of vertically stacked rows of tube. The optimum of nine vertical rows depends on the canyon effect in which diffuse light penetration is assumed comparable to that between plates. Considering yearly areal productivity only, systems with more than ten rows in the vertical seem

unreasonable. However, tubular PBRs with more vertical rows are being operated in practice [117]. The relative effect of the number of rows and vertical distance is similar for the Netherlands and Algeria. Shading and canyon effects are comparable for the two locations, but overall productivities differ as light intensities are higher in Algeria than in the Netherlands.

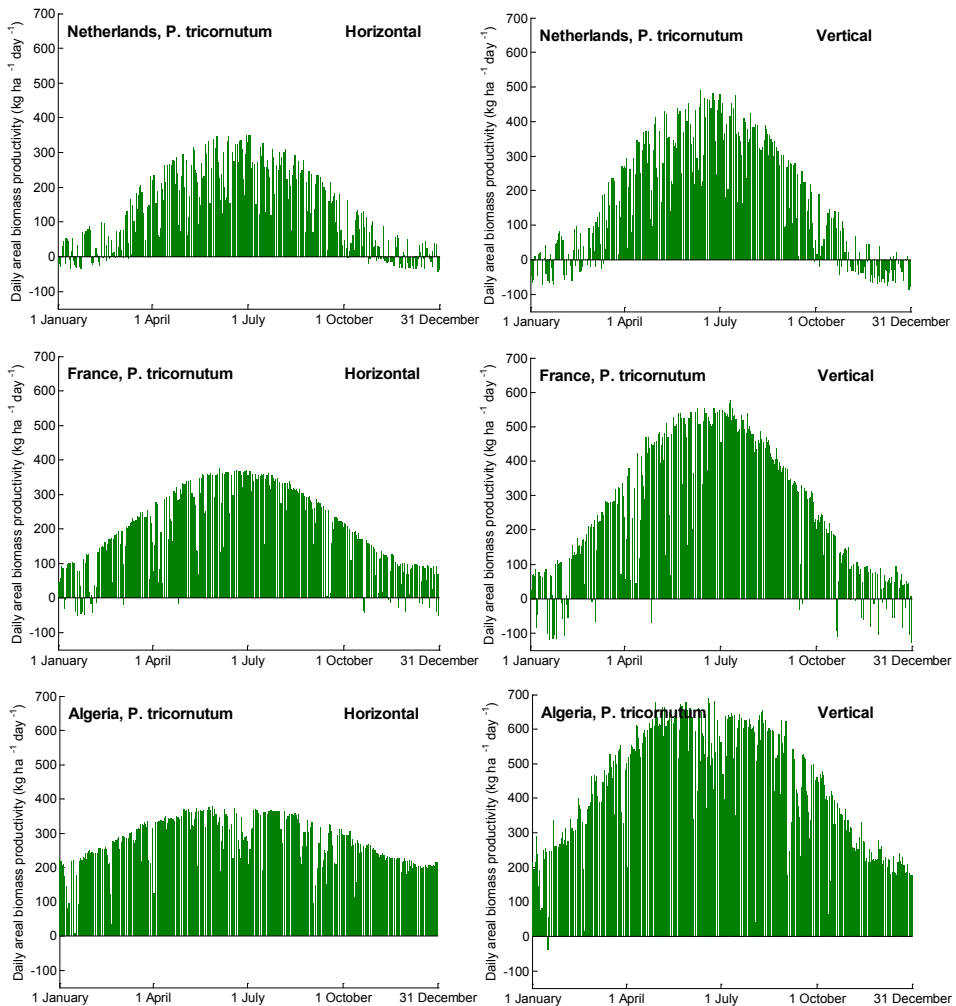


Figure 4. Daily areal biomass production ( $\text{kg ha}^{-1} \text{day}^{-1}$ ) during 2009 for production of *P. tricornutum* in horizontal (left) and vertical (right) tubular PBRs. Tube diameter is 0.06 m and vertical tubular PBRs have 9 vertical rows with 0.01 m vertical distance in between. For every situation, the best horizontal distance and best constant biomass concentration are used (see Table 2).

The effect of horizontal distance between tubes on yearly areal productivity in horizontal and vertical tubular PBRs using a standard tube diameter of 0.06 m is shown in Figure 6. Standard settings for these simulations are listed in Table 1. The effect of horizontal distance between the tubes on simulated productivities shows a similar trend for the various scenarios. An optimal distance is present for all three locations. For small distances between tubes the decline in light received per tube is compensated by the increase in number of tubes resulting in increased productivities. However, at some point, the decrement in light input caused by small horizontal distances is too high to compensate with the number of tubes.

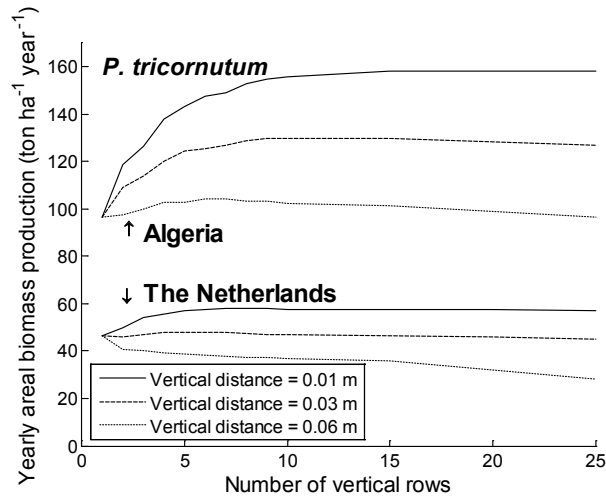


Figure 5. The effect of number of vertical rows and vertical distance between tubes on yearly areal biomass production ( $\text{ton ha}^{-1} \text{ year}^{-1}$ ) in vertical tubular PBRs. Results are shown for the Netherlands and Algeria using the species *P. tricornutum*. For every point best constant biomass concentrations and horizontal distance are used, tube diameter is 0.06 m.

The highest areal productivities in horizontal tubular PBRs of 0.06 m diameter are reached for a distance of 0.03-0.04 m between tubes. In general, higher productivities are estimated for the algae species *P. tricornutum*, which was also seen for raceway ponds and vertical flat panel PBRs [110, 111]. The growth characteristics of this algae species are more beneficial for production compared to *T. pseudonana*. As a rule of thumb, a horizontal distance equal to  $\frac{1}{2}$ - $\frac{2}{3}$  diameter can be recommended for the distance between horizontal tubes, for the three countries and both algae species (results not shown).

Areal biomass productivity for vertical tubular PBRs show the same trends with design parameters as horizontal tubular PBRs. The system height affects the canyon effect for

light penetration and the shading pattern. Thus, larger horizontal distances should be used for vertical tubular PBRs. The best horizontal distance between vertical tubular PBRs is 0.25 m in the Netherlands. For France and Algeria, the best distance is 0.20 m and 0.15 m respectively. Vertical tubular PBRs can be put closer to each other at lower latitudes for two reasons. First, solar angles are higher and shading effects occur at smaller distances. Shading can be beneficial as growth is more efficient at lower light intensities. Second, light intensities at locations like France and Algeria are higher than in the Netherlands. Therefore, diffuse light intensities are higher despite the canyon effect for diffuse light penetration.

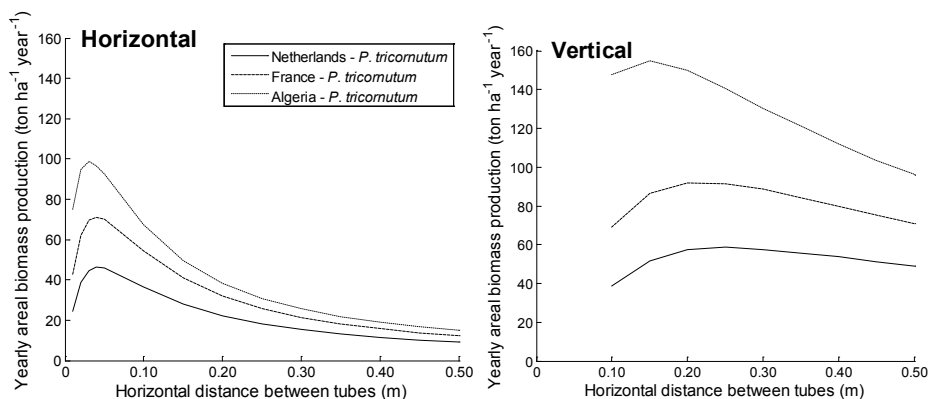


Figure 6. The effect of horizontal distance between tubes on yearly areal biomass production ( $\text{ton ha}^{-1} \text{year}^{-1}$ ) with horizontal (left) and vertical (right) tubular PBRs. Algae species is *P. tricorutum*, tube diameter is 0.06 m, vertical tubular PBRs have nine vertical rows with a vertical distance of 0.01 m. For every point best constant biomass concentration is used.

Table 2. Best yearly areal productivities Prod. ( $\text{ton ha}^{-1} \text{year}^{-1}$ ), PE (%) and biomass concentration Cx ( $\text{kg m}^{-3}$ ) following from Figure 6. Tube diameter is 0.06 m, vertical PBRs have 9 horizontal tubes above each other with 0.01 m in between. Results are given for the best distance between rows.

	Horizontal						Vertical					
	<i>T. pseudonana</i>			<i>P. tricorutum</i>			<i>T. pseudonana</i>			<i>P. tricorutum</i>		
	Prod.	Prod.	Prod.	Prod.	PE	Cx	Prod.	PE	Cx	Prod.	PE	Cx
Netherlands	27.1	27.1	27.1	46.3	1.4	1.6	31.9	1.6	0.9	58.6	3.0	2.6
France	43.9	43.9	43.9	71.2	1.5	2.1	56.6	2.0	1.1	91.8	3.2	3.3
Algeria	59.7	59.7	59.7	96.8	1.5	2.5	97.0	2.4	1.3	154.8	3.8	4.0

The best-simulated areal productivities, corresponding photosynthetic efficiencies (PE) and applied biomass concentrations are listed in Table 2. The results indicate that areal biomass productivity in vertical tubular photobioreactors is 25%-70% higher than in horizontal systems. The vertical design enables the use of more light.

However, the increase in productivity is restricted since shading and the canyon effect for light penetration affect vertical systems more than horizontal systems. As expected, productivities in both systems are the lowest in the Netherlands and the highest in Algeria. Solar angles and light intensities are lower at northern locations and as a result, vertical tubular systems receive lower light intensities at those latitudes. For the Netherlands, these conditions are especially limiting growth in winter.

Previously estimated best yearly areal productivities for raceway ponds and flat panels are listed in Table 3 as comparison [110, 111]. Raceway ponds are expected to have the lowest productivities; dark zones often occur in the 0.30 m deep systems. These dark zones are prevented in systems with a smaller light path, therefore production increases with closed horizontal tubular PBRs. Productivity increases further when vertical systems are used and in general flat panels result in the highest productivities. As mentioned before, light angles and light intensities of a location are important aspects for vertical systems. By comparing Tables 2 and 3, it is seen that productivity in vertical tubular PBRs may reach the productivities of flat panel reactor, but only for locations at lower latitudes and with high light intensities.

Table 3. Best yearly areal productivities (ton ha<sup>-1</sup> year<sup>-1</sup>) for 0.30 m deep raceway ponds and flat panels with a light path of 0.03 m [for more details see 110, 111].

	Raceway ponds [110]		Flat panels [111]	
	<i>T. pseudonana</i>	<i>P. tricornutum</i>	<i>T. pseudonana</i>	<i>P. tricornutum</i>
Netherlands	8.0	41.5	54.7	119.6
France	<sup>a</sup>	<sup>a</sup>	60.9	128.6
Algeria	14.9	63.7	74.9	157.6

<sup>a</sup> Productivities for France are unknown due to lack of climatologic data (air temperature, relative humidity, wind velocity and air pressure) for this location.

The effect of biomass concentration on yearly areal biomass production in the Netherlands using *P. tricornutum* is illustrated in Figure 7. Every tube diameter has a different optimal biomass concentration and deviation from the best biomass concentration results in a decrease of biomass production. Below the optimal biomass concentrations, light is not fully used and at higher biomass concentrations large dark zones exist for most of the year.

Moreover, biomass production in small diameter tubes is less sensitive to changes in biomass concentration than production in tubes with larger diameters. The light pattern in tubes with larger diameters is more affected by changes in biomass concentration, which does not benefit growth. Similar trends are seen for the other algae species and

for the locations France and Algeria (results not shown), but at these locations, the optimal biomass concentrations are higher. The results of Figure 7 show that high biomass concentrations should be used for small diameter tubes to optimally use the available light, while larger diameters require low biomass concentrations. Areal productivities are lower in tubes with larger diameters of e.g. 0.12 or 0.30 m. Up to 16% higher yearly areal productivities are achievable in tubular PBRs using smaller diameters. In addition, biomass concentrations obtained in large diameter tubes are substantially lower compared to smaller diameter tubes. This has a large effect on water usage and centrifugation costs. However, tubular algae systems with tube diameters of 0.30-0.41 m are used commercially [37, 118]. For vertical tubular PBRs also an optimal tube diameter for yearly areal production exists .

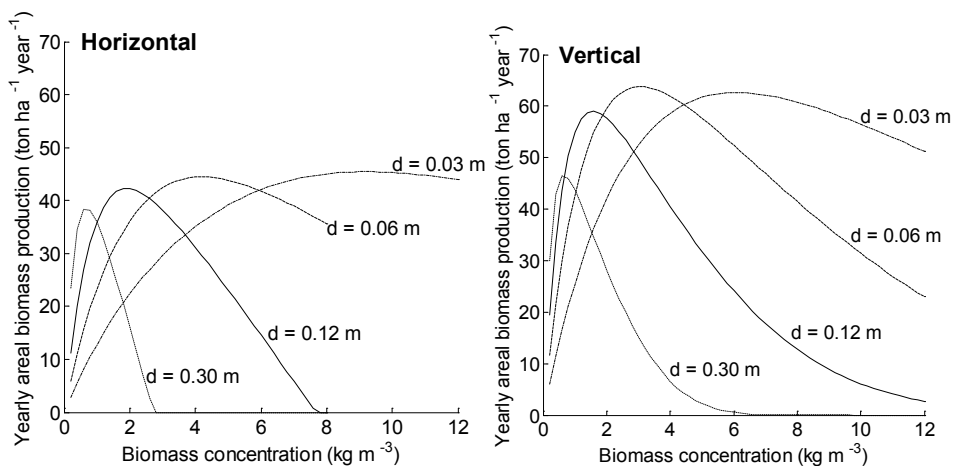


Figure 7. The effect of biomass concentration and tube diameter on yearly areal biomass production ( $\text{ton ha}^{-1} \text{year}^{-1}$ ) for *P. tricornutum* in the Netherlands using horizontal (left) and vertical (right) tubular PBRs. A constant system height of 0.62 m was used for vertical systems. For both systems, the best horizontal distance between tubes is used.

## Materials

Yearly areal biomass production depends on the reflection characteristics of the ground material. The reflectivity of white plastic was used in all previous simulations. Figure 8 illustrates the relative effect of ground reflectivity on predicted areal productivities. As reference the areal productivity of systems without reflection of the ground material is used.

Some ground reflection of light increases the productivity of horizontal tubular PBRs significantly. The increment is similar for the three locations and algae species. Similar trends are visible for vertical tubular PBRs. In the Netherlands, ground reflectivity affects productivity in vertical systems a bit less by than in horizontal tubular PBRs.

In France and Algeria reflected light on average has a higher intensity. Therefore, it contributes more to the internal light profile at these locations resulting in increased production. This positive effect is stronger in vertical systems than in horizontal systems. Light levels at the bottom part of vertical reactor systems are usually low, caused by shading and the canyon effect for diffuse light. Therefore, productivity in vertical tubes at locations with high light intensities is affected more positively by ground reflectivity as a high intensity light is reflected back to the reactor surface.

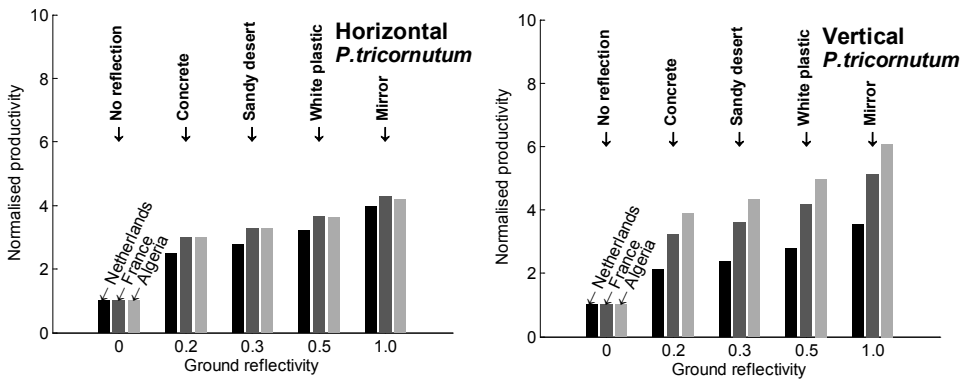


Figure 8. Relative effect of ground material on yearly areal biomass production for horizontal and vertical tubular PBRs. Productivity is normalised to the yearly areal biomass productivity without light reflection from ground material (most left situation in both figures). Tube diameter is 0.06 m, the vertical systems has 9 vertical rows and 0.01 m vertical distance between them. For every point, the best constant horizontal distance and biomass concentration were used.

Some companies are interested in sophisticated tube materials to enhance algae production by reducing reflection of light and increasing tube material transparency. Yearly areal biomass production using various tube materials are shown in Figure 9. The simulation results indicate that characteristics like refractive index and transparency have a minor impact on yearly areal algae productivity. The tube material PMMA results in slightly lower productivities compared to glass and PVC. The refractive indices of glass and PMMA differ similarly to glass and PVC, which does not have a significant effect on productivity. Differences in refractive indices between glass and PVC result in only a small change in biomass production. PMMA is 92% transparent while glass is 100% and obviously, this slightly affects productivity. A perfect material that transmits all the light increases production noticeably. However, still the difference in productivity is less than 10%. The results are similar for other locations and algae species.

Relatively large changes in light intensity in the concentrated algae suspensions are needed to improve yearly areal biomass production in tubular PBRs, as productivity

is a combination of light profile and biomass concentration. In this study, the biomass was already optimised to achieve conditions leading to the best possible productivity. Under such optimised conditions the increase in light intensity by using other tube materials is marginal. Thus, only small improvements in algae production are achieved.

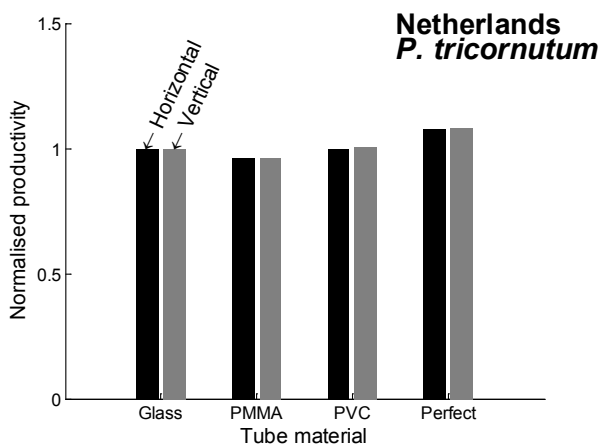


Figure 9. Relative effect of tube materials on yearly areal biomass production using horizontal and vertical tubular PBRs. Results are shown for cultivation of *P. tricornutum* in the Netherlands in 0.06 m diameter tubes. Productivity is normalised to yearly areal biomass production using glass as tube material, which was done separately for horizontal and vertical tubular PBRs. A perfect material transmits all light to the culture volume. Best distance between tubes and best constant biomass concentrations are used.

### Height dependent biomass concentrations

In vertical tubular PBRs, diffuse light levels between horizontal tubes decrease from top to bottom. Lower tubes receive less light and therefore benefits can be obtained by applying a height dependent biomass concentration. Figure 10 shows that yearly areal biomass productivities improve by using for example, two levels of biomass concentration each optimised for the prevailing conditions. The effect is more pronounced for higher reactor systems with 20 vertical rows. The effect is especially important for locations with lower solar angles and lower light intensities like the Netherlands. At such locations, the need to diminish dark zones in the lower part of the system would require a low biomass concentration. However, light cannot be used effectively in the upper part of the reactor system when a single low biomass concentration is used in the entire system. Hence, a low biomass concentration in the lower part and a higher concentration in the upper part result in better light use.

The results in Figure 10 indicate that the best horizontal distance between vertical tubes remains the same when height dependent biomass concentrations are used. Biomass

concentrations can thus be used to improve reactor performance, without changing the reactor design.

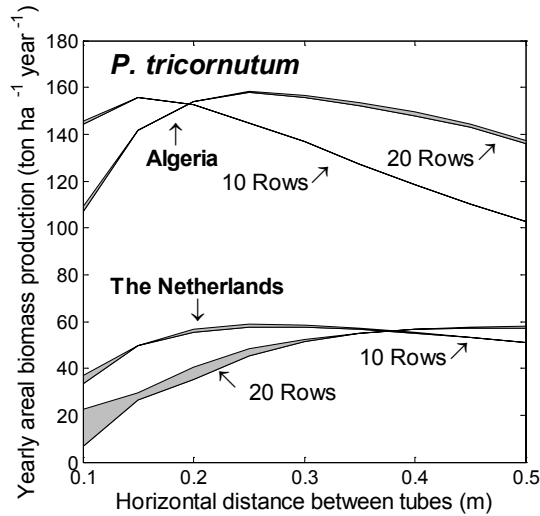


Figure 10. Yearly areal biomass production (ton ha<sup>-1</sup> year<sup>-1</sup>) in vertical systems with 10 and 20 vertical rows, using one (lower lines) or two (upper lines) constant best biomass concentrations. The increase in biomass productivity using two biomass concentrations is indicated in grey. Productivity is given for *P. tricornutum* in the Netherlands and Algeria using a tube diameter of 0.06 m.

## CONCLUSIONS

Experimental data on algae productivity in horizontal and vertical tubular PBRs is limited. In addition, the effect of design variables in large-scale systems has not been studied in detail. Tubular PBR performance depends on the internal light profile, which is influenced by location, reactor configuration (horizontal or vertical), reactor distance, tube diameter, biomass concentration, growth characteristics of algae species and for vertical tubular PBRs, the number of rows and vertical distance. Simulations are therefore a feasible alternative to assess design options and scenarios for photobioreactors. In this work, we present a simulation tool to analyse biomass production in various scenarios. With this tool, horizontal and vertical PBRs are compared using scenario studies. While experimental validation is needed to confirm the details, the comparison of system configurations and location can be considered to be reliable, as the models are based well-documented knowledge of algae parameters and light penetration properties.

High productivities are reached on locations at low latitudes like Algeria. Locations at higher latitudes like France and the Netherlands have lower yearly biomass productivities

and weather conditions affect day-to-day production patterns. Productivities in vertical tubular PBRs are higher than in horizontal systems. The best distance between tubular PBRs depends on location and reactor set-up (horizontal vs. vertical), since light conditions differ. Horizontal tubular PBRs should be placed close to each other, about  $\frac{1}{2}$  to  $\frac{2}{3}$  of the diameter. Vertical tubular PBRs need a larger distance between tubes. We found that vertical tubular PBRs do not need to be higher than nine rows; there is a limit to useful height due to the canyon effect. Each situation requires a specific biomass concentration. Higher biomass concentrations are beneficial in tubes with a small diameter. PBRs with smaller diameters are affected less by deviations from the best biomass concentration. In addition, optimal tube diameters exist and productivity reductions as high as 20% were found in systems with tube diameters that are larger than necessary.

In vertical systems, the top of the reactor receives more light than the bottom part. Some benefits can be obtained by having higher biomass concentrations in the upper tubes than in the lower tubes. Productivity increases when using two different biomass concentrations within one reactor, especially for locations at higher latitudes. Ground reflectivity is an important aspect for large-scale algae cultivation. Light reflecting materials below the reactor system improve reactor performance. Concrete already behaves as a good reflection material. Altering the transparency and reflectivity properties of tube wall material appears to have no significant effect.

Yearly areal productivities with tubular PBRs lie between the productivities for raceway ponds and flat panels. Productivity increases from raceway ponds to horizontal tubular PBRs, to vertical tubular PBRs and flat panels. Productivity in vertical tubular PBRs is similar to that in flat panels for locations at lower latitudes and with high light intensities.

## **ACKNOWLEDGEMENTS**

This work was performed in the cooperation framework of Wetsus, centre of excellence for sustainable water technology ([www.wetsus.nl](http://www.wetsus.nl)). Wetsus is co-funded by the Dutch Ministry of Economic Affairs and Ministry of Infrastructure and Environment, the European Union Regional Development Fund, the Province of Fryslân, and the Northern Netherlands Provinces. The authors like to thank the participants of the research theme Algae for the discussions and their financial support.

## APPENDIX A. LIGHT INPUT OF A TUBULAR PBR

Light falling on the earth's surface consist of direct and diffuse light. Diffuse light is scattered in the atmosphere and by clouds. The amount of direct and diffuse light falling on a tubular PBR depends on the time, ay and location. The direct and diffuse light inputs of the tubular PBRs are calculated separately.

### A.1 Direct light input

The direct light falling on a tubular reactor varies with the solar position. The same model to determine the solar incidence angle is used as in [111]. Figure A.1 shows how the solar incidence angle  $\theta$  ( $^\circ$ ) on a tubular reactor depends on the slope of a point on the reactor wall with respect to the ground surface  $\beta$  ( $^\circ$ ), the orientation  $\gamma$  ( $^\circ$ ) and the solar hour angle  $\omega$  ( $^\circ$ ). The zenith angle  $\theta_z$  ( $^\circ$ ) and complementary solar elevation  $\alpha_v$  ( $^\circ$ ) are also shown.

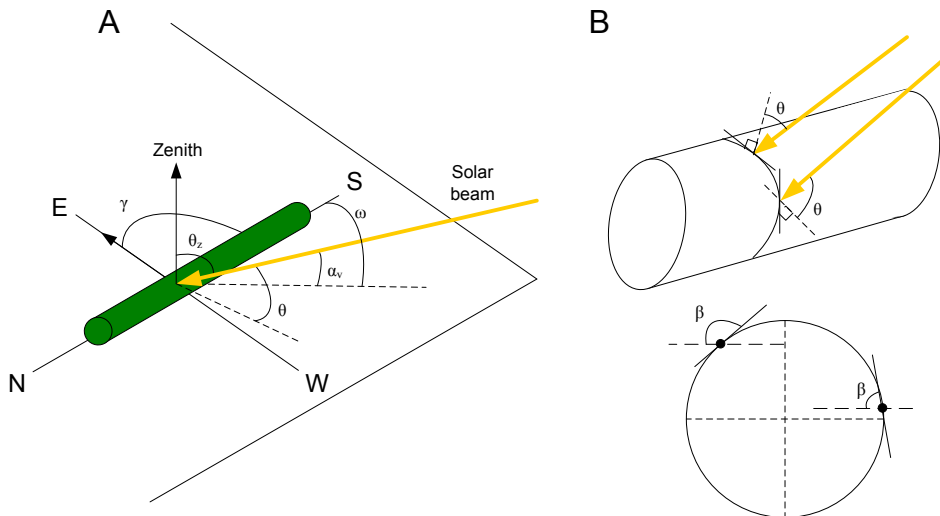


Figure A.1 Various angles are used to describe how light beams fall on the tubular reactor. Figure A illustrates the majority where  $\gamma$  is a reactor characteristic and  $\omega$ ,  $\theta$ ,  $\theta_z$  and  $\alpha_v$  depend on time. Figure B shows how the solar incidence angle  $\theta$  varies with  $\beta$  for every point on the reactor wall.

Angles  $\beta$  and  $\gamma$  are fixed reactor characteristics during time and angle  $\omega$  depends on the solar hour. The orientation of the reactor  $\gamma$  is measured from the normal of the reactor on the horizontal plane to the south. It is positive for a position in the S-E / N-W plane and negative for a position in S-W / N-E. The solar incidence angle at a given point of the tube with slope  $\beta$  is taken to the normal of this point (see Figure A.1B). Hour angle  $\omega$  is also measured to the south and is negative in the morning and positive in the afternoon.

The solar incidence angle  $\theta$ , solar zenith angle  $\theta_z$ , reactor slope  $\beta$  and orientation  $\gamma$  are used to calculate the amount of direct light falling on the tubular reactor at a given point  $I_{direct}$  ( $\text{W m}^{-2}$ ) by [119]:

$$I_{direct}(\beta, t) = I_{direct, horizontal} G_{direct}(\beta, \gamma) \quad (\text{A.1})$$

where  $I_{direct, horizontal}$  ( $\text{W m}^{-2}$ ) is the measured direct light on a horizontal surface and  $G_{direct}$  (-) the geometric factor for direct light, which is calculated as:

$$G_{direct}(\beta, \gamma) = \frac{\cos(\theta(\beta, \gamma))}{\cos(\theta_z)} \quad (\text{A.2})$$

Shading by neighbouring tubes prevents points from receiving direct light as shown in Figure A.2A & B. The shadow height  $h_{shadow}$  (m) is calculated using:

$$h_{shadow} = h - \tau \tan(90 - \theta_z') = h - \tau \tan(\lambda) \quad (\text{A.3})$$

where  $h$  (m) is the total height of the reactor system,  $\tau$  (m) the horizontal distance between the tubes and  $\theta_z'$  ( $^\circ$ ) the projection of the zenith on the plane perpendicular to the reactor. We refer with  $\lambda$  to the complementary of  $\theta_z'$ . The shadow height depends on the number of tubes  $N$  (-), the tube diameter  $d$  (m) and the vertical distance between tubes  $\tau_1$  (m) through the reactor height:

$$h = Nd + (N - 1)\tau_1 \quad (\text{A.4})$$

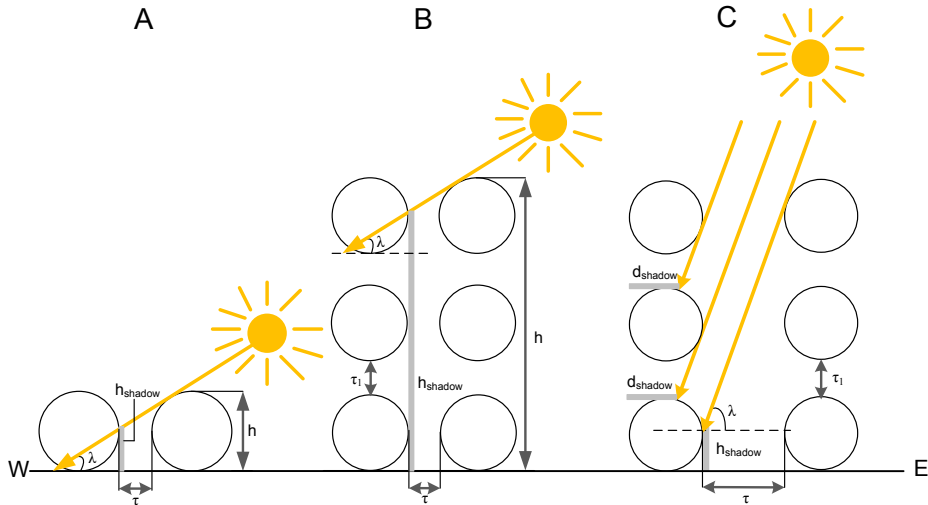


Figure A.2 Illustration of shading on A) horizontal tubular PBRs, B&C) vertical tubular PBRs.

Figure A.2C shows that vertical stacked tubes are also shaded by tubes above them. The shadow depth  $d_{shadow}$  (m) is calculated as:

$$d_{shadow} = d - \left( \frac{(\tau_1 + y_1 + y_2)}{\tan(\lambda)} + \left( \frac{1}{2}d - x_1 \right) \right) \quad (\text{A.5})$$

Line pieces  $x_1$ ,  $y_1$  and  $y_2$  are illustrated in Figure A.3.

The direct light input is removed for all points on the reactor surface that are shaded. Tubes at the border of the algae plant receive different light patterns than the tubes in the middle of the plant. This effect is negligible for large-scale production, so in the simulations all tubes are treated similarly.

## A.2 Diffuse light input

The amount of diffuse light on the tubular reactor  $I_{diffuse}$  ( $\text{W m}^{-2}$ ) is calculated with [119]:

$$I_{diffuse}(\beta, t) = I_{diffuse, horizontal} G_{diffuse}(\beta, h') \quad (\text{A.6})$$

where  $I_{diffuse, horizontal}$  ( $\text{W m}^{-2}$ ) is the measured direct light on a horizontal surface and  $G_{diffuse}$  (-) the geometric factor for diffuse light. All diffuse light is considered isotropic. Diffuse light penetration is obstructed by the so-called ‘‘canyon effect’’ that depends on the distance between two objects and the total height [105]. For vertical reactor systems  $G_{diffuse}$  is a function of the reactor surface angle  $\beta$  and the height  $h'$  (m) measured from half of the highest row and the distance between the tubes:

$$G_{diffuse}(\beta, h') = \frac{1 + \cos(\beta + u(h'))}{2} \quad (\text{A.7})$$

where the sky view angle  $u$  (-) depends on the height  $h'$  and the distance between the tubes [105]:

$$u(h') = \tan^{-1} \left( \frac{h'}{\tau} \right) \quad (\text{A.8})$$

The geometric factor also corrects for diffuse sky light penetration as illustrated in Figure A.4 [see also 105, 111]. The upper half of the top row is not hindered so there the amount of diffuse light only depends on the slope  $\beta$  (situation 1). For all the other points the sky view angle  $u$  has to be included as well (situation 2). Angle  $u$  is approximated using the projection of a point on the vertical line and a slope of  $90^\circ$ . Ground reflected light contributes to the total amount of diffuse light falling on the reactor [119]. The total amount of reflected light  $I_{groundreflected}$  ( $\text{W m}^{-2}$ ) is calculated by:

$$I_{groundreflected}(\beta, t) = G_{groundreflected}(\beta) \left( I_{diffuse}(\beta, t) \cos(\delta_1) + \frac{I_{shadow} - \tau}{\tau} I_{direct}(\beta, t) \right) \quad (\text{A.9})$$

with the geometric factor for ground reflected light  $G_{groundreflected}$  (-), the sky view angle for ground reflection  $\delta_i$  (°) and shadow length  $l_{shadow}$  (m). The geometric factor  $G_{groundreflected}$  is calculated by:

$$G_{groundreflected}(\beta, h) = \rho \frac{1 - \cos(\beta + u(h))}{2} \quad (A.10)$$

using the reflectivity of the ground  $\rho$  (-). The sky view angle  $u$  is a function of height  $h$  (m) measured from bottom and the distance between the tubes  $\tau$ :

$$u(h) = \tan^{-1}\left(\frac{h}{\tau}\right) \quad (A.11)$$

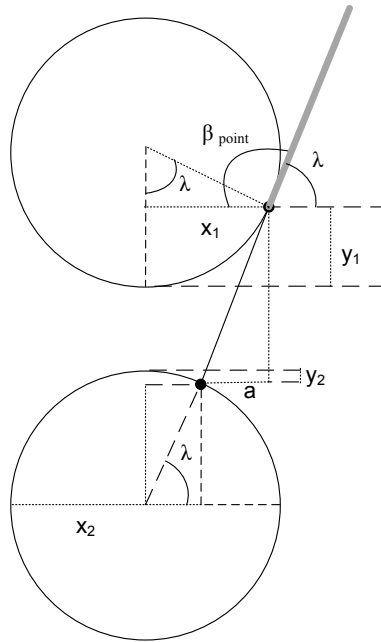


Figure A.3 Sketch of different line pieces used to calculate vertical shadow depth  $d_{shadow}$ .

Angle  $\delta_i$  in equation A.9 is illustrated in Figure A.4 and calculated as:

$$\delta_i = \tan^{-1}\left(\frac{h - 0.5d}{0.5\tau}\right) \quad (A.12)$$

The shadow length  $l_{shadow}$  of equation A.9 is calculated by:

$$l_{shadow} = \frac{h}{\tan(\lambda)} \quad (A.13)$$

### A.3 Local light gradient in reactor volume

Not all light that falls on the reactor surface reaches the algae inside the tube. Losses occur due to reflection of different interfaces: from air to tube material and from tube material to algae solution. The amount of reflected light depends on the difference in refractive index of two interfaces. The angle of refracted light to the normal is calculated with Snell's law [see 111]. Reflection of direct light occurs in one direction. For diffuse light, an angle of  $60^\circ$  is taken as angle of incidence [103]. The amount of reflection by the tube follows from the Fresnel equations [see 111]. In addition, the tube material can absorb light. The total light intensity is used to calculate the light gradient in the reactor volume with Lambert-Beer's law. The light path is taken perpendicular to the reactor wall for each point.

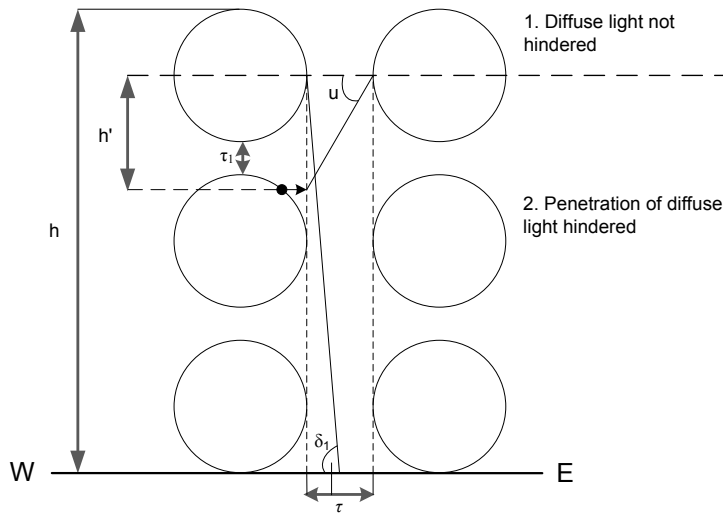


Figure A.4 Penetration of diffuse light depends on the horizontal distance between tubes  $\tau$  and height  $h'$ .

## APPENDIX B. MODEL SIMULATIONS

Mathworks® MATLAB is used to perform the model calculations. The simulations are based on a grid with equal areas and twelve disk-shaped segments from outside to inside.

Table B1. Algae specific parameter values.

Parameter	<i>T. pseudonana</i>	<i>P. tricornutum</i>	Reference
Absorption coefficient (m <sup>2</sup> kg <sup>-1</sup> )	269 <sup>#</sup>	75 <sup>*</sup>	*[47] #[107]
Functional cross-section photosynthetic apparatus (g C mol <sup>-1</sup> photons m <sup>2</sup> g <sup>-1</sup> Chl <i>a</i> )	2	2	[42]
Maximum chlorophyll <i>a</i> and carbon ratio in the cell (g <sup>1</sup> Chl <i>a</i> g <sup>-1</sup> C)	0.08	0.08	[42]
Maximum specific growth rate (day <sup>-1</sup> )	3.29	1.40	[42]
Respiration rate (day <sup>-1</sup> )	0.05	0.05	[42]

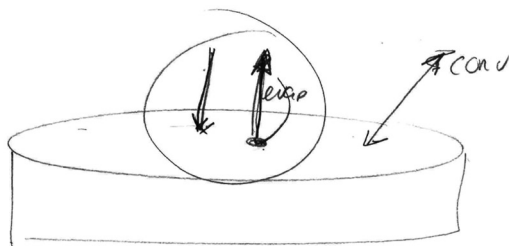
Chl *a* = chlorophyll *a*

# SCENARIO EVALUATION OF OPEN POND MICROALGAE PRODUCTION

$$N_1 = k_1 A (C_1 - \frac{C_2}{m})$$

$$1000 \frac{g}{hour} = \frac{k_1 A}{\zeta} (C_1 - \frac{C_2}{m})$$

$$\frac{1}{P_g}$$



THIS CHAPTER IS PUBLISHED AS:

P.M. SLEGGERS, M.B. LÖSING, R.H. WIJFFELS, G. VAN STRATEN, A.J.B. VAN BOXTEL  
 SCENARIO EVALUATION OF OPEN POND MICROALGAE PRODUCTION  
 ALGAL RESEARCH (2013), 2(4): 258-368

## **ABSTRACT**

To evaluate microalgae production in large-scale open ponds under different climatologic conditions, a model-based framework is used to study the effect of light conditions, water temperature and reactor design on trends in algae productivity. Scenario analyses have been done for two algae species using measured weather data of the Netherlands and Algeria. The effects of temperature control, photo-inhibition and employing monthly or yearly fixed biomass concentrations are estimated by a sensitivity analysis. The calculation-based results show that climate conditions such as solar irradiation and temperature dynamics play an important role in open raceway ponds. In moderate climate zones low and high temperatures over a season suppress growth. At high latitudes this effect is important as light levels vary much during the day and between seasons. Optimal biomass concentrations in ponds depend on location, pond depth and algae species. Pond design, location and algae species interact and productivity cannot be based solely on general or assumed efficiencies. It is essential to select algae species that have a suitable growth rate, light absorption coefficient and the ability to grow over a broad temperature range. The presented approach gives a framework to validate specific cultivation systems.

*Keywords: open ponds, scenario analysis, microalgae, production estimates, model, decision variables*

## INTRODUCTION

Currently, microalgae gain a lot of attention for their potential to produce high value products like pigments, omega-3 fatty acids and proteins, and their ability to produce lipids for the production of biofuels [13]. Microalgae employed for these applications are cultivated in a variety of cultivation systems. Open raceway ponds are the most basic cultivation systems and are used for the production of algae as food supplement and for pigments. Biomass productivities in raceway ponds are low, but are compensated by high product prices and low construction and operating costs [25].

The use of microalgae for biofuel production in open pond systems has recently been assessed [26, 70, 78, 79, 94, 120]. These studies concern algae cultivation in connection with a series of processing steps to convert lipids into biofuel. General algae productivities are used to estimate algae productivity and although open ponds are straightforward systems there is a wide variation in the employed estimates. Some life cycle assessments (LCA) assume biomass productions as high as 110 ton ha<sup>-1</sup> year<sup>-1</sup> for open ponds [70, 79, 120], and even higher productivities have been mentioned before [94]. Borowitzka [20] has reported an average yearly production of 91 ton ha<sup>-1</sup> year<sup>-1</sup> in Australia, which seems to be close to the upper production limit. In contrast to these high estimates, Jorquera *et al* [78] assume more modest productivities of 39 ton ha<sup>-1</sup> year<sup>-1</sup>. This estimate is close to yearly areal productivities reported for experimental sites at higher latitudes. For example, productivities of 30 ton ha<sup>-1</sup> year<sup>-1</sup> have been reported for experimental ponds in Spain [35] and an average best productivity of 20 ton ha<sup>-1</sup> year<sup>-1</sup> for Italy [34]. According to Tredici [121] long-term productivities in commercial raceway ponds rarely exceed 47 ton ha<sup>-1</sup> year<sup>-1</sup>. In contrast to the other LCA studies, Wigmosta *et al* derive potential local microalgae biodiesel productivities from fixed photosynthetic efficiencies (PE) and a factor to account for temperature effects [26]. However, such fixed PEs are not sufficient to account for the effect of location, algae species and other growth conditions [122]. It is obvious that the actual values have an important influence on the interpretation of the feasibility of microalgae cultivation systems [81, 123]. As shown by Slegers *et al* [111] the productivity of algae cultivation systems is strongly linked to the location of production, the layout of the production system, algae species and weather conditions. For example, a flat panel system in Algeria has different production yields than the same system in the Netherlands due to differences in solar radiation, latitude and day length. Extrapolation of available experimental and production data to other situations for LCAs is thus not straightforward, which may be one of the reasons of the wide variety of numbers found in literature.

Model simulations are a good approach to estimate the productivities to be expected under a range of conditions. Pond models are mostly available in waste water treatment, such as CO<sub>2</sub> modelling of algae and bacteria co-cultures under simulated diurnal cycles [124]. In microalgae research several empirical models exist, such as the empirically derived model for the effect of light, temperature, pH and oxygen on *Spirulina* production in Spain [35]. Also the penetration of various wavelengths of light in algae ponds has been studied in detail [125]. Algae productivities and water temperatures in ponds have been compared by James and Boriah [126], but unfortunately comparison with literature data is missing. Water temperature has been studied widely and also specifically for raceway ponds [127]. Hydrodynamics play a role for the design of pond dimensions [128] and mixing velocities [126]. Models on photo-adaptation and photo-inhibition effects including the associated timescales are very limited [129].

Models that derive algae productivities at a specific location, using various types of reactor design and algae species will provide a common basis for LCA studies. It enables a consistent comparison when studying different cases. Therefore, we have combined existing models on algae growth kinetics, light conditions and transport phenomena to predict productivities using various pond depths, weather conditions and algae species. The effect of light and temperature is analysed on estimated productivities, prior to validation. This work is part of a series of studies for modelbased comparison of the expected productivity of various system designs at various locations. The framework is intended as a guideline for the assessment of the feasibility of alternate choices in future production scenarios, which is possible after model validation.

## **METHOD**

Open pond cultivation of algae is mostly performed in so-called raceway ponds. Algae grow under daily light conditions and during growth CO<sub>2</sub> is taken up while produced oxygen is released from the pond. Additional CO<sub>2</sub> is injected at relevant positions in the system to enhance growth. Although algae ponds do not need arable land, they do require large amounts of water when cultivated on a commercial scale. Therefore, using marine algae species and salt water is beneficial and more sustainable. A paddle wheel moves the water in the system to obtain sufficient mixing in the system. The mixing effect is important and if well-designed it is effective for the whole “raceway cycle” [128]. Direct and diffuse light penetrate the liquid. Algae absorb the light and therefore, the light intensity decreases towards the bottom of the raceway pond.

## **Calculation overview**

This work compares algae productivity in raceway ponds under a range of decision

variables such as location, algae species and system design using a modelbased framework. Open pond productivity in various scenarios is considered. The open pond calculations consist of three elements: calculating light input, calculating water temperature and assessing algae productivity as function of light and temperature. The calculation structure is given in Figure 1. The prediction of algae productivities is based on measured weather conditions, i.e. direct and diffuse light, temperature, wind velocity, relative humidity and air pressure.

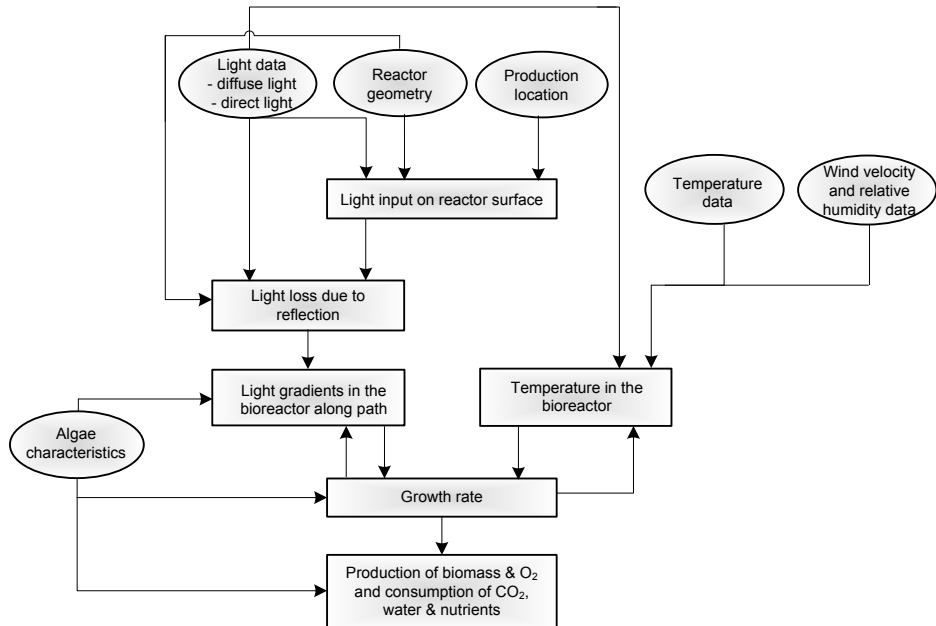


Figure 1. Calculation scheme for evaluating algae productivity in open raceway ponds. □ = Calculation, ○ = Model inputs like data and design parameters.

### Determining light input of ponds

The light model of Slegers *et al* [111] for flat panel photobioreactors is used as basis and was adapted to the conditions and design for raceway ponds. Thereby, the effect of shading on the light input due to objects in the surroundings was excluded. The first step in the procedure is to calculate the amount of received sunlight on the horizontal water surface [111]. Local solar irradiation measurements are used to include a dynamic light pattern during the day and the year. The loss of light by reflection at the water surface is taken into account as function of sun elevation and season. The light gradient due to extinction and absorption of light by the algae is described by the law of Lambert-Beer and results in local light intensities. The light path is taken perpendicular to the water surface. This is justified as algae solutions are strongly scattering media with particles

in an order of magnitude larger than the wave length, meaning that scattered light is mainly reflected [114].

### Calculating raceway pond water temperature

The raceway pond energy balance was applied to determine the dynamic temperature of the pond water. A recently developed approach uses dimensionless numbers for heat transfer and evaporation phenomena [127], while the classical approach is based on well-established empirical relationships. In this work the last approach is used. The energy flows due to solar irradiation, light absorption by algae, convection, evaporation, condensation, conduction and longwave radiation are considered (see Figure 2). Changes in water volume due to evaporation or precipitation are assumed to be balanced by an overflow/inflow system that does not affect the energy balance. The system is considered to be well-mixed with a constant volume and a flat and opaque water surface. The solar irradiance input is derived from weather data and reflected light is removed from the energy flow. Longwave radiation from both pond and air are calculated using the Stefan-Boltzmann expression [103]. Estimation of evaporative flows from saline water bodies is not straightforward [130] and detailed information on the most appropriate method for raceway ponds is lacking [127]. Evaporation rates are calculated from the heat exchange coefficient introduced by McMillan [131]. Convection is related to evaporation and follows from the Bowen relation [132]. Conduction between the pond and soil is based on Fourier's law. The soil is considered as an infinite source for heat transfer as a first approximation. Further explanation and an overview of the used equations for the energy balance can be found in Appendix A.

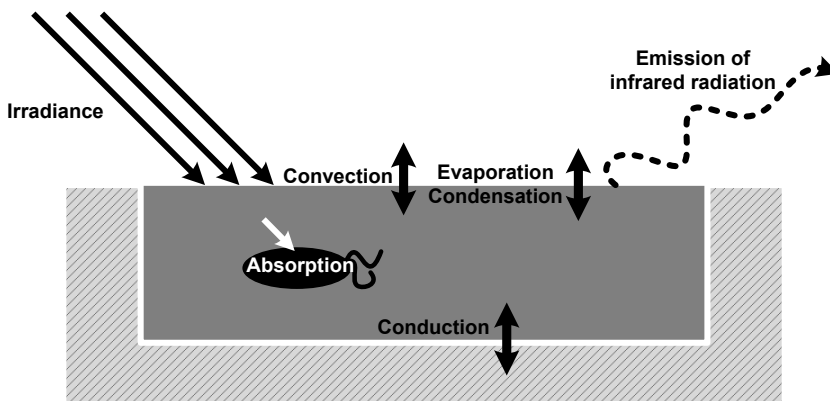


Figure 2. Overview of the energy fluxes in outdoor raceway ponds. The arrows indicate whether the energy fluxes enter and/or leave the water volume of the pond.

### Estimating algae growth in raceway ponds

The growth model as given by Geider *et al* [42] and used in Slegers *et al* [111] is used to predict algae growth as function of light. The growth model enables to estimate algae growth under dynamic light conditions, which are common in all algae systems under outdoor conditions. This growth model includes photo-adaptation and is in this work extended to include the effect of temperature on growth using a multiplicative reduction factor (see Appendix B). Steady state conditions are applied for growth and a constant biomass concentration is employed. Hence, it is assumed that the pond is operated in “turbidostat mode”. The presented results are based on a fixed biomass concentration yielding the highest productivity during the year, the so-called “best” biomass concentration.

Photosynthetic efficiencies (%) are determined using:

$$PE = \frac{h_{comb} \int Y_{areal}(t) dt}{A \int I_{surface}(t) dt} \cdot 100\% \quad (1)$$

with  $h_{comb}$  (J kg<sup>-1</sup> algae) the combustion energy of algae biomass,  $Y_{areal}$  (kg algae ha<sup>-1</sup> s<sup>-1</sup>) areal biomass production rate which is integrated for a full year,  $A$  (m<sup>2</sup>) size of a hectare and  $I_{surface}$  (J m<sup>-2</sup> s<sup>-1</sup>) total light falling on the pond which is also integrated for a year.

### Input data

The framework has been applied to various scenarios for location, i.e. the Netherlands and Algeria, algae species, i.e. *Thalassiosira pseudonana* and *Phaeodactylum tricornutum*, and pond design, i.e. pond depth, algae biomass concentration and control of water temperature. Weather data from the World Radiation Monitoring Centre (WRMC) are used for direct and diffuse light, air temperature, relative humidity and air pressure data [95, 96, 133]. For Algeria the WRMC also supplied data on wind velocity and dew point temperature. Wind data for the Netherlands are obtained from the Cabauw Experimental Site Atmospheric Research [134]. Soil temperature data at 50 cm depth for the Netherlands are obtained from the Coordinated energy and water cycle observation project [135]. Since soil temperature data are not measured in Algeria, they were considered to be equal to the soil temperature at 30 cm depth in Israel. Data for Israel are obtained from the Ben Gurion University of the Negev [136]. The parameter values for energy balance and algae growth are given in Appendix C.

## RESULTS

### Climatologic effects on water temperature

The changes in water temperature using 30 cm deep raceway ponds for the Netherlands and Algeria are shown in Figure 3. Each line represents the pond temperature during a day, which is indicated on the vertical axis with the colour map. Some lines partly

overlap and as a result wider bands occur. The water temperature in the Netherlands clearly shows a strong trend with the seasons. In winter months the daily average water temperature is around 0°C. Temperatures below the freezing point are possible as salt water is used, which is continuously moved by the paddlewheels in the raceway pond. In summer the temperature varies between 12°C and 30°C. The high water temperatures during the day are reduced again at night time. For Algeria the water temperature shows a more constant pattern during the year. Water temperatures lay around 5-10°C during night and during the day around 20°C.

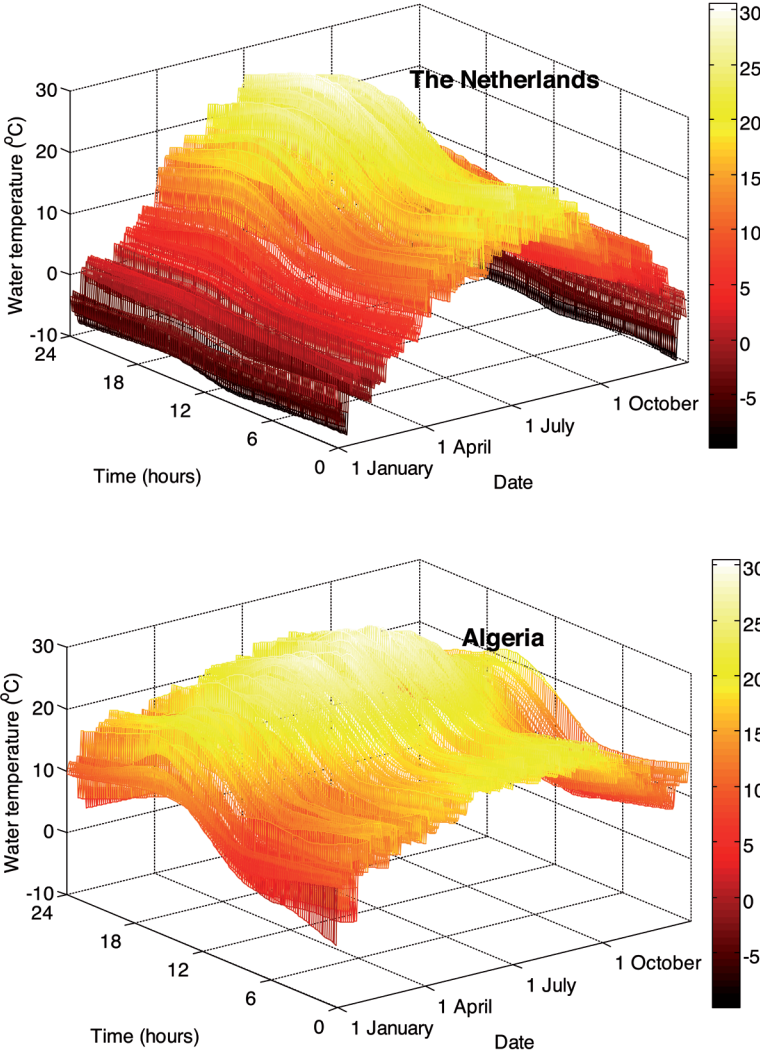


Figure 3. Water temperature in 30 cm deep raceway ponds during the year for the Netherlands and Algeria.

Figure 4 shows the heat flows during a summer day. Sunlight, evaporation and convection are the main contributors to the water temperature in summer. From the figures we learn that the overall longwave radiation flow is small. Similarly, dynamics of the conduction flow will not have a significant effect since it is very low for both locations. These results are comparable to those presented by Béchet *et al* [127]. Additional scenario calculations show that in winter, in the Netherlands the overall energy flow is dominated by longwave radiation and by solar radiation during the light hours. Longwave radiation has a relative high contribution during periods with low light, as the other flows except solar radiation are minimal. Estimated evaporation rates for the Netherlands are similar to those reported by Jacobs *et al* [137].

### Location-specific algae productivity

The effect of location and algae species on biomass production is illustrated in Figure 5. The patterns for daily biomass production during one year in the Netherlands and in Algeria are given for the algae species *T. pseudonana* and *P. tricornutum* assuming a stable monoculture. For both locations a pond depth of 30 cm was applied and the best constant turbidostat biomass concentration was applied during the year, i.e.  $C_x=0.1 \text{ kg m}^{-3}$  for *T. pseudonana* and  $C_x=0.3 \text{ kg m}^{-3}$  for *P. tricornutum*.

The production pattern is a full combination of local light, water temperature and the other meteorological conditions, where the water temperature is dynamic and thus uncontrolled. The results in Figure 5 show that biomass production depends strongly on the local climate conditions which are influenced by latitude, solar irradiation, time of the year and day length. This results in an almost constant production pattern over the year in Algeria and a bell-shaped pattern for the Netherlands. Biomass production in the Netherlands is negative during winter as dark respiration exceeds biomass growth, which is caused by the low ambient and water temperatures, low solar radiation level and short day lengths (see also Figure 3). The effect of very low and negative water temperatures on algae growth is further discussed in the next section. In practice, raceway systems will only be operated during the growing season when positive productivities prevail. The results illustrate what would happen with the pond temperature and algae productivity if a system would run a full year.

The estimated yearly production values in raceway ponds for the Netherlands and Algeria for the two algae species are listed in Table 1. Full year productivities are given, which include also simulated negative productivities. Exclusion of these will result in higher productivities for the Netherlands; for *P. tricornutum* a productivity of  $42.9 \text{ ton ha}^{-1} \text{ year}^{-1}$  would be predicted and for *T. pseudonana*  $9.82 \text{ ton ha}^{-1} \text{ year}^{-1}$ .

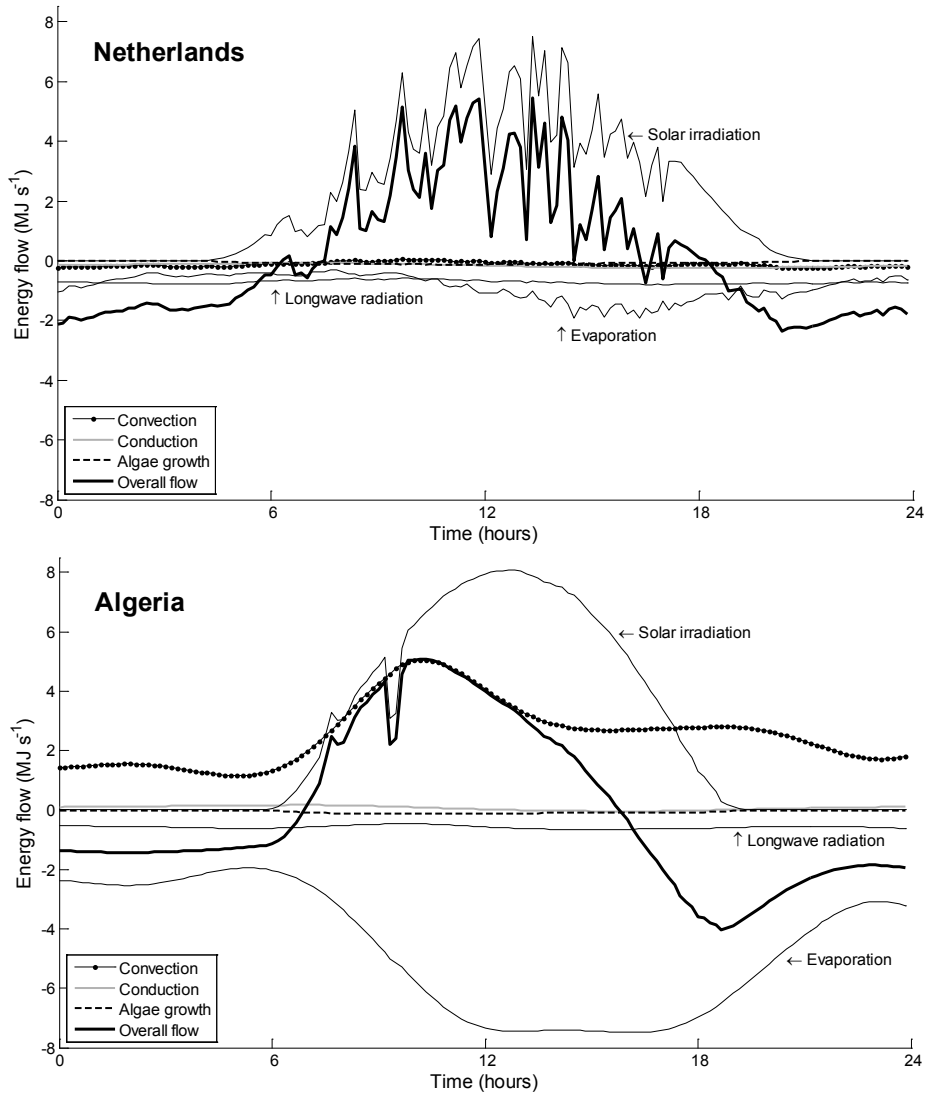


Figure 4. Energy flows ( $J s^{-1}$ ) for the Netherlands and Algeria on a typical summer day in a 30 cm deep raceway pond.

Table 1. Estimated yearly biomass production ( $ton ha^{-1} year^{-1}$ ) for the Netherlands and Algeria based on weather data of 2009. The photosynthetic efficiencies are given between brackets.

	<i>T. pseudonana</i>	<i>P. tricornutum</i>
The Netherlands	8.00 (0.40%)	41.5 (2.09%)
Algeria	14.9 (0.36%)	63.7 (1.56%)

For both algae species, the yearly areal biomass production in Algeria is higher than in the Netherlands. Although *T. pseudonana* grows faster than *P. tricornutum* higher productivities can be achieved with *P. tricornutum* because of its significant lower absorption coefficient. The photosynthetic efficiencies (PE) in the given reactor design vary from  $\pm 0.3\%$  to  $2.1\%$  depending on both species and locations. The characteristics of *T. pseudonana* lead to low PEs, while the upper limit for raceway ponds is almost reached by *P. tricornutum* at both locations. In Algeria there is an excess of light that cannot be converted to biomass, therefore the PE is lower than that for the Netherlands. The different climatic conditions and characteristics of algae species make it difficult to compare the success of cultivation based only on PE.

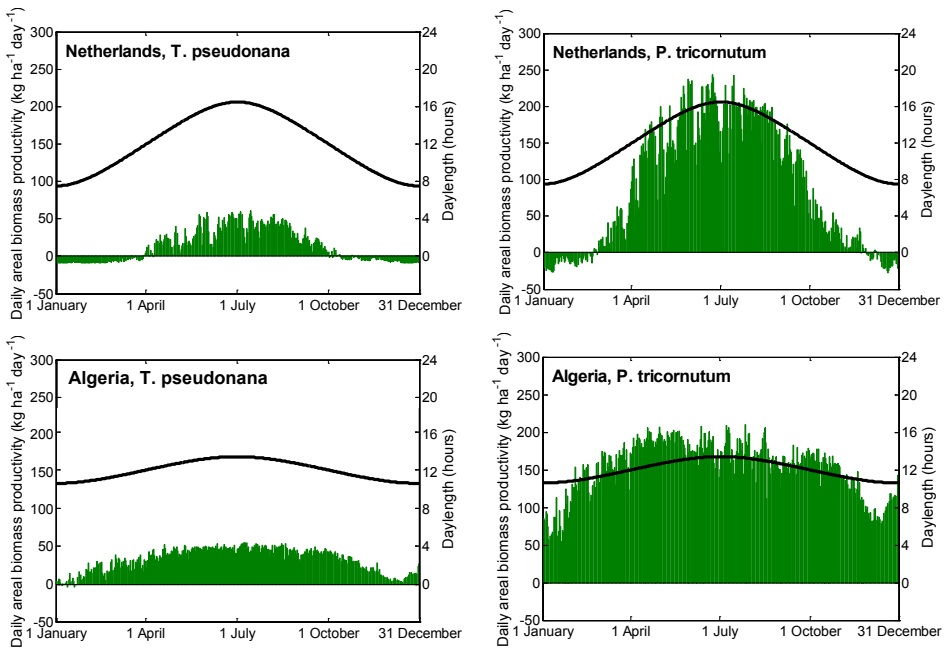


Figure 5. Daily areal biomass production ( $\text{kg ha}^{-1} \text{day}^{-1}$ ) in a 30 cm deep raceway pond as a function of dynamic light and temperature regime, using a constant biomass concentration during the year. The bar plots give the daily areal biomass production. The bold lines show the day length in hours (right y-axes).

### Temperature effect on algae growth

Low water temperatures significantly affect growth. In Figure 6 an analysis of the effect of temperature on growth of *P. tricornutum* is given. It shows the temperature factor (equation B.6) as function of temperature. At the optimal growth temperature algae growth is solely influenced by sunlight, so the temperature function is equal to one. Below and above the optimal growth temperature growth is negatively influenced

by the water temperature. According to the model growth is possible at negative water temperatures (see Figure 6). This is caused by the parameter estimation, which is based on measurements done between 5 and 30 °C. The equation allows growth below 5°C, however it is unlikely that these algae grow substantially around 0°C [138, 139]. So the model slightly overestimates production at these temperatures. For the Netherlands using *P. tricornutum* the simulated overall yearly productivity would reduce 7% if the specific growth rate is set to zero below 5°C and 2% if set to zero below 0°C. Similar effects are calculated for *T. pseudonana*. However, in practice raceway ponds are only operated during periods with a positive production, so not during winter.

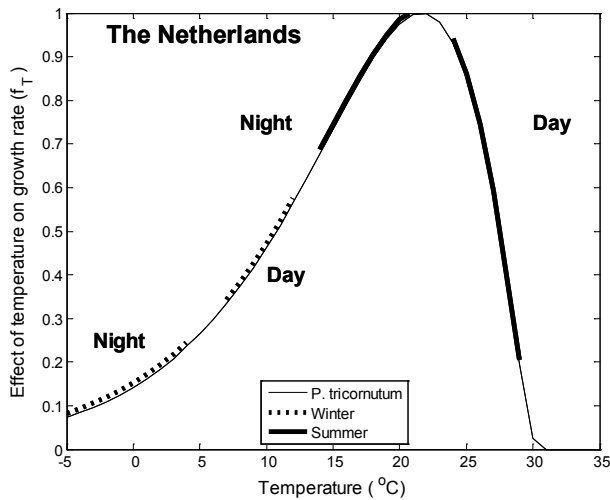


Figure 6. Effect of temperature on the specific growth rate of *P. tricornutum*. If the temperature function is 0 no growth is possible, independent of sunlight intensity. If the temperature function is 1 growth is only influenced by sunlight conditions. The dotted lines indicate the temperature range that algae experience in winter in the Netherlands, the bold solid lines the temperature ranges for summer.

Figure 6 shows that in the Netherlands growth of *P. tricornutum* is reduced to 35-55% of the potential growth. In summer maximum specific growth rates are possible during the day, but the water temperature in the Netherlands often exceeds the optimal growth temperature. This affects production negatively and for this algae species the full production potential cannot be reached. In Algeria the water temperatures are more constant during the year and at this location algae productivity is affected less by the temperature. During the day temperatures are close to the optimal growth temperature of *P. tricornutum*, while at night temperatures are low therefore reducing respiration.

## Effect of pond design

The design and operational conditions of the raceway pond also play an important role in productivity. The effect of biomass concentration and pond depth on yearly areal productivity in Algeria is shown in Figure 7. It is important to operate using the best biomass concentration to avoid loss of light or loss of biomass in the dark zone of the pond. Below the optimal biomass concentrations excess sunlight energy cannot be employed for growth, while self-shading of algae as a consequence of too high biomass concentrations results in enhanced cellular respiration. Especially deep ponds are sensitive to this decrease in productivity as is illustrated in Figure 7. This pattern is similar for the Netherlands. So the best pond design depends on location, algae species and thresholds for culture stability.

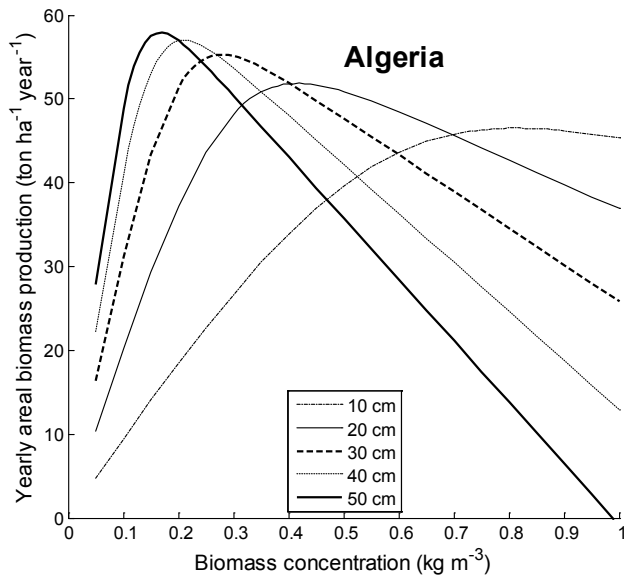


Figure 7. Yearly areal biomass production ( $\text{ton ha}^{-1} \text{year}^{-1}$ ) using *P. tricornutum* as a function of biomass concentration ( $\text{kg m}^{-3}$ ) and pond depth (cm).

Pond depth also affects the maximum yearly areal production. For the Netherlands and Algeria the use of deeper ponds results in high productivities. The water temperatures in deeper ponds are beneficial for algae growth compared to the more dynamic water temperatures. This is especially apparent in Algeria, where yearly areal production is significantly higher in deeper ponds, e.g. of 50 cm. However, for other locations and climate conditions other pond depths will be optimal. For example, the effect is less significant in the Netherlands compared to Algeria. The water temperatures are beneficial in deeper ponds as the water serves as a temperature buffer. Figure 8

illustrates the buffering effect of pond depth on the pond temperature on a summer day. The temperature variations in a 10 cm deep pond are approximately two times higher than a 50 cm deep pond. In these deeper systems low biomass concentrations have to be applied to achieve higher productivities. The downside is that this is accompanied by increased energy costs that are necessary for harvesting the algae cells from the very dilute solution.

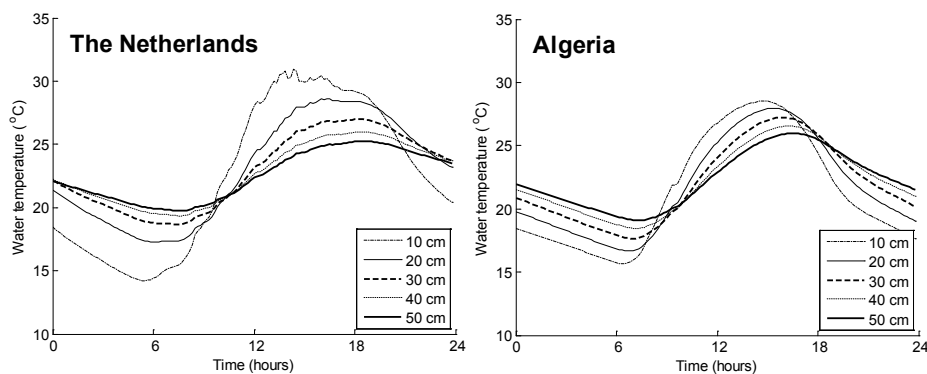


Figure 8. The variation in water temperature during a summer day.

## DISCUSSION

The increasing interest in algae cultivation and subsequent feasibility and LCA studies demand for a simulation framework that analyses open pond productivity at different locations using various production scenarios. As a first step, a model to predict raceway pond productivity under a range of decision variables was developed. The difference in production patterns for the two locations with different climatic conditions and the effect of species characteristics and design variables showed that algae productivities cannot simply be extrapolated to different production circumstances. The model is capable of including these characteristics and provides a suitable basis to include the effect of location and species in techno-economic analyses and LCAs. The results are used to compare different systems using the same set of assumptions. Raceway ponds have the lowest yearly areal productivity compared to horizontal tubular photobioreactors (PBR), vertically stacked horizontal tubular PBRs and flat panel PBRs (Table 2). In any of these systems it is important to consider algae species, light angles and light intensities of a location [see also 122].

### Comparison with experimental data

The production values based on an optimal constant biomass concentration and weather data of 2009 are of the same order of magnitude as experimental productivities reported

in literature. It has to be noticed that the assumptions behind literature values may not fully comply with the assumptions made in the current study, thus making a direct comparison difficult. Average productivities in open ponds of 20 ton ha<sup>-1</sup> year<sup>-1</sup> and 30 ton ha<sup>-1</sup> year<sup>-1</sup> have been found with other algae species in respectively Italy and Spain [34, 35]. Cultivation of *P. tricornutum* in England using 0.4 m deep tanks resulted in an average productivity around 25 ton ha<sup>-1</sup> year<sup>-1</sup> [32], and is comparable to the predicted productivity in the Netherlands using the same species. A productivity of around 60 ton ha<sup>-1</sup> year<sup>-1</sup> has been achieved with *P. tricornutum* in California [31], which has a similar latitude and climate as Algeria. The model result of 63.7 ton ha<sup>-1</sup> year<sup>-1</sup> is thus also in line with the reported productivity.

Table 2. Overview of estimated yearly areal biomass productivities (ton ha<sup>-1</sup> year<sup>-1</sup>) for *P. tricornutum* in raceway ponds, horizontal and vertically stacked horizontal tubes, “vertical tubes” [122] and flat panel PBRs [111].

	Raceway ponds	Horizontal tubes	Vertical tubes	Flat panels
Netherlands	41.5	46.3	62.8	120
France	-	71.2	94.8	129
Algeria	63.7	96.8	155	158

### Considering other operating strategies

While the current analysis is considered to be sufficient for comparative studies of various algae production scenarios, sensitivity analysis and model validation are two further steps to be taken to assess the uncertainty range in the current projections of algae production. As an example, a sensitivity analysis on temperature control is given here. The difference in daily areal biomass production based on a controlled water temperature and uncontrolled dynamic water temperature are shown for the Netherlands in Figure 9. The best yearly constant biomass concentration is used, i.e.  $C_x = 0.3$  kg m<sup>-3</sup> for both *controlled* and *uncontrolled*.

In the winter season biomass production is low or negative for the uncontrolled dynamic water temperature at low light levels (see Figure 6). Biomass production improves when the water temperature is controlled constantly to the optimal growth temperature (see Table C.2). The relative effect of temperature control on yearly areal biomass production is shown in Table 3. Especially for the Netherlands the increase in productivity is accompanied by higher costs for temperature control, i.e. heating in winter and cooling in summer (see also Figure 3).

The control of biomass concentration to one fixed value per year in turbidostat operation may have a significant effect on the productivity. The overall ‘best’ biomass

concentration is a compromise between the preference for low biomass concentration during periods with low light levels (winter) and for higher biomass concentrations during periods with high light intensities (summer). Therefore, yearly areal biomass productivities with monthly best biomass concentrations are estimated (Table 3). The effect of this operation strategy is marginal. In Algeria the light pattern is fairly constant during the year and monthly best biomass concentrations are comparable to the yearly best biomass concentration. In the Netherlands monthly biomass concentrations are low between November and February. The values indicate that cultivation in the pond is not feasible during these months. Reduced productivities during these months are balanced by using higher biomass concentrations resulting in elevated productivities in summer, compared to the standard case with a yearly fixed biomass concentration. However, overall the effect is marginal as ponds are deep and dark zones prevail.

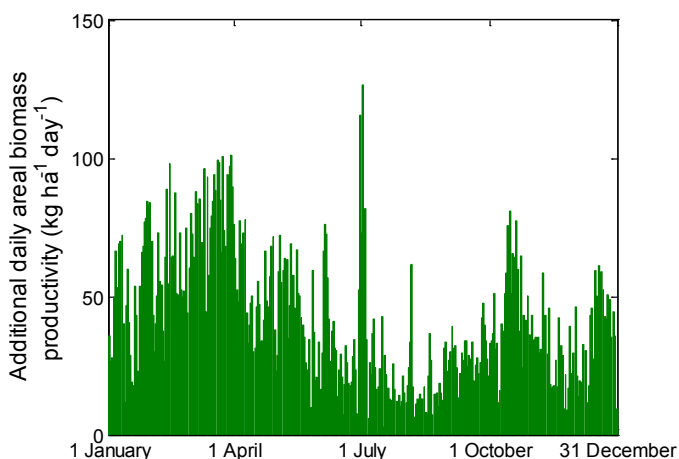


Figure 9. Additional daily areal biomass production ( $\text{kg ha}^{-1} \text{ day}^{-1}$ ) during one year for *P. tricornutum* in the Netherlands for controlled water temperature equal to the optimal growth temperature of *P. tricornutum*.

Table 3. Relative effect of applying temperature control, varying biomass concentrations per month and including mimicked photo-inhibition. The yearly areal biomass productivities ( $\text{ton ha}^{-1} \text{ year}^{-1}$ ) of the standard location-specific simulations are used as a reference. The ranges of monthly best biomass concentrations ( $\text{kg m}^{-3}$ ) are given between brackets.

	Standard	Temperature controlled	Monthly biomass concentration	Growth with mimicked photo-inhibition
NL, <i>T. pseudonana</i>	1	2.166	1.043 (0-0.08)	0.902
NL, <i>P. tricornutum</i>	1	1.559	1.048 (0-0.28)	0.930
AL, <i>T. pseudonana</i>	1	1.478	1.003 (0.07-0.08)	0.877
AL, <i>P. tricornutum</i>	1	1.236	1.001 (0.26-0.30)	0.880

## Reflection on algae growth characteristics

In the standard simulations the effects of light and temperature on growth were considered and included photo-acclimation. However, photo-inhibition effects, i.e. decrease of productivity at high light intensities due to decay of the photosynthetic apparatus, were not quantified for these algae species. Experimental work is needed to assess the exact magnitude of this effect [129]. The effect of photo-inhibition in raceway ponds is not expected to be large as algae on average do not experience high light intensities for a long time during their travel through the pond. The possible effect of photo-inhibition on our results was evaluated in a sensitivity analysis, using equation B.7 to mimic photo-inhibition with data from [140-142]. Growth curves for *P. tricornutum* and *T. pseudonana* including photo-inhibition effects are shown in Figure 10. The results in Table 3 show that including the assumed pattern for photo-inhibition reduces the estimated yearly areal productivity by 7-12%. The effect is algae specie and location dependent. Productivity in Algeria is affected more as it is characterised by higher light intensities.

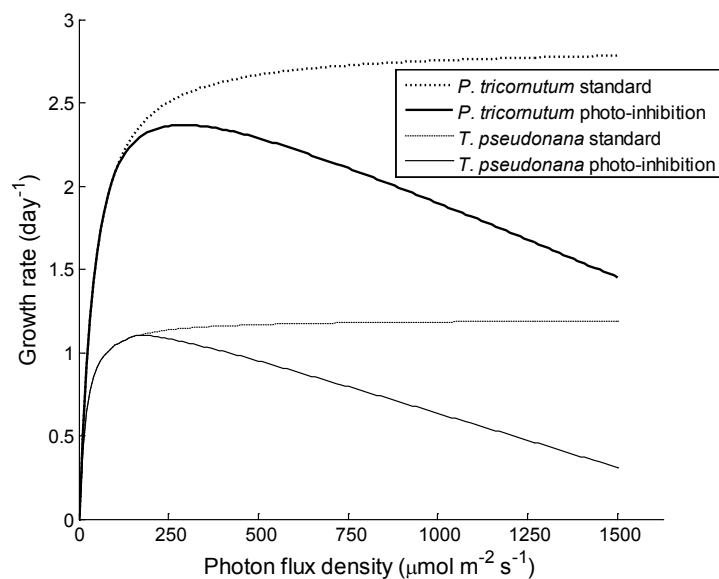


Figure 10. Estimated specific growth rates ( $\text{day}^{-1}$ ) with mimicked and without photo-inhibition.

In addition, one of the assumptions in the growth model is that the chlorophyll *a*:carbon ratio is changing instantaneously with the changing light conditions [42]. We expect that the chlorophyll *a* and carbon content do not change at such fast rates and the exact ratio will depend on the light intensity to which algae are acclimated [129]. It is challenging to determine this light adaptation effect under constantly changing

outdoor conditions. In the model framework this would require another state variable and experimental data are missing. Therefore, in this study the effect has been modelled in accordance with the cited literature. As a first approximation of the possible effects, a sensitivity analysis could be performed by adjusting the chlorophyll *a*:carbon ratio in accordance to the average solar irradiation per day, month or even season.

As mentioned earlier, maximising biomass productivity is not equivalent to maximising economic return. Further studies on simultaneous optimisation of biomass productivity and energy consumption, post processing, process costs or life cycle assessment under varying operating conditions and design will result in a comprehensive analysis of algae production.

## CONCLUSION

Climate conditions play an important role in algae production in open raceway ponds. Water temperature is influenced by sunlight input, ambient air temperature, soil temperature, dew point temperature, wind velocity and the saturated and partial water pressure. This work presents a framework to estimate the effect of each of these different aspects on yearly algal productivity on the basis of well-established relationships.

The results showed that radiation and temperature dynamics have a major effect on productivity. During the seasons the pond temperature can be significantly below and above the optimal cultivation temperature and suppress the potential growth of algae. In moderate climate zones, the effect can be significant. Therefore, it is essential to select algae besides on the specific growth rate and adsorption coefficient on their ability to grow over a broad temperature range. The optima for pond depth and biomass depend on the production location. Deep ponds have to be combined with low biomass concentrations and shallow ponds with high biomass concentrations to reach peak productivities. The choice of pond depth, however, depends also on the paddle wheel design and the costs for concentrating the diluted solutions in downstream processing. The overall PE depends on the algae species and location. As expected, algae with a high light adsorption coefficient have a low PE, while cultivations in countries with a moderate climate use the available light more efficiently.

The open pond model was developed to get insight in the complexity of algae growth in raceway ponds. The model enables us to study the effect of changes in location, pond design and operation condition on the light and growth processes and on pond performance. To evaluate the success of cultivation cannot be based only on photosynthetic efficiency. The presented method enables us to calculate location-dependent optimal pond depths and biomass concentrations.

## **ACKNOWLEDGEMENT**

This work was performed in the cooperation framework of Wetsus, centre of excellence for sustainable water technology ([www.wetsus.nl](http://www.wetsus.nl)). Wetsus is co-funded by the Dutch Ministry of Economic Affairs and Ministry of Infrastructure and Environment, the European Union Regional Development Fund, the Province of Fryslân, and the Northern Netherlands Provinces. The authors like to thank the participants of the research theme Algae for the discussions and their financial support.

## APPENDIX A. TEMPERATURE MODEL OF RACEWAY PONDS

The dynamic temperature of the liquid in the pond is calculated from the energy balance of raceway ponds. The energy balance is given by:

$$V_w C_p \rho_w \frac{dT_w}{dt} = Q_{irradiance} - Q_{algaegrowth} - Q_{radiation} - Q_{evaporation} - Q_{convection} - Q_{conduction} \quad (A.1)$$

with  $V_w$  ( $m^3$ ) the volume of the pond,  $C_p$  ( $J\ kg^{-1}\ ^\circ C^{-1}$ ) the heat capacity of the growth medium,  $\rho_w$  ( $kg\ m^{-3}$ ) the density of the growth medium,  $T_w$  ( $^\circ C$ ) the temperature in the pond,  $Q_{irradiance}$  (W) the heat flow to the pond by sun light,  $Q_{algaegrowth}$  (W) the light energy flow to algae during growth,  $Q_{radiation}$  (W) the heat flow by emission of longwave radiation in the infrared region,  $Q_{evaporation}$  (W) the heat flow caused by either evaporation or condensation,  $Q_{convection}$  (W) the heat flow by convection and  $Q_{conduction}$  (W) the heat flow between the pond and the ground via conduction.

The water in the pond is heated by sunlight that enters the culture volume. Solar energy that is not used by algae for growth is considered as thermal energy. The total heat flow by the sunlight is given by:

$$Q_{irradiance} = A_w I_{surface}(t) \quad (A.2)$$

with  $A_w$  ( $m^2$ ) the water surface area of the pond and  $I_{surface}$  ( $J\ m^{-2}\ s^{-1}$ ) total light falling on the pond, where loss of light by reflection is accounted for. Part of this light is absorbed by algae for growth:

$$Q_{algaegrowth} = h_{comb} \mu_{growth} C_x V_w \quad (A.3)$$

which is a function of the combustion energy of algae biomass  $h_{comb}$  ( $J\ kg^{-1}$ ), the specific growth rate  $\mu_{growth}$  ( $s^{-1}$ ) and the biomass concentration  $C_x$  ( $kg\ m^{-3}$ ).

The water in the pond emits thermal energy by longwave radiation. The overall longwave radiation flow between the water in the pond and the sky is calculated using [103]:

$$Q_{radiation} = A_w \varepsilon_w \sigma \left( (T_w + 273.15)^4 - T_{sky}^4 \right) \quad (A.4)$$

where  $\varepsilon_w$  (-) is the emissivity of the water in the infrared region,  $\sigma$  ( $W\ m^{-2}\ K^{-4}$ ) the Stefan-Boltzmann constant and  $T_{sky}$  (K) the equivalent sky temperature for clear sky days, which is expressed in terms of easily measurable variables by [103]:

$$T_{sky} = (273.15 + T_a) \left( 0.711 + 5.6 \cdot 10^{-3} T_{dew} + 7.3 \cdot 10^{-5} T_{dew}^2 + 0.13 \cos(15 t_{solar}) \right)^{0.25} \quad (A.5)$$

where  $T_a$  ( $^\circ C$ ) is the air temperature,  $T_{dew}$  ( $^\circ C$ ) the dew point temperature and  $t_{solar}$  (-) the number of hours after solar midnight. The effect of cloud cover is not included in the calculation of the sky temperature due to lack of monitored data. Clouds increase the sky temperature and hence may have a substantial impact on the longwave radiation flow.

Evaporation has a large contribution to the water temperature, especially at locations such as Algeria with low humidity and high wind velocities. The evaporation rate depends on the shape of the water area, wind velocity, thus also movement of the water [130]. Here we use a basic model for the energy flows between the pond with salt, moving water and ambient air by evaporation or condensation and by convection for large water surfaces as described by Woolley *et al* [132]. The evaporation flow is driven by the difference of water vapour pressures between the ambient air and the saturated water body. The evaporation energy flow is given by:

$$Q_{evaporation} = A_w h_{evap} (p'_s - p'_a) \quad (A.6)$$

The evaporation flow depends on the heat exchange coefficient for evaporation  $h_{evap}$  ( $\text{W m}^{-2} \text{Pa}^{-1}$ ), the saturated water pressure  $p'_s$  (Pa) at water temperature  $T_w$  and the water pressure of air  $p'_a$  (Pa) at air temperature  $T_a$ . The evaporation rates were calculated using the heat exchange coefficient  $h_{evap}$  introduced by McMillan[131]:

$$h_{evap} = (3.6 + 2.5v) \cdot 10^{-2} \quad (A.7)$$

with  $v$  the wind speed ( $\text{m s}^{-1}$ ).

The Antoine equation is applied to calculate the saturated water pressure  $p'_s$  (Pa) at water temperature  $T_w$ , the water pressure of the air  $p'_a$  (Pa) at air temperature  $T_a$  and the dew point temperature  $T_{dew}$ :

$$p' = RH 10^{\left( \frac{8.07 + 10 \log\left(\frac{1.01 \cdot 10^5}{760}\right)}{233.43 + T} \right) - \frac{1730.63}{233.43 + T}} \quad (A.8)$$

where RH (-) is the relative humidity and  $T$  ( $^{\circ}\text{C}$ ) the temperature.

Convection and evaporation are related processes. The flow for passive and forced convection at the water surface mainly depends on the difference between water and air temperature. The convection flow is given by [132]:

$$Q_{convection} = C_{bowen} \frac{p_a}{p_{ref}} \frac{T_w - T_a}{p'_s - p'_a} Q_{evaporation} \quad (A.9)$$

where  $C_{bowen}$  is the Bowen constant ( $\text{Pa } ^{\circ}\text{C}^{-1}$ ),  $p_a$  is the ambient pressure (Pa) and  $p_{ref}$  the reference pressure (Pa),  $p'_s$  and  $p'_a$  are derived using equation A.8.

Conductive heat transfer takes place between the open pond and the soil. The soil is assumed to be an infinite source for heat transfer. This heat transfer calculation is derived from Fourier's law:

$$Q_{conduction} = h_{soil} A_{soil} (T_w - T_{soil}) \quad (A.10)$$

where  $h_{soil}$  ( $\text{W m}^{-2} \text{ } ^{\circ}\text{C}^{-1}$ ) is the heat transfer coefficient of the surrounding soil layer,  $A_{soil}$  ( $\text{m}^2$ ) is the area of the pond that is embedded in the soil and  $T_{soil}$  ( $^{\circ}\text{C}$ ) is the temperature of the soil surrounding the pond.

## APPENDIX B. CALCULATING BIOMASS PRODUCTION IN PONDS

The accumulation of biomass in the pond under the CSTR assumption is given by:

$$\frac{dC_x(z,t)}{dt} = (\mu_{growth}(z,t) - r_m - D(t))C_x(z,t) \quad (B.1)$$

where  $C_x$  (kg m<sup>-3</sup>) is the biomass concentration,  $D$  (s<sup>-1</sup>) the dilution rate,  $\mu_{growth}$  (s<sup>-1</sup>) the specific growth rate and  $r_m$  (s<sup>-1</sup>) the maintenance metabolic coefficient as a function of the position in pond depth  $z$  (m) and time  $t$  (s). In this study the system is operated in steady state, so the biomass concentration is independent of time and the dilution rate equals the effective specific growth rate.

The areal biomass production rate (kg s<sup>-1</sup>) is given by the integral over the depth of the pond  $d$  (m):

$$Y_{areal}(t) = \eta_L A \int_0^d (\mu_{growth}(z,t) - r_m) C_x(z,t) dz \quad (B.2)$$

where  $\eta_L$  is the fraction of land used for the water and  $A$  (m<sup>2</sup>) the surface area of one hectare. The biomass concentration is considered to be constant through the water volume.

Nutrients and pH are assumed not to limit growth. The effect of light on the specific growth rate is modelled using a growth model developed by Geider *et al* [42]. The growth model connects the photosynthetic activity of algae cells to the current light intensity and the irradiance dependent chlorophyll *a*:carbon ratio. In contrast to acclimation, photo-inhibition is not taken into account. The specific growth rate is given by:

$$\mu_{growth}(z,t) = P_m^c \left( 1 - \exp\left(\frac{-\alpha I_{PF D}(z,t) \Theta_a(z,t)}{P_m^c}\right) \right) \quad (B.3)$$

where the specific growth rate depends on the chlorophyll *a* and carbon ratio in the cell  $\Theta_a$  (g Chl *a* g<sup>-1</sup> C) and on the photon flow density  $I_{PF D}$  ( $\mu\text{mol m}^{-2} \text{s}^{-1}$ ) experienced by the algae cell at the position in pond depth  $z$  (m) and time  $t$ . The cells adapt the ratio between chlorophyll *a* and carbon in their cells according to the light intensity. The specific growth rate also depends on the maximum carbon specific rate of photosynthesis  $P_m^c$  (s<sup>-1</sup>), the functional cross section of the photosynthetic apparatus  $\alpha$  (g C (mol<sup>-1</sup> photons) m<sup>2</sup> g<sup>-1</sup> Chl *a*) and the maintenance metabolic coefficient.

The functional cross section  $\alpha$  is taken constant. The chlorophyll *a*:carbon ratio is given by:

$$\Theta_a(z,t) = \Theta_{a,max} \frac{1}{1 + \frac{\Theta_{a,max} \alpha I_{PF D}(z,t)}{2P_m^c}} \quad (B.4)$$

The maximum carbon specific rate of photosynthesis depends on the maximum specific growth rate  $\mu_{max}$  (s<sup>-1</sup>) and the maintenance metabolic coefficient as given by:

$$P_m^c = \mu_{max} f_T + r_m \quad (\text{B.5})$$

With  $f_T$  the temperature function affecting the specific growth rate. The effect of temperature on the specific growth rate and maintenance metabolic coefficient is included using a non-linear temperature effect model [143]. The resulting temperature factor  $f_T$  varies between zero and one and is given by:

$$f_T = \left( \frac{T_{let} - T_w}{T_{let} - T_{opt}} \right)^{\beta_T} \exp \left( -\beta_T \left( \frac{T_{let} - T_w}{T_{let} - T_{opt}} - 1 \right) \right) \quad (\text{B.6})$$

in which  $T_{let}$  (°C) is the lethal temperature,  $T_{opt}$  (°C) the optimal growth temperature and  $\beta_T$  (-) the curve modulating constant.

The effect of photo-inhibition is approximated by:

$$\mu_{growth+PInh}(z, t) = \mu_{growth}(z, t) - \overbrace{f_{PInh} \frac{I_{PInh} - I_{PPFD}(z, t)}{I_{PInh}}}^{\text{when } I > I_{PInh}} \quad (\text{B.7})$$

With  $\mu_{growth+PInh}$  (s<sup>-1</sup>) the growth rate if the effect of photo-inhibition is included,  $f_{PInh}$  (s<sup>-1</sup>) the photo-inhibition factor and  $I_{PInh}$  (μmol m<sup>-2</sup> s<sup>-1</sup>) the light intensity used to include photo-inhibition effects.

## APPENDIX C. PARAMETER VALUES

The general parameters and their values assumed in this study are given in Table C.1 and the algae dependent parameters in Table C.2.

Table C.1. General parameters.

Parameter	Value	Unit	Reference
$A_{soil}$	9602	m <sup>2</sup>	
$A_w^a$	8000	m <sup>2</sup>	
$C_{bowen}$	61.3	Pa °C <sup>-1</sup>	[132]
$Cp_w$	4180	J kg <sup>-1</sup> °C <sup>-1</sup>	
$d^b$	0.30	m	
$h_{soil}$	0.601	W m <sup>-1</sup> °C <sup>-1</sup>	[144]
$P_{ref}$	101325	Pa	[145]
$V_w$	2400	m <sup>3</sup>	
$\epsilon_w$	0.96		[146]
$\eta$	0.8		
$\rho_w$	1000	kg m <sup>-3</sup>	
$\sigma$	5.77*10 <sup>-8</sup>	W m <sup>-2</sup> K <sup>-4</sup>	

<sup>a</sup> Per hectare 80% of the surface area is considered as cultivation surface. The remaining area is necessary for infrastructure

<sup>b</sup> Pond depth

Table C.2. Algae dependent parameters.

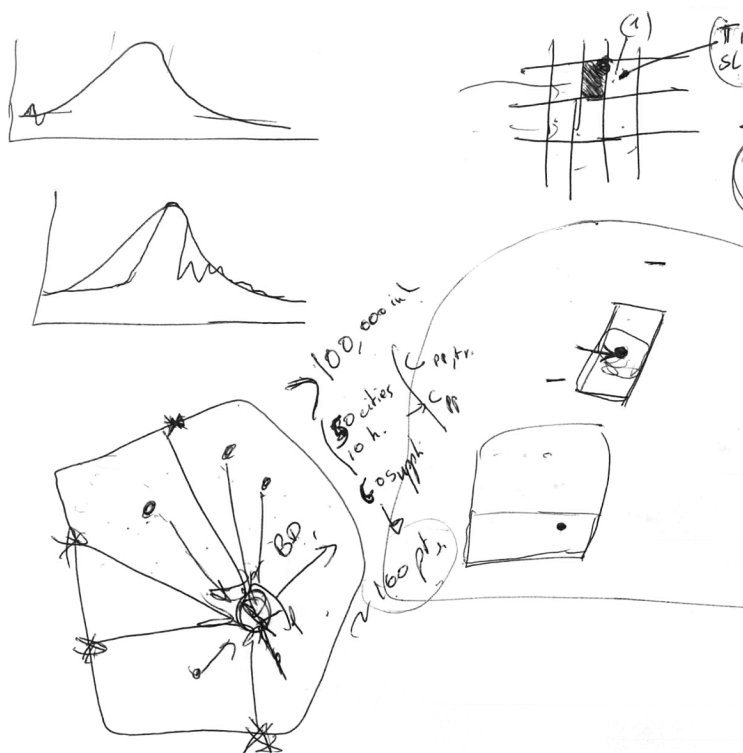
Parameter	<i>T. pseudonana</i>	<i>P. tricornutum</i>	Dimensions	Reference
$f_{PInh}$	1.1 <sup>s</sup>	1.3 <sup>*</sup>	s <sup>-1</sup>	*[141] <sup>s</sup> [140, 142]
$h_{comb}$	20*10 <sup>6a</sup>	20*10 <sup>6a</sup>	J kg <sup>-1</sup> algae	[147]
$I_{PInh}$	100 <sup>s</sup>	170 <sup>*</sup>	μmol m <sup>-2</sup> s <sup>-1</sup>	*[141] <sup>s</sup> [140, 142]
$k_a^b$	269 <sup>#</sup>	75 <sup>i</sup>	m <sup>2</sup> kg <sup>-1</sup>	#[107], <sup>i</sup> [47]
$r_m$	0.05	0.05	d <sup>-1</sup>	[42]
$T_{opt}$	24.73 <sup>#</sup>	21.64 <sup>c</sup>	°C	#[107]
$T_{let}$	31.40 <sup>#</sup>	30.31 <sup>c</sup>	°C	#[107]
$\alpha$	10	10	g C mol <sup>-1</sup> photons m <sup>2</sup> g <sup>-1</sup> Chl <i>a</i>	[42]
$\beta$	1.83 <sup>#</sup>	1.57 <sup>c</sup>	Dimensionless	[107]
$\Theta_{a,max}$	0.08	0.08	g <sup>1</sup> Chl <i>a</i> g <sup>-1</sup> C	[42]
$\mu_{max}$	3.29	1.40	d <sup>-1</sup>	[42]

<sup>a</sup> By the lack of specific data on the combustion energy of the algae species, the commonly accepted average value for algae is used

<sup>b</sup> Spectrally averaged light absorption coefficient

<sup>c</sup> Parameter values were generated by fitting equation B.6 to data obtained by [148, 149]

# ANALYSIS OF ALGAE CULTIVATION SUPPLY LOGISTICS



THIS CHAPTER IS SUBMITTED FOR PUBLICATION AS:

P.M. SLEGGERS, S. LEDUC, R.H. WIJFFELS, G. VAN STRATEN, A.J.B. VAN BOXTEL  
ANALYSIS OF ALGAE CULTIVATION SUPPLY LOGISTICS

## ABSTRACT

A regional algae facility allocation study is presented to analyse the energy share of supply transport in large-scale algae cultivation. This is done by integrating algae cultivation models with the quantitative logistic decision model 'BeWhere' for the regions Benelux (Northwest Europe), southern France and Sahara. This so-called 'BeWhere Algae' model is used to 1) assess how resource allocation influences the size and optimal locations of algae cultivation, and 2) analyse the transport energy consumption and distances for water and CO<sub>2</sub> supply.

The optimisation results show that in the Benelux large algae cultivation areas should be planned at locations nearby the sea with a high CO<sub>2</sub> availability. In southern France the plants are scattered over the region and for the Sahara cultivation is planned at locations with a minimised water transport. Given a realistic number of areas for algae cultivation, the energy consumed for transport of resources turns out to be a small percentage of the energy contained in the algae biomass. The transport energy consumption is the lowest in the Benelux due to good availability of water and CO<sub>2</sub>. In southern France and the Sahara water and CO<sub>2</sub> have to be transported over significant larger distances, but the proportion of transport energy is still low. In general, the share of transport energy is the lowest for photobioreactors and the highest for cultivation in raceway ponds, which is mainly attributed to the difference in evaporative losses.

*Keywords: logistics, quantitative analysis, algae, transport, resources*

## INTRODUCTION

Microalgae are an attractive source for production and biorefinery of commodities, such as fuels, chemicals, food and feed. Large-scale algae production facilities are one of the potential alternatives to fulfil the global demand of these products [14]. Commercial large-scale algae cultivation for production of these commodities, however, does not yet occur.

The success of cultivation depends strongly on reactor design and local weather conditions [110, 111, 122].

The decision where to locate algae cultivation is more complex than just selecting a region with good weather conditions: also the availability of water, nutrients and land may be limiting [26, 52, 56, 57, 150]. Large plants require large quantities of resources that can only be supplied if the infrastructure satisfies, while in areas with limited availability of water, CO<sub>2</sub> and nutrients small plants may be a better alternative. Logistic analyses commonly start with selecting suitable areas for production based on geographical properties of regions. GIS methods are used to construct maps that indicate preferable production areas, whereby areas with high land slopes, cities and protected areas are excluded. The exclusion steps are combined with a qualitative analysis of e.g. the potential productivity and availability of resources. Several authors have studied the potential algae cultivation in various regions (Table 1).

*Table 1. Literature overview of regional suitability analyses for algae production.*

<b>Description</b>	<b>Reference</b>
GIS approach for algae potential based on algae productivity, resource availability using three transport distances for CO <sub>2</sub> transport.	[56]
Priority map for algae plants based on spatial analysis of algae cultivation in the US using geographical information on algae productivity and fresh water availability and economic modeling of algae lipid production, freshwater pumping (based on head losses) and lipid transport costs (Euclidian distance to biorefinery).	[150]
GIS analysis of algae cultivation in Australia to derive a priority map for distance to port, distance to saline water from the coast and CO <sub>2</sub> pipeline distances based on the closest available source.	[54]
Logistic framework for waste water treatment plants in Canada including solar irradiance, land use, pipeline connections to closest CO <sub>2</sub> and water source and biomass production costs.	[55]

The approaches applied for algae location planning in the above cases are the first step in the logistic analysis and are rather qualitative. In contrast, for first and second generation biofuels, quantitative analyses are available. Cost estimates for biomass logistics have been derived and based on this the best locations for feedstock processing

have been planned (Table 2). An extreme example of the role of transportation is in sugar beet processing where the transport contributes to up to 50% of production costs [151]. Another example is methanol production from wood, where feedstock transport accounts for 16% of the production costs and methanol transportation for 12% [152].

The energy requirements and costs of algae cultivation have been assessed before [25]. However, despite the studies in Table 1, a quantitative analysis of how much energy is required for resource transport is still lacking. Furthermore, it is not clear how resource availability and cultivation supply logistics affect the planning of algae cultivation sites.

In this work these aspects are studied through a quantitative logistic analysis in which models on algae productivity are integrated with existing logistic models. The effect of allocation of algae cultivation sites is explained. In addition, energy requirements and transport distances are determined for several regions and cultivation systems to get insight in the share of transport energy in different regions. Moreover, a projection on the implications of future developments on the allocation is discussed.

*Table 2. Literature overview of logistic cost analyses for conventional biofuel production with other biomass feedstocks than algae.*

<b>Feedstock</b>	<b>Description</b>	<b>Reference</b>
Forest wood, coppice, straw and miscanthus.	Overview of biofuel supply chain considerations on process level (how to harvest) including the effects on transport costs.	[153]
Unspecified	Detailed economic evaluation of logistic costs for bio-energy. Including an analysis of lower and upper bounds for logistic variables like specific transport costs and distribution density.	[154]
Lignocellulosic feedstocks	Optimisation of biofuel production plant siting using various options for energy production and on various scales: municipality, region, country and Europe.	[58, 59, 152]
Cotton stalks and almond tree prunings	Economic study on the effect of feedstock storage costs while considering integration of biomass supply chains.	[155]
Miscanthus, poplar and willow	Feedstock allocation study for bioenergy production using GISbased biomass yield maps and optimisation of total costs (production and delivery)	[156]

## **METHODOLOGY AND INPUT DATA**

### **BeWhere Algae**

The algae supply logistics are analysed quantitatively with the logistic bioenergy optimisation model ‘BeWhere’ [157]. This model is developed for determining optimal locations and sizes of biofuel production plants with constraints for feedstock locations

and energy demands. In BeWhere the study area is divided in a grid. In each grid cell the availability of resources and the potential biomass productivity is determined. The selection of supply cells and production cells, and the connection between them are obtained by optimisation that takes the transport distances into account. An extensive description of the mathematical formulation of BeWhere is given in by Leduc *et al* and Wetterlund *et al* [59, 157].

In this work BeWhere is adapted for application to algae cultivation supply logistics. In ‘BeWhere Algae’ the area used for algae cultivation in each grid cell is determined by optimisation taking into account the resource demand of the grid cell and a supply constraint for each resource. Grid cells for which the required transportation energy is larger than the energy contained in the algae biomass will not be selected. The potential algae production per region is constrained by the total availability of water and CO<sub>2</sub> and by the weather conditions. The decision variables are 1) whether a grid cell is employed for algae cultivation (binary), 2) the area of the grid cell that is used (continuous), and 3) the amount of resources transported between supply cells and cultivation cells. The analysis is performed for four alternative reactor systems and two algae species.

The objective function applied in BeWhere Algae aims to maximise the difference between the energy contained in the produced algae biomass and the energy required for transport. Optimisation of BeWhere Algae results in the selection of the decision variables and supply network with the largest difference in energy contained in the produced algae and energy consumed for resource transport. The optimisation problem is given by:

$$\text{find} \quad x_j^{LS}, z_{ijR}^L, y_j^S \quad \forall i, j, R \quad (1)$$

$$\text{such that} \quad E_{algae} - E_{transport} \quad \text{is maximised} \quad (2)$$

$$\text{where} \quad E_{algae} = \sum_j E_{algae,j} = \sum_j x_j^{LS} y_j^S P_A^{LS} e_A \quad (3)$$

$$E_{transport} = \sum_j E_{transport,j} = \sum_{i,j,R,L} z_{ijR}^L d_{ij}^L c_R^L \quad (4)$$

$$\text{subject to} \quad E_{transport,j} \leq E_{algae,j} \quad \forall j \quad (5)$$

$$\sum_i z_{ijR}^L = x_j^{LS} y_j^S P_A^{LS} q_{RA}^{LS}, \quad \forall j, R \quad (6)$$

$$\sum_j z_{ijR}^L \leq S_{iR}^L, \quad \forall i, R \quad (7)$$

$$\sum_S x_j^{LS} \leq 1, \quad \forall j \quad (8)$$

$$0 \leq \sum_S y_j^S \leq Y, \quad \forall j, S \quad (9)$$

$$0 \leq \sum_{j,S} x^{LS} \leq N, \quad (10)$$

$$L \in \{Benelux, southern France, Sahara\} \quad (11)$$

$$S \in \{raceway pond, flat panel, horizontal tube, vertical tube\} \quad (12)$$

$$R \in \{water, CO_2\} \quad (13)$$

$$A \in \{P.tricornutum, T.pseudonana\} \quad (14)$$

$$x_j^{LS} \in \{0,1\} \quad \forall j \quad (15)$$

Table 3. Nomenclature

$x_j^{LS}$	binary decision variable for grid cell j for each region L and for reactor system S
$z_{ijR}^L$	amount of resource R that is transported from the supply grid cell i to grid cell j in region L (ton resource yr <sup>-1</sup> )
$y_j^S$	the land-use for algae production with reactor system S in grid cell j (ha)
$E$	annual energy equivalent (MWh yr <sup>-1</sup> )
$P_A^{LS}$	algae productivity of species A in region L and for reactor system S (ton dry weight ha <sup>-1</sup> yr <sup>-1</sup> )
$d_{ij}^L$	distance between the supply grid cell i and grid cell j in region L (km)
$e_A$	energy content of species A (MWh ton <sup>-1</sup> dry weight)
$q_{RA}^{LS}$	the relative demand of resource R for algae species A in region L and for reactor system S (ton resource ton <sup>-1</sup> dry weight)
$c_R^L$	distance and weight specific transport energy requirements for resource R in region L (MWh km <sup>-1</sup> ton <sup>-1</sup> resource)
$S_{iR}^L$	maximum availability of resource R from grid cell i in region L (ton resource yr <sup>-1</sup> )
$N$	maximum number of grid cells to be selected
$Y$	maximum land-use per grid cell (ha)

#### Indices

Lower case	Upper case
$A$	algae species
$algae$	produced algae biomass
$i$	supply grid cell
$j$	cultivation grid cell
$R$	resource type
$transport$	for resource transport

where  $E_{algae}$  (kWh yr<sup>-1</sup>) is the energy contained in the annually produced algae biomass (eq. 3) and  $E_{transport}$  (kWh yr<sup>-1</sup>) the annual energy consumption of resource transport to the algae plants (eq. 4). We refer to the objective function value as “energy value” (eq. 2) and this should always be positive for each selected grid cell, i.e. cells where and hence also for all selected cells together (eq. 5). The total supply to grid cell  $j$  should be equal to the total demand (eq. 6) and the total supply from grid cell  $i$  cannot exceed the maximum availability (eq. 7). Every grid cell contains at most one reactor system (eq. 8). The land-use for algae cultivation per grid cell cannot be larger than the given maximum (eq. 9), as it is unrealistic to assume that the full grid can be used for algae growth. The number of grid cells to be selected for cultivation is constrained (eq. 10). The idea behind this is as follows. In an unconstrained case, the number of cells selected for cultivation will increase until the ever increasing transport energy demand equals the energy in the algae for this last selected cell. However, as production also requires energy this situation is unrealistic and such facilities will never be realised. In fact, it cannot be expected that the total area available for algae production exceeds a certain value that is determined by competing land use. Hence, in this study the maximum number of cells is set to 10, which is a realistic number of sites given the total land area ( $10 \cdot 500^2 \cdot 0.4$  ha) and CO<sub>2</sub> availability (see supplementary information). BeWhere Algae considers this as a mixed integer problem which is solved using standard mixed integer program techniques. BeWhere Algae is solved with CPLEX in GAMS [158].

### Research case

Three regions with different weather and infrastructure conditions are considered (Figure 1). The studied regions are divided in grids cells of 0.5 degrees (~50 km x 50 km) each. Mountain areas (Pyrenees, Alps, Atlas Mountains) are not considered. In order to make the results comparable the number of grid cells that are potentially available for cultivation is set the same for each region and equals 78. The “Benelux” region located in Northwest Europe is characterised by an abundant presence of industry, high population density, low light intensities and low average temperatures (see Table 4 for indicative values). “Southern France” is thinly populated compared to the Benelux, has less industry and generates most electricity at low CO<sub>2</sub> emissions using nuclear, wind and solar power [159, 160]. The most southern region “Sahara” has a desert climate, characterised by uniform weather conditions with high light intensities and high average temperatures. The inhabitants and industry are concentrated near the coast.

Various reactor designs, i.e. open ponds, flat panels, horizontal & vertical tubes and a maximum total cultivation area of 100000 ha (40% of the grid cell area) applies for each grid cell. The maximum land-use of 40% is chosen such that it does not conflict with water and urban zones, which are uniformly assessed to be at most 60% of the grid cell area. Note that per grid cell just the aggregated land-use for algae cultivation is considered, so a grid cell may contain one big cultivation plant or a number of small plants with the same overall land-use.



Figure 1. Overview of the 3 regions considered. The blue dots indicate the stations that supplied the weather data.

Table 4. Light input, temperatures at noon and daylength during winter (January) and summer (July).

	Light input (MJ m <sup>-2</sup> day <sup>-1</sup> )		Temperature (°C)		Daylength (hours:minutes)	
	Winter	Summer	Winter	Summer	Winter	Summer
Benelux	3.2	19.4	1.8	20.5	7:30	16:30
southern France	5.9	27.1	5.6	29.2	8:40	15:20
Sahara	16.3	27.6	17.9	34.0	10:35	13:25

Algae productivities for each specific region and reactor type are shown in Table 5 and follow from advanced model calculations involving local light dynamics, weather

conditions, reactor characteristics and the effect of reactor design parameters [110, 111, 122]. In order to not overly complicate the calculations for this purpose it is assumed that each region is meteorologically homogeneous.

Water and CO<sub>2</sub> are the major substrates for algae cultivation and the requirements are also given in Table 5. The two case-study algae species *P. tricornutum* and *T. pseudonana* are marine species and therefore salt water is needed. This choice is made to protect scarce fresh water sources. Algae plants are intended to contribute to sustainable production and thus it would not make much sense to waste energy or water for cooling and heating. It is therefore assumed that the heating and/or cooling of photobioreactors (PBR) is realised by heat pumps coupled to aquifers. Hence, no additional water for the temperature control of closed PBRs is required. In the current study, the consumption of other nutrients and minerals are not included.

For the supply of water and CO<sub>2</sub> an additional grid cell layer is employed, which also contains grid cells outside the grid for cultivation of Figure 1. This supply layer contains seawater supply by pipelines from the North Sea, Atlantic Ocean and Mediterranean Sea. The CO<sub>2</sub> is obtained from electricity plants [161]. This gives a good indication of regional availability which often depends on population density. Similar trends are seen for cement and steel industry exhausts as shown in the supplementary information. For the Benelux CO<sub>2</sub> from Luxemburg is also included, in southern France from the mountainous regions and in the Sahara from the coastal area.

Distances for pipelines are the direct distance between two points based on the centre of a grid cell. A distance of 25 km is applied for transport within a grid cell. CO<sub>2</sub> can be transported by pipelines (pure and compressed) or trucks (bottled gas). However, as the energy for truck transport is much higher (see supplementary information) pipeline transport is always selected.

## RESULTS AND DISCUSSION

### Allocation of algae cultivation sites

The allocation of algae cultivation sites with raceway ponds and horizontal tubes is illustrated in Figure 2 for the algae species *P. tricornutum*. The results for the other algae species and the vertical reactor types are similar and are not shown here. The number of cells selected, the total area for algae production, the total annual biomass production and the total annual CO<sub>2</sub> mitigation that result from the optimisation are presented in Table 6. Due to the more efficient production characteristics the highest production is achieved with horizontal tubes.

Table 5. Yearly areal productivities based on Slegers et al [110, 111, 122], water consumption, for raceway ponds yearly areal evaporation of water is given in brackets, CO<sub>2</sub> consumption and energy content of algae biomass [100]. The water and CO<sub>2</sub> ratios per ton of algae are also given. A yearly fixed best biomass concentration is used to determine the optimal yearly areal productivity (see supplementary information). Cultivation systems run for 24 hours a day and for 365 days a year: Tp is *T. pseudonana*, Pt is *P. tricornutum*.

Symbol	Raceway ponds			Flat panels			Horizontal tubular			Vertical tubular		
	Benelux	S. France	Sahara	Benelux	S. France	Sahara	Benelux	S. France	Sahara	Benelux	S. France	Sahara
Biomass productivity (ton ha <sup>-1</sup> year <sup>-1</sup> )	4.57	a	11.8	54.7	60.9	74.9	27.1	43.9	59.7	31.9	56.6	97.0
P <sub>A</sub> <sup>LS</sup>	Pt		a	55.3	129	158	46.3	71.2	96.8	58.6	91.8	155
CO <sub>2</sub> consumption <sup>d</sup> (ton ha <sup>-1</sup> year <sup>-1</sup> )	14.2	a	36.4	169	189	232	56.0	90.7	123	65.9	117	200
q <sub>RA</sub> <sup>LS</sup>	Pt		a	174	404	495	96.8	149	203	123	192	324
CO <sub>2</sub> ratio <sup>e</sup>	Tp		a	3.1	3.1	3.1	2.1	2.1	2.1	2.1	2.1	2.1
(ton CO <sub>2</sub> ton <sup>-1</sup> algae)	Pt		a	3.1	3.1	3.1	2.1	2.1	2.1	2.1	2.1	2.1
Water consumption <sup>b</sup> (1000 m <sup>3</sup> ha <sup>-1</sup> year <sup>-1</sup> )	10.7 (4.52)	a	45.5 (35.7)	4.4	4.5	5.6	0.9	1.2	1.4	2.1	3.0	4.4
q <sub>RA</sub> <sup>LS</sup>	Pt		a	47.8 (35.4)	3.0	3.1	3.7	0.7	0.8	0.9	1.4	1.8
Water ratio <sup>c</sup>	Pt		a	864	25	24	23	14	11	10	24	19
(ton water ton <sup>-1</sup> algae)	Tp		a	2348	80	74	35	26	23	66	53	46
Energy content (MWh ton <sup>-1</sup> algae)	Pt		a	5.56								
	Tp		a	5.56								

<sup>a</sup> Algae cultivation in open ponds in southern France is not regarded due to lack of suitable weather data (i.e. wind velocity, dew point and soil temperature).

<sup>b</sup> Four factors have been accounted for: 1) water consumption by algae during growth, 2) the water volume of the reactor system (assume one complete flush per year), 3) estimated losses of water during harvesting and, 4) evaporative loss of water in open ponds. Closed PBRs are cooled and heated using heat pumps coupled to aquifers. Therefore, no additional water is needed for PBRs. An extensive description of the parameters and calculations is given in the supplementary information.

<sup>c</sup> The water ratios are derived from the water consumptions (1000 m<sup>3</sup> ha<sup>-1</sup> year<sup>-1</sup>), the density of water and the yearly areal productivities (ton ha<sup>-1</sup> year<sup>-1</sup>).  
<sup>d</sup> CO<sub>2</sub> consumption is directly coupled to algae growth and the efficiency depends on the cultivation system used. The calculations are given in the supplementary information.

<sup>e</sup> The CO<sub>2</sub> ratios are derived by dividing the CO<sub>2</sub> consumption (ton ha<sup>-1</sup> year<sup>-1</sup>) and the yearly areal productivities (ton ha<sup>-1</sup> year<sup>-1</sup>).

The high availability of CO<sub>2</sub> in the Benelux leads to the high biomass production and CO<sub>2</sub> mitigation. Figure 2 shows for the Benelux and Sahara a clear trend for locations near the coast. Figure 2 shows also a striking difference in land-use between the regions. Once a cell is selected in the Benelux it is best to exploit it to the maximum allowable area to use all available CO<sub>2</sub>, whereas in southern France and the Sahara the optimum locations are not fully exploited. Plenty of CO<sub>2</sub> is available throughout the Benelux so the number of selected grid cells is equal to the allowable number, i.e. ten cells, and there is no advantage to diminish the land-use within the selected cells. In southern France and the Sahara the size and distribution of local CO<sub>2</sub> sources as well the total CO<sub>2</sub> availability limit both the number of cells as well as the area for production within a cell. Additional availability of CO<sub>2</sub> from other sources than power plants, such as cement and steel industry, is expected to increase the optimal land-use per selected grid cell in southern France and the Sahara.

Comparing horizontal tubes with raceway ponds shows that with tubes relatively more cells are selected that are not situated at the border of the region. Horizontal tubes require less water than raceway ponds and this relaxes the water transport distances. The same trend was observed for flat panel and vertical tubular photobioreactors. The best locations are reactor system dependent.

### **Characteristic logistic elements**

This section gives an overview of the transport distances, transport energy consumption and share of transport energy. The quantitative results are outcomes of the optimisation of BeWhere Algae and presented here only for the optimal number of plants, which is maximally 10.

#### **Transport distance**

The average transport distances (i.e. total transport divided by number of supply points) per region and algae species is given in Figure 3. For *P. tricorntum* the distance for water supply is on average 25, 98 and 223 km for respectively the Benelux, southern France and Sahara, and 46, 126 and 171 km for CO<sub>2</sub> supply. For *T. pseudonana* it is on average 25, 28 and 178 km for respectively the Benelux, southern France and Sahara, and 25, 178 and 175 km for CO<sub>2</sub> supply. The large CO<sub>2</sub> transport distances in southern France and the Sahara, compared to the Benelux, are caused by the dispersed and limited availability of CO<sub>2</sub>.

A cultivation site can be supplied from multiple neighbouring supply points, which results in the average transport distance.

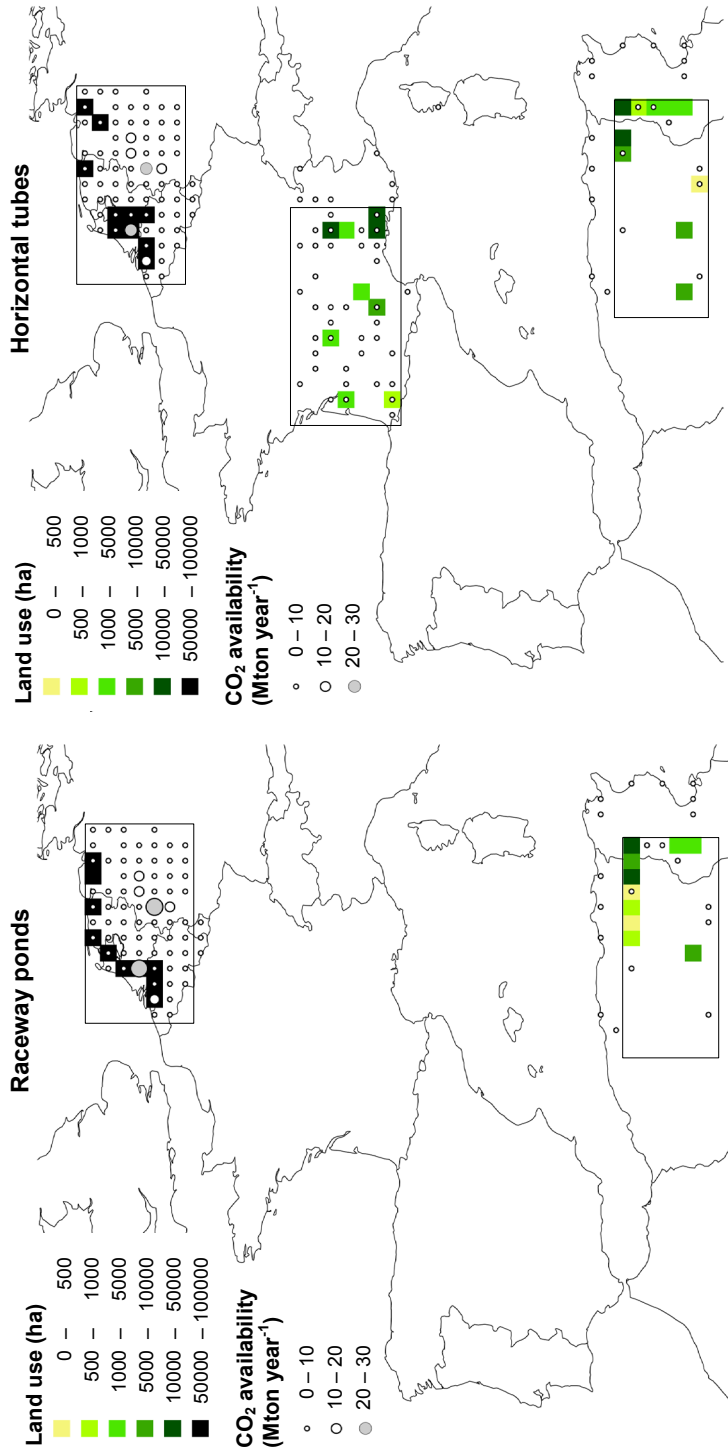


Figure 2. The allocation of algae cultivation sites with *P. tricornutum*, left for raceway ponds and right for horizontal tubes. The boxes indicate the area of each region considered for algae cultivation. Selection of grid cells for algae cultivation is indicated by the squares, also indicating the selected land-use of each grid cell. CO<sub>2</sub> availability from electricity plants is given by the circles (Mton CO<sub>2</sub> available per year).

Table 6. Biomass production and CO<sub>2</sub> mitigation for the planning shown in Figure 2.

	Number of cells	Total land-use (ha)	Total regional biomass production (Mton yr <sup>-1</sup> )	Total regional CO <sub>2</sub> availability (Mton yr <sup>-1</sup> )	Total regional CO <sub>2</sub> mitigation by the planned algae cultivation (Mton year <sup>-1</sup> )
Benelux	Ponds	1.00·10 <sup>6</sup>	41.5	195.7	86.9
	Hor tubes	1.00·10 <sup>6</sup>	46.3		96.9
S. France	Ponds	n.a.	n.a.	13.5	n.a.
	Hor tubes	8.33·10 <sup>4</sup>	5.9		12.3
Sahara	Ponds	4.84·10 <sup>4</sup>	3.1	18.7	6.5
	Hor tubes	4.76·10 <sup>4</sup>	4.6		9.6

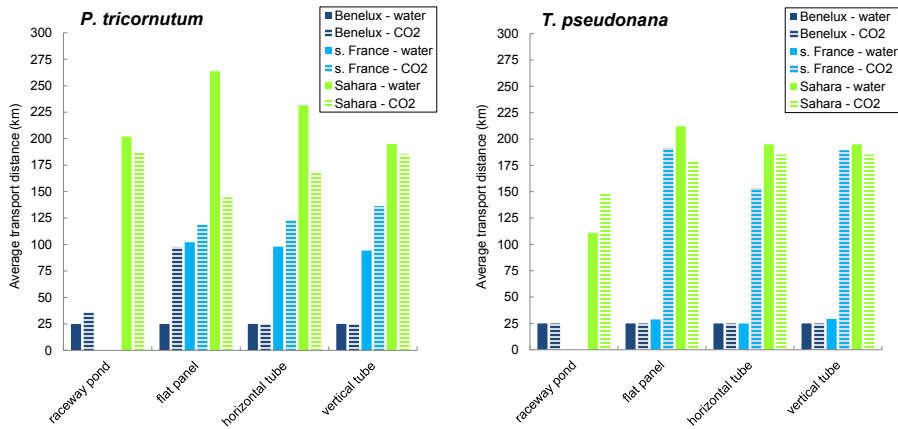


Figure 3. Average transport distance (km) per supply point for water and CO<sub>2</sub> for *P. tricornutum* (left) and *T. pseudonana* (right).

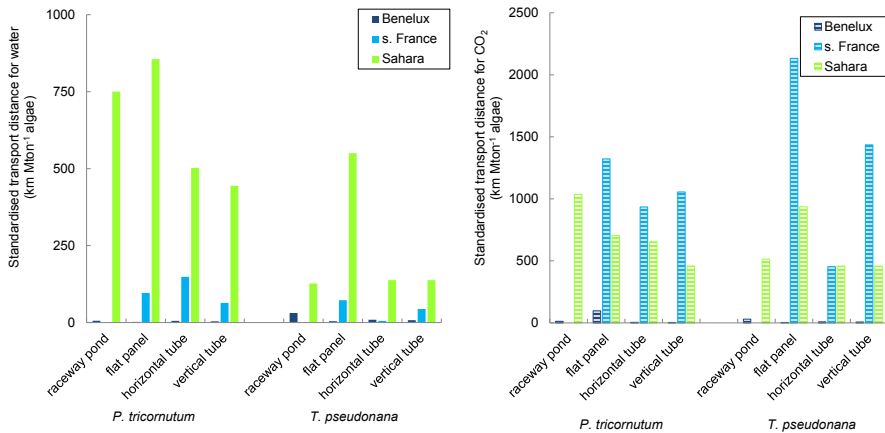


Figure 4. Standardised transport distances (km Mton<sup>-1</sup> algae) for water (left) and CO<sub>2</sub> (right).

The total required pipeline length is then the number of supply points times the average distance, which is much longer than the average distance. Moreover, the productivity varies between regions. To compensate for these two aspects the standardised transport distance per region is given in Figure 4. This standardised transport distance is the ratio between the total transport distance for all supply points and the total algae production. The contrast between the locations becomes much bigger with the standardised transport distances. Sites in the Benelux have a high productivity and use a small number of supply points, and therefore have a very low standardised

transport distance. In southern France and the Sahara the production is low and many supply points are used with large transport distances, thus resulting in much higher standardised transport distances. The standardised transport distance in the Sahara is much larger than for the other regions and can reach up to 750 kilometres per megaton for water. Similarly, in southern France the CO<sub>2</sub> standardised transport distance can reach up to 2000 kilometres per megaton.

**Supply transport energy consumption**

Clearly, the regional energy consumption for water and CO<sub>2</sub> is a result of the demand and transport distance. Figure 5 shows the absolute specific energy consumption for water and CO<sub>2</sub> transport. The Sahara always has the highest transport energy consumption for both water and CO<sub>2</sub> compared to the Benelux and southern France. The high water energy requirement is caused by the large transport distances. Still, large transport distances are possible without resulting in high energy requirements. For example, transport distances for CO<sub>2</sub> are very large for southern France, but the energy requirements per ton algae are still lower than for the Sahara (Figure 5). This is a result of the larger absolute demands for CO<sub>2</sub> per grid cell.

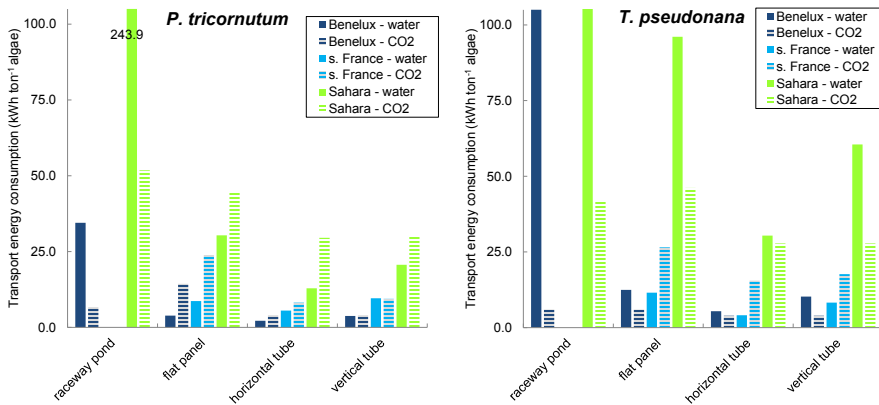


Figure 5. Energy consumption for water and CO<sub>2</sub> transport (kWh ton<sup>-1</sup> algae) for *P. tricornutum* (left) and *T. pseudonana* (right).

Comparing the transport energy needs over systems reveals that they are, overall, the lowest for horizontal tubes. The low amounts of water and CO<sub>2</sub> required compensate the transport distances which are not always the lowest for horizontal tubes (Figure 4). The transport energy is the highest for raceway ponds, which is caused by the high consumption of water especially to compensate for evaporation losses.

Production systems with *P. tricornutum* consume less transport energy than with

*T. pseudonana*. The large water consumption of the lower productive *T. pseudonana* (see the water ratio in Table 5) is reflected in the energy requirements, especially for the Sahara.

### Share of transport energy

The relative specific transport energy consumption is illustrated in Figure 6. The share of transport energy is the highest for the Sahara and much lower for the Benelux and southern France, for all reactor systems. The share of transport energy accounts for less than 6% of the energy contained in algae biomass and is in most cases below 2%. The cultivation of *T. pseudonana* in raceway ponds in the Sahara is a significant exception with 38.5% of the biomass energy consumed for resource transport. The horizontal tubes have the lowest transport share, while it is the highest for raceway ponds.

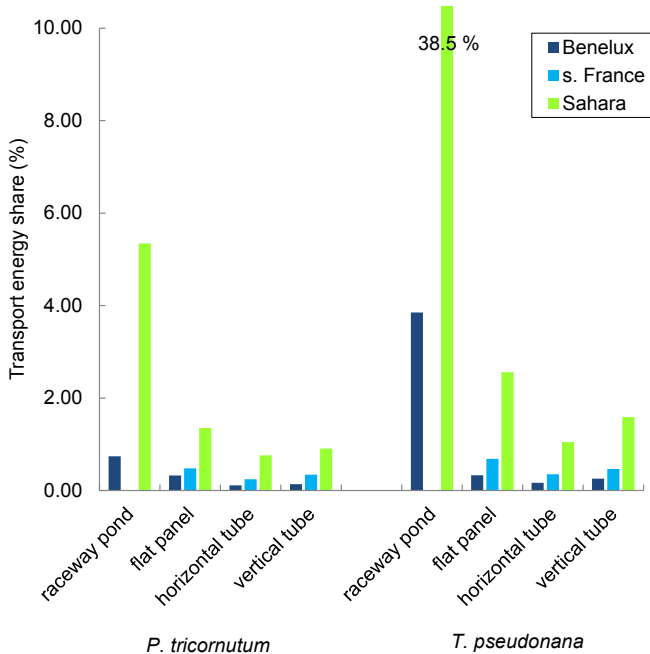


Figure 6. Transport energy share (%) compared to the energy contained in biomass.

### Summarising remarks

Obviously, cultivation near the supply points for water and CO<sub>2</sub> results in the lowest transport energy consumption. The current quantitative analysis shows that proximity of CO<sub>2</sub> and water is not essential for energy efficient algae cultivation. Transport energy is only a small share of the biomass energy content. Despite that for southern France

and the Sahara transport distances reach up to 223 km and standardised distances up to 850 kilometres per megaton for water. For CO<sub>2</sub> the distance goes up to 178 km and the standardised transport distance up to 2000 kilometres per megaton. These large distances are in contrast to previous studies [54, 150, 162] that concluded, on the basis of GIS approaches combined with several qualitative indicators, that algae plants have to be located as close as possible to the supply points. Indeed, proximity to resource supply points results in the lowest energy requirements for transport, but this proximity is not essential to achieve a positive energy balance for cultivation.

### **Implications of future developments**

In the current analysis exhausts from large point sources were considered as CO<sub>2</sub> source for algae cultivation, but CO<sub>2</sub> can also be acquired from local sources within the radius of 25 kilometres. In the Benelux the average transport distance for water and CO<sub>2</sub> is small, while in southern France and the Sahara CO<sub>2</sub> is transported over significant distances (see also Figure 4). Regional CO<sub>2</sub> supply from mobile sources, small industries and agriculture is possible, for example from biogas generation at farm-scale by processing manure and other waste stream, or at larger scale in cities to generate electricity from biomass waste that cannot be brought to value [163-165]. Another possibility is to absorb CO<sub>2</sub> out of the air [166], a technique that could be applied in remote areas for example in the Sahara.

The allocation of algae cultivation sites changes by using other sources of the resources and new calculations are necessary once these sources are quantified. Nevertheless, to get an impression on the potential effects of local supply we translate the transport energy consumption per ton of algae produced of Figure 5 to energy consumption per ton of resource used. As the supply in the Benelux is virtually local, the energy costs per amount of resource can be seen as characteristic for energy costs of local supplies. Next, a scenario is considered where transport energy requirements in southern France and the Sahara are reduced to the level of the Benelux. The differences between the current transport energy consumption and those derived from the Benelux are expressed as the potential energy reduction for local supply in Figure 7.

The values in Figure 7 can also be seen as the maximum affordable energy investment (per ton of resource) for obtaining the water and CO<sub>2</sub> from local sources. These vary between the regions, reactor systems and algae species. The potential energy reduction per ton of water is lower compared to CO<sub>2</sub>, so the maximum affordable energy investment is also limited. However, the amounts are much larger and therefore, a small reduction in transport energy through local supply may significantly contribute to the overall energy requirements. For example, overall large improvements are

possible for the Sahara for cultivation in raceway ponds or with *T. pseudonana* (Figure 5). Still, despite the existence of saline aquifers the local availability of salt water in the Sahara is limited [167, 168] and much lower than sea water supply.

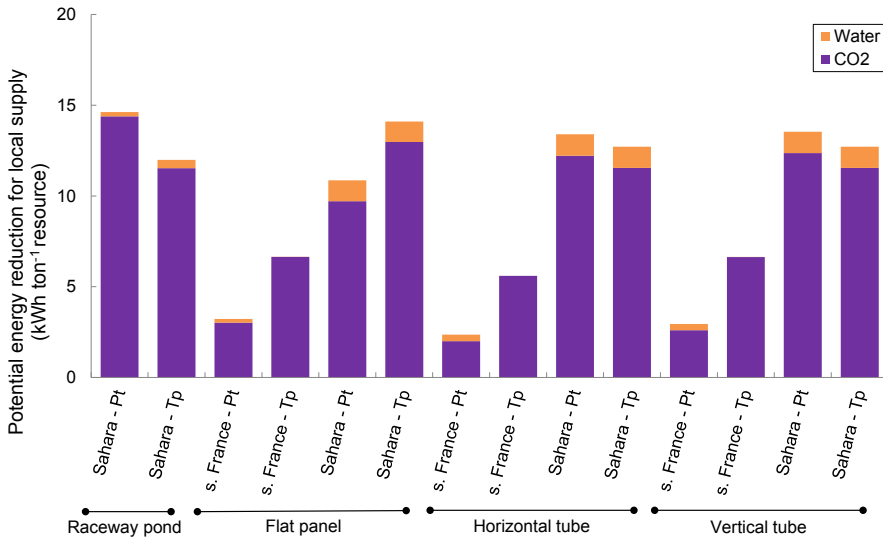


Figure 7. Potential energy reduction for local supply of water and CO<sub>2</sub> (kWh ton<sup>-1</sup> resource). Pt refers to *P. tricornutum* and Tp to *T. pseudonana*. The potential reduction is the difference between the supply energy required in the illustrated situations compared to the Benelux, where the resource supply is local.

## CONCLUSIONS

This results of this work show that the logistic requirements and trends depend greatly on cultivation characteristics (location, algae species, reactor system) and logistic aspects (transport distance, transport energy consumption, availability of resources). The many interactions and complicated relations make it indispensable to use a tool like ‘BeWhere Algae’ for solving algae cultivation site allocation.

This study is the first to quantify the energy consumption for resource transport of algae cultivation. With the realistic constraint applied to the number of grid cells, transport energy consumption represents in general only a small fraction of the total algae biomass energy. Horizontal tubular reactors have the lowest transport energy consumption and raceway ponds the highest. The transport requirements are the lowest for the Benelux (Northwest Europe) due to the good infrastructure and availability of water and CO<sub>2</sub> in large amounts at many places. The limitations of supply transport are less adverse than previously thought. The low energy requirements for transport allow

significant average transport distances per supply point of 223 km for water and up to 178 km per supply point for CO<sub>2</sub> in southern France and the Sahara.

In the Benelux location sites along the coast are preferred and it is beneficial to exploit the available area in these sites to the maximum. In southern France, with a lower availability of CO<sub>2</sub> the land-use per site is lower and the selected sites are spread over the full region. In the Sahara sites with the lowest water transport distance are preferred. The lack of CO<sub>2</sub> leads to the low land-use per site. In southern France and the Sahara CO<sub>2</sub> from local sources creates potential to reduce energy requirements for transport and to increase algae productivity. Water transport contributes significantly to the energy requirements due to the large amounts necessary. Local supply of water with minimum energy required for processing besides transport is challenging.

The fact that transport energy is only a small proportion of the energy contained in the produced algae in this study does not imply that transport logistics is not important. As shown here resource location, regional distribution, resource availability and transport networks have a profound effect on the allocation of algae cultivation sites.

## **ACKNOWLEDGEMENTS**

This work was initiated at IIASA during the Young Scientists Summer Programme (YSSP) 2011 with funding from the Netherlands Organisation for Scientific Research (NWO). This work was performed in the cooperation framework of Wetsus, centre of excellence for sustainable water technology ([www.wetsus.nl](http://www.wetsus.nl)). Wetsus is co-funded by the Dutch Ministry of Economic Affairs and Ministry of Infrastructure and Environment, the European Union Regional Development Fund, the Province of Fryslân, and the Northern Netherlands Provinces. The authors like to thank the participants of the research theme Algae for the discussions and their financial support.

## SUPPLEMENTARY INFORMATION

### S. 1 Determining biomass productivity

The productivity of algae is a function of sunlight input and water temperature. The latitude of the location determines the solar elevation and day length and thereby the growth period [110, 111, 122]. Furthermore, the cultivation technology, algae species and reactor design have an impact on the light input and distribution in the reactor and thus on productivity. The water temperature in raceway ponds is influenced by ambient conditions like air temperature, wind velocity, relative humidity and dew point temperature, and is evaluated with a model [110]. In closed PBRs it is assumed that temperature control is applied. A model-framework to study algae cultivation in open ponds, flat panel and two types of tubular PBRs is used to predict yearly areal biomass production [110, 111, 122].

Meteorological data from measuring sites in Cabauw, the Netherlands, Carpentras, France and Tamanrasset, Algeria have been collected as input [95-97, 133-135, 169]. The best yearly areal algae productivities from Slegers *et al* [110, 111, 122] for the four cultivation systems using the algae species *T. pseudonana* and *P. tricornutum* are given in Table 5. The species *T. pseudonana* has a lower productivity than *P. tricornutum*. The best fixed yearly biomass concentration and best fixed distance between reactor elements for the Benelux, southern France and Sahara have been derived and are given in Table S.1.

Table S.1. Biomass concentration  $C_x$  ( $\text{kg m}^{-3}$ ) and distance  $d$  (m) used to determine yearly areal productivities ( $\text{ton ha}^{-1} \text{ year}^{-1}$ ) for *T. pseudonana* (*Tp*) and *P. tricornutum* (*Pt*) at three locations and in four different cultivation systems; raceway ponds, flat panels, horizontal and vertically stacked horizontal “vertical” tubular photobioreactors.

		Benelux		southern France		Sahara	
		$C_x^a$	d	$C_x^a$	d	$C_x^a$	d
Raceway pond	<i>Tp</i>	0.1	n.a	<sup>b</sup>	n.a.	0.1	n.a.
	<i>Pt</i>	0.2	n.a.	<sup>b</sup>	n.a.	0.3	n.a.
Flat panel	<i>Tp</i>	0.8	0.35	0.8	0.40	0.8	0.30
	<i>Pt</i>	2.8	0.35	2.9	0.35	3.0	0.30
Horizontal tubular	<i>Tp</i>	1.6	0.04	2.1	0.04	2.5	0.03
	<i>Pt</i>	4.3	0.04	5.6	0.04	6.4	0.03
Vertical tubular	<i>Tp</i>	0.9	0.20	1.1	0.15	1.3	0.10
	<i>Pt</i>	2.6	0.25	3.3	0.20	4.0	0.15

<sup>a</sup> The best yearly fixed biomass concentration and distance between the reactors were determined for each algae species, cultivation system and location.

<sup>b</sup> Algae cultivation in open ponds in southern France was not computed due to lack of suitable weather data (i.e. wind velocity, dew point and soil temperature)

## S.2 Substrate requirements

### S.2.1 Water

The water requirement depends on the cultivation system used. Four factors have been accounted for: 1) water consumption by algae during growth (photosynthesis), 2) the water volume of the reactor system for one complete flush per year for cleaning purpose, 3) water losses during harvesting and, 4) evaporative loss of water in open ponds. Closed photobioreactors can be cooled and heated using heat pumps coupled to aquifers. Therefore, no additional water to balance evaporation is needed for closed photobioreactors. The water consumption is given by:

$$\phi_{\text{water}} = \overbrace{P_{\text{biomass}} \frac{f_{\text{water}}}{\rho_{\text{water}}}}^{\text{algae growth}} + \overbrace{V_{\text{water}}}^{\text{water volume}} + \overbrace{\eta_{\text{water}} \frac{P_{\text{biomass}}}{C_x}}^{\text{water losses DSP}} + \overbrace{\frac{\Phi_{\text{evap}}}{\rho_{\text{water}}}}^{\text{evaporation}} \quad (\text{S.1})$$

in which  $\phi_{\text{water}}$  ( $\text{m}^3 \text{ hectare}^{-1} \text{ year}^{-1}$ ) is the water consumption,  $P_{\text{biomass}}$  ( $\text{kg dry matter hectare}^{-1} \text{ year}^{-1}$ ) the biomass productivity,  $f_{\text{water}}$  the stoichiometric factor of water consumption for growth and  $\rho_{\text{water}}$  ( $\text{kg m}^{-3}$ ) the density of water. The water volume  $V_{\text{water}}$  ( $\text{m}^3 \text{ hectare}^{-1} \text{ year}^{-1}$ ) is expressed using the parameters  $A_{\text{water}}$  ( $\text{m}^2 \text{ hectare}^{-1} \text{ year}^{-1}$ ) which is the water surface of open ponds, the diameter or depth of the system  $d$  (m), the height of the panel  $h$  (m), the length of the panels or tubes  $L$  (m) and the number of reactor systems  $N_{\text{total}}$  ( $\text{hectare}^{-1} \text{ year}^{-1}$ ):

$$V_{\text{water}}(\text{ponds}) = A_{\text{water}} d; V_{\text{water}}(\text{panels}) = h d L N_{\text{total}}; V_{\text{water}}(\text{tubes}) = 0.25 L \pi d^2 N_{\text{total}} \quad (\text{S.2})$$

Water losses during harvesting, i.e. water that cannot be recycled are estimated using the efficiency  $\eta_{\text{water}}$ , biomass productivity  $P_{\text{biomass}}$  and biomass concentration  $C_x$  ( $\text{kg m}^{-3}$ ). Water loss by evaporation is calculated using the evaporation flux  $\phi_{\text{evap}}$  ( $\text{kg hectare}^{-1} \text{ year}^{-1}$ ). Precipitation is neglected, but for some locations it could balance evaporation. Therefore, this is a worst-case scenario for water consumption.

Parameter values used to determine the water consumption are given in Tables S.2 and S.3. The distance between the systems varies between regions (Table S.1), resulting in a different number of reactor elements per hectare. The number of closed photobioreactors is based on 100 m long systems and on the number of vertical rows used. The resulting yearly water consumptions in the cultivation systems for different regions are given in Table 5 in the paper.

Table S.2. Number of reactor elements per hectare ( $N_{total}$  in equation S.2).

		Benelux	southern France	Sahara
Raceway pond	$Tp$	n.a.	n.a.	n.a.
	$Pt$	n.a.	n.a.	n.a.
Flat panel	$Tp$	259	229	297
	$Pt$	259	259	297
Horizontal tubular	$Tp$	943	943	1041
	$Pt$	943	943	1041
Vertical tubular	$Tp$	3375	4158	5418
	$Pt$	2844	3375	4158

Table S.3. System and species specific parameter values for water and  $CO_2$  consumption.

	Raceway pond	Flat panel	Horizontal & vertical tubular
$A_{water}$ (m <sup>2</sup> )	8000	n.a.	n.a.
$d$ (m)	0.30	0.03	0.06
$f_{CO_2}$ (kg kg <sup>-1</sup> ) <i>T. pseudonana</i>	2.0651	2.0651	2.0651
$f_{CO_2}$ (kg kg <sup>-1</sup> ) <i>P. tricornutum</i>	2.0928	2.0928	2.0928
$f_{water}$ (kg kg <sup>-1</sup> ) <i>T. pseudonana</i>	0.6239	0.6239	0.6239
$f_{water}$ (kg kg <sup>-1</sup> ) <i>P. tricornutum</i>	0.6609	0.6609	0.6609
$h$ (m)	n.a.	1	n.a.
$L$ (m)	n.a.	100	100
Number of vertical rows	n.a.	n.a.	1 (hor), 9 (vert)
$\eta_{CO_2}$	1.5	1.5	1
$\eta_{water}$	0.05	0.05	0.05

Table S.4. Distance ( $D$ ) dependent energy requirements (kWh ton<sup>-1</sup>) for  $CO_2$  and water transport.

	Pipe line		Truck	
	<200 km	>200 km	<200 km	>200 km
$CO_2$	0.076D <sup>a</sup>	0.064D <sup>a</sup>	200 <sup>b</sup>	1D <sup>b</sup>
Water	0.0062D	0.0062D	n.a.	n.a.

<sup>a</sup> Based on projections of onshore compressed  $CO_2$  transport [170] which are in line with the requirements for natural gas transport on the Yamal-European pipeline.

<sup>b</sup> Transport of bottled compressed  $CO_2$  by truck [171].

### S.2.2 $CO_2$

$CO_2$  consumption is directly coupled to algal growth. The requirement of  $CO_2$  in the three cultivation systems is given by:

$$\phi_{CO_2} = P_{biomass} f_{CO_2} \eta_{CO_2} \quad (S.3)$$

in which  $\phi_{CO_2}$  (kg hectare<sup>-1</sup> year<sup>-1</sup>) is the  $CO_2$  consumption,  $P_{biomass}$  (kg hectare<sup>-1</sup> year<sup>-1</sup>) the biomass production,  $f_{CO_2}$  the stoichiometric factor of  $CO_2$  consumption for growth and  $\eta_{CO_2}$  the assimilation efficiency of  $CO_2$ . The parameter values for *P. tricornutum* and

three locations can be found in Table S.3. The resulting CO<sub>2</sub> consumption per year is listed in Table 5.

### S.3 Energy consumption for transport

The energy consumptions for transport of CO<sub>2</sub> and water are given in Table S.4.

The energy consumption for water transport are obtained by:

$$E = \frac{g(h_f + h_{static})\rho_w f_E}{D\eta} \quad (\text{S.4})$$

where the energy consumption  $E$  (kWh ton<sup>-1</sup> km<sup>-1</sup>) depends on the gravitational constant  $g$  (m s<sup>-2</sup>), the head loss  $h_f$  (m), the static lift  $h_{static}$  (m), the density  $\rho_w$  (kg m<sup>-3</sup>), the conversion factor  $f_E$  (2.78\*10<sup>7</sup> kWh W<sup>-1</sup>), the volume flow of water  $Q$  (m<sup>3</sup> s<sup>-1</sup>) and the pump efficiency  $\eta$  (-) which is taken to be 0.7. The head loss due to friction is described using the Darcy-Weisbach relation:

$$h_f = f \frac{D}{d} \frac{v^2}{2g} \quad (\text{S.5})$$

With the friction factor  $f$  (-), the length or distance  $D$  (m), the diameter  $d$  (m) and the velocity  $v$  (m s<sup>-1</sup>). The friction factor  $f$  depends on the diameter and the roughness  $k_r$  (m):

$$f = \left( 1 / \left( 4 \log \left( \frac{3.7d}{k_r} \right) \right) \right)^2 \quad (\text{S.6})$$

the roughness for concrete pipes is used (2\*10<sup>4</sup> m). For pumping of water a common static lift of 0.5 m km<sup>-1</sup>, a tube diameter of 1 m and a pumping velocity of 2.5 m s<sup>-1</sup>.

### S.4 CO<sub>2</sub> supply

Figure S.1 shows the CO<sub>2</sub> availability for electricity plants (left) and for cement and steel industry (right). The yearly CO<sub>2</sub> availability per grid cell and per region is given. Southern France has a low CO<sub>2</sub> availability as France generates most electricity at low CO<sub>2</sub> emissions using nuclear, wind and solar power [159, 160]. Flue gasses from electricity plants are used in the calculations as CO<sub>2</sub> source for algae cultivation, as they are a good indicator for industrial CO<sub>2</sub> availability per region. Table S.5 shows for several substrates the CO<sub>2</sub> emissions per MJ energy produced that were used to derive the emissions from plant capacities (based on [161]).

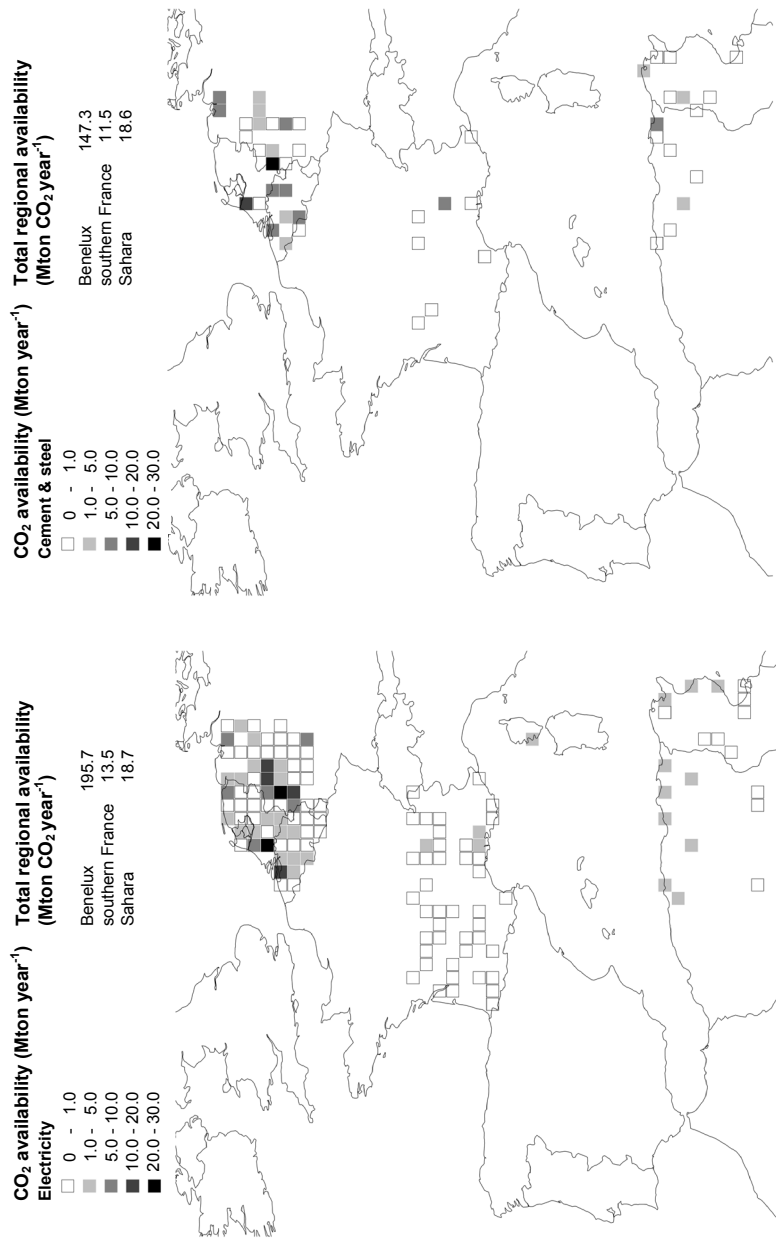


Figure S.1 Distribution of CO<sub>2</sub> supply points (squares, in Mton year<sup>-1</sup>) in the three regions. Left for electricity plants (based on Platts' electricity dataset [161]), using the average energy value and the average CO<sub>2</sub> emission per kg of processed substrate entity (see Table S.5), right for cement and steel plants (derived from the USGS mineral year book of the different locations [172], using only emissions from the raw materials). Yearly regional availability is also given.

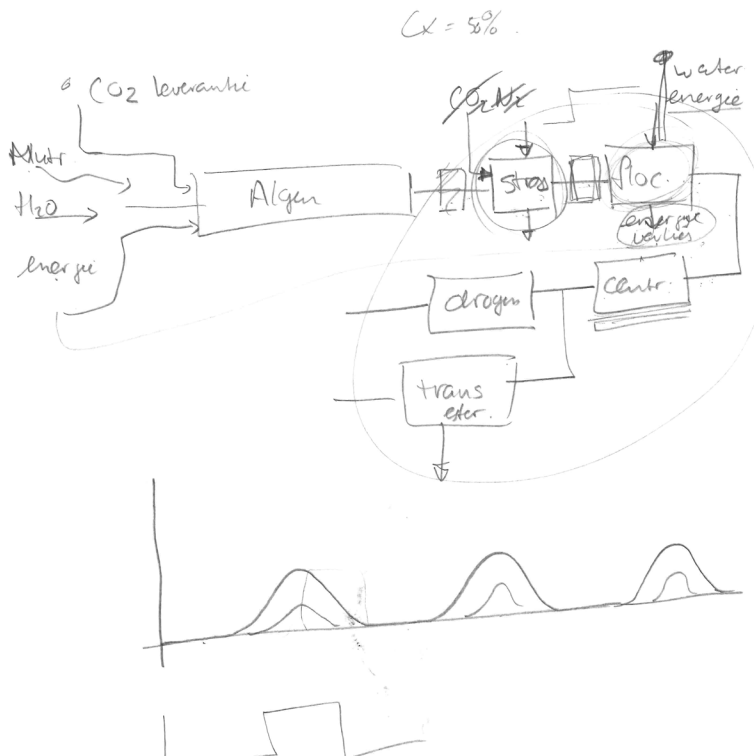
Table S.5. Overview of the different substrates used for electricity production in Europe and the Sahara, the heating value of the substrates ( $\text{MJ kg}^{-1}$ ) and  $\text{CO}_2$  emissions ( $\text{kg MJ}^{-1}$  and  $\text{kg kg}^{-1}$ ). References are given in [ ].

Name	Heating value ( $\text{MJ kg}^{-1}$ ) <sup>a</sup>	$\text{CO}_2$ emission ( $\text{kg MJ}^{-1}$ )	$\text{CO}_2$ emission ( $\text{kg kg}^{-1}$ )
<b><u>Electricity plants</u></b>			
Blast-furnace gas	2.68 [173]	0.209	0.56 [174]
Biogas from wood or other biomass or gasification of organic material such as manure or sludge or food waste	21.26 [175]	0.211	4.48 [175]
Biomass including agricultural waste and energy crops	10.00 [176]	0.184	1.84 [177]
Bio-derived liquid fuel, biodiesel or bio-oil			2.85 [178]
Coal	24.00 [179]	0.108	2.60 [180]
Coke oven gas	37.50 [174]	0.048	1.79 [174]
Digester gas (from sewage sludge or agricultural waste)	23.32 [181]	0.012	0.2 [182]
Natural gas			2.81 [174]
Landfill gas	14.41 [183]	0.022	0.31 [182]
Mine gas (low-BTU waste gas or methane from coal mines)	48.49 [180]	0.006	0.29 [180]
Naphtha	45.01 [174]	0.073	3.30 [174]
Fuel oil			2.98
Refuse (municipal solid waste)	8.40 [180]	0.119	1.00 [180]
Refinery off-gas	48.15 [173]	0.067	3.21 [184]
Oil shale	8.60 [174]	0.107	0.92 [174]
Scrap tires	34.86 [185]	0.073	2.55 [186]
Wood or wood-waste fuel	16.00 [176]	0.110	1.76 [187]
Wastewater sludge	11.30 [188]	0.004	0.05 [189]
<b><u>Cement plants</u></b>			
Cement			0.42 [190]
Clinker			0.42 [190]
<b><u>Steel plants (blast furnices)</u></b>			
Iron			1.99 [191]
Steel			1.99 [191]

<sup>a</sup> Based on the lower heating value



# A MODEL-BASED COMBINATORIAL OPTIMISATION APPROACH FOR ENERGY-EFFICIENT PROCESSING OF MICROALGAE



6

THIS CHAPTER IS SUBMITTED FOR PUBLICATION AS:

P.M. SLEGGERS, B.J. KOETZIER, F. FASAEI, R.H. WIJFFELS, G. VAN STRATEN, A.J.B. VAN BOXTEL  
A MODEL-BASED COMBINATORIAL OPTIMISATION APPROACH FOR ENERGY-EFFICIENT PROCESSING OF  
MICROALGAE.

## ABSTRACT

The analysis of energy consumption of algae biorefineries is commonly based on fixed performance data for each processing step. In this work we demonstrate a model-based combinatorial approach to derive the design-specific energy consumption and biodiesel yield in the production of biodiesel from microalgae. Process models based on mass and energy balances and conversion relationships are presented for several possible process units in the algae processing train. They allow incorporating the effects of throughput capacity and process conditions, which is not possible in the data-based approach. The process models are organised in a superstructure to evaluate all combinations of routings. First this is done for selected fixed design conditions, and next for process conditions that are optimised by maximising the net energy ratio (NER) of each route. The optimised process conditions yield NER values which are up to 38% higher than those for fixed process conditions. In addition, the approach allows a bottleneck analysis for each process route which shows that the best process conditions of a single unit depend upon the entire route. The model-based approach proves to be a versatile tool for the design of efficient microalgae processing systems. Keywords: *microalgae, net energy ratio, combinatorial optimisation, process design, models*

## INTRODUCTION

Producing biodiesel from microalgae biomass requires the processing steps harvesting, dewatering, disruption, extraction and lipid conversion. Various processing units are available, ranging from traditional ones like centrifugation and filtration to innovative algae specific processing units such as microwave assisted conversion [192]. Table 1 gives an overview of possible processing units for each main step in the processing to biodiesel. Several combinations of processing units are possible in the process design. Process engineers normally use a step-wise approach to design process routings whereby for every function the unit with the best performance is chosen. However, each choice in the route affects the performance of units downstream. As a consequence, an early choice may have a negative effect on other process units further in the processing route.

The processing algae biomass has an important role in the sustainability performance of algae biodiesel production. Several authors evaluate the energy use and other impacts of processing options in LCA studies as shown in Table 2. Each study considers a specific processing route and assumes a specific lipid content, while in addition some consider allocation of energy to co-products which decreases the energy use for biodiesel production. In these works standard characteristics of processing units are employed and basic processing routes with limited variation are studied. Brentner *et al* [63] recognised the limitations of such an approach and studied all possible combinations of units that can be applied in the processing of algae. In that study the route of chitosan flocculation followed by supercritical methanol conversion was evaluated as best, with the lowest use of water and energy.

All the authors above, including Brentner *et al*, use an approach whereby the performance of single process units is derived from standard databases. The disadvantage is that the performance is not affected by process conditions or other decision variables. The relevance to include the process conditions in the performance analysis is illustrated by the next example. Algae solutions are often first concentrated 10 times, followed by dewatering to reach a solid concentration above 15% [198]. An algae solution of 4 g L<sup>-1</sup> would thus get 10 times concentrated during harvesting and 4 times during dewatering. However, other combinations of concentration factors are also possible. The energy requirement for two centrifuges in series with different combinations of concentration factors was calculated based on Wileman *et al* [199]. Figure 1 shows that the solution with the lowest energy requirement is obtained by 4 times concentration in harvesting and subsequently 10 times concentration during dewatering. The energy saving with respect to the customary 10x4 treatment is 38%.

Table 1. Overview of some possible processing units for biodiesel production from algae

<b>Harvesting</b>	<b>Dewatering</b>	<b>Disruption</b>	<b>Extraction</b>	<b>Conversion</b>
Centrifugation	Centrifugation	Bead milling	Traditional solvent (hexane)	Acid catalyst
Pressure filtration	Pressure filtration	Homogenisation	Mixed solvent	Alkali catalyst
Vacuum filtration	Vacuum filtration	Ultrasound	Supercritical CO <sub>2</sub>	Heterogeneous catalyst
Tangential cross flow filtration	Drying	Supersonic wave treatment	Ionic liquids	Enzymatic with lipases
Ultrasound sedimentation	Steam evaporation	Pulsed electric field	Two-phase systems	
Chemical flocculation		Acid treatment	Switchable solvents	
Biological flocculation		Enzymatic cell wall degradation	Surfactants	
Autoflocculation		French press		
Dissolved air flotation				
Suspended air flotation				
Electrolytic flotation				
			Supercritical methanol extraction and conversion	
			Microwave assisted extraction and conversion	

Table 2. Literature overview of energy requirements for processing microalgae to biodiesel.

Cultivation based on	Lipid content	Cultivation (co-product allocation) included?	Processing route	Energy requirement (GJ ton <sup>-1</sup> biodiesel)	Reference	Scenario name
Raceway pond	25%	No (no)	Centrifugation – drying – pressure filtration – hexane extraction – esterification	255	[63]	Base
Flat panel PBR	25%	No (no)	Chitosan flocculation – supercritical methanol extraction and conversion	44	[63]	Best
Raceway pond	18-39%	No (no)	Flocculation – rotary press – belt drying – oil milling – hexane extraction – transesterification	100-46	[70]	Dry
Raceway pond	18-39%	No (no)	Flocculation – rotary press – oil milling – hexane extraction – transesterification	32-15	[70]	Wet
Flat panel PBR	50%	No (no)	Centrifugation – shear mixing – hexane extraction – conversion	23	[193]	
Raceway pond	23%	No (yes)	Centrifugation – cell lyses – solvent extraction – methanol conversion	41	[194]	
Raceway pond	40%	Yes (no)	Settling tank – drying – hexane extraction – conversion with acidic catalysis	34	[195]	Base
Raceway pond	40%	Yes (no)	Settling tank – drying – hexane extraction – conversion with acidic catalysis (with energy and material integration)	23	[195]	Integrated
Raceway pond	25%	Yes (no)	Bioflocculation – dissolved air flotation – centrifugation – homogeniser – hexane extraction	23	[196]	
Raceway pond	20-50%	Yes (yes)	Centrifugation – thermal drying – hexane extraction – transesterification – anaerobic digestion	44-33 (with 25-75% probability)	[197]	Reference
PBRs and raceways combined	20-50%	Yes (yes)	Bed drying – wet lipid extraction – hydrotreating – anaerobic digestion	23-17 (with 25-75% probability)	[197]	Innovative

An alternative for the data-based approach is a model-based approach. Hereby, the characteristics of the flows, for example flow rate, algae concentration and lipid content, are linked to the mass and energy balances for every processing unit. By connecting the models of all processing units the performance of each route can be quantified and optimized with respect to the routing and operational conditions [197, 200].

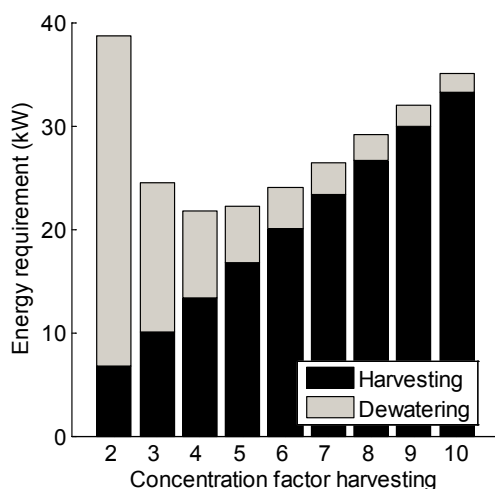


Figure 1. Relative energy requirements for concentrating a solution 40 times with two centrifugation steps in series based on Wileman et al [199]. The first concentration step is called harvesting and the second dewatering. The energy requirements are relative to the highest requirement, which is achieved at 2 times concentration for harvesting. Black shows the contribution of harvesting and grey the contribution of dewatering.

In this work we demonstrate the model-based approach for a combinatorial evaluation of several options of process functions. In the combinatorial evaluation, first the energy performance of all combinations of processing units with fixed standard process conditions is quantified. Note that this is not the same as using fixed performance indicators per unit as is customary in the data-based approach. The results illustrate typical net energy ratios (NER) of groups of processing units. Next, the possibilities to increase the NER values are investigated by optimising the operational conditions in all possible product routings.

## MODEL-BASED COMBINATORIAL APPROACH

### Superstructure and processing units

The first step in the model-based combinatorial approach is the selection of processing units for algae to biodiesel, shown in the superstructure in Figure 2. The selection is based on the availability of process relations and data, and contains both traditional

and innovative process units. The traditional processes have proven their success in other applications, like food and biotechnology, but generally process conditions can be improved when using algae. Innovative processes are more specifically developed for algae or combine several processing steps. This mostly results in lower energy consumption and less room for improvement.

The downstream processing starts with harvesting to separate microalgae from the cultivation solution. Six process units are considered for the harvesting step. In “mechanical harvesting” energy is applied to separate the algae from the cultivation solution; this includes centrifugation, vacuum filtration, pressure filtration and ultrasound sedimentation. “Flocculation” uses energy to mix the microalgae with flocculent, after which the algae precipitate. Harvesting is commonly followed by dewatering to produce a concentrated algae stream and a waste stream that contains water and a low amount of algae [198]. In “mechanical dewatering” a force is used to separate the cells. The processing units considered for mechanical dewatering are centrifugation, vacuum filtration and pressure filtration. In order to conform with available data about the subsequent steps, and to not excessively complicate the analysis, the biomass concentration after dewatering is fixed to 100 g L<sup>-1</sup>.

Several extraction processes require to disrupt the cells first, e.g. by exposing microalgae to a force which destroys the cell structure. Bead milling is considered here. In the extraction procedure the slurry with disrupted algae are mixed with a solvent to transfer the lipids to the solvent phase. Traditional hexane extraction is considered, next to supercritical CO<sub>2</sub> extraction.

In the last processing step the extracted lipids, especially triacylglycerides, are converted to biodiesel using a catalyst to form fatty acid methyl esters. Acidic and alkaline catalysts are considered. Enzymatic conversion to biodiesel can be directly applied after disruption. “Microwave assisted conversion” combines the disruption, extraction and conversion step in one process unit, but the algae need to be dried using thermal energy as microwave conversion has only been tested on dried algae samples. Methanol acts as solvent and reactant to form fatty acid methyl esters. “Supercritical methanol conversion” also combines disruption, extraction and conversion in one processing unit. Methanol is added to the algae slurry and the mixture is brought to supercritical conditions to destroy the cells. The methanol is used as a solvent and at the same time for conversion to fatty acid methyl esters.

The process routes are grouped according to the extraction and conversion process which leads to seven processing groups (the right hand side of Figure 2). There are six processing options for harvesting and three for dewatering (the left hand side of Figure 2), so each process group consists of 18 possible routes.

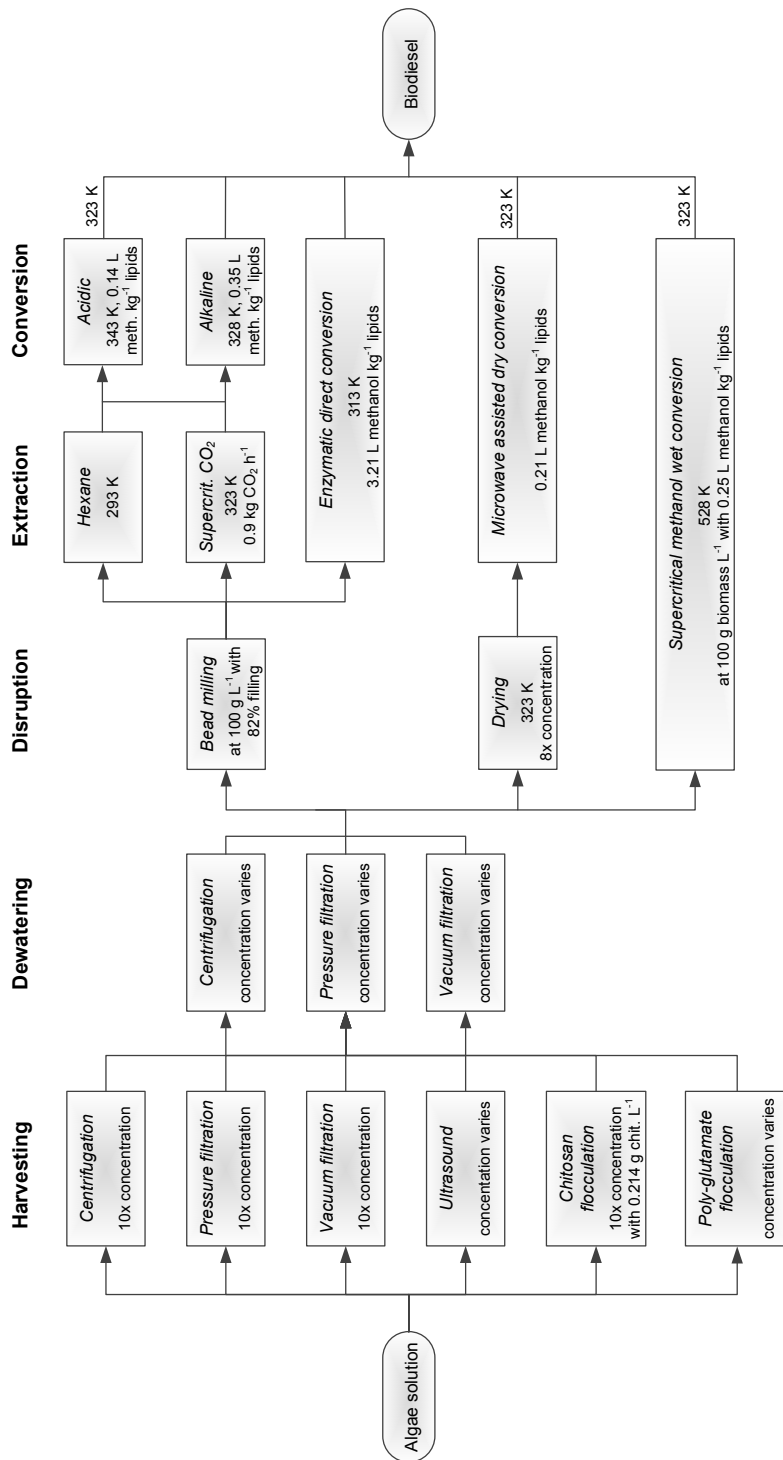


Figure 2. Superstructure of processing units in the downstream processing of microalgae to biodiesel considered in this study. The processing units are described by squares, the start and end by ovals and the lines describe the possible combinations of process units. For each unit the process conditions and outgoing temperatures as used in the combinatorial analysis with fixed process conditions are given (see references [63, 198, 201–209]). Harvesting and dewatering processes are performed at room temperature. The concentration factors for ultrasound and poly-glutamate flocculation are linked to the flow and concentration of the algae solution. Moreover, in the dewatering step the concentration factor is related to the results in the harvesting step. Additional information is given in the appendices.

## Process models

Mass and energy balances form the backbone of the model-based approach. The overall equations (1) and (2) are given below. The general expression for the mass balance for each component is:

$$F_{m,in}C_{X,m,in} + F_{co}C_{X,co,in} = F_{m,out}C_{X,m,out} + F_{co,out}C_{X,co,out} - q_X \quad (1)$$

where  $F$  are the in/out flow rates for the main stream  $m$  and co-streams  $co$  ( $\text{m}^3 \text{s}^{-1}$ ),  $C_X$  the concentration of component  $X$  ( $\text{kg m}^{-3}$ ) in each stream and  $q_X$  the conversion rate ( $\text{kg s}^{-1}$ ). The energy input for each processing unit concerns heating, cooling, pressurising, mixing, specific processing unit requirements, regeneration of solvents and pumping the liquids to the next processing unit. The total energy input rate for each unit operation  $H_{unit}$  ( $\text{J s}^{-1}$ ) is given by:

$$H_{unit} = H_s + H_h + H_c + H_{pr} + H_m + H_r + H_p \quad (2)$$

with  $H_s$  the mechanical energy ( $\text{J s}^{-1}$ ) input for each processing unit,  $H_h$  ( $\text{J s}^{-1}$ ) the energy for heating,  $H_c$  ( $\text{J s}^{-1}$ ) the energy for cooling,  $H_{pr}$  ( $\text{J s}^{-1}$ ) the energy to pressurize the mixture,  $H_m$  ( $\text{J s}^{-1}$ ) the energy for mixing,  $H_r$  ( $\text{J s}^{-1}$ ) the energy to regenerate the solvents and  $H_p$  ( $\text{J s}^{-1}$ ) the energy to pump to the next processing unit.

The key of the process models is to relate mass and energy balance terms to process conditions, such as volumetric and mass flows, biomass concentration, process temperatures and pressure.

Whenever available these relations have been included in the processing unit models as given in Appendix B.

Most of the process models were derived for laboratory or pilot scale equipment. The process models are considered to scale linearly to large-scale conditions. It is also assumed that mechanical heat generated during harvesting, dewatering and disruption is not heating the algae solution, which can be achieved by proper temperature control if needed.

## Combinatorial approach with fixed process conditions

The main process conditions applied in the combinatorial analysis are given in Figure 2. Additional process conditions can be found in Appendix A. The simulations consider the processing of algae from one hectare with a productivity of  $80 \text{ ton ha}^{-1} \text{ year}^{-1}$ , operational time of 330 days a year and biomass concentration of  $2 \text{ kg m}^{-3}$  which leads to a year-round mean algae flow of  $5 \text{ m}^3 \text{ h}^{-1}$  to be processed. The lipid content is taken to be  $0.30 \text{ kg kg}^{-1}$ , so the maximum biodiesel yield is  $3.5 \text{ L h}^{-1}$ . The process conditions are constant and based on literature results (see data of [63, 198, 201-209]).

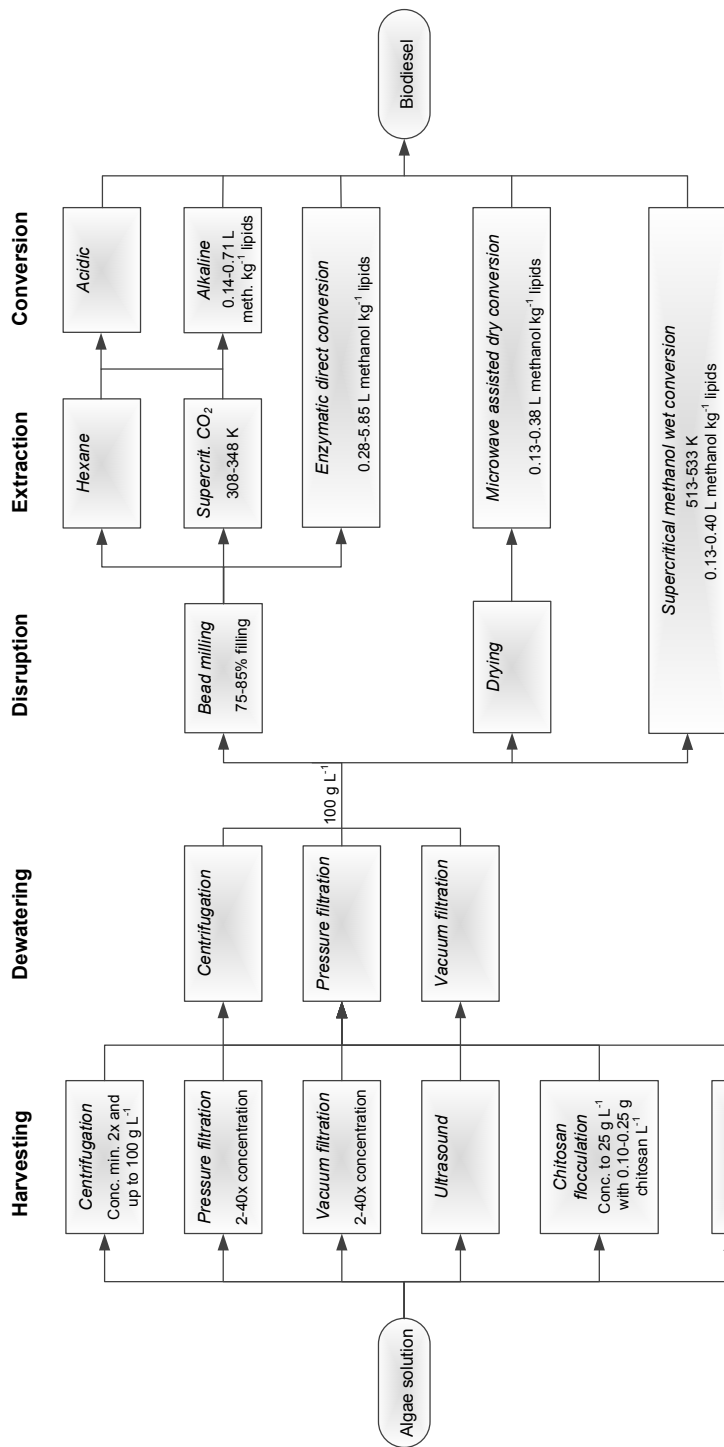


Figure 3. The applied ranges of process conditions in the superstructure optimisation.

The combinatorial approach with fixed process conditions resembles the approach used by Brentner *et al* [63], but in our work the constant process conditions are applied to process models for each processing unit. Therefore, the characteristics of the ingoing algae solution such as biomass concentration and volumetric flow rate affect the model results. The energy requirement, biodiesel yield and net energy ratio (NER) are calculated for each of the routes from the superstructure in Figure 2.

### Combinatorial approach with optimised process conditions

In the optimisation five possible decision variables are employed. These are, where appropriate, the concentration factor – when not defined by a process relation, chitosan concentration, the filling degree of the bead mill (bead filling), extraction temperature and methanol flow. None of the routes has all decision variables, but there is at least one, and at most four at the same time depending upon the route. The concentration factors in ultrasound sedimentation, poly-glutamate flocculation and the dewatering steps are linked to the volumetric flow of algae and the biomass concentration. Thus, in these process models the concentration factor is a function of the process conditions instead of a predefined value. Due to lack of information on the effect on extraction yield or energy use, the extraction temperature in hexane extraction, enzymatic conversion and microwave assisted conversion are not considered as decision variables and the temperature is taken constant based on [63, 207]. The microwave reaction temperature is unknown [210] and not included in the process model.

In the superstructure optimisation the decision variables  $x_d$  are varied to find the maximum NER for each processing route. The NER is the energy of the produced biodiesel divided by the energy used. The optimisation problem is defined as:

$$\text{Find } x_d \quad \forall d \quad (3)$$

$$\text{Such that } NER = Y_{route} / H_{route} \quad \text{is maximised} \quad (4)$$

$$\text{Where } Y_{route} = F_{mass,biodiesel} E_{biodiesel} \quad (5)$$

$$H_{route} = H_{harv} + H_{dew} + H_{drying} + H_{disr} + H_{ext} + H_{conv} \quad (6)$$

$$\text{Subject to } \text{equations B.3-B.62 in Appendix B} \quad (7)$$

$$X_d^{LB} \leq x_d \leq X_d^{UB} \quad (8)$$

$$x_d \in \left\{ \begin{array}{l} \text{concentration factor, chitosan concentration, bead filling,} \\ \text{extraction temperature, methanol flow} \end{array} \right\} \quad (9)$$

Here  $Y_{route}$  (kWh (kg algae hr<sup>-1</sup>)<sup>-1</sup>) is the biodiesel energy gained in the process route from the given inflow of biomass.  $Y_{route}$  is equal to the mass flow of produced biodiesel  $F_{mass,biodiesel}$  (kg (kg algae hr<sup>-1</sup>)<sup>-1</sup>) and the energy content of biodiesel  $E_{biodiesel}$  (kWh kg<sup>-1</sup>) (eq. 4). The energy consumption in the route for the given inflow of biomass  $H_{route}$

(kWh (kg algae hr<sup>-1</sup>)<sup>-1</sup>) is the sum of energy consumption in the used processing units, i.e. harvesting  $H_{harv}$ , dewatering  $H_{dew}$ , drying  $H_{drying}$ , disruption  $H_{disr}$ , extraction  $H_{ext}$ , and conversion  $H_{conv}$  (eq. 5). The optimisation uses the process models as given in Appendix B (eq. 6). The decision variables  $x_d$  are constrained by a lower bound  $X_d^{LB}$  and upper bound  $X_d^{UB}$  (eq. 7) which are given in Figure 3. The possible process routes are defined in a superstructure matrix, which is used to call the process models involved in the 126 routes. The optimisation problem is solved by enumeration with discrete decision variable values over the ranges indicated in Figure 3.

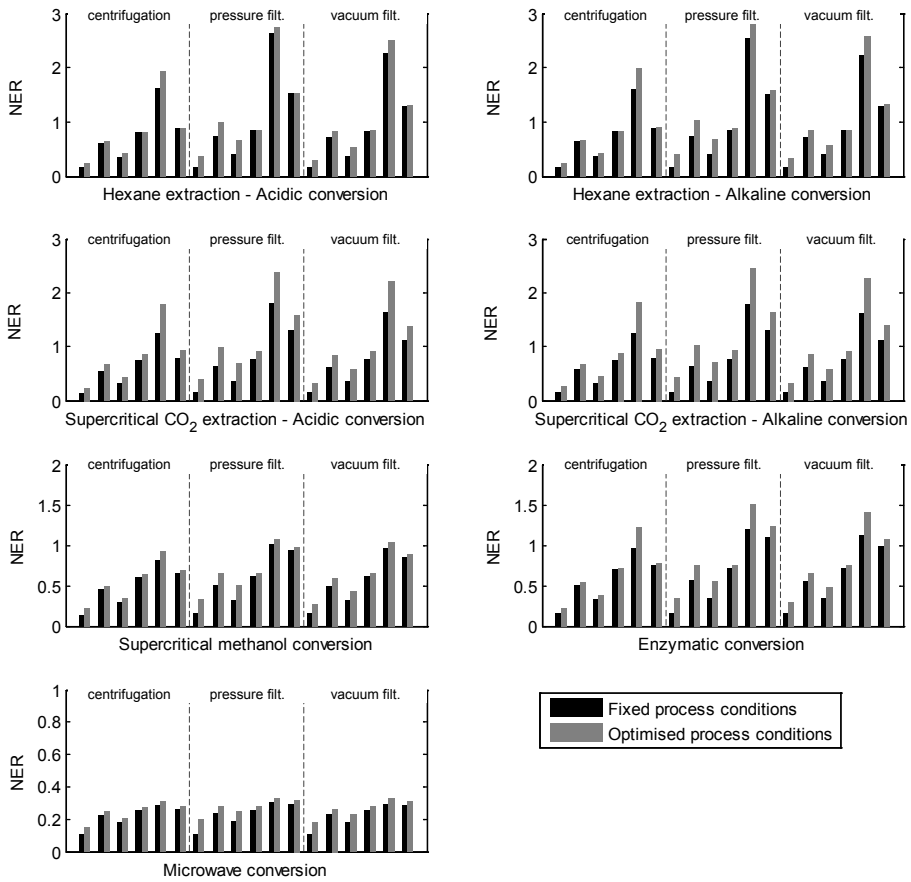


Figure 4. NER of each process route given in the superstructure with fixed (black) and optimised (grey) process conditions. The scales differ between the subplots. Each bar represents one process route. The results are grouped based on the choice for extraction and conversion so each group contains 18 process routes which are further clustered based on the dewatering step. Each cluster contains 6 routes which are ordered by the harvesting step, being 1) centrifugation, 2) pressure filtration, 3) vacuum filtration, 4) ultrasound, 5) chitosan flocculation and 6) polyglutamate flocculation.

## RESULTS AND DISCUSSION

### Evaluation NER

The NER for the fixed and optimised process conditions are shown in Figure 4. The results are grouped based on the choice for extraction and conversion. Both for the fixed (Figure 2) and optimised process conditions (Figure 3) the routes with hexane extraction have the highest NER. Hexane extraction with alkali catalysed conversion achieves the highest NER followed by the acid catalysed conversion. Supercritical CO<sub>2</sub> extraction is the second best group.

Supercritical methanol conversion reaches NERs just above one. Microwave conversion always has a NER below one, which is mainly caused by the drying step. The best routes are those using chitosan flocculation followed by pressure filtration. The worst routes are using two consecutive centrifugations steps. The NER varies widely, even within the seven conversion groups as given in Figure 4.

Optimisation of the process conditions improves for all routes the NER. The improvements in NER are given in Table 3 as percentage compared to the fixed process conditions. Based on the median NER of each group, optimisation of the process conditions leads to at least 8% improvement and goes up to 31%. The group of supercritical CO<sub>2</sub> extraction with acid catalysed conversion improves the most. The best process routes improve up to 38%.

The improvement depends on 1) the quality of the choice for fixed process conditions and 2) on the level of detail in the process models. Less detail means less room for improvement, for example the yields are fixed for hexane extraction and acid catalysed conversion and the energy consumption depends only on the incoming flows.

*Table 3. Increase in NER between fixed and optimised process conditions based on the median values of all 18 routes in each group (median) and for the route with the highest NER (best route) with optimised process conditions compared to that route with fixed process conditions.*

	Median	Best route
Hexane – acidic	8%	5%
Hexane – alkaline	10%	12%
Supercritical CO <sub>2</sub> – acidic	29%	32%
Supercritical CO <sub>2</sub> – alkaline	31%	38%
Supercritical methanol	14%	7%
Enzymatic	16%	25%
Microwave	11%	8%

Optimised process conditions for the best processing route in each group are given in Figure 5. All the best routes first apply chitosan flocculation to concentrate 12.5 times followed by 4 times concentration by pressure filtration.

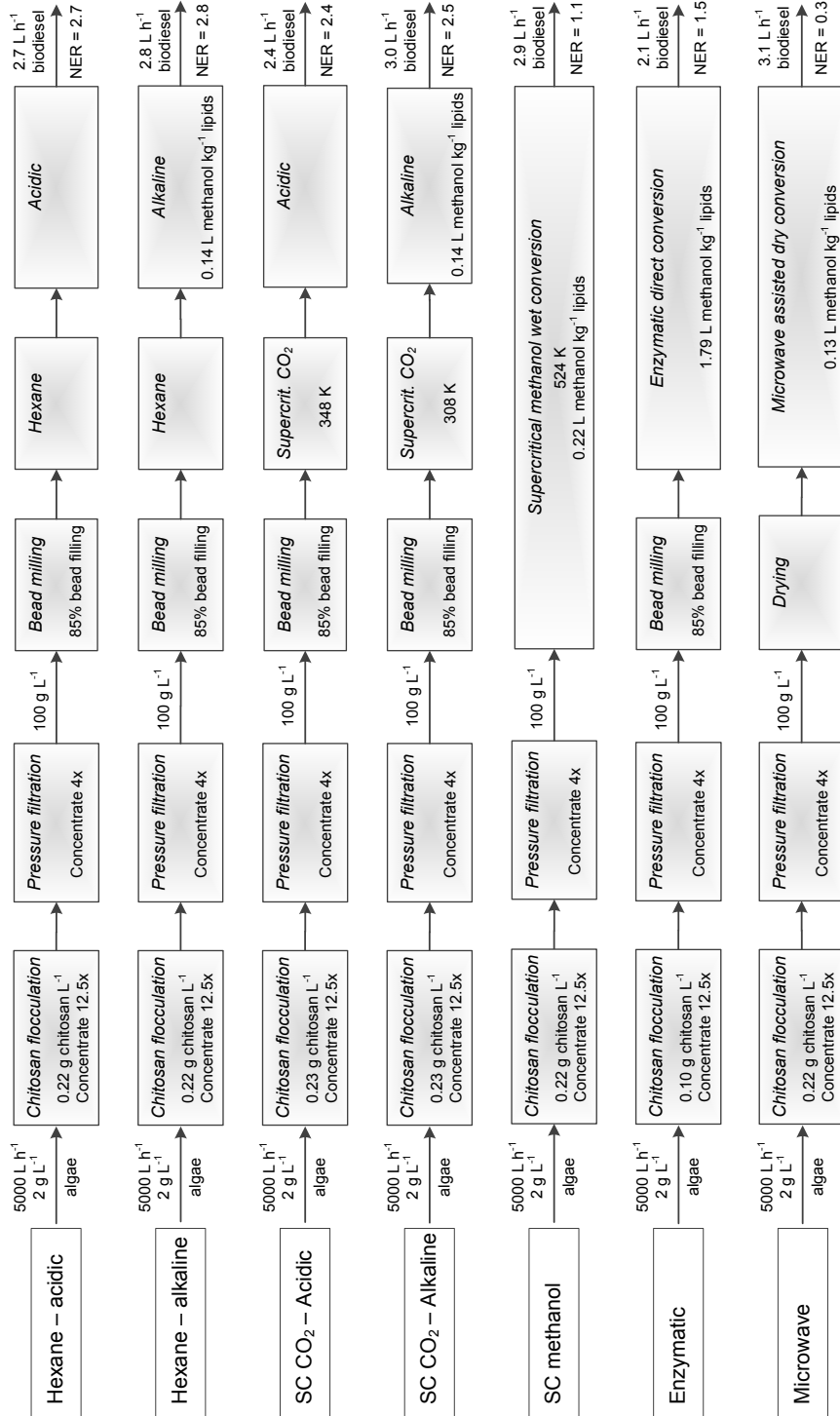


Figure 5. The optimal process conditions for each processing group. Estimated biodiesel yield and NER are given as well.

Chitosan dosages vary between the groups and differ from the fixed dosage of 0.214 kg chitosan m<sup>-3</sup> and extraction temperatures also differ from the fixed process temperature. Biodiesel yields are different for all routes; the lowest biodiesel yield is obtained with enzymatic direct conversion (59% of theoretical yield) and the highest yield with microwave conversion (88% of theoretical yield).

### Bottleneck analysis

The model-based combinatorial approach enables a bottleneck analysis for each process group. Figure 6 illustrates for the best process route in each group given in Figure 5, the relative energy consumption of every processing step as a percentage of the total energy consumption.

Disruption contributes 25-34% to the total energy consumption. For the groups with separate extraction and conversion steps, at least 50% of the energy is consumed by the extraction. Hexane extraction requires most energy for hexane regeneration, while supercritical CO<sub>2</sub> extraction consumes a lot of energy in pressurising the mixture and for mixing. Enzymatic conversion needs 67% of the energy for conversion, which is due to the energy requirements for mixing and solvent regeneration. In supercritical methanol conversion almost all energy is consumed in the conversion steps (95%) for heating the solutions. To achieve a NER above 1.0, significant improvements should be made there. For microwave conversion obviously drying is very energy-intensive and consumes 94% of the total energy required.

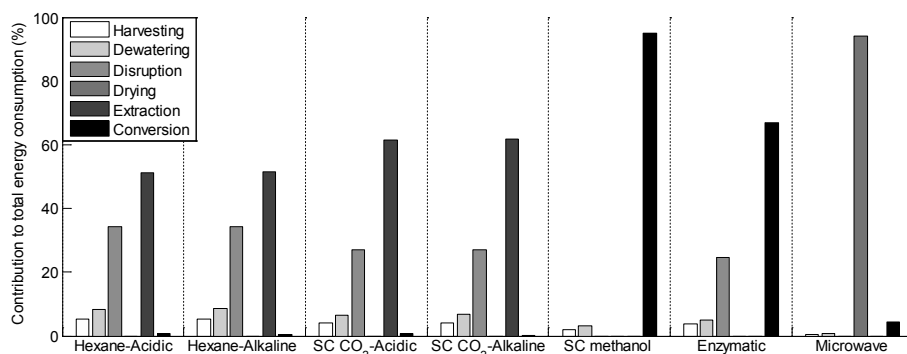


Figure 6. Contribution of process steps to total energy consumption (%) for the best processing route in each process group

It clearly depends on the process route considered which processing steps are the most important to improve. It should be noted that in non-optimal routes other steps can be bottlenecks. Furthermore, the exact contribution depends on the conditions of the ingoing algae stream, i.e. volumetric flow, biomass concentration and lipid content.

## DISCUSSION

The indicated trends in the NER for the 126 routes are discussed in this section. Moreover, the discussion concerns the role of the process models and underlying assumptions.

### Results

To substantiate the model-based method as developed here, a comparison to other published results is useful. A direct comparison is not always possible as routes may differ. The route in this work that resembles the route used by Brentner *et al* (two subsequent centrifugation steps, followed by disruption, hexane extraction and acidic conversion) has a NER of 0.22, which is in the same order of magnitude. The maximum NER achieved with supercritical methanol conversion is slightly higher than 1.0, comparable to the results of Brentner *et al* [63]. In the group of hexane extraction methods the maximum NER with optimized process conditions is 2.8 when preceded by chitosan flocculation, pressure filtration and bead milling and followed by alkali catalysed conversion (route 2 in Figure 5). With fixed process conditions a NER of 2.5 was achieved. This is much higher than the hexane process analysed by Brentner *et al* which has a NER of 0.16. However they considered another processing route that involved centrifugation, drying, disruption by drill pressing, hexane extraction and acidic catalysis. Delrue *et al* [197] found NER values in the range of 0.95-1.26 for process routes with hexane extraction. In their results the energy required for cultivation minus energy recovery from the residual biomass is included, in addition to drying the biomass from 2.5-3.5% to 90% solids content. All together this contributes to a lower NER value than found in our work.

The routes with alkaline conversion perform better in NER and biodiesel yield than those with acidic conversion. Alkaline routes are promising for algae refinery because of the existing industrial experience with these routes [211].

The NER for supercritical methanol conversion with optimised process conditions is low compared to that of the other routes, while this technique is often described as promising (see also Brentner *et al* [63]). However, processing diluted lipid solutions from algae require more energy and have a lower yield than concentrated lipid solutions obtained from other biomass [212].

The NER for microwave conversion is also very low, while often innovative techniques are known for their improved energy usage. The available data were derived from lab-scale experiments and scaled to resemble larger scales of processing. It is expected that in upscaling of this technique significant efficiency improvements can be made.

Our results show a wide variety in NER which depend on the processing steps selected. The effect of biomass productivity in cultivation on the energy demand in the total production of biodiesel has been studied by Sills *et al* [81]. Their results also show large variations in the required process energy between a dry and wet extraction route. In a next step the conditions for algae cultivation such as biomass concentration, volumetric flow and lipid content can be included in the analysis. For very dilute streams from raceway ponds a preharvesting step may be considered.

The comparison shows the high sensitivity of NER values to process routes, which underlines the benefits of model-based combinatorial analysis.

### **Models and assumptions**

All process models are based on overall mass and energy balances that are linked to the process conditions. The relations in the process models for industrial centrifugation, filtration, hexane extraction and acidic conversion of algae biomass are less detailed due to limited availability of experimental information. More data on the effect of process conditions on yield and energy use will assist in more detailed analysis of these process routes. Similarly, any other processing unit can be added to the framework when there is enough information available to relate the process conditions to process yield and energy consumption.

In this study the biomass concentration after dewatering was set to a fixed value. Instead, once more data become available, it can also be used as a decision variable. This can help to improve the NER in the supercritical methanol conversion and microwave assisted conversion.

To deal with the lack of large-scale data and detailed process models, uncertainty and sensitivity analyses are tools to indicate uncertain elements in the framework and models, and to provide a further basis to guide the future development, both of critical process steps, as well as suitable process models.

Currently, disruption is the only process step for which just one processing unit is included.

It is worthwhile to extend the framework with process models for other disruption techniques, such as those that are in use for processing plant materials. However, before this can be done additional experimental knowledge is needed about disruption of unicellular algae cells with rigid cell walls [213].

## **CONCLUSION**

In this work a model-based approach for combinatorial analysis of algae processing is introduced. In contrast to the common use of fixed performance indicators for processing units in literature, the presented model-based approach offers possibilities to take into account the effect of process conditions on the performance of processing routes. It is demonstrated that the framework can be applied to identify promising process routes and also to indicate bottlenecks that should be studied further. The results show that optimisation of the process conditions for algae biodiesel production leads to at least a 5% higher NER, and can go up to 38%.

The analysis shows that each main production route has a different NER and limiting processing step. Stand-alone optimisation of a bottleneck step in a particular route does not necessarily yield good results in another route. Therefore, tailor-made improvements in process unit design should be made.

In the current work, laboratory and pilot data from frequently used refinery units is used. The developments in this field are fast and new information is expected to be generated in the nearby future. The proposed approach provides the flexibility to incorporate new information and to explore new process designs. In addition, when more accurate process models for (large-scale) processing units become available from new data, they can easily be incorporated, thus improving the accuracy of the predicted NER values.

This work illustrates the potential of this model-based approach for process design and can also be linked to other performance indicators such as economics, material inputs or greenhouse warming potential.

## **ACKNOWLEDGEMENT**

This work was performed in the cooperation framework of Wetsus, centre of excellence for sustainable water technology ([www.wetsus.nl](http://www.wetsus.nl)). Wetsus is co-funded by the Dutch Ministry of Economic Affairs and Ministry of Infrastructure and Environment, the European Union Regional Development Fund, the Province of Fryslân, and the Northern Netherlands Provinces. The authors like to thank the participants of the research theme Algae for the discussions and their financial support. We thank Mrs. L.B. Brentner for the interesting discussions on downstream processing of algae to biodiesel.

## APPENDIX A. PROPERTIES, PROCESS CONDITIONS AND SPECIFIC ENERGY USE

The physical properties of microalgae biomass, oil and biodiesel are given in Table A1. The specific energy requirements for some processing units are given in Table A2. The fixed process conditions are given in Table A3.

Table A1. Properties of microalgae biomass, oil and biodiesel.

	Value	Reference
Density microalgae biomass (kg m <sup>-3</sup> )	1050	[201]
Density microalgae biodiesel (kg m <sup>-3</sup> )	864	[213]
Density microalgae oil (kg m <sup>-3</sup> )	918	Similar to soybean oil [214]
Energy content microalgae biodiesel (J kg <sup>-1</sup> )	41·10 <sup>6</sup>	[213]
Heat capacity microalgae biomass (J kg <sup>-1</sup> K <sup>-1</sup> )	4181.3	Equal to water
Heat capacity microalgae oil (J kg <sup>-1</sup> K <sup>-1</sup> )	1670	Equal to vegetable oil
Molecular weight microalgae biodiesel (kg mol <sup>-1</sup> )	0.287	[215]
Molecular weight microalgae oil (kg mol <sup>-1</sup> )	0.789	[207]

Table A2. Specific energy requirements for some processing units.

Process	Specific energy requirement (MJ m <sup>-3</sup> of inflow)	Energy input per apparatus (W unit <sup>-1</sup> ) [Maximum throughput] (m <sup>3</sup> day <sup>-1</sup> )	Reference
Centrifugation	12.0		[199]
Pressure filtration	2.0		Average from [198, 199]
Vacuum filtration	4.4		Average from [198, 199]
Flocculation	0.36		[63]
<i>Chitosan &amp; poly-glutamate</i>			
Bead milling		3300 [10.8]	[204]
Ultrasound sedimentation		30 [432.0]	[216]
Microwave assisted conversion		1400 [345.6]	[210]

Table A3. Standard process conditions. The decision variable values are given in Figure 2

Processing unit	Pressure (bar)	Residence time (min)	Stirring speed (rpm)	Other conditions	Reference
Ultrasound sedimentation		3			[201]
Chitosan flocculation			150		[202]
Poly-glutaminate flocculation				0.022 kg polyglutaminate m <sup>-3</sup> , 20 kg salt m <sup>-3</sup>	[203]
Bead milling				beads 0.5 mm, 14 m s <sup>-1</sup> velocity	[204]
Supercritical CO <sub>2</sub> extraction	225	180	600	3 hexane: 1 methanol, 15 g CO <sub>2</sub> min <sup>-1</sup>	[205, 206]
Acidic conversion		60	600		[63, 206]
Alkaline conversion		60	600	0.0088 kg catalyst kg <sup>-1</sup> lipids	[206]
Enzymatic direct conversion		2880	600		[207]
Microwave assisted conversion		10	1000	0.057 kg catalyst kg <sup>-1</sup> lipids	[192]
Supercritical methanol conversion	82.7	30	600		[208, 209]

## APPENDIX B. MASS AND ENERGY BALANCES FOR PROCESSING UNITS

The general expression for the mass balance for each component is:

$$F_{m,in}C_{X,m,in} + F_{co}C_{X,co,in} = F_{m,out}C_{X,m,out} + F_{co,out}C_{X,co,out} - q_X \quad (\text{B.1})$$

where  $F$  are the in/out flow rates for the main stream  $m$  and co-streams  $co$  ( $\text{m}^3 \text{s}^{-1}$ ),  $C_X$  the concentration of component  $X$  ( $\text{kg m}^{-3}$ ) in each stream and  $q_X$  the conversion rate ( $\text{kg s}^{-1}$ ). The total energy input rate for each unit operation  $H_{unit}$  ( $\text{J s}^{-1}$ ) is given by:

$$H_{unit} = H_s + H_h + H_c + H_{pr} + H_m + H_r + H_p \quad (\text{B.2})$$

with  $H_s$  the mechanical energy ( $\text{J s}^{-1}$ ) input for each processing unit,  $H_h$  ( $\text{J s}^{-1}$ ) the energy for heating,  $H_c$  ( $\text{J s}^{-1}$ ) the energy for cooling,  $H_{pr}$  ( $\text{J s}^{-1}$ ) the energy to pressurize the mixture,  $H_m$  ( $\text{J s}^{-1}$ ) the energy for mixing,  $H_r$  ( $\text{J s}^{-1}$ ) the energy to regenerate the solvents and  $H_p$  ( $\text{J s}^{-1}$ ) the energy to pump to the next processing unit.

### B.1 Pumping

The pumping energy to transport the algae, lipid or biodiesel slurry between process units is considered for every processing unit. The energy input rate is derived from the Bernoulli equation:

$$H_p = 2f_F \rho_A \frac{F_A^3 L}{A^2 d} \quad (\text{B.3})$$

Where  $f_F$  is the Fanning friction factor,  $L$  the length of the tube (m),  $A$  is the cross-sectional area ( $\text{m}^2$ ),  $d$  is the diameter of the tube (m) and  $Re$  is the Reynolds number. The fanning friction factor for laminar flow of viscous algae solutions is calculated with:

$$f_F = \frac{16}{Re} \quad (\text{B.4})$$

A modified Reynolds number which takes the rheological properties of the algae solution into account is given by Wileman *et al* [199]:

$$Re = \frac{\rho_a v^{2-n} d^n}{8^{n-1} K} \quad (\text{B.5})$$

Where  $v$  is the velocity ( $\text{m s}^{-1}$ ),  $K$  is the consistency factor ( $\text{Poise m}^{-1}$ ) and  $n$  is the behaviour index which depends on the biomass concentration;  $n=1$  below  $C_A = 50 \text{ kg m}^{-3}$  and  $n=0.8$  above that. The consistency factor  $K$  is based on the average as given in Wileman *et al* [199]:

$$K = \left( 7 + \frac{C_A}{\sqrt{1 + 0.005(C_A - 100)^2}} \right) 10^{-4} \quad (\text{B.6})$$

With the algae concentration  $C_A$  ( $\text{kg m}^{-3}$ ).

## B.2 Harvesting and dewatering

During harvesting microalgae are separated from the cultivation solution by mechanical separation or by flocculation. Both harvest systems are described by the following mass balance and additional equations:

$$0 = F_{A,in} C_{A,in} - F_{A,out} C_{A,out} - F_{A,waste} C_{A,waste} \quad (B.7)$$

$$C_{A,out} = C_{A,in} Cf \quad (B.8)$$

$$F_{A,out} = \frac{F_{A,in} C_{A,in} R}{C_{A,out}} \quad (B.9)$$

$$C_{A,waste} = \frac{F_{A,in} C_{A,in} (1-R)}{F_{A,in} - F_{A,out}} \quad (B.10)$$

Where  $F$  is the volumetric flow rate ( $\text{m}^3 \text{s}^{-1}$ ),  $C$  the concentration ( $\text{kg m}^{-3}$ ),  $Cf$  is the concentration factor (-) and  $R$  the microalgae recovery ( $\text{kg kg}^{-1}$ ). The subscript  $A$  indicates algae and  $waste$  the waste stream.

The energy requirements for harvesting are:

$$H_{harv} = H_s + H_p \quad (B.11)$$

Values for are given in Table A2, the energy requirements for pumping in Appendix B1. The processing units centrifugation, pressure filtration and vacuum filtration are also used as dewatering step for further concentration of the algae solution.

### B.2.1 Mechanical harvesting

A microalgae recovery of 95 % is expected for all mechanical harvesting processes considered [63]. The desired concentration factor is given as input. According to Wileman *et al* [199] the energy input is:

$$H_s = EF_{A,in} Cf \quad (B.12)$$

With  $E$  ( $\text{J m}^{-3}$ ) the specific energy requirement for each process, as given in Table A2.

### B.2.2 Ultrasound sedimentation

Ultra-sound sedimentation is a novel harvesting technique. The surface response model from Bosma *et al* [201] is used to estimate the recovery  $R$  (eq. B.13) and concentration factor  $Cf$  (eq. B.14):

$$R = 0.75 + 1.2 \cdot 10^{-9} C_{A,in}^* + 0.052 F_{A,in}^* - 3.3 \cdot 10^{-3} \tau^* + 3.2 \cdot 10^{-3} H^* - 4.1 \cdot 10^{-3} F_{A,in}^{*2} + 8.5 \cdot 10^{-6} \tau^{*2} - 6.6 \cdot 10^{-11} C_{A,in}^* F_{A,in}^* - 1.4 \cdot 10^{-10} C_{A,in}^* H^* + 2.7 \cdot 10^{-3} F_{A,in}^* H^* \quad (B.13)$$

$$Cf = 18 - 2.7 \cdot 10^{-8} C_{A,in}^* + 1.3 F_{A,in}^* - 1.6 \left( \frac{F_{A,out}}{F_{A,in}} \right)^* - 0.077 F_{A,in}^{*2} + 3.1 \cdot 10^{-9} C_{A,in}^* \left( \frac{F_{A,out}}{F_{A,in}} \right)^* \quad (B.14)$$

In which  $C_{A,in}^*$ ,  $F_{A,in}^*$ ,  $\tau^*$  and  $H^*$  are coded values as used by [201] for the algae concentration, flow rate, residence time (min) and energy input (J s<sup>-1</sup>):

$$C_{A,in}^* = \frac{C_{A,in} - 17}{16} \quad (\text{B.15})$$

$$F_{A,in}^* = \frac{F_{A,in} - 10}{8} \quad (\text{B.16})$$

$$\tau^* = \frac{\tau - 180}{120} \quad (\text{B.17})$$

$$H^* = \frac{H_s - 6}{82} \quad (\text{B.18})$$

$$\left( \frac{F_{A,out}}{F_{A,in}} \right)^* = \frac{\frac{F_{A,out}}{F_{A,in}} - 6}{4} \quad (\text{B.19})$$

The energy requirement results of Bosma *et al* [201] of 0.018 m<sup>3</sup> day<sup>-1</sup> at 8 W unit<sup>-1</sup> in the BioSep are scaled to larger ultrasound sedimentation devices with a capacity of 432 m<sup>3</sup> day<sup>-1</sup> at 30 W unit<sup>-1</sup> [216].

### B.2.3 Flocculation

The energy input for flocculation is mainly used for mixing and is given by:

$$H_s = E(F_{A,in} + F_{F,in}) \quad (\text{B.20})$$

The specific energy requirement is given in Table A2.

The flocculation efficiency of chitosan flocculation is expressed by a polynomial expression derived by Riano *et al* [202]:

$$R = (84.3 + 17.5C_F^* - 1.3S^* - 11.1C_F^{*2} - 3.7S^{*2} - 2.6C_F^*S^*)10^{-2} \quad (\text{B.21})$$

Where  $C_F^* = \frac{C_F - 0.128}{0.086}$  and  $S^* = \frac{S - 325}{194}$ , with  $C_F$  the flocculant concentration (kg m<sup>-3</sup>) and  $S$  stirring speed (rpm). The processing conditions are related to those applied by Riano *et al* [202]. The recovery cannot get below zero.

In poly-glutamate flocculation the microalgae recovery and concentration factor are affected by biomass concentration, poly-glutamate concentration and salinity  $C_{salt}$  (kg m<sup>-3</sup>). The recovery  $R$  is given by equation B.22 and the concentration factor  $Cf$  by equation B.23, based on Zheng *et al* [203]:

$$R = (336.2 + 48.9C_F^* + 45.1C_A^* + 3.4C_{salt} - 1.2C_F^{*2} - 23.7C_A^{*2} - 0.1C_{salt}^2 + 1.0C_F^*C_A^* + 0.1C_F^*C_{salt} - 3.5C_A^*C_{salt})10^{-3} \quad (\text{B.22})$$

$$Cf = 17.57 + 4.56C_F^* - 3.28C_A^* - 0.55C_{salt}^* - 0.12C_F^{*2} - 1.45C_A^{*2} - 5.010^{-3}C_{salt}^{*2} - 0.14C_F^*C_A^* + 0.02C_F^*C_{salt}^* - 0.14C_A^*C_{salt}^* \quad (\text{B.23})$$

$C_A^*$  and  $F_A^*$  are coded values in the regression model of [203] and are defined as:

$$C_F^* = \frac{C_F - 20}{5000} \quad (\text{B.24})$$

$$C_A^* = \frac{C_A - 1}{0.5} \quad (\text{B.25})$$

$$C_{salt}^* = \frac{C_{salt} - 20}{10} \quad (\text{B.26})$$

### B.3 Drying

In thermal drying heat is used to evaporate water from the algae slurry, the algae mass balance is given by:

$$0 = F_{A,in} C_{A,in} - F_{A,out} C_{A,out} \quad (\text{B.27})$$

$$C_{A,out} = C_{A,in} C_f \quad (\text{B.28})$$

Drying of algae to a solid content of 800 kg algae m<sup>3</sup> is required for the microwave conversion.

The energy input rate for convective thermal drying is:

$$H_{drying} = H_h + H_s + H_p \quad (\text{B.29})$$

$$H_h = F_{A,in} \rho_A c p_A (T_s - T_{in}) \quad (\text{B.30})$$

$$H_s = \Delta H_{vap} F_w \rho_w \frac{(T_a - T_s)}{(T_a - T_{in})} \quad (\text{B.31})$$

Where  $\Delta H_{vap}$  the heat of evaporation for water (J kg<sup>-1</sup>), the amount of evaporated water (m<sup>3</sup>),  $T_a$  the temperature of heated air (°C),  $T_s$  the temperature in the dryer and of the outgoing stream (°C),  $T_{in}$  the temperature of ingoing algae solution (°C),  $(T_a - T_s)/(T_a - T_{in})$  expresses the energy efficiency in drying.

### B.4 Disruption

The mass balance for disruption relates the released lipids to the lipid content of the microalgae.

The mass balance for lipids is given by:

$$0 = F_A C_{A,in} f_L - F_A C_{L,release} - F_A C_{L,algae} \quad (\text{B.32})$$

$$C_{L,release} = C_{A,in} D f_L \quad (\text{B.33})$$

$$C_{L,algae} = C_{L,in} (1 - D) f_L \quad (\text{B.34})$$

Where  $f_L$  is the algae oil content (kg kg<sup>-1</sup>) and  $D$  the disruption efficiency (kg kg<sup>-1</sup>). The subscript  $L$  is for lipids. *Release* indicates the released lipids and *algae* the lipids remained in intact algae cells.

The degree of disruption  $D$  for bead milling has been derived by Doucha *et al* [204] and is given by:

$$D = 17.48 F_{A,in}^{n_1} d_b^{n_2} B^{n_3} v^{n_4} C_{A,in}^{n_5} \quad (\text{B.35})$$

Where  $d_b$  is the diameter of the beads (mm),  $B$  the percentage of the chamber that is filled with beads (%) and  $v$  the rotation speed (m s<sup>-1</sup>). The constants are  $n_1 = -0.0356$ ,  $n_2 = 0.326$ ,  $n_3 = 0.0768$ ,  $n_4 = 0.248$ ,  $n_5 = -0.763$ . The energy input rate is given by the following equation:

$$H_{disr} = H_s + H_p \quad (\text{B.36})$$

The process conditions are related to the maximum feasible flow rate at lab conditions of 0.96 m<sup>3</sup> day<sup>-1</sup> [204]. The total number of bead mills is based on the maximum flow for large-scale systems, which is 10.8 m<sup>3</sup> day<sup>-1</sup> [204].

## B.5 Extraction

The lipid mass balance for extraction is:

$$0 = F_A C_{L,in} - F_{waste} C_{L,waste} - F_L C_{L,out} \quad (\text{B.37})$$

$$C_{L,out} = \frac{F_A C_{L,in} Y_L}{F_L} \quad (\text{B.38})$$

$$C_{L,waste} = \frac{F_A C_{L,in} (1 - Y_L)}{F_{waste}} \quad (\text{B.39})$$

Where  $Y_L$  is the extracted lipid yield (kg kg<sup>-1</sup> lipids). The lipid yield depends on the process parameters as discussed below.

### B.5.1 Hexane extraction

Process models on algae lipid extraction yields with hexane extraction are not available. Therefore a fixed extraction yield of 91% at 20°C was assumed [63]. The hexane dosage is 15 v/v % of the algae solution [217]. The energy input rate is given by:

$$H_{ext} = H_h + H_m + H_r + H_p \quad (\text{B.40})$$

The heating input rate is expressed as:

$$H_h = \sum_X c p_X \rho_X F_X (T_s - T_X) \quad (\text{B.41})$$

Where  $X$  represents the each component  $X$ .

The input rate for mixing is given by Wesselingh and Krijgsman [218]:

$$H_m = \left( \sum_X F_X \rho_X \right) k_{power} \rho_{av} u^3 \left( \frac{1}{2} \sqrt[3]{ \left( 4 \sum_X F_X \frac{\tau}{\pi} \right) } \right)^5 \quad (\text{B.42})$$

With the power constant  $k_{power}$  equal to 0.4, the average density  $\rho_{av}$  (kg m<sup>-3</sup>), the stirrer speed  $u$  (s<sup>-1</sup>) and the residence time  $\tau$  (s).

The energy input for hexane regeneration is [218]:

$$H_r = (5+1) F_x \frac{\rho_X}{MW_X} \quad (\text{B.43})$$

### B.5.2 Supercritical CO<sub>2</sub> extraction

The extraction yield with supercritical CO<sub>2</sub> was derived by Char *et al* [205] as a function of the temperature, pressure and the ratio between hexane and methanol:

$$Y_L = (0.57 - 1.44T^* + 1.38p^* + 0.61r_{HM}^* + 1.07T^{*2} + 0.64p^{*2} + 0.81r_{HM}^{*2} - 0.19T^*p^* + 4.3 \cdot 10^{-3}r_{HM}^*T^* + 0.44r_{HM}^*p^*) / 5.03 \quad (\text{B.44})$$

Where  $r_{HM}^*$  is the ratio between hexane and methanol. The yield is relative to the maximum extractable yield of lipids. The maximum yield is set to one.  $T^*$  and  $p^*$  are coded values from [205] based on the temperature  $T$  (K) and the pressure  $p$  (bar):

$$T^* = \frac{(T_s - 273) - 50}{10} \quad (\text{B.45})$$

$$p^* = \frac{p - 225}{75} \quad (\text{B.46})$$

$$r_{HM}^* = \frac{r_{HM} - 2}{1} \quad (\text{B.47})$$

With  $T_s$  (K) the temperature in the system. The energy input rate for supercritical carbon dioxide extraction is given by:

$$H_{ext} = H_h + H_{pr} + H_m + H_p \quad (\text{B.48})$$

Regeneration of hexane and methanol is not required at the temperature is above the boiling points of these components which are 70°C and 65°C respectively. The energy for pressurising is calculated based on the total volume flow and the pressure by [218]:

$$H_{pr} = (F_A + F_{CO2} + F_H + F_M)p \cdot 10^5 \quad (\text{B.49})$$

### B.6 Conversion

The conversion of algae lipids to biodiesel using catalysts is described by mass balances for lipids  $L$  (eq. B.50), biodiesel  $B$  (eq. B.51) and methanol  $M$  (eq. B.52 & 53):

$$0 = F_L C_{L,in} - F_L C_{L,out} - q_L \quad (\text{B.50})$$

$$0 = q_L \frac{Y_{BL} MW_B}{MW_L} - F_L C_{B,out} \quad (\text{B.51})$$

$$0 = F_{M,in} \rho_M - F_{M,out} \rho_M - q_M \quad (\text{B.52})$$

$$q_M = q_L \frac{y_{ML} MW_M}{MW_L} \quad (\text{B.53})$$

Where  $q_L$  is the lipid conversion rate (kg s<sup>-1</sup>),  $q_M$  the methanol consumption rate (kg s<sup>-1</sup>),  $MW$  the molecular weight (kg mol<sup>-1</sup>),  $Y_{BL}$  the biodiesel production yield (kg biodiesel kg<sup>-1</sup> lipids) and  $y_{ML}$  the ratio of methanol consumed per lipid (kg kg<sup>-1</sup>).  $Y_{BL}$ ,  $y_{ML}$  and  $q_L$  depend on process conditions and specific process choices as described in the sections below.

The energy input rate for the conversion processes is given by:

$$H_{conv} = H_h + H_m + H_r + H_p \quad (\text{B.54})$$

Where  $H_h$ ,  $H_m$  and  $H_r$  are derived from equations B.41-B.43. Regeneration is only considered for process temperatures below the boiling point of methanol (65°C).

### B.6.1 Acid catalysed transesterification

In this process the conversion is catalysed by hydrochloric acid. At 70°C 98% of the lipids are converted to biodiesel [63].

### B.6.2 Alkali catalysed transesterification

The lipid yield from alkali catalysed transesterification is based on the results for rice bran oil by Rashid *et al* [206]:

$$Y_{BL} = -2.22 - 0.016r_{ML} + 0.063c_{cat} + 2.92T_{cel,s} + 2 \cdot 10^{-4}\tau + 3 \cdot 10^{-4}r_{ML}^2 - 5 \cdot 10^{-4}c_{cat}^2 - 1.37T_{cel,s}^2 - 3 \cdot 10^{-5}\tau^2 + 6 \cdot 10^{-4}r_{ML}c_{cat} - 8 \cdot 10^{-4}r_{MA}T_{cel,s} - 3 \cdot 10^{-4}r_{ML}\tau - 0.010c_{cat}T_{cel,s} + 8 \cdot 10^{-5}c_{cat}\tau + 2.1 \cdot 10^{-3}T_{cel,s}\tau \quad (\text{B.55})$$

Where  $r_{ML}$  is the molar ratio between methanol and algae oil (kg m<sup>-3</sup>),  $c_{cat}$  the catalyst concentration (%),  $T_{cel,s}$  the reaction temperature (°C) and  $\tau$  the residence time (min). In this work the catalyst concentration is not considered as decision variable.

### B.6.3 Enzymatic transesterification

The extraction of lipids and conversion to biodiesel is considered simultaneously with lipase-catalysed transesterification [207]. The conversion yield is given by Tran *et al* [207] by using the relation:

$$Y_{BL} = \frac{r_{ML}}{70} \exp\left(1 - \frac{r_{ML}}{70}\right) \quad (\text{B.56})$$

### B.6.4 Microwave assisted conversion

Microwave assisted conversion combines extraction and conversion and does not need separate disruption but requires dried biomass as input. The biodiesel yield from dry algae biomass  $Y_{BA}$  (kg biodiesel kg<sup>-1</sup> dry algae) is given by by Patil *et al* [210]:

$$Y_{BA} = (260 + 32.0H^* + 35.0c_{cat}^* + 7.1r_{AM}^* + 11.0\tau^* + 6.9H^*c_{cat}^* + 5.2H^*r_{AM}^* + 7.5H^*\tau^* + 8.3c_{cat}^*r_{AM}^*)10^{-3} \quad (\text{B.57})$$

With

$$H^* = \frac{H_s - 1050}{350} \quad (\text{B.58})$$

$$c_{cat}^* = \frac{c_{cat} - 2}{1} \quad (\text{B.59})$$

$$r_{AM}^* = \frac{r_{AM} - 12}{3} \quad (\text{B.60})$$

$$\tau^* = \frac{\tau - 7}{3} \quad (\text{B.61})$$

$c_{cat}$  (%) is the catalyst concentration and  $r_{AM}$  (kg m<sup>-3</sup>) the ratio algae methanol. The catalyst concentration is not considered as decision variable in this work.

For scale-up the microwave units are assumed to deal with continuous flows. The total number of apparatus required is based on the maximum current capacity without dissipation of heat energy. The energy input rate for the overall process is:

$$H_{conv} = H_s + H_m + H_p \quad (\text{B.62})$$

### B.6.5 Supercritical methanol conversion

Supercritical methanol conversion combines disruption, extraction and conversion. Drying the biomass is not necessary. The biodiesel yield is given by as suggested by Patil *et al* [209]:

$$Y_{BL} = (77 + 11T^* + 7.1r_{AM}^* + 11\tau^* - 20T^{*2} - 10r_{AM}^{*2} + 6.6\tau^{*2} + 5.6T^*r_{AM}^* - 4.7T^*\tau^* - 2.0r_{AM}^*\tau^*)10^{-2} \quad (\text{B.63})$$

With the accompanying code equations as derived by [209]:

$$T^* = \frac{T_s - 250}{10} \quad (\text{B.64})$$

$$r_{AM}^* = \frac{r_{AM} - 8}{4} \quad (\text{B.65})$$

$$\tau^* = \frac{\tau - 20}{10} \quad (\text{B.66})$$

The energy input rate is given by:

$$H_{conv} = H_h + H_c + H_{pr} + H_m + H_p \quad (\text{B.67})$$

With  $H_c$  the input rate for cooling the biodiesel:

$$H_c = cp_F \rho_F F_{XF} (T_s - T_{out}) \quad (\text{B.68})$$

The other energy input rates are calculated based on equations S.3, S.41, S.43 and S.49.

## Nomenclature for appendix

$A$	cross-sectional area ( $\text{m}^2$ )
$B$	percentage of bead mill chamber filled with beads (%)
$C$	concentration ( $\text{kg m}^{-3}$ )
$c_{cat}$	catalyst concentration (%)
$Cf$	concentration factor (-)
$cp$	heat capacity ( $\text{J kg}^{-1} \text{K}^{-1}$ )
$D$	disruption efficiency ( $\text{kg kg}^{-1}$ )
$d$	diameter of the tube (m)
$d_b$	diameter of the beads
$E$	specific energy requirement for each process ( $\text{J m}^{-3}$ )
$F$	Volumetric flow rate ( $\text{m}^3 \text{s}^{-1}$ )
$f_F$	Fanning friction factor
$f_L$	algae oil content ( $\text{kg kg}^{-1}$ )
$H$	energy input rate ( $\text{J s}^{-1}$ )
$K$	consistency factor (Poise $\text{m}^{-1}$ )
$k_{power}$	power constant
$L$	tube length (m)
$MW$	molecular weight ( $\text{kg mol}^{-1}$ )
$n$	behaviour index for pumping
$p$	pressure (bar)
$q_L$	lipid conversion rate ( $\text{kg s}^{-1}$ )
$q_M$	methanol consumption rate ( $\text{kg s}^{-1}$ )
$R$	microalgae recovery ( $\text{kg kg}^{-1}$ )
$r_{AM}$	ratio between algae and methanol ( $\text{kg m}^{-3}$ )
$Re$	Reynolds number
$r_{HM}$	ratio between hexane and methanol
$r_{LM}$	ratio between lipids and methanol ( $\text{kg m}^{-3}$ )
$S$	stirring speed (rpm)
$T$	temperature (K)
$T_{cel}$	temperature ( $^{\circ}\text{C}$ )
$u$	stirrer speed ( $\text{m s}^{-1}$ )
$v$	velocity ( $\text{m s}^{-1}$ )
$Y_{BA}$	biodiesel yield from dry biomass ( $\text{kg biodiesel kg}^{-1}$ dry algae)
$Y_{BL}$	biodiesel yield ( $\text{kg biodiesel kg}^{-1}$ lipids)
$Y_L$	lipid extraction yield ( $\text{kg kg}^{-1}$ )
$y_{ML}$	ratio of methanol consumed per lipid
$\Delta H_{vap}$	heat of evaporation ( $\text{J kg}^{-1}$ )
$\rho$	density ( $\text{kg m}^{-3}$ )
$\tau$	residence time (s)

### Subscripts

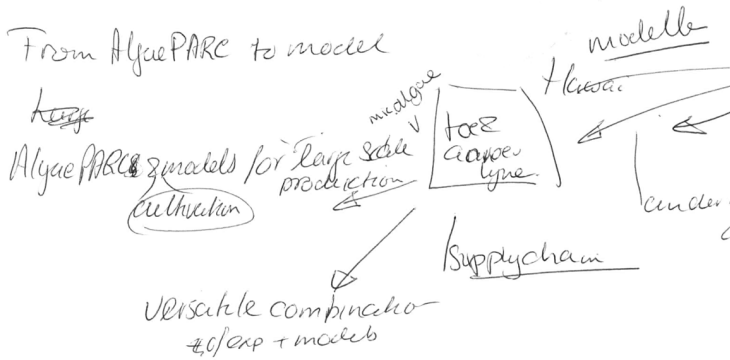
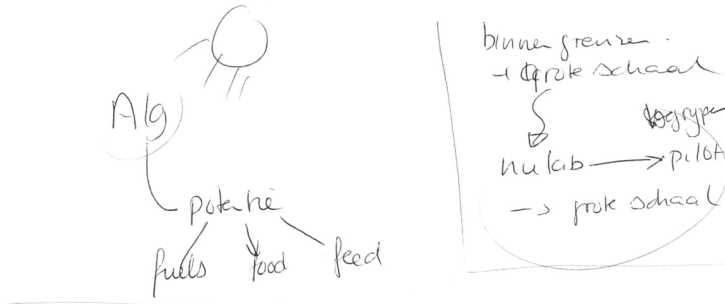
$A$	algae
$algae$	remaining in algae cells
$av$	average

<i>B</i>	biodiesel
<i>c</i>	cooling
<i>CO<sub>2</sub></i>	carbon dioxide
<i>conv</i>	conversion
<i>dew</i>	dewatering
<i>disr</i>	disruption
<i>drying</i>	drying
<i>ext</i>	extraction
<i>F</i>	flocculant
<i>h</i>	heating
<i>H</i>	hexane
<i>harv</i>	harvesting
<i>in</i>	ingoing
<i>L</i>	lipids
<i>m</i>	mixing
<i>M</i>	methanol
<i>out</i>	outgoing
<i>p</i>	pumping
<i>pr</i>	pressurising
<i>r</i>	regeneration of solvents
<i>Release</i>	released lipids
<i>route</i>	for the process route
<i>s</i>	for the specific processing unit
<i>salt</i>	salinity
<i>W</i>	water
<i>waste</i>	waste
<i>X</i>	component X

### **Superscripts**

\* coded value

# FOOD COMMODITIES FROM MICROALGAE



THIS CHAPTER IS PUBLISHED AS:

R.B. DRAAISMA, R.H. WIJFFELS, P.M. SLEGGERS, L.B. BRENTNER, A. ROY, M.J. BARBOSA  
 FOOD COMMODITIES FROM MICROALGAE

CURRENT OPINION IN BIOTECHNOLOGY (2013),24 (SPECIAL ISSUE: FOOD BIOTECHNOLOGY): 169-177

## **ABSTRACT**

The prospect of sustainable production of food ingredients from photoautotrophic microalgae was reviewed. Clearly, there is scope for microalgae oils to replace functions of major vegetable oils, and in addition to deliver health benefits to food products. Furthermore, with a limited production surface, a substantial portion of the European Union market could be supplied with edible oils and proteins from microalgae. Yet, before microalgae ingredients can become genuinely sustainable and cost effective alternatives for current food commodities, major breakthroughs in production technology and in biorefinery approaches are required. Moreover, before market introduction, evidence on safety of novel microalgae ingredients, is needed. In general, we conclude that microalgae have a great potential as a sustainable feedstock for food commodities.

## INTRODUCTION

In a biobased economy, agricultural crops are not only used for production of food and feed but also for chemicals, materials and biofuels. Due to the scarcity of available fossil feedstocks for non-food products, there is an increasing demand for supply of biobased feedstocks for both food and non-food ingredients. As a result, there is a debate on whether production capacity of biomass for both food and non-food products can be sufficient. Especially with the world population rising to nine billion in 2050, with many inspiring to a western life style and diet, this challenge should be addressed urgently. Availability of arable land, fresh water and fertiliser usage and effects on biodiversity are major factors that need to be taken into account in sustainable agriculture [219, 220].

Microalgae are considered one of the most promising feedstocks for sustainable supply of commodities for both food and non-food products [13, 17, 19, 221, 222]. Microalgae do not need to be grown on arable land, can be grown on seawater, can be grown on residual nutrients, have a high areal productivity, are rich in lipids, proteins and carbohydrates and via biorefinery the algae biomass can be fractionated into both food and non-food products [14]. Within Europe food and fuel could be produced using microalgae without being dependent on fossil fuels and imported agricultural feedstocks as calculated in [13].

Eukaryotic microalgae have a great potential for production of food commodities such as edible oils, protein and starch. Only eukaryotic microalgae are capable of natural triacylglyceride production, unlike the prokaryotic microalgae (cyanobacteria) and macroalgae. Therefore this work addresses the potential of eukaryotic microalgae while the reader is referred to other recent reviews [223, 224] for recent developments on cyanobacteria and macroalgae.

Oleaginous eukaryotic microalgae can accumulate up to 50-70% oil [112, 225, 226]; under different conditions the protein content in microalgae can reach values as high as 60% [15]. Furthermore, under yet again different circumstances, accumulation of carbohydrates up to 60% was shown in these microalgae [45, 225].

This work describes the potential, challenges and economics of sustainable production of food ingredients by microalgae. An estimate of the market volumes in which microalgae products can play a role to replace agricultural crops is provided, the technology of production will be described as well as potential locations and designs for production for the European market. Finally, the sustainability of algae production

and agriculture crops for the food market will be compared and safety of microalgae ingredients in food will be discussed. An overview of the key features, which need to be considered to allow successful production and application of food commodities from microalgae, is given in Figure 1.

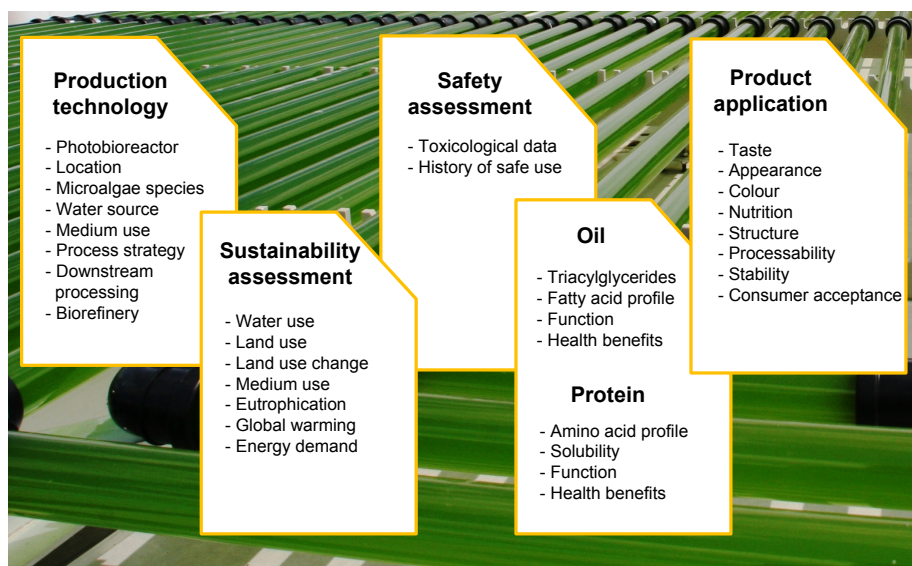


Figure 1. Food commodities from microalgae: overview of key features to consider prior to successful sustainable, cost effective and safe product applications.

## FOOD INGREDIENTS

Currently edible oils, proteins and carbohydrates are consumed through a variety of food products, which contain ingredients from both plant and animal origin. Commodities such as cereals, starchy roots, legumes, seeds, nuts, protein crops as well as fruit and vegetables are the most important sources for vegetable proteins, while oil crops are the prime source of vegetable oils. Meat, milk, eggs, fish and seafood products are considered the main animal sources for proteins and lipids. Cereals and starchy roots are the key commodities containing carbohydrates [227].

Edible oils and proteins deliver nutritional and functional properties to food products. While vegetable oils contribute to the nutritional value, taste and structure of many food products, such as mayonnaise and margarine, proteins can have functions in nutrition, structure, binding, viscosity, gelation, emulsification and foam formation [228]. These functional properties of proteins are related to their stability and solubility under pH conditions typical for foods (pH 3.5-7.0). In addition, practical aspects

such as processability, taste, appearance, colour and stability (temperature and pH) are significant factors for successful product applications of any food ingredient. Moreover, before bringing a food ingredient to the market, consumer acceptance should be checked and food safety should be guaranteed.

### **Microalgae oils**

For most applications in food products, oil present as triacylglycerides (TAG) is preferred, which is the lipid class used by oleaginous eukaryotic micro-organisms to store their fatty acids under stress conditions [229]. The accumulation of fatty acids by oleaginous photoautotrophic microalgae is well established and recently reviewed [226, 230, 231]. Under stress conditions; such as limitation or depletion of specific nutrients, a sub optimal pH, high salinity and high light conditions, a reduction of the degree of unsaturation of intracellular fatty acids was shown [232-236]. Accumulation of fatty acids in TAG under nitrogen limitation or depletion has been confirmed for a number of microalgae [45, 225, 232, 236, 237].

The microalgae fatty acids listed in Table 1, provided they are present in TAG, offer options to in part replace functions of the currently used vegetable oils. For instance the presence of linoleic (C18:2) and alpha-linolenic acid (C18:3) may in part substitute the essential fatty acid contribution from rape seed (canola), soy or sunflower oils, while palmitic acid (C16:0) in microalgae oils can contribute to structuring in food products. The presence of long-chain polyunsaturated fatty acids such as eicosapentaenoic acid (C20:5), docosahexanoic acid (C22:6) and the C20:5 precursor, stearidonic acid (C18:4) are of interest because of their cardio vascular health benefits [238, 239]. Contribution to product taste by microalgae oils and any adverse effect of less common fatty acids in the fatty acid profiles will need to be evaluated prior to application.

Strain improvement for increased TAG productivity and for designing ‘a la carte’ fatty acid profiles by both metabolic and evolutionary engineering is a potential route to improve the competitiveness of the process, although at present relatively little is known about pathways leading to TAG production. Comparison of specific genomic information of microalgae and higher plants contributes to further insights in these metabolic routes. For example, searches on sequenced microalgae genomes disclosed that most microalgae have several copies of putative specific enzymes active in final conversion step towards TAG, in this case diacylglycerol acyltransferases, whereas other eukaryotes have single genes [240]. For recent comprehensive studies and reviews on molecular tools used to study, optimise and modify performance of microalgae, we refer to [241-243].

Table 1. Comparison of the fatty acid (FA) profiles of various oleaginous microalgae and major vegetable oils. Specific fatty acids present below 1 % were not included. All microalgae were cultivated under nitrogen deplete or limiting conditions, which resulted in a total FA content above 20 % (w/w) in all cases, suggesting the presence of TAG. FA profiles from different strains of microalgae species were pooled, with the exception of *Neochloris oleabundans*, where results from the same strain were used. In cases where results were pooled, FA content was averaged and relative standard deviation was calculated (without subscript indicates a relative standard deviation in 1 to 30 % range).

Fatty acids	C10:0	C14:0	C16:0	C16:1	C16:2	C16:3	C18:0	C18:1	C18:2	C18:3	C18:4	C20:3	C20:4	C20:5	C22:6	References
Microalgae																
<i>Ankistrodesmus falcatus</i>	11	1	3	3	53	14	12									[244]
<i>Chlorella vulgaris</i>	17	1 <sup>a</sup>	3	6	4 <sup>a</sup>	9	13									[233, 244]
<i>Chlorella zofingiensis</i>	15	1	4	2	3	47	8									[233]
<i>Cylindrotheca fusiformis</i>	6	35	35	1	9	3	3	2	5	3						[244]
<i>Isochrysis</i> sp.	20 <sup>b</sup>	16	3	2 <sup>b</sup>	33	3	4	10								[233, 244]
<i>Nannochloropsis</i> sp.	5	40	29	1	16	1	4									[226, 244] <sup>d</sup>
<i>Neochloris oleabundans</i>	23	2 <sup>b</sup>	2 <sup>a</sup>	2	4	44	21	4 <sup>c</sup>								[233, 244]
<i>Phaeodactylum tricorutum</i>	5 <sup>c</sup>	24	47	2 <sup>a</sup>	2	1 <sup>a</sup>	5 <sup>b</sup>	1 <sup>a</sup>								[233, 244, 245]
<i>Scenedesmus</i> sp.	19 <sup>a</sup>	3 <sup>b</sup>	4	2 <sup>b</sup>	5	48	12 <sup>b</sup>	4 <sup>b</sup>	1							[233, 244]
<i>Thalassiosira pseudonana</i>	7 <sup>c</sup>	10	28	32	4	4	4									[245]
Palm	44				4	39	11									[246]
Rapeseed (canola)	4				2	62	22	10								[246]
Soy	8				4	24	53	6								[246]
Sunflower	6				4	25	63									[246]

<sup>a</sup> Relative standard deviation 30 – 40%

<sup>b</sup> Relative standard deviation 40 – 106%

<sup>c</sup> Only present in FA profiles [233]

<sup>d</sup> FA profile of neutral lipids was used of Hu et al [226]

<sup>e</sup> Only present in FA profiles [245]

## **Microalgae proteins**

In terms of amino acid content the nutritional value of proteins from several microalgae, compare favourable to egg, soy and wheat protein as well as to WHO/FAO requirements [15, 247, 248]. Isolation of a colourless protein fraction from *Tetraselmis* sp., water soluble on and above pH 5.5 was shown to be feasible [248]. Without doubt, substitution of meat, milk or egg protein by microalgae protein represents an exciting sustainable sourcing option.

## **Microalgae carbohydrates**

Microalgae can store carbohydrates in starch grains (pyrenoids) [249]. In addition, the cell wall can also act as a reservoir for carbohydrates [250]. Polysaccharides found in the cell wall vary with microalgae genera and species as well as with growth phase. Sugars such as arabinose, xylose, mannose, galactose and glucose can be found as well as less common sugars such as rhamnose, fucose and uronic acids [250-252].

Carbohydrates are commodities, which are becoming scarce and expensive at a fast pace. Using microalgae as a sustainable source of carbohydrates is an opportunity which should be further explored as these compounds can represent a large fraction of microalgae biomass.

For all ingredients derived from microalgae, serious R&D efforts and further consumer understanding are required to provide proof of principle for application in foods. In the future most likely commercialisation of all major and valuable biomass fractions is required to enable viable business cases.

## **MICROALGAE PRODUCTION TECHNOLOGY, SCENARIOS AND COSTS**

It is an enormous challenge to transfer the microalgae cultivation technology used for high value niche products to a production technology for commodities. Production scale and price still remain a challenge for microalgae cultivation technology, despite the large efforts going on in this field [13]. There are, however, clear options to reduce price of production considerably. It has been determined that production costs at large scale cultivation could be reduced from approximately 5.50 € kg<sup>-1</sup> dry biomass today to 0.68 € kg<sup>-1</sup> dry biomass if the technology develops [25].

Table 2. Biomass production costs including harvesting, yearly areal biomass productivity, biomass concentration and average daily dilution rate using the algae species *T. pseudonana* (Tp) and *P. tricornutum* (Pt).

Location	Raceway ponds				Flat panel				Horizontal tubular PBR				Vertical tubular PBR			
	Southern Europe	Eastern Europe	Southern Europe	Eastern Europe	Southern Europe	Eastern Europe	Southern Europe	Eastern Europe	Southern Europe	Eastern Europe						
Algae species	Pt	Tp	Pt	Tp	Pt	Tp	Pt	Tp	Pt	Tp	Pt	Tp	Pt	Tp	Pt	Tp
Biomass production cost (£ kg DW <sup>-1</sup> )	12.72	11.41	7.08	4.43	10.12	5.98	9.97	5.2	3.84	3.13	4.92	3.33	7.97	5.95	12.17	7.3
Biomass productivity (ton ha <sup>-1</sup> year <sup>-1</sup> )	14.9	63.8	8.0	41.5	60.9	128.6	54.7	119.7	43.9	71.2	27.1	46.3	56.6	91.8	31.9	58.6
Biomass concentration (g L <sup>-1</sup> )	0.1	0.3	0.1	0.3	0.8	2.9	0.8	2.8	2.0	5.6	1.6	4.3	1.1	3.3	0.9	2.6
Average daily dilution rate (%)	17	72	3	14	26	58	7	15	13	29	3	6	7	14	1	4

Many cultivation systems are variations of the basic design principles found in the four most well-known systems: raceway ponds, horizontal tubular photobioreactors (PBR), vertically stacked horizontal tubular PBR and flat panels. Using simulation models [110, 111, 122] the capacity of microalgae technology to replace 25% and 50% of the total European consumption of proteins and vegetable oils, respectively was evaluated. The outcome of these simulations is presented in Table 2 and Table 3. Distinct scenarios based on state-of-the-art technology (the four cultivation systems mentioned above), two different geographical locations (southern Europe and eastern Europe), each with 50% share of the total European production capacity and two different microalgae species both rich in protein and lipids (*Thalassiosira pseudonana* and *Phaeodactylum tricornutum*) have been considered. The scenarios for location and species are random and merely demonstrate the impact of technology. The two locations provide different cases with either a lot of sunshine (southern Europe) or large differences between summer and winter (eastern Europe).

Table 3. Land requirement ( $10^3$  ha) to replace 25% and 50% of the total 2011 European market of proteins and oils respectively<sup>a</sup> using the algae species *T. pseudonana* (Tp) and *P. tricornutum* (Pt). The percentage of non-arable land required for these scenarios are given between brackets.

Location	Algae species	Southern Europe		Eastern Europe	
		Tp	Pt	Tp	Pt
Raceway ponds		748 (2.0)	174 (0.5)	1390 (7.4)	268 (1.4)
Flat panel		182 (0.5)	86 (0.2)	203 (1.1)	93 (0.5)
Horizontal tubular		253 (0.7)	156 (0.4)	410 (2.2)	240 (1.3)
Vertical tubular		196 (0.5)	121 (0.3)	348 (1.9)	190 (1.0)

<sup>a</sup> The 2011 market figures show a vegetable oil consumption in the European Union (EU) of 13 million metric ton [253]. The total 2011 protein consumption excluding fish, fruit and vegetables is estimated for the EU to be 16 million metric ton [227].

The estimated productivities are shown in Table 2. The impact of cultivation strain on productivity is clear; with *P. tricornutum*, two to five fold higher biomass productivities can be reached at the same location and with the same cultivation system, in comparison to *T. pseudonana*. This shows the importance of strain selection and the potential of strain development for overall process performance. In addition, both cultivation system and location determine the exact difference in productivity.

Translating these results to biomass production costs in a 100 hectare plant, assuming operation parameters identical to those described in [171], costs range from 3.10 to 12.70 € kg<sup>-1</sup> dry weight (Table 2) with state-of-the-art technology. The costs depend on the system and there is no linear relation between productivity and production costs. In open ponds production costs are strongly related to biomass concentration due to the high costs related to harvesting (both energy and capital expenditure).

Assuming a biomass composition of 40% oils, 20% proteins, 20% carbohydrates and 20% ash and a recovery of 90%, the land required to replace 25% and 50% of the total 2011 European Union market of proteins and oils, respectively was calculated. Protein is the determining factor in terms of land requirement and the required land is given in Table 3. In Poland 0.5-7.4% of total non-arable land would be necessary to produce the required amounts of protein and lipid, and in Spain 0.2-2.0% of non-arable land. It is clear that the high areal productivities of the algae cultivation systems result in relatively low land requirements, indicating the huge potential of the use of microalgae as a novel food crop.

Downstream cost of 0.50 € kg<sup>-1</sup> product are assumed, resulting in oils and proteins production costs of at least 8.30 and 16.15 € kg<sup>-1</sup> product, respectively. In order to be competitive this value should decrease at least ten times, if present market values are used as reference.

The current technology available for algae cultivation is still immature, while at present, effective technology for biorefinery is even completely lacking. Nevertheless, it is expected that biomass can be produced at commercial scale for a cost price less than 0.68 € kg<sup>-1</sup> dry biomass in the next 10 to 15 years. This corresponds to oil and protein production costs of 2.13 and 3.75 € kg<sup>-1</sup> product, respectively if the downstream production costs are considered the same as above (0.50 € kg<sup>-1</sup> product). Despite still being higher than current prices, it is worth mentioning that if all biomass components are sold at current market prices, in a biorefinery perspective algae biomass would have a total value of 1.65 € kg<sup>-1</sup> dry biomass, which will make algae competitive for commodities [14]. [2]

## **SUSTAINABILITY ASSESSMENT**

Life cycle assessment (LCA) is a technique to assess environmental impacts associated with all stages of the life cycle of a product. A LCA of microalgae biomass, produced in the above scenarios was done and compared to the production of conventional vegetable oil and protein sources for the European market (21.0% palm, 21.1% rapeseed, 9.7% soy, 25.1% sunflower and 23.1% other oils for which data averaged from the former were applied (data obtained from United States Department of Agriculture [253]).

The LCA applies the same methodology as previously published [63, 77], based on the productivity parameters as given in Table 2 and a wet, supercritical CO<sub>2</sub> extraction process. It is a cradle-to-port analysis, meaning all inputs and outputs are considered from cultivation of microalgae through the transport of the microalgae products to the destination port (e.g. harbour of Rotterdam), including the embodied energy and environmental footprint of the materials and chemicals used. Impacts are allocated

on mass basis, assuming that protein and oil are the only useable fractions of the microalgae production systems and are produced by the same system.

Table 4 compares the basic raceway pond production system with low productivity microalgae species to the flat panel system with highly productive microalgae species to produce microalgae oil and protein with the conventional sources of vegetable oils and protein, highlighting the potential gains through technology advancement in both reactor design and microalgae productivity. In a closed system, microalgae have an advantage over conventional agricultural products, in energy consumption and freshwater consumption, assuming that seawater is used for cultivation.

The Global Warming Potential (GWP) profile of the flat panel and raceway pond growing *P. tricornerutum* in southern Europe show the different sources of impacts (Figure 2). It is clear that energy applied for lipid extraction, for water delivery and to produce synthetic fertilisers are the biggest burdens to overcome in the life cycle of microalgae production. It is the energy required for additional reactor materials, and the energy for water delivery, due to lower achievable biomass concentrations, that makes the biggest difference in impact between the two scenarios. If the use of nitrogen fertilisers is reduced through the use of seawater and wastewater inputs [80], then the GWP of both systems would decrease dramatically.

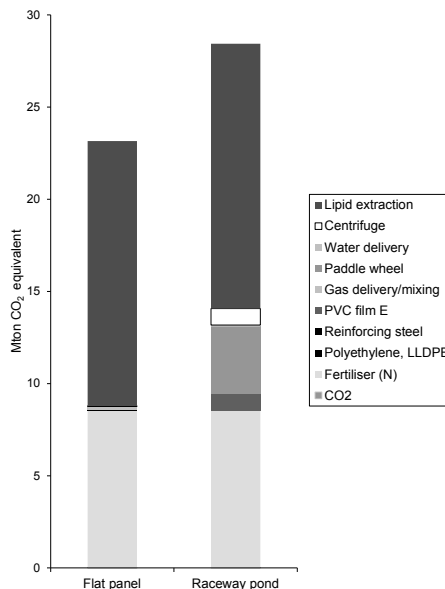


Figure 2. The global warming potential profile in Mton CO<sub>2</sub> equivalent for flat panels and raceway ponds, located in southern Europe and growing *P. tricornerutum*, showing the distribution of impacts in the life cycle of the microalgae oil production systems to meet the 50% of the European market demand for oil (6 million tons).

Table 4. Comparison of resource demands and environmental impacts for protein and oil produced by conventional agriculture or by the microalgae scenarios, Tp is *T. pseudonana*, Pt is *P. tricornutum*). Greenhouse gas (GHG) emission is given per kg product produced with and without land use change (LUC).

Production scenario	Conventional agriculture		Open pond		Flat panel		Conventional agriculture		Raceway pond		Flat panel	
	oil <sup>a</sup>	Pt	Tp	oil	Pt	oil	(Soybean) protein	Tp	protein	Pt	protein	Pt
Product												
Cumulative energy demand (MJ)	5.79·10 <sup>11</sup>		8.17·10 <sup>11</sup>	3.78·10 <sup>11</sup>			1.35·10 <sup>11</sup>	4.96·10 <sup>11</sup>			2.29·10 <sup>11</sup>	
Eutrophication (kg NO <sub>3</sub> equivalent)	2.41·10 <sup>8</sup>		5.46·10 <sup>7</sup>	1.14·10 <sup>8</sup>			5.38·10 <sup>7</sup>	6.93·10 <sup>7</sup>			3.31·10 <sup>7</sup>	
Fertiliser use, nitrogen (g kg product <sup>-1</sup> )	63.9		157	157			3.14	153			153	
Fertiliser use, phosphorus (g kg product <sup>-1</sup> )	4.735		16.9	16.9			6.07	16.5			16.5	
Freshwater demand (L kg product <sup>-1</sup> )	98.8		2450	1.41			321	2390			1.38	
Total freshwater demand (m <sup>3</sup> )	6.42·10 <sup>7</sup>		1.96·10 <sup>10</sup>	2.13·10 <sup>7</sup>			1.28·10 <sup>9</sup>	9.56·10 <sup>9</sup>			5.50·10 <sup>6</sup>	
GHG per kg product (kg CO <sub>2</sub> equivalent kg <sup>-1</sup> )	3.24		7.12	3.88			1.65	7.03			3.83	
GHG per kg product with LUC (kg CO <sub>2</sub> equivalent kg <sup>-1</sup> )	4.85		7.12	3.88			3.73	7.03			3.83	

<sup>a</sup> Oils produced by conventional agriculture include the distribution of plant sources for oil based on European market demands from 2011 (6 million tons total consisting of 21.0% palm, 21.1% rapeseed, 9.7% soy, 25.1% sunflower and 23.1% other oils for which data averaged from the former were applied).

As microalgae production systems are still at an early stage of development, LCA can provide a tool to show the directions toward which technology should develop, to overcome bottlenecks and improve sustainability. Further improvement of photobioreactor design, use of seawater and development of productive microalgae strains would enforce the potential for microalgae to become a more sustainable resource than our current agricultural systems. Microalgae represent a new food source that do not require arable lands and may be grown in regions where land use change is not a concern. Thus, as demand for food increases with global populations it represents an important sustainable resource for future generations.

## **SAFETY ASSESSMENT**

Before a novel ingredient can be introduced to the market as food ingredient for human consumption, market approval is required from regulatory authorities. For this market approval, safety of the ingredients has to be established. Food ingredients derived from microalgae such as microalgae oils and proteins are unique due to the non-traditional nature of the source organism used for their production and to ensure the consumer safety of these ingredients some essential elements of safety assessments need to be considered [254].

Chemical and physical characterisation of the products is important as safety considerations often revolve around its individual components. In addition to this, the products must be examined to determine the potential for toxicity (including mutagenicity, systemic toxicity, repro- and multi-generation toxicity), the possibility for naturally occurring toxins (from the source organism), heavy metals, and hazardous levels of pathogenic microorganisms, as well as potential by-products, formed from the degradation of certain pathways or introduced from production processing. The safety of the source organism is also critical in evaluating the toxicity of the products.

For some source organisms, the ‘history of safe use’ approach can be employed to understand the consumer safety of the oil [255]. For instance *Chlorella* species have been used as a food supplement in some countries and there is available history of use. Although there is not a complete package on toxicity of products from *Chlorella*, there is information on relevant toxicology parameters [256] and human consumption trials on this organism [244].

Using both the history of use and available toxicological data information, top line views on the organism and food ingredients can be formulated to either support human consumption or identify gaps that need to be addressed with toxicity testing.

## **CONCLUSIONS**

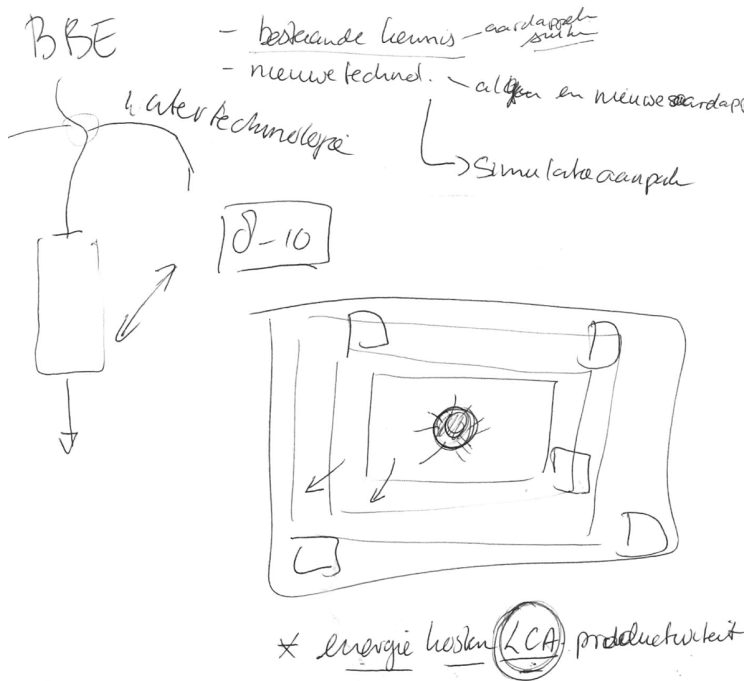
The potential of using photoautotrophic microalgae as a biomass source for food applications was reviewed. An overview of the most important elements, which need to be considered prior to successful production and application of food commodities from microalgae, is provided in Figure 1. Where certain microalgae oils might in part substitute functionalities of major vegetable oils, other microalgae oils containing long-chain polyunsaturated fatty acids might be added to food products to provide cardio vascular health benefits. The prospect of microalgae proteins and microalgae carbohydrates to replace current vegetable or animal sources needs further evaluation. We showed that a limited surface area of land would be required to produce and supply edible oils and proteins in Europe for the European market. Provided the technology of microalgae production matures and algae biorefinery is developed, the future market price of microalgae oils and proteins might compete with commodity prices. Additional sustainability analysis showed that with respect to land use microalgae have enormous advantages over current land crops. Food safety analysis already provided evidence for some of products and microalgae strains used, but more evidence on safety needs to be built up. Overall, we conclude that microalgae have a great potential as a feedstock for food commodities.

## **ACKNOWLEDGEMENTS**

We would like to thank everyone from Wageningen UR and Unilever who gave advice and contributed to inspiring discussions, in particular Ivan Muñoz, Balkumar Marthi, Peter Haring and Rob Hamer from Unilever. In addition, we are grateful for the support in preparation of the graphical abstract by Emile Verdegaal. We would also like to thank the US National Science Foundation for support of L.B. Brentner through International Research Fellowship Program (OISE-1064672).

# SCENARIO STUDIES FOR ALGAE PRODUCTION

## ACHIEVEMENTS, INSIGHTS AND NEW CHALLENGES





## INTRODUCTION

Algae biorefinery systems are under development. The first step is to cultivate algae. The success of cultivation is affected by many factors, such as weather conditions, characteristics of algae species, reactor design and operating conditions. Estimates of algae productivity under various conditions are necessary to project experimental results to large-scale facilities and to compare production at various locations. However, large databases for algae productivities are not available and at the beginning of this thesis work productivity models that are applicable for a range of production systems under varying conditions were missing. At the upstream end, algae production is connected to the supply of resources. Suitable regions for algae production have been indicated using qualitative geographical analyses [26, 52, 54-57, 150], but these studies were unable to indicate how much transport energy for supply of resources contributes to the overall energy balance of the algae production chain. At the downstream end, various techniques have been proposed for algae biorefinery processing [62], with a focus on algae biofuel production [12]. However, comprehensive insight in how to find the most promising routes and how to estimate the energy required for algae biomass processing was lacking.

The starting point for this work was the recognition that the three elements mentioned above have a strong interaction and would require an integrated study. In this thesis partial integration between these different elements was realised (Figure 1B). The interaction asks for methods that are able to estimate, amongst others algae productivities and energy consumption, under a wide range of process conditions. In this thesis model frameworks have been developed to assess algae productivity, transport energy consumption and biomass processing energy requirements. The frameworks are based on mass and energy balances, and bio-physical process descriptions.

Scenario studies are often used to analyse the effects of uncertainties in assumptions, possible model outcomes or future scenarios of new technology [85, 86]. Scenario studies were applied in this work to deal with the complexity and uncertainty arising in the various data and models. The Scenarios were employed here to explore the potential of algae production under various conditions and reactor designs, to indicate bottlenecks and to guide future research.

In the previous chapters the different aspects of the research work have been discussed in detail. In this chapter the achievements and insights of this research are discussed in the context of algae cultivation and processing. The research also opened views on new horizons and challenges for future research, which are presented as well.

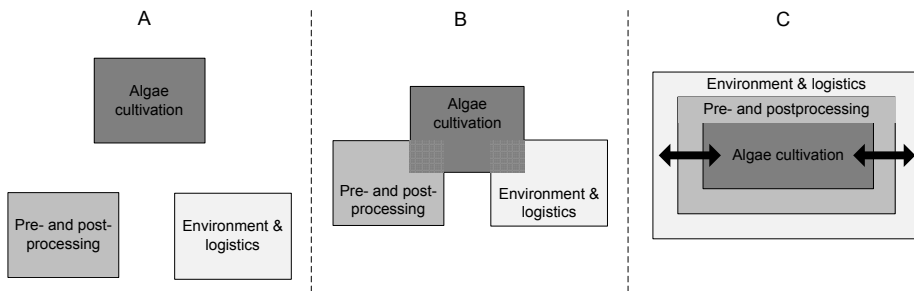


Figure 1. System division, A) the current approach where different system elements such as cultivation and processing are studied separately; B) design and analysis of system elements using information from other elements as realised in this thesis; C) utopic systems analysis where the interactions between the different system elements are fully integrated.

## SCENARIO STUDIES

Algae cultivation, processing and algae-based products are in an initial phase. In this phase, developing basic knowledge and realising actual processes are parallel activities. Techno-economic and life cycle analyses cannot take advantage of years of experience from pilot plants or industry. In this situation, the only alternative for developing ideas on large-scale algae production is by developing models based on the best available knowledge. These models are used in this thesis to predict the performance, explore trends and to indicate critical points and bottlenecks; we refer to this as “scenario studies”.

The scenarios considered in this thesis concern different levels, from design, processing and logistics to impact. In Chapters 2-4 wide ranges of reactor designs are explored with scenarios, in Chapter 5 the algae cultivation supply logistics, in Chapter 6 a model-based approach is presented to determine the best process routes for biomass processing, and in Chapter 7 scenario-based data on algae productivity are used as the input for impact analysis of food commodity production. Figure 2 shows the position of the elements of this thesis in the uncertainty and complexity space.

The accuracy of the predictions depends on the quality of the available information. Every day, new information is generated about algae. Therefore, the predictions cannot be considered to be final, if this state can ever be achieved. But, they do provide good indicators and allow the comparison of alternatives on their strength and weakness. In complex systems like algae cultivation and processing, the deviation between predictions, data and information is, together with the results of bottleneck analysis, a strong drive to improve insight and provide focus for further research.

<sup>2</sup> The definition of scenario studies is wide. In general, the results of scenario studies can 1) point out bottlenecks that need to be solved to reach the desired goal [86], 2) help to explore and understand the effects of measures, technical developments or alternative designs [86-88] or 3) indicate the consequences of uncertainty [189].

## SCENARIO ANALYSIS FOR ALGAE CULTIVATION

Algae productivity is affected by the combination of location, reactor design and algae species. Although this is recognised in the literature, often generic productivity values are used. Chapters 2-4 in part 1 focus on algae production under varying conditions. The main research challenge in these chapters was to understand how algae productivity is affected by location, reactor design and algae species characteristics, and to include these elements in a productivity modelling framework.

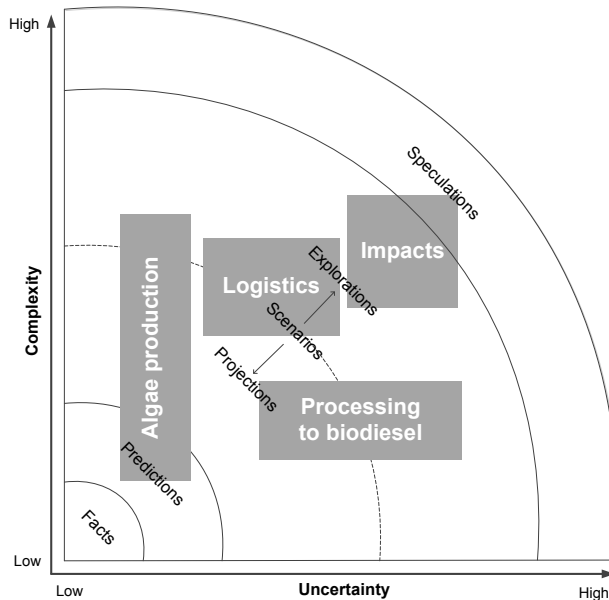


Figure 2. Position of thesis frameworks and scenario studies in the domain of complexity and uncertainty. The four scenario studies are indicated with the grey boxes. Figure adapted from Zurek and Henrichs [90]

### Achievements

Figure 3 gives an overview of the productivity framework.

The framework uses location specific light angles, day lengths and reported direct and diffuse light intensities, reactor variables like geometry and wall material, ground material and algae characteristics. For closed PBRs the temperature is assumed to be controlled to the optimal growth temperature. For raceway ponds physical relations are combined with reported weather data on wind velocity, light intensity, air temperature, relative humidity, air pressure and soil temperature in order to derive dynamic water temperatures. In the framework detailed bio-physics-based models are applied to determine the light input on the reactor surface and the light gradient in the bioreactor. In addition, the canyon effect for the penetration of diffuse light between parallel

reactor systems is included. Specific growth rates are related to these light gradients and for raceway ponds also to the water temperature. The specific growth rate leads to biomass formation or to loss of biomass when not enough light is present to yield a net positive specific growth rate.

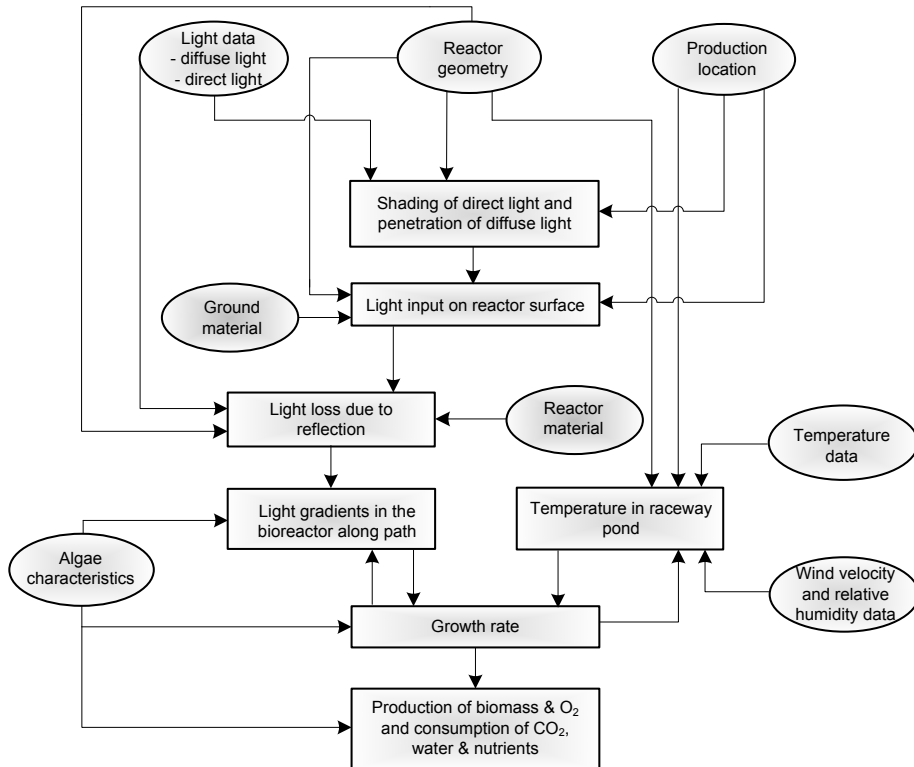


Figure 3. Productivity framework.

In this thesis several design and location scenarios were applied to the productivity framework to quantify and compare these effects. The results show that regional weather conditions, solar angles and algae species determine what is the best choice for the specific reactor design. The distances between parallel units and the height of units have to be adapted accordingly. Choosing non-optimal values often results in a sharp decrease of maximum achievable biomass production. The optimal height of vertical systems is mainly affected by the canyon effect for diffuse light which has a large effect on the penetration of light in between two parallel systems. The actual biomass concentration that must be maintained to maximise the yield varies between the reactor systems, locations and algae species. As weather and light conditions are of utmost importance for the growth of algae, it is recommended to link the algae

species selection to the regional light and temperature conditions. In regions with strong weather variations it is even an option to cultivate different algae species during the year each suitable for a particular season.

The simulations were performed for the algae species *P. tricornutum* and *T. pseudonana*, which are both marine diatoms well-known for their high poly-unsaturated fatty acid contents. The species differ much in maximum specific growth rate and in light absorption coefficient and are thus interesting examples for the scenarios. The species indicate the range of productivities to be expected, with the results of *T. pseudonana* indicating the lower end and *P. tricornutum* the higher end. Based on the growth characteristics it is expected that the productivity of most common other species will lay between these two extremes. For example, *Neochloris* has an absorption coefficient and specific growth rate that lay between the values used in this study (see [257]). The species *Nannochloropsis* has a low absorption coefficient like *P. tricornutum* which is beneficial for productivity, but it also has a much lower growth rate [41] which reduces the productivity.

### **Additional features of the productivity framework**

The developed productivity models aid in optimising reactor designs and algae biomass concentrations for a given situation. Tailor-made system designs result in the highest productivities. The framework is flexible enough to accommodate other locations, reactor types and algae species. For each location weather data are required, for the reactor design the geometry, and for the algae species the growth characteristics.

The growth relation developed by Geider *et al* [258] can be exchanged by others. The light absorption coefficient was taken constant, but in areas with large variations in light (e.g. the Netherlands) incorporating varying absorption coefficients during the day and year may be appropriate [116, 259]. The effect of photo-inhibition has been studied for raceway ponds by sensitivity analysis (Chapter 3). At locations with high light intensities or for algae that are sensitive to light it is important to include this aspect, as it was found that including photo-inhibition biomass may reduce production estimated by up to 12%.

### **Further insights**

#### **Trends in photosynthetic efficiencies**

It is common practice to assume that productivities and associated with that PEs as well, always increase going from raceway ponds (1-2%), to horizontal tubes (3%) and to vertical systems (4-5%) which could be a flat panel or a vertically stacked tubular reactor [19, 23, 25, 260]. However, the PEs are a result of the combination of reactor geometry, species characteristics and location specific weather conditions, daylengths

and light angles. Figure 4 illustrates the photosynthetic efficiencies (PE) of the studied combinations of reactor system (raceway ponds, flat panels and horizontal and vertical tubular photobioreactors), location (Netherlands, France and Sahara) and algae species (*P. tricornutum* and *T. pseudonana*).

The results in Figure 4 show that PE is more complex, for example flat panels and vertical tubular reactors in Algeria achieve similar PEs while in the Netherlands panels perform much better than vertical tubes. In the Netherlands for panels the PE is even higher than that for panels in France or Algeria as the flat vertical reactor surface fits better to the generally low solar angles in the Netherlands. Generic reactor specific PEs are thus not representative for each location. A model framework such as presented in this thesis is advantageous compared to generic PEs to predict the productivity under various conditions.

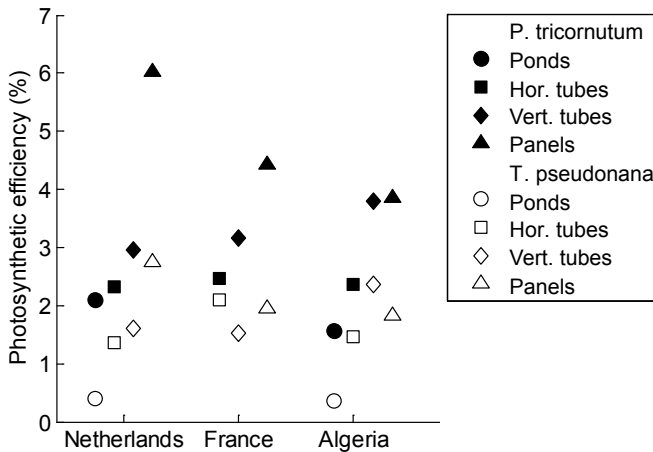


Figure 4. Photosynthetic efficiencies (%)

### Uncertainty and sensitivity analysis

An initial global uncertainty and sensitivity analysis for single standing flat panels was performed. In contrast to a local sensitivity analysis which uses one at a time variation around the operation point, this global analysis includes the interaction between parameters in a search space. The sensitivity analysis is based on a Monte Carlo sampling which means that each parameter varies randomly between the given minimum and maximum value (Table 1). The ranges are based on current knowledge. The uncertainty ranges are used as inputs to determine the Saltelli-Sobol coefficients based on Saltelli [261]. The Total Sobol coefficients quantitatively indicate the influence of each parameter on the variance of the predicted productivities and are a measure of the importance of each parameter on the model prediction.

Table 1. The minimum and maximum parameter deviation applied for Monte Carlo sampling.

	+ / -
Absorption coefficient	50%
Diffuse light angle	10%
Diffuse light input	3%
Direct light input	3%
Functional cross section	40%
Ground reflectivity	5%
Light input reactor wall	15%
Max. respiration rate	20%
Max. specific growth rate	20%
Maximum Chl <i>a</i> :C ratio	8%
Outgoing light Lambert-Beer	10%

The results of the sensitivity analysis are shown in Figure 5 and show that the spectrum-averaged light absorption coefficient, maximum specific growth rate and functional cross section of the photosynthetic apparatus<sup>3</sup> are the essential parameters of the productivity models. From the analysis it follows that addressing the uncertainty in these parameters has the potential to reduce the variance in predicted biomass productivity with 96%. Thus, most focus should be put on these three parameters. More extensive uncertainty and sensitivity analyses should shed light on the most important parameters in the other reactor types, but there are no reasons to believe that the results will be much different.

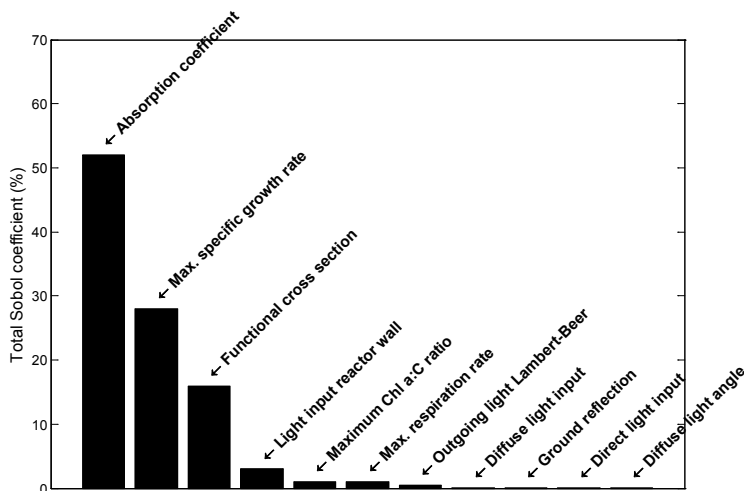


Figure 5. Total Sobol coefficients (%) for 11 model parameters. The coefficient values indicate the influence on the variance of the predicted productivity. The values give a measure of the importance to the variance.

<sup>3</sup> The functional cross section of the photosynthetic apparatus indicates how much carbon can be produced per mol photons when having a certain area of photosynthetic apparatus per gram chlorophyll *a*.

Variation in yearly weather conditions is another uncertainty factor in the application of the current model. Employing datasets of several years will give insight in the year-to-year variation that can be expected, but could not yet be performed within the time frame of this research.

### Operating conditions

The current simulations were performed for growth with turbidostat conditions with a fixed biomass concentration during the year. The approach allows applying other operating conditions, such as turbidostats with best biomass concentrations for shorter periods (seasons, months, days or based on weather forecasts). A preliminary analysis predicts a moderate potential improvement for raceway ponds of up to 4.8% and for flat panels up to 2.8% using seasonal and monthly adaptation of biomass concentration compared to yearly best biomass concentrations (Table 2). As the light conditions vary the most in the Netherlands, this is also the location where the relatively largest improvements are possible. However, the increase is marginal for flat panels systems. A similar trend was observed for the advanced luminostat operation, which stands for a constantly diluted system that has a constant amount of light leaving the rear of the reactor. Research by Cuaresma *et al* [262] shows that it is difficult to achieve higher PEs with luminostat conditions compared to chemostat conditions.

For raceway ponds other operating strategies such as semi-batch production may be more practical for achieving higher productivities.

Table 2. The relative increase with seasonal and monthly biomass concentrations on the yearly areal biomass productivity, compared to the use of yearly biomass concentrations for raceway ponds and flat panels, using the species *T. pseudonana* (Tp) and *P. tricornutum* (Pt).

		Raceway ponds		Flat panels	
		Seasonal	Monthly	Seasonal	Monthly
Netherlands	Tp	3.55%	4.77%	1.31%	1.66%
Netherlands	Pt	4.10%	4.12%	2.21%	2.80%
France	Tp	-	-	0.47%	0.70%
France	Pt	-	-	0.87%	1.08%
Algeria	Tp	0.08%	0.31%	0.08%	0.11%
Algeria	Pt	0.03%	0.12%	0.17%	0.21%

## Development of the framework

### Validation and calibration

A next step that still must be done is to validate and calibrate the current biomass productivity estimates with experimental data under outdoor conditions. Various pilot plant systems around the world are beginning to produce data that might be an excellent starting point for validation and calibration. Examples are parallel experiments in

Chili, Norway, Spain and the Netherlands in the EU MICRACLES project, in the Netherlands, Spain, Italy and Israel for FUEL4ME and the Netherlands and Spain for SPLASH. Comparing productivities in different systems at the same locations will demonstrate the similarity between the systems and the implemented models. The biomass productivity can be compared on yearly basis, but the framework also enables analysis on a more detailed basis with monthly or even daily production data. The pilot experiments also allow to further develop our insights in the growth characteristics of various algae species.

### Energy consumption

The practical implications of the reactor designs or the energy consumption have not been evaluated in this work. Currently, some cost estimates are available for various reactor systems [25], but a detailed analysis of how reactor design contributes to the operational energy consumption during the cultivation process is still lacking. The productivity framework is a good basis that can be extended to include calculations on the effect of reactor design on the cultivation's energy consumption. As an illustration a preliminary calculation was made leading to Figure 6 that shows the effect of the light path of a flat panel PBR on the energy consumption for aeration, cooling and heating (to the optimal growth temperature) which is based on process models for these process elements. Such an expended energy framework can also be used to improve degasser designs for tubes, mixing in all systems and air supply systems for flat panels.

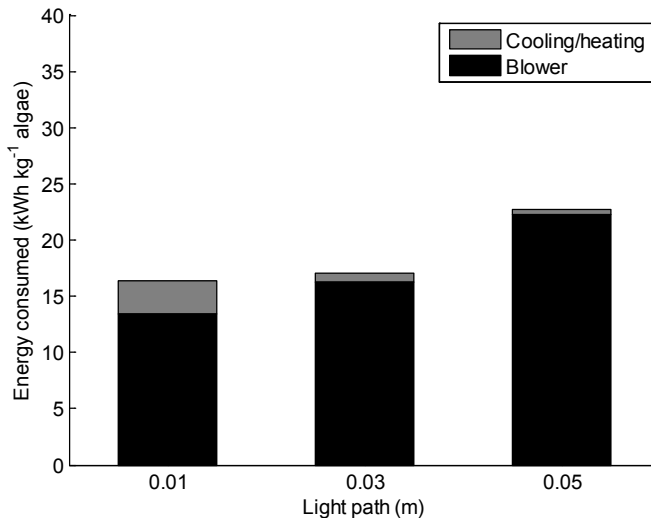


Figure 6. Energy consumption (kWh kg<sup>-1</sup> algae) for cooling/heating and aeration in a flat panel with varying light paths.

The suggested energy framework is also a tool to study advanced temperature control mechanisms for closed PBRs that reduce the energy required for heating and cooling reactor systems. Respiration rates reduce during the night at lower temperatures [263]. Furthermore, heating the algae solution before sunrise enhances growth at the start of the day [264]. Thus, energy can be saved by not constantly heating or cooling. This energy reduction should be balanced with the productivity, which may be lower at non-optimal growth temperatures. The inclusion of these ideas into an optimal control strategy is a challenging and exciting task for the future.

### **Biomass composition**

The framework focusses on biomass production. For specialised products a specific biomass composition is required, for example with high lipid, protein or carbohydrate content. Customising the biomass composition by manipulation of the cultivation conditions [265] belongs to the possibilities. However, such specialised biomass compositions are achieved after submitting the algae to stress conditions, which also goes as the expense of growth. Therefore, the effect of a changed biomass composition is not straightforward. Performing scenario studies for large-scale production under stress conditions and using these control options and the effect on biomass composition and productivity is a new aspect and a challenging extension of the developed framework

### **Conclusion – algae cultivation**

As production data are limited available and very specific, scenario studies using the modelling framework are currently the only way to study large-scale outdoor algae production. The productivity framework predicts biomass productivity and photosynthetic efficiencies under various conditions. By comparing scenario results the best choice for the type of reactor can be made for given regional weather conditions, solar angles and growth characteristics. The scenario analysis proved that reactor specific photosynthetic efficiencies differ for each location and cannot be generally employed. The simulations also revealed the most critical parameters that cause variation in algae productivity, i.e. the light absorption characteristics and maximum specific growth rates of algae species. Understanding these phenomena will improve the quality of prediction, while control of these aspects during production will reduce the variation in productivity. The scenario results indicate that fine-tuning of operating conditions has a minor positive effect on the overall productivity.

In future projects, with more full scale plant data available, calibration and adjustment of the framework models can play a more prominent role. Other important next steps are to expand the models in order to predict the biomass composition and productivity under stress conditions, and the energy consumption of cultivation.

## SCENARIO EVALUATION OF ALGAE LOGISTICS

The supply logistics of algae cultivation are often ignored, except perhaps for planning of suitable regions based on GIS analysis [26, 52, 54-56, 150]. The energy necessary for resource transport has not been analysed yet. Differences between regions and reactor systems are expected due to different infrastructure and resource demands. In addition, it is unknown how algae cultivation sites should be allocated with a given set of resource supply points. In Chapter 5 (in part 2) the interaction between resource availability and demand through algae production was analysed based on a quantitative logistic study.

### Achievements

The allocation of algae sites varies between the regions studied. In the Benelux (in Northwest Europe) large algae cultivation areas should be planned at locations nearby the sea with a high CO<sub>2</sub> availability. In southern France the plants should be scattered over the region because of the low CO<sub>2</sub> per supply point and for the Sahara cultivation should be planned at locations with a minimised water transport. The availability, distribution and demand of resources has a dominant effect on the feasibility of regions for algae cultivation.

The feasible average transport distances for resource supply are higher than commonly thought and can reach up to 225 km for water and 180 km for CO<sub>2</sub> per supply point, without reducing the productivity potential. So, clearly algae cultivation does not necessarily need to take place in proximity of CO<sub>2</sub> supply. The largest difference in transport distance between the Benelux and the Sahara is 10.5 times for water transport and 7.4 times for CO<sub>2</sub>.

We suggest to employ a standardised transport distance (total transport distance divided by productivity) that encompasses the differences in number of supply points and productivity. The standardised transport distances vary much stronger between the regions, as there are also large differences in the number of supply points utilised and in algae productivity. The largest difference is 400 times for water between the Benelux and the Sahara, and 250 times for CO<sub>2</sub>. The difference in water is the largest for raceway ponds, which require large amounts of water to compensate for evaporative losses. The closed PBRs are assumed to be cooled and heated by heat pumps coupled to aquifers and therefore no additional water for cooling and heating has been accounted for. The standardised transport distances can reach up to 860 km Mton<sup>-1</sup> water in the Sahara and up to 2000 km Mton<sup>-1</sup> CO<sub>2</sub> in southern France.

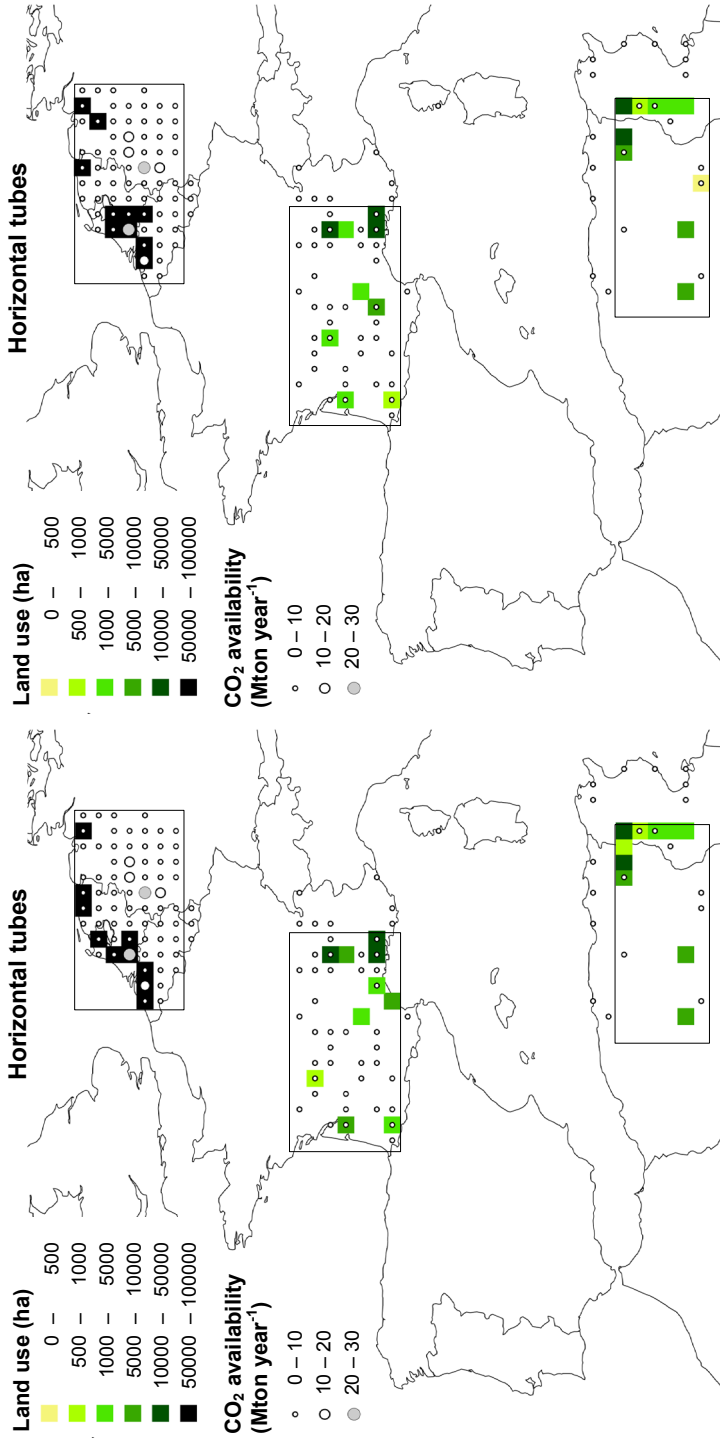


Figure 7. The distribution of algae plants with horizontal tubes for *T. pseudonana* (left) and *P. tricornutum* (right).

The results of Chapter 5 show that most transport energy is required for raceway ponds and for the Sahara region. Horizontal tubular reactors consume the least energy for resource transport. In general, under realistic assumptions of the total space available for algae production, the transport energy consumption is low compared to the energy contained in the algae biomass (4-5%), so the share of transport to the energy balance is not a bottleneck in the algae production chain. Reducing the energy used for cultivation and during processing need most attention. However, supply logistics is essential for planning algae cultivation as not every location achieves a positive energy balance for transport.

## **Insights in supply chain design**

### **Planning algae cultivation**

The investigation considered regions which were divided in areas of 50 by 50 km. This grid gives a good indication of the possibilities within a region for algae production and the transport energy consumption. Figure 7 illustrates the planning of algae cultivation with horizontal tubes for the algae species *T. pseudonana* and *P. tricornutum*. These results show similar trends in selection of cells for both algae species. However, *T. pseudonana* requests for a higher water demand, so there is a slightly higher preference for cultivating this species at locations near the coast. A similar trend in the distribution was seen in Chapter 5 when comparing cultivation of *P. tricornutum* in raceway ponds and horizontal tubes.

The results of this work can be translated to the planning of specific algae plants, but to determine the exact sizes and locations more information on the economy of scale for large-scale algae cultivation is necessary. In addition, for areas with a dense pipeline infrastructure a smaller grid of, for example of 10 by 10 km might give more detailed local information (see also [60]).

### **Water and CO<sub>2</sub> sources**

For the regions southern France and the Sahara the exclusive use of CO<sub>2</sub> exhausts from industrial sources seems less appropriate, due to the very limited capacity of this CO<sub>2</sub> supply. This also constrains the potential production (Chapter 5), while the weather conditions are very favourable for algae growth (Chapter 2-4). Therefore, it is important to consider other sources for CO<sub>2</sub> for large-scale production of algae products in those regions. This increases the production potential and simultaneously reduces the energy requirements for transport. Regional available sources can be biogas installations near cities, CO<sub>2</sub> absorption from the air and exhausts from smaller industries which were not yet included in this thesis.

From the results in Chapter 5 it follows that critical factors for reducing the transport energy consumption are region dependent. In the Benelux resources are obtained locally and transport distances are short and transport energy consumption is low. It is difficult to reduce the energy consumption further. In southern France and the Sahara the transport energy consumption is slightly higher, which is a result of the dispersed and limited availability of CO<sub>2</sub>. This also increases the transport distances for water. Increased availability of water and CO<sub>2</sub> is expected to reduce the average transport distance, standardized transport distance and transport energy share. In the Sahara the transport energy consumption for raceway ponds is very large, due to the large amounts of water that evaporate.

Such a higher energy demand for resource transport can be compensated by the higher productivity at a location with beneficial light and climate conditions. Improved pond designs that reduce the evaporation, or enable recycling of the evaporated water through condensation sheets will significantly reduce the transport requirements. In addition, saline aquifers are available in the Sahara region which can supply salt water more regionally, although the capacities are most likely limited [167, 168]. Other options are to reduce the water consumption by an intensive water recovery system and to gain CO<sub>2</sub> from the air. The most favourable location has a light input leading to productivity and a high availability of water and CO<sub>2</sub>.

The largest potential energy reduction per amount of resource can be achieved through local supply of CO<sub>2</sub> (on average 8.7 kWh ton<sup>-1</sup> CO<sub>2</sub>). Local water supply has a much lower potential energy reduction (on average 0.6 kWh ton<sup>-1</sup> water). Nevertheless, large improvements in the energy consumption for water can be achieved as larger amounts of water are required compared to CO<sub>2</sub>.

## **New challenges for algae logistics**

### **Extended planning scenarios**

The scenario results illustrate that the planning of algae cultivation is strongly related to the demand, which follows from the regional algae biomass productivity on one hand and the availability and distribution of resources on the other hand. The two algae species used in this work give for the four reactor designs a good indication of the expected ranges of biomass productivity and resource demand.

However, the availability and distribution of water, CO<sub>2</sub> and other resources is much more diverse than the basic scenario of electricity plants and sea water that was applied in this work.

An interesting follow-up is to compare the energy consumption and location planning for various scenarios with other resource inputs. For example, local supply of CO<sub>2</sub> through biogas installations, CO<sub>2</sub> absorption from the air, saline water from aquifers or waste-water use. It is also interesting to apply theoretical scenarios where the availability of resource supply can be assigned to some locations to study the implications on the planning and transport energy consumption.

In addition, the transport distances and energy consumption patterns can be studied in more detail. With an increasing number of plants the transport distance and thus also the energy consumption rise. Studying these patterns will give more insight in the potential algae production in a given region and in the balance between increase in biomass production and a simultaneous increase in energy consumption for transport. Such study will help to indicate the maximum feasible transport distances for a given scenario of resource supply and areal biomass productivity and to provide the energy consumption associated with this maximum distance.

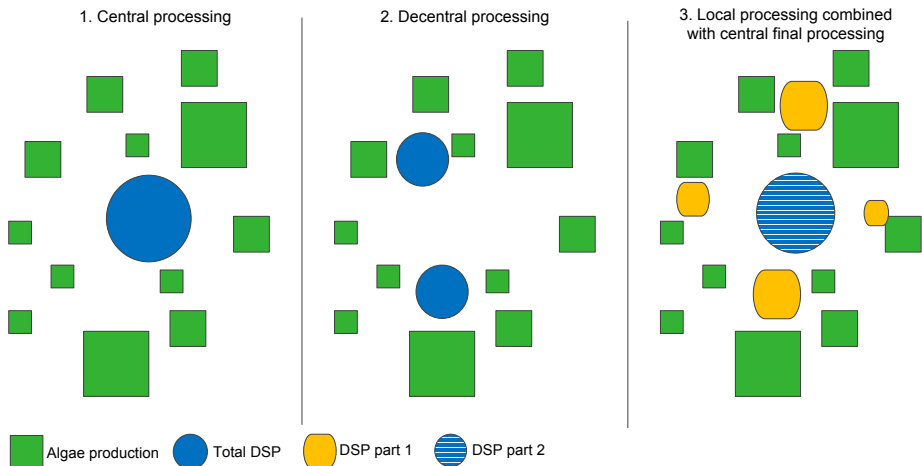


Figure 8. Three scenarios for the processing of algae biomass.

### Logistics of algae processing

The logistics of processing of algae biomass is also important for planning the total algae production chain. The processing of algae biomass into products can take place centrally or can be divided over several processing plants (Figure 8). For example, scenario 3 depicts a process where biomass is first concentrated locally and then transported to a central facility that processes the biomass further. It is challenging to study which processing infrastructure is most suitable and to understand which characteristics and conditions lead to the selection of the specific optimal logistic network.

## **Conclusion - logistics**

Conventional scenarios on resource supply, i.e. seawater and CO<sub>2</sub> from electricity plants, show that feasible average transport distances per supply point can reach up to 223 km for water and 178 km for CO<sub>2</sub>, without significant reduction of the productivity potential. Under realistic assumptions of the space available for algae cultivation, only 4-5% of the energy in biomass is consumed during resource transport. However, large demands of water such as for raceway ponds in the Sahara can increase the consumption to reach 38% of the biomass energy.

So, generally the energy consumption for resource transport is not a bottleneck. Still, algae supply logistics are important for the planning of algae sites. The planning strongly depends on the availability and distribution of resource supply. Other sources for water, CO<sub>2</sub> and other resources are possible and should be studied in future scenario studies. To reduce the transport energy consumption these techniques should not require more than 8.7 kWh ton<sup>-1</sup> CO<sub>2</sub> and 0.6 kWh ton<sup>-1</sup> water on additional process energy (compared to the use of seawater and CO<sub>2</sub> from electricity plant flue gasses).

Future research should focus on extending the current scenarios for resource supply with other sources. Insight on the patterns in transport distance and associated energy consumption with increasing production areas are important to also indicate for example maximum feasible transport distances. In addition, the processing of algae biomass should not be neglected.

## **SCENARIO STUDIES ON THE PROCESSING OF ALGAE**

The processing of algae biomass to biodiesel is affected by the cultivation conditions by for instance the biomass concentration and the lipid content. The development of processing algae to biodiesel is still in a developmental stage [14]. Often the performance of single process units is described or a data-based approach is applied [63, 70, 75, 193, 194]. We introduced a model-based combinatorial approach to study the effect of process design and processing conditions on the biodiesel yield, energy consumption and net energy ratio (Chapter 6 in part 2). The performances of the obtained process routes with optimised process conditions have been compared to the combinatorial approach with fixed process conditions.

## **Achievements**

A flexible model-based combinatorial framework was applied to select process units and to predict the effect of process conditions on the biodiesel yield and net energy ratio (NER). In this framework, mass and energy balances are combined with additional relations to calculate the process yields and energy consumption of each process unit. The main process conditions are biomass concentration, concentration

factor, throughput, co-stream flow and concentration (flocculant, catalyst, methanol), residence time, pressure and process temperature. The framework is applied to 126 possible process routes for biodiesel production (Figure 9), which are grouped based on the employed extraction and conversion process.

The most promising process routes harvest algae with chitosan flocculation, followed by the dewatering with pressure filtration. The best route extracts the lipids with hexane and applies alkaline catalysed conversion to yield biodiesel. The next best route uses supercritical CO<sub>2</sub> extraction.

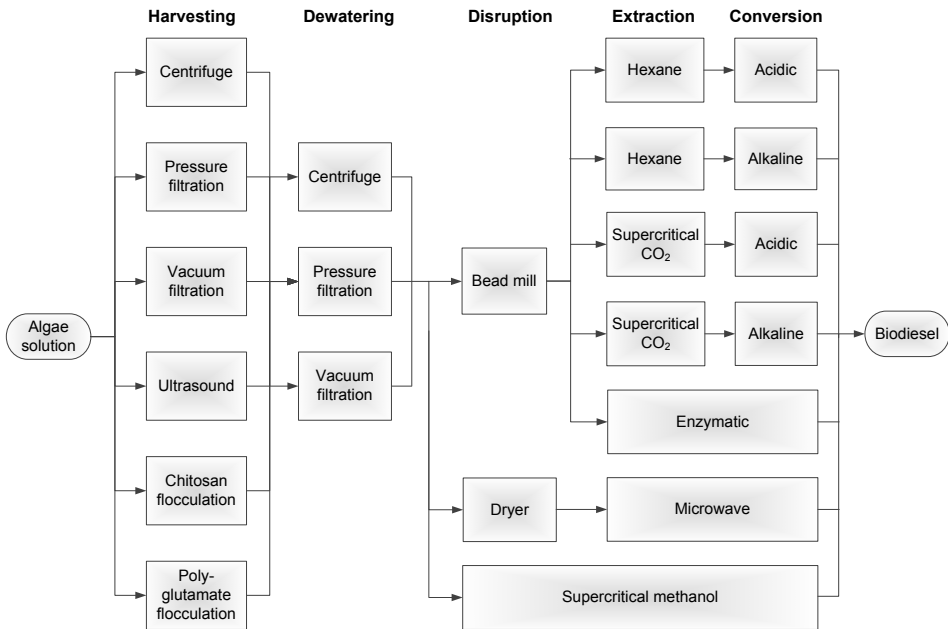


Figure 9. Superstructure for biodiesel production from microalgae, with all 126 process routes analysed in this work. The routes are divided into seven groups based on the extraction and conversion process units.

The framework allows optimisation of the process conditions, which leads to increased biodiesel yields and NER values. Optimisation of the main process conditions (concentration factor, chitosan flocculation, filling of the bead mill, extraction temperature and methanol flow) leads, compared to a combinatorial approach with standard fixed process conditions, for the best routes in the seven process groups to at least 5% higher NER values, and can go up to 38%. The best NER is again achieved for the route chitosan flocculation – pressure filtration – bead milling – hexane extraction – alkaline conversion. The highest biodiesel yield is obtained for supercritical CO<sub>2</sub> extraction combined with alkaline conversion.

A bottleneck analysis of the best process routes of each group shows the contribution of each process step to the total energy requirement. Routes with hexane and supercritical CO<sub>2</sub> extraction required 27-34% of the process energy for disruption and 51-62% for lipid extraction. The enzymatic routes combine extraction and conversion and require even 95% for conversion. The figures for the supercritical methanol route are 67% for conversion and 24% for disruption. The microwave route consumes 94% of the energy for drying. So each route has a specific limiting processing step and improvements in process unit design should be tailor-made for each route.

Despite the important progress that has been shown in the processing of algae biomass into biodiesel, the current results of the model-based framework cannot be regarded as a definitive prediction of the NER and biodiesel yield. In this thesis, laboratory and pilot data from frequently used refinery units is used. The selection of processes was limited to process units that had sufficient information available to model the effect of process conditions like biomass flow, biomass concentration, solvent flow, temperature or pressure on the concentration factor, recovery or energy consumption. This limits the inclusion of promising techniques for algae biomass DSP such as enzymatic cell wall degradation, pulsed electric field perforation or ionic liquids for extraction and separation. The developments in this field are fast and new information is expected to be generated in the nearby future.

## **New challenges for biomass processing**

### **Flexibility**

The performance of the processing chain is affected by the ingoing biomass concentration, flows and properties of algae (see Chapter 5). Moreover, the properties of the algae feed solution to the processing systems, such as rheological properties, cells wall properties and lipid content, vary during the year [259], but also during biomass processing. As a consequence, the choices for process conditions are affected and possibly the process routing as well [197]. The processing system should be able to anticipate to these variations.

The effect of varying flow rates and biomass concentration on the NER of biomass processing is illustrated in a preliminary sensitivity analysis (Figure 10). The results indicate that for the routes with hexane or supercritical CO<sub>2</sub> extraction the use of a lower biomass concentration or flow rate decreases the NER relative to the value obtained under the reference conditions of Chapter 6. A higher concentration and flow does not lead to higher NER values for the routes with supercritical CO<sub>2</sub> extraction. This is also visible for the routes with enzymatic conversion. In contrast, the NER values for the routes with supercritical methanol and microwave conversion are barely affected by

changing the input conditions. This might originate from the experimental conditions applied in the laboratory experiments used for the models. These preliminary results indicate that further optimisation of the process routes including cultivation conditions is an essential step to forward the performance of algae processing. To accommodate future innovations, the knowledge on the process models and process units should also develop further.

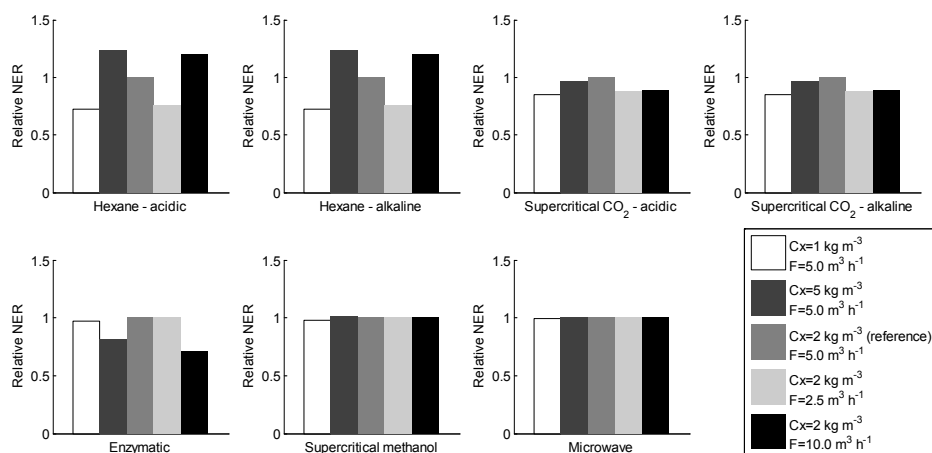


Figure 10. NER for two biomass concentrations and two flow rates, relative to the NER achieved with a biomass concentration of  $2 \text{ kg m}^{-3}$  and  $5 \text{ m}^3 \text{ h}^{-1}$  flow rate. Relative NER values are given for the best route (under reference conditions) in each process group.

### Multiproduct algae biorefineries

Algae contain many interesting molecules. In a next step the simultaneous superstructure and process conditions optimisation should be extended to other products such as functional proteins, feed or carbohydrates as bulk chemicals for chemical industry. This requires additional process information on the effect of process conditions on the functionality of the products and other process steps that are aiming at the recovery of proteins, carbohydrates or pigments. Optimisation of the process routes will lead to suggestions for efficient processing of algae biomass to several products.

### Data-based models

To illustrate the approach of simultaneous combinatorial route selecting and optimisation of process conditions overall input-output models were employed in this thesis. The value and impact of the results increases when the models are extended with characteristics of the algae solution and algae cells obtained from laboratory, pilot-plant and industrial data.

The current research in this area will supply new knowledge to incorporate into the models. The new data and knowledge can be collected in a library of process models, to be used in a general simulation environment.

## **Conclusion – biomass processing**

The developed model-based framework for algae biomass processing gives the opportunity to analyse and illustrate the potential of processing routes. In addition, it is a tool to improve the performance of the process routes by optimisation of the processing conditions. The currently available process models for algae biorefinery are relatively limited. The proposed approach is flexible enough to incorporate new information and to explore new process designs. In addition, the process models can be linked to other performance indicators such as economics, material inputs or greenhouse warming potential.

## **IMPACT ANALYSIS BASED ON SCENARIO STUDIES**

Several performance indicators are suitable to analyse processes and products. In many technical studies the performance is indicated with productivities (see Chapters 2-4) or through energy consumption (see Chapter 6). Economic performance indicators are most appropriate for fully developed processes, although they are also used to indicate the current status of algae biorefinery [14, 25, 65, 266]. Life cycle assessments (LCA) are often applied to compare the algae production process with crop-based or fossil-based production [67, 70, 76, 80, 267]. The impact of the productivity scenarios on land-use requirements and life cycle indicators of algae food commodity production was studied in Chapter 7 (part 3 of this thesis).

## **Achievements**

The impact of algae cultivation in four cultivation systems and two algae species on land-use requirements and life cycle impacts for food commodity production has been compared for two locations, i.e. southern Europe (Spain) and eastern Europe (Poland). The results show that a limited production surface is required to grow algae for replacing 25% of the proteins and 50% of vegetable oils currently consumed in Europe. As a consequence of the lower protein content of algae compared to lipids it is the protein productivity that determines the required land area. In Spain 0.2-2.0% of the non-arable land would be required and in Poland 0.5-7.4%, hereby both producing 50% of the desired target. The production costs vary between the two regions and also between the algae species as a result of the different biomass productivity and biomass concentration. In general, the current production costs should reduce ten times to become competitive, based on the current market values of the products. However, it is

expected that in 10 to 15 years algae will be competitive for production of commodities when produced in a biorefinery [14].

The results of the environmental sustainability analysis of algae production show that in closed systems with productive algae species less water is required compared to conventional agriculture with soy or palm. The fertiliser demand and impact of fresh water use for algae can be further reduced by using sea water and waste water. Another advantage of algae is their high productivity compared to that of traditional agriculture crops [268]. The main difference in greenhouse warming potential between raceway ponds and flat panels is the energy required for reactor material and for water delivery due to the lower achievable biomass concentration. Producing a species that is able to grow at higher biomass concentrations is thus beneficial in terms of environmental impacts.

### **Insights scenario-based impact analysis**

Clearly, the differences in algae productivity, production costs, land-area use of the regions and sustainability impact affect the implications of food commodity production with algae. The scenario-based analysis is a valuable basis for policy making and technology implementation.

### **Next challenge: multi-criteria analysis**

In a full system analysis the algae productivity, economics and sustainability impacts should be optimised simultaneously. These impacts can be studied on a comparable level by expanding the here developed frameworks for algae productivity and biomass processing. Additional modules must be included to quantify the energy consumption during cultivation, costs of the processes and various sustainability impacts. Once available, this same optimisation methodology can be used, but as shown previously, sustainable impacts and economics are often conflicting [72, 197, 269]. It is always difficult to compare diverse aspects. Sustainability impacts are often translated to CO<sub>2</sub> equivalent emissions, greenhouse warming potentials or are normalised [270], but cost cannot be expressed as emissions or a warming potential. Pareto plots from multi-criteria optimisation may be a solution to deal with the various indicators, as they visualise how various choices affect the balance between sustainability and cost.

## **CONCLUDING REMARKS**

Algae cultivation and biorefinery are developing and will play an important role in the biobased economy. System analysis is an important principle to reach flexible and robust process and chain designs. In this thesis model-based approaches are combined

with scenario studies to incorporate, expand and exploit existing knowledge and data on algae cultivation, supply logistics and biomass processing. Algae cultivation was partially integrated with supply logistics and biomass processing to biodiesel.

The scenario studies can be further developed based on the results of this work. New challenges mainly lie in the calibration of the productivity models, extended scenarios for location planning, extension and expansion of the model library for biomass processing and implementation of other performance indicators. It is hoped and expected that the scenario methodology as developed here will be a source of inspiration for the analysis of other biobased processes and biorefineries.

REFERENCES

SUMMARY

SAMENVATTING

DANKWOORD

ABOUT THE AUTHOR

PUBLICATIONS

OVERVIEW OF COMPLETED TRAINING ACTIVITIES





## REFERENCES

- [1] Pellerin W, Taylor DW. Measuring the biobased economy: A Canadian perspective. *Industrial Biotechnology*. 2008;4:363-6.
- [2] Vandermeulen V, Van der Steen M, Stevens CV, Van Huylenbroeck G. Industry expectations regarding the transition toward a biobased economy. *Biofuels, Bioprod Bioref*. 2012;6:453-64.
- [3] van Dam JEG, de Klerk-Engels B, Struik PC, Rabbinge R. Securing renewable resource supplies for changing market demands in a bio-based economy. *Industrial Crops and Products*. 2005;21:129-44.
- [4] Ragauskas AJ, Williams CK, Davison BH, Britovsek G, Cairney J, Eckert CA, et al. The path forward for biofuels and biomaterials. *Science*. 2006;311:484-9.
- [5] Landeweerd L, Pierce R, Kinderlerer J, Osseweijer P. Bioenergy: A potential for developing countries? *CAB Reviews: Perspectives in Agriculture, Veterinary Science, Nutrition and Natural Resources*. 2012;7.
- [6] Kajikawa Y, Takeda Y. Structure of research on biomass and bio-fuels: A citation-based approach. *Technological Forecasting and Social Change*. 2008;75:1349-59.
- [7] González-Delgado Á-D, Kafarov V. Microalgae based biorefinery: issues to consider *Ciencia, tecnología y futuro*. 2011;4:5-22.
- [8] Carroll A, Somerville C. Cellulosic biofuels. *Annual Review of Plant Biology*. 2009;60:165-82.
- [9] Borines MG, McHenry MP, de Leon RL. Integrated macroalgae production for sustainable bioethanol, aquaculture and agriculture in Pacific island nations. *Biofuels, Bioprod Bioref*. 2011;5:599-608.
- [10] John RP, Anisha GS. Macroalgae and their potential for biofuel. *CAB Reviews: Perspectives in Agriculture, Veterinary Science, Nutrition and Natural Resources*. 2011;6:1-15.
- [11] Wijffels RH. Potential of sponges and microalgae for marine biotechnology. *Trends in Biotechnology*. 2008;26:26-31.
- [12] Konur O. The scientometric evaluation of the research on the algae and bio-energy. *Applied Energy*. 2011;88:3532-40.
- [13] Wijffels RH, Barbosa MJ. An outlook on microalgal biofuels. *Science*. 2010;329:796-9.
- [14] Wijffels RH, Barbosa MJ, Eppink MHM. Microalgae for the production of bulk chemicals and biofuels. *Biofuels, Bioprod Bioref*. 2010;4:287-95.
- [15] Becker EW. Micro-algae as a source of protein. *Biotechnology Advances*. 2007;25:207-10.
- [16] de la Noue J, de Pauw N. The potential of microalgal biotechnology: A review of production and uses of microalgae. *Biotechnology Advances*. 1988;6:725-70.
- [17] Milledge J. Commercial application of microalgae other than as biofuels: a brief review. 2011;10:31-41.
- [18] Daroch M, Geng S, Wang G. Recent advances in liquid biofuel production from algal feedstocks. *Applied Energy*. 2013;102:1371-81.
- [19] Tredici MR. Photobiology of microalgae mass cultures: understanding the tools for the next green revolution. *Biofuels*. 2010;1:143-62.

- [20] Borowitzka MA. Commercial production of microalgae: ponds, tanks, tubes and fermenters. *Journal of Biotechnology*. 1999;70:313-21.
- [21] Lee Y-K. Commercial production of microalgae in the Asia-Pacific rim. *Journal of Applied Phycology*. 1997;9:403-11.
- [22] Carvalho AP, Meireles LA, Malcata FX. Microalgal reactors: A review of enclosed system designs and performances. *Biotechnol Progress*. 2006;22:1490-506.
- [23] Posten C. Design principles of photo-bioreactors for cultivation of microalgae. *Eng Life Sci*. 2009;9:165-77.
- [24] Pulz O. Photobioreactors: production systems for phototrophic microorganisms. *Applied Microbiology and Biotechnology*. 2001;57:287-93.
- [25] Norsker N-H, Barbosa MJ, Vermuë MH, Wijffels RH. Microalgal production - A close look at the economics. *Biotechnology Advances*. 2011;29:24-7.
- [26] Wigmosta MS, Coleman AM, Skaggs RJ, Huesemann MH, Lane LJ. National microalgae biofuel production potential and resource demand. *Water Resources Research*. 2011;47:1-13.
- [27] Wogan DM, da Silva AK, Webber M. Assessing the potential for algal biofuels production in Texas. *ASME Conference Proceedings*. 2009;2009:145-54.
- [28] Crowe B, Attalah S, Agrawal S, Waller P, Ryan R, Van Wagenen J, et al. A comparison of *Nannochloropsis salina* growth performance in two outdoor pond designs: Conventional raceways versus the arid pond with superior temperature management. *International Journal of Chemical Engineering*. 2012.
- [29] Moheimani N, Borowitzka M. The long-term culture of the coccolithophore *Pleurochrysis carterae* (Haptophyta) in outdoor raceway ponds. 2006;18:703-12.
- [30] Huntley M, Redalje D. CO<sub>2</sub> mitigation and renewable oil from photosynthetic microbes: a new appraisal. *Mitigation and Adaptation Strategies for Global Change*. 2007;12:573-608.
- [31] Thomas WH, Seibert DLR, Alden M, Neori A, Eldridge P. Yields, photosynthetic efficiencies and proximate composition of dense marine microalgal cultures. I. Introduction and *Phaeodactylum tricornutum* experiments. *Biomass*. 1984;5:181-209.
- [32] Ansell AD, Raymont JEG, Lander KF, Crowley E, Shackley P. Studies on the mass culture of *Phaeodactylum*. II. The growth of *Phaeodactylum* and other species in outdoor tanks. *Limnology and Oceanography*. 1963;8:184-206.
- [33] Olguín E, Galicia S, Mercado G, Pérez T. Annual productivity of *Spirulina* (*Arthrospira*) and nutrient removal in a pig wastewater recycling process under tropical conditions. 2003;15:249-57.
- [34] Tredici MR, Materassi R. From open ponds to vertical alveolar panels: the Italian experience in the development of reactors for the mass cultivation of phototrophic microorganisms. *Journal of Applied Phycology*. 1992;4:221-31.
- [35] Jiménez C, Cossío BR, Niell FX. Relationship between physicochemical variables and productivity in open ponds for the production of *Spirulina*: A predictive model of algal yield. *Aquaculture*. 2003;221:331-45.
- [36] Roebroek E. Personal communication, productivity at LGem. 2012.
- [37] Olaizola M. Commercial development of microalgal biotechnology: from the test tube to the marketplace. *Biomolecular Engineering*. 2003;20:459-66.

- [38] Ación Fernández FG, Fernández Sevilla JM, Magán JJ, Molina-Grima E. Production cost of a real microalgae production plant and strategies to reduce it. *Biotechnology Advances*. 2012;30:1344-53.
- [39] Barbosa MJ. personal communication BTME productivity. 2012.
- [40] Richmond A, Zhang C-W. Optimization of a flat plate glass reactor for mass production of *Nannochloropsis* sp. outdoors. *Journal of Biotechnology*. 2001;85:259-69.
- [41] Quinn J, de Winter L, Bradley T. Microalgae bulk growth model with application to industrial scale systems. *Bioresource Technology*. 2011;102:5083-8092.
- [42] Geider RJ, MacIntyre HL, Kana TM. A dynamic model of photoadaptation in phytoplankton. *Limnology and Oceanography*. 1996;41:1-15.
- [43] Bosma R, van Zessen E, Reith JH, Tramper J, Wijffels RH. Prediction of volumetric productivity of an outdoor photobioreactor. *Biotechnol Bioeng*. 2007;97:1108-20.
- [44] Pruvost J, Cornet JF, Goetz V, Legrand J. Theoretical investigation of biomass productivities achievable in solar rectangular photobioreactors for the cyanobacterium *Arthrospira platensis*. *Biotechnol Progress*. 2012;28:699-714.
- [45] Pruvost J, Van Vooren G, Le Gouic B, Couzinet-Mossion A, Legrand J. Systematic investigation of biomass and lipid productivity by microalgae in photobioreactors for biodiesel application. *Bioresource Technology*. 2011;102:150-8.
- [46] Pruvost J, Cornet JF, Goetz V, Legrand J. Modeling dynamic functioning of rectangular photobioreactors in solar conditions. *AIChE J*. 2011;57:1947-60.
- [47] Ación Fernández FG, García Camacho F, Sánchez Pérez JA, Fernández Sevilla J, Molina Grima E. A model for light distribution and average solar irradiance inside outdoor tubular photobioreactors for the microalgal mass culture. *Biotechnol Bioeng*. 1997;55:701-14.
- [48] Ación Fernández FG, García Camacho F, Sánchez Pérez JA, Fernández Sevilla JM, Molina Grima E. Modeling of biomass productivity in tubular photobioreactors for microalgal cultures: Effects of dilution rate, tube diameter, and solar irradiance. *Biotechnol Bioeng*. 1998;58:605-16.
- [49] Molina Grima E, García Camacho F, Sánchez Pérez JA, Fernández Sevilla JM, Ación Fernández FG, Contreras Gómez A. A mathematical model of microalgal growth in light-limited chemostat culture. *Journal of Chemical Technology & Biotechnology*. 1994;61:167-73.
- [50] Ación Fernández FG, Fernández Sevilla JM, Sánchez Pérez JA, Molina Grima E, Chisti Y. Airlift-driven external-loop tubular photobioreactors for outdoor production of microalgae: assessment of design and performance. *Chemical Engineering Science*. 2001;56:2721-32.
- [51] Molina Grima E, Fernández Sevilla J, Ación Fernández FG, Chisti Y. Tubular photobioreactor design for algal cultures. *Journal of Biotechnology*. 2001;92:113-31.
- [52] Pate R, Klise G, Wu B. Resource demand implications for US algae biofuels production scale-up. *Applied Energy*. 2011;88:3377-88.
- [53] Skarka J. Microalgae biomass potential in Europe. *Technikfolgenabschätzung - Theorie und Praxis*. 2012;21:72-9.
- [54] Borowitzka MA, Boruff BJ, Moheimani NR, Pauli N, Cao Y, Smith H. Identification of the optimum sites for industrial-scale microalgae biofuel production in WA using a GIS model. *Centre for Research into Energy for Sustainable Transport*; 2012.

- [55] Klise GT, Roach JD, Passell HD. A study of algae biomass potential in selected Canadian regions. Livermore, California: Sandia National Laboratories; 2011.
- [56] Quinn J, Catton K, Johnson S, Bradley T. Geographical assessment of microalgae biofuels potential incorporating resource availability. *BioEnergy Research*. 2013;6:591-600.
- [57] Venteris ER, Skaggs RL, Coleman AM, Wigmosta MS. A GIS cost model to assess the availability of freshwater, seawater, and saline groundwater for algal biofuel production in the United States. *Environmental Science & Technology*. 2013;47:4840-9.
- [58] Leduc S, Starfelt F, Dotzauer E, Kindermann G, McCallum I, Obersteiner M, et al. Optimal location of lignocellulosic ethanol refineries with polygeneration in Sweden. *Energy*. 2010;35:2709-16.
- [59] Wetterlund E, Leduc S, Dotzauer E, Kindermann G. Optimal localisation of biofuel production on a European scale. *Energy*. 2012;41:462-72.
- [60] Natarajan K, Leduc S, Pelkonen P, Tomppo E, Dotzauer E. Optimal locations for second generation Fischer Tropsch biodiesel production in Finland. *Renewable Energy*. 2014;62:319-30.
- [61] Giarola S, Zamboni A, Bezzo F. Spatially explicit multi-objective optimisation for design and planning of hybrid first and second generation biorefineries. *Computers & Chemical Engineering*. 2011;35:1782-97.
- [62] Vanthoor-Koopmans M, Wijffels RH, Barbosa MJ, Eppink MHM. Biorefinery of microalgae for food and fuel. *Bioresource Technology*. 2013;135:142-9.
- [63] Brentner LB, Eckelman MJ, Zimmerman JB. Combinatorial Life Cycle Assessment to inform process design of industrial production of algal biodiesel. *Environmental Science & Technology*. 2011;45:7060-7.
- [64] Bello BZ, Nwokoagbara E, Wang M, Ian David Lockhart B, Michael F. Comparative techno-economic analysis of biodiesel production from microalgae via transesterification methods. *Computer Aided Chemical Engineering*; Elsevier; 2012. p. 132-6.
- [65] Davis R, Aden A, Pienkos PT. Techno-economic analysis of autotrophic microalgae for fuel production. *Applied Energy*. 2011;88:3524-31
- [66] Rickman M, Pellegrino J, Hock J, Shaw S, Freeman B. Life-cycle and techno-economic analysis of utility-connected algae systems. *Algal Research*. 2013;2:59-65.
- [67] Collet P, Hélias A, Lardon L, Ras M, Goy R-A, Steyer J-P. Life-cycle assessment of microalgae culture coupled to biogas production. *Bioresource Technology*. 2011;102:207-14.
- [68] Slade R, Bauen A. Micro-algae cultivation for biofuels: Cost, energy balance, environmental impacts and future prospects. *Biomass and Bioenergy*. 2013;53:29-38.
- [69] Clarens AF, Resurreccion EP, White MA, Colosi LM. Environmental life cycle comparison of algae to other bioenergy feedstocks. *Environmental Science & Technology*. 2010;44:1813-9.
- [70] Lardon L, Hélias A, Sialve B, Steyer J-P, Bernard O. Life-cycle assessment of biodiesel production from microalgae. *Environmental Science and Technology*. 2009;43:6475-81.
- [71] Corsano G, Vecchiotti AR, Montagna JM. Optimal design for sustainable bioethanol supply chain considering detailed plant performance model. *Computers & Chemical Engineering*. 2011;35:1384-98.
- [72] Zondervan E, Nawaz M, de Haan AB, Woodley JM, Gani R. Optimal design of a multi-product biorefinery system. *Computers & Chemical Engineering*. 2011;35:1752-66.

- [73] Richardson JW, Johnson MD, Outlaw JL. Economic comparison of open pond raceways to photo bio-reactors for profitable production of algae for transportation fuels in the Southwest. *Algal Research*. 2012;1:93-100.
- [74] Beal CM, Hebner RE, Webber ME, Ruoff RS, Seibert AF, King CW. Comprehensive evaluation of algal biofuel production: experimental and target results. *Energies*. 2012;5:1943-81.
- [75] Frank ED, Elgowainy A, Han J, Wang Z. Life cycle comparison of hydrothermal liquefaction and lipid extraction pathways to renewable diesel from algae. *Mitigation and Adaptation Strategies for Global Change*. 2013;18:137-58.
- [76] Liang S, Xu M, Zhang T. Life cycle assessment of biodiesel production in China. *Bioresource Technology*. 2013;129:72-7.
- [77] Brentner L, Wijffels RH. Life cycle assessment of microalgae as a replacement commodity for palm and soy imports in the Netherlands. submitted.
- [78] Jorquera O, Kiperstok A, Sales EA, Embiruçu M, Ghirardi ML. Comparative energy life-cycle analyses of microalgal biomass production in open ponds and photobioreactors. *Bioresource Technology*. 2010;101:1406-13.
- [79] Stephenson AL, Kazamia E, Dennis JS, Howe CJ, Scott SA, Smith AG. Life-Cycle Assessment of potential algal biodiesel production in the United Kingdom: a comparison of raceways and air-lift tubular bioreactors. *Energy & Fuels*. 2010;24:4062-77.
- [80] Yang J, Xu M, Zhang X, Hu Q, Sommerfeld M, Chen Y. Life-cycle analysis on biodiesel production from microalgae: Water footprint and nutrients balance. *Bioresource Technology*. 2011;102:159-65.
- [81] Sills DL, Paramita V, Franke MJ, Johnson MC, Akabas TM, Greene CH, et al. Quantitative uncertainty analysis of Life Cycle Assessment for algal biofuel production. *Environmental Science & Technology*. 2012;47:687-94.
- [82] Chum HL, Overend RP. Biomass and renewable fuels. *Fuel Processing Technology*. 2001;71:187-95.
- [83] Jenkins T. Toward a biobased economy: examples from the UK. *Biofuels, Bioprod Bioref*. 2008;2:133-43.
- [84] De Meester S, Callewaert C, De Mol E, Van Langenhove H, Dewulf J. The resource footprint of biobased products: a key issue in the sustainable development of biorefineries. *Biofuels, Bioprod Bioref*. 2011;5:570-80.
- [85] Zhu Z, Bai H, Xu H, Zhu T. An inquiry into the potential of scenario analysis for dealing with uncertainty in strategic environmental assessment in China. *Environmental Impact Assessment Review*. 2011;31:538-48.
- [86] European Environment Agency (EEA). Catalogue of scenario studies — Knowledge base for Forward-Looking Information and Services. Technical report No 1/20112011.
- [87] Thompson JR, Wiek A, Swanson FJ, Carpenter SR, Fresco N, Hollingsworth T, et al. Scenario studies as a synthetic and integrative research activity for long-term ecological research. *BioScience*. 2012;62:367-76.
- [88] Rabbinge R, van Oijen M. Scenario studies for future agriculture and crop protection. 1997;103:197-201.
- [89] Duinker PN, Greig LA. Scenario analysis in environmental impact assessment: Improving explorations of the future. *Environmental Impact Assessment Review*. 2007;27:206-19.

- [90] Zurek MB, Henrichs T. Linking scenarios across geographical scales in international environmental assessments. *Technological Forecasting and Social Change*. 2007;74:1282-95.
- [91] Acién Fernández FG, Sánchez Pérez JA, Fernández Sevilla JM, García Camacho F, Molina Grima E. Modeling of eicosapentaenoic acid (EPA) production from *Phaeodactylum tricornutum* cultures in tubular photobioreactors. Effects of dilution rate, tube diameter and solar irradiance. *Biotechnol Bioeng*. 2000;68:173-83.
- [92] Zijffers J-W, Janssen M, Tramper J, Wijffels R. Design process of an area-efficient photobioreactor. *Marine Biotechnology*. 2008;10:404-15.
- [93] Campbell PK, Beer T, Batten D. Greenhouse gas sequestration by algae - energy and greenhouse gas life cycle studies. *Proceedings of the 6th Australian Conference on Life Cycle Assessment*. Melbourne: Commonwealth Scientific and Industrial Research Organisation (CSIRO); 2009. p. 24.
- [94] Kadam KL. Environmental implications of power generation via coal-microalgae cofiring. *Energy*. 2002;27:905-22.
- [95] Knap W. Basic measurements of radiation at station Cabauw. Koninklijk Nederlands Meteorologisch Instituut, De Bilt; 2009.
- [96] Mimouni M. Basic measurements of radiation at station Tamanrasset. National Meteorological Office of Algeria; 2009.
- [97] Morel J-P. Basic measurements of radiation at station Carpentras. Centre Radiometrique; 2009.
- [98] Janssen M. Microalgal photosynthesis and growth. *Advanced Marine Biotechnology*. Wageningen2009. p. 54.
- [99] Shen Y, Yuan W, Pei ZJ, Wu Q, Mao E. Microalgae mass production methods. *Transactions of the ASABE*. 2009;52:1275-87.
- [100] Meiser A, Schmid-Staiger U, Trösch W. Optimization of eicosapentaenoic acid production by *Phaeodactylum tricornutum* in the flat panel airlift (FPA) reactor. *Journal of Applied Phycology*. 2004;16:215-25.
- [101] Masci P, Grogard F, Bernard O. Microalgal biomass surface productivity optimization based on a photobioreactor model. *Proceedings of Computer Applications in Biotechnology (CAB 2010)*. Leuven2010.
- [102] Hu Q, Fairman D, Richmond A. Optimal tilt angles of enclosed reactors for growing photoautotrophic microorganisms outdoors. *Journal of Fermentation and Bioengineering*. 1998;85:230-6.
- [103] Duffie JA, Beckman WA. *Solar engineering of thermal processes*. 2 ed. Toronto: Wiley-Interscience; 1991.
- [104] Sukhatme SP. *Solar Energy. Principles of thermal collection and storage*. 2 ed. New Delhi: McGraw-Hill; 1991.
- [105] Robinson D, Stone A. Solar radiation modelling in the urban context. *Solar Energy*. 2004;77:295-309.
- [106] Anderson LA. On the hydrogen and oxygen content of marine phytoplankton. *Deep sea research part I: Oceanographic research papers*. 1995;42:1675-80.
- [107] Clauquin P, Probert I, Lefebvre S, Veron B. Effects of temperature on photosynthetic parameters and TEP production in eight species of marine microalgae. *Aquatic Microbial Ecology*. 2008;51:1-11.

- [108] del Pilar Sánchez-Saavedra M, Voltolina D. Effect of blue-green light on growth rate and chemical composition of three diatoms. *Journal of Applied Phycology*. 1996;8:131-7.
- [109] Ho T-Y, Quigg A, Finkel ZV, Milligan AJ, Wyman K, Falkowski PG, et al. The elemental composition of some marine phytoplankton. *Journal of Phycology*. 2003;39:1145-59.
- [110] Slegers PM, Lösing MB, Wijffels RH, van Straten G, van Boxtel AJB. Scenario evaluation of open pond microalgae production. *Algal Research*. 2013;2:358-68.
- [111] Slegers PM, Wijffels RH, van Straten G, van Boxtel AJB. Design scenarios for flat panel photobioreactors. *Journal of Applied Energy*. 2011;88:3342-53.
- [112] Chisti Y. Biodiesel from microalgae. *Biotechnology Advances*. 2007;25:294-306.
- [113] Rorrer GL, Mullikin RK. Modeling and simulation of a tubular recycle photobioreactor for macroalgal cell suspension cultures. *Chemical Engineering Science*. 1999;54:3153-62.
- [114] Jenkins FA, White HE. Absorption and scattering. *Fundamentals of optics*. 4 ed: McGraw-Hill Book Company; 1976. p. 457-73.
- [115] Sousa C, de Winter L, Janssen M, Vermuë MH, Wijffels RH. Growth of the microalgae *Neochloris oleoabundans* at high partial oxygen pressures and sub-saturating light intensity. *Bioresource Technology*. 2012;104:565-70.
- [116] Cuaresma M, Janssen M, Vilchez C, Wijffels RH. Horizontal or vertical photobioreactors? How to improve microalgae photosynthetic efficiency. *Bioresource Technology*. 2011;102:5129-37.
- [117] Pulz O, Gross W. Valuable products from biotechnology of microalgae. *Applied Microbiology and Biotechnology*. 2004;65:635-48.
- [118] AlgaeLINK®. 2012.
- [119] Liu BYH, Jordan RC. The interrelationship and characteristic distribution of direct, diffuse and total solar radiation. *Solar Energy*. 1960;4:1-19.
- [120] Campbell PK, Beer T, Batten D. Life cycle assessment of biodiesel production from microalgae in ponds. *Bioresource Technology*. 2011;102:50-6.
- [121] Tredici MR. Mass production of microalgae: photobioreactors. In: Richmond A, editor. *Handbook of microalgal culture*. 4 ed. Oxford: Blackwell Publishing; 2007. p. 178-214.
- [122] Slegers PM, van Beveren PJM, Wijffels RH, van Straten G, van Boxtel AJB. Scenario analysis of large-scale algae production in tubular photobioreactors. *Applied Energy*. 2013;105:395-406.
- [123] Handler RM, Canter CE, Kalnes TN, Lupton FS, Kholiqov O, Shonnard DR, et al. Evaluation of environmental impacts from microalgae cultivation in open-air raceway ponds: Analysis of the prior literature and investigation of wide variance in predicted impacts. *Algal Research*. 2012;1:83-92.
- [124] Yang A. Modeling and evaluation of CO<sub>2</sub> supply and utilization in algal ponds. *Industrial & Engineering Chemistry Research*. 2011;50:11181-92.
- [125] Kroon B, Ketelaars H, Fallowfield H, Mur L. Modelling microalgal productivity in a High Rate Algal Pond based on wavelength dependent optical properties. *Journal of Applied Phycology*. 1989;1:247-56.
- [126] James SC, Boriah V. Modeling algae growth in an open-channel raceway. *Journal of Computational Biology*. 2010;17:895-906.

- [127] Bechet Q, Shilton A, Park JBK, Craggs RJ, Guieysse B. Universal temperature model for shallow algal ponds provides improved accuracy. *Environmental Science & Technology*. 2011;45:3702-9.
- [128] Hadiyanto H, Elmore S, Van Gerven T, Stankiewicz A. Hydrodynamic evaluations in high rate algae pond (HRAP) design. *Chemical Engineering Journal*. 2013;217:231-9.
- [129] Bernard O. Hurdles and challenges for modelling and control of microalgae for CO<sub>2</sub> mitigation and biofuel production. *Journal of Process Control*. 2011;21:1378-89.
- [130] Sartori E. A critical review on equations employed for the calculation of the evaporation rate from free water surfaces. *Solar Energy*. 2000;68:77-89.
- [131] McMillan W. Heat dispersal — Lake Trawsfynydd cooling studies. Symposium on freshwater biology and electrical power generation. 1971;1:41-80.
- [132] Woolley J, Harrington C, Modera M. Swimming pools as heat sinks for air conditioners: Model design and experimental validation for natural thermal behavior of the pool. *Building and Environment*. 2011;46:187-95.
- [133] Mimouni M. Meteorological synoptical observations from station Tamanrasset. National Meteorological Office of Algeria; 2009.
- [134] Cabauw experimental site atmospherical research CESAR. Meteorological data measured on surface (Wind speed). In: KNMI, editor. De Bilt: KNMI; 2009.
- [135] Bosveld F. Soil temperature and soil moisture data set Cabauw (part of the Coordinated Energy and Water Cycle Observation Project). NCAR Earth Observing Laboratory; 2009.
- [136] Klepach D. Meteorological data from Sede Boqer. Ben Gurion University of the Negev, Department of Solar Energy and Environmental Physics: Desert Meteorology; 2009.
- [137] Jacobs AFG, Heusinkveld BG, Holtslag AAM. Eighty years of meteorological observations at Wageningen, the Netherlands: precipitation and evapotranspiration. *Int J Climatol*. 2010;30:1315-21.
- [138] Bitaubé Pérez E, Caro Pina I, Pérez Rodríguez L. Kinetic model for growth of *Phaeodactylum tricornutum* in intensive culture photobioreactor. *Biochemical Engineering Journal*. 2008;40:520-5.
- [139] Berges JA, Varela DE, Harrison PJ. Effects of temperature on growth rate, cell composition and nitrogen metabolism in the marine diatom *Thalassiosira pseudonana* (Bacillariophyceae). *Marine Ecology Progress Series*. 2002;225:139-46.
- [140] Aydın GŞ, Kocataş A, Büyükişik B. Effects of light and temperature on the growth rate of potentially harmful marine diatom: *Thalassiosira allenii* Takano (Bacillariophyceae). *African Journal of Biotechnology*. 2009;8:4983-90.
- [141] Lamers P. Personal communication (2013).
- [142] Nelson DM, D'Elia CF, Guillard RRL. Growth and competition of the marine diatoms *Phaeodactylum tricornutum* and *Thalassiosira pseudonana*. II. Light limitation. 1979;50:313-8.
- [143] Blanchard GF, Guarini JM, Richard P, Gros P, Mornet F. Quantifying the short-term temperature effect on light-saturated photosynthesis of intertidal microphytobenthos. *Marine Ecology Progress Series*. 1996;134:309-13.
- [144] Ek MB, Holtslag AAM. Evaluation of a land-surface scheme at Cabauw. *Theoretical and Applied Climatology*. 2005;80:213-27.

- [145] Bowen IS. The ratio of heat losses by conduction and by evaporation from any water surface. *Physical Review*. 1926;27:779.
- [146] Hahne E, Kübler R. Monitoring and simulation of the thermal performance of solar heated outdoor swimming pools. *Solar Energy*. 1994;53:9-19.
- [147] Das P, Obbard JP. Incremental energy supply for microalgae culture in a photobioreactor. *Bioresource Technology*. 2011;102:2973-8.
- [148] William KWL, Morris I. Temperature adaptation in *Phaeodactylum tricornutum* bohlin: Photosynthetic rate compensation and capacity. *Journal of Experimental Marine Biology and Ecology*. 1982;58:135-50.
- [149] Montagnes DJS, Franklin DJ. Effect of temperature on diatom volume, growth rate, and carbon and nitrogen content: Reconsidering some paradigms. *Limnology and Oceanography*. 2001;46:2008-18.
- [150] Davis R, Fishman D, Frank ED, Wigmosta MS, Aden A, Coleman AM, et al. Renewable diesel from algal lipids: an integrated baseline for cost, emissions, and resource potential from a harmonized model.: U.S. Department of Energy Biomass Program; 2012.
- [151] Cosun. Bietenlogistiek steeds efficiënter. *Cosun Magazine*. 2009:10-1.
- [152] Leduc S, Lundgren J, Franklin O, Dotzauer E. Location of a biomass based methanol production plant: A dynamic problem in northern Sweden. *Applied Energy*. 2010;87:68-75.
- [153] Allen J, Browne M, Hunter A, Boyd J, Palmer H. Logistics management and costs of biomass fuel supply *International Journal of Physical Distribution & Logistics Management*. 1998;28:463-77.
- [154] Caputo AC, Palumbo M, Pelagagge PM, Scacchia F. Economics of biomass energy utilization in combustion and gasification plants: effects of logistic variables. *Biomass and Bioenergy*. 2005;28:35-51.
- [155] Rentizelas AA, Tolis AJ, Tatsiopoulos IP. Logistics issues of biomass: The storage problem and the multi-biomass supply chain. *Renewable and Sustainable Energy Reviews*. 2009;13:887-94.
- [156] Bauen AW, Dunnett AJ, Richter GM, Dailey AG, Aylott M, Casella E, et al. Modelling supply and demand of bioenergy from short rotation coppice and *Miscanthus* in the UK. *Bioresource Technology*. 2010;101:8132-43.
- [157] Leduc S. Development of an optimization model for the location of biofuel production plants [PhD thesis]. Sweden: Lulea University of Technology; 2009.
- [158] McCarl BA, Meeraus A, van den Eijk P, Bussieck M, Dirkse S, Steacy P. McCarl Expanded GAMS user Guide Version 22.9. GAMS Development Corporation; 2008.
- [159] IEA. Key world energy statistics. 2012.
- [160] Schneider M. France's great energy debate. *Bulletin of the Atomic Scientists*. 2013;69:27-35.
- [161] Platts. Electric power plants. 2005.
- [162] Quinn J, Catton K, Wagner N, Bradley T. Current large-scale US biofuel potential from microalgae cultivated in photobioreactors. *BioEnergy Research*. 2012;2:49-60.
- [163] Rubio-Romero JC, Arjona-Jiménez R, López-Arquillos A. Profitability analysis of biogas recovery in Municipal Solid Waste landfills. *Journal of Cleaner Production*. 2013;55:84-91.

- [164] Bajaj M, Winter J. Biogas and biohydrogen production potential of high strength automobile industry wastewater during anaerobic degradation. *Journal of Environmental Management*. 2013;128:522-9.
- [165] Pastor L, Ruiz L, Pascual A, Ruiz B. Co-digestion of used oils and urban landfill leachates with sewage sludge and the effect on the biogas production. *Applied Energy*. 2013;107:438-45.
- [166] Veselovskaya JV, Derevschikov VS, Kardash TY, Stonkus OA, Trubitsina TA, Okunev AG. Direct CO<sub>2</sub> capture from ambient air using K<sub>2</sub>CO<sub>3</sub>/Al<sub>2</sub>O<sub>3</sub> composite sorbent. *International Journal of Greenhouse Gas Control*. 2013;17:332-40.
- [167] BGR, UNESCO. Groundwater resources of Africa. 2008.
- [168] Edmunds WM. Limits to the availability of groundwater in Africa. *Environmental Research Letters*. 2012;7:021003.
- [169] Zangvil A. Meteorological synoptical observations from station Sede Boqer. The Jacob Blaustein Institutes for Desert Research, Sede Boqer; 2009.
- [170] Zero Emissions Platform. The costs of CO<sub>2</sub> transport. Post-demonstration CCS in the EU. Brussels, Belgium: European Technology Platform for Zero Emission Fossil Fuel Power Plants; 2011.
- [171] Norsker N-H. Transportation costs for carbon dioxide. Wageningen2011.
- [172] U.S. Geological Survey (USGS). Minerals yearbook. 2011.
- [173] Komori T, Yamagami N, Hara H. Design for blast furnace gas firing gas turbine. 2004. p. 1-12.
- [174] Simmons T. CO<sub>2</sub> Emissions from stationary combustion of fossil fuels. Good practice guidance and uncertainty management in national greenhouse gas inventories: IPCC; 2000.
- [175] Börjesson P, Berglund M. Environmental systems analysis of biogas systems—Part I: Fuel-cycle emissions. *Biomass and Bioenergy*. 2006;30:469-85.
- [176] Friedl A, Padouvas E, Rotter H, Varnuza K. Prediction of heating values of biomass fuel from elemental composition. *Analytica Chimica Acta*. 2005;544:191-8.
- [177] Turhollow AF, Perlack RD. Emissions of CO<sub>2</sub> from energy crop production. *Biomass and Bioenergy*. 1991;1:129-35.
- [178] Kalnes T, Marker T, Shonnard DR. Green diesel: A second generation biofuel. *International Journal of Chemical Reactor Engineering*. 2007;5.
- [179] Argonne National Lab (ANL). GREET, The greenhouse gases, regulated emissions, and energy use In transportation model, GREET 1.8d.1, developed by Argonne. 2010.
- [180] IPCC. Revised 1996 IPCC guidelines for national greenhouse gas inventories: reference manual. 1996.
- [181] Waukesha Engine Dresser Inc. Digester gas - Premium gas engine fuel. 1993.
- [182] Niska J, Rensgard A, Ekman T. Oxyfuel combustion of low calorific blast furnace gas for steel reheating furnace. 2009.
- [183] Gardner N, Manley B, Probert SD. Harnessing land-fill gas from refuse-dumping sites in the UK. *Applied Energy*. 1988;29:201-15.
- [184] Malik ZI, Slack JW. How to treat refinery gases and make them suitable to recover valuable liquids. p. 1-21.

- [185] Smith CB, Martin L, Cárdenas-Lailhacar C. Lesser known energy sources: A study of biogas and tire-based fuel. *Cogeneration and distribution generation journal*. 2008;23:35-66.
- [186] Sediqi A. A preliminary assessment of air quality in Kabul. Kabul2008.
- [187] Dixon RK, Krankina ON. Forest fires in Russia: carbon dioxide emissions to the atmosphere. *Canadian Journal of Forest Research*. 1993;23:700-5.
- [188] Gerhardt T, Cenni R, Siegle V, Spliethoff H, Hein KRG. Fuel characteristics of sewage sludge and other supplemental fuels regarding their effect on the co-combustion process with coal. *Combustion chemistry of traditional and non-traditional fuels*. Dallas, US: American Chemical Society; 1998. p. 197-202.
- [189] Werther J, Ogada T. Sewage sludge combustion. *Progress in Energy and Combustion Science*. 1999;25:55-116.
- [190] Cement & Beton Centrum (CBC). Cement, beton en CO<sub>2</sub>. Feiten en trends (Brochure 472).
- [191] TATA steel. The carbon footprint of steel. 2002.
- [192] Patil PD, Gude VG, Mannarswamy A, Cooke P, Munson-McGee S, Nirmalakhandan N, et al. Optimization of microwave-assisted transesterification of dry algal biomass using response surface methodology. *Bioresource Technology*. 2011;102:1399-405.
- [193] Batan L, Quinn J, Willson B, Bradley T. Net energy and greenhouse gas emission evaluation of biodiesel derived from microalgae. *Environmental Science & Technology*. 2010;44:7975-80.
- [194] Beal C, Hebner R, Webber M, Ruoff R, Seibert A. The energy return on investment for algal biocrude: Results for a research production facility. *Bioenergy Research*. 2011;5:341-62.
- [195] Chowdhury R, Viamajala S, Gerlach R. Reduction of environmental and energy footprint of microalgal biodiesel production through material and energy integration. *Bioresource Technology*. 2012;108:102-11.
- [196] Frank ED, Han J, Palou-Rivera I, Elgowainy A, Wang MQ. Methane and nitrous oxide emissions affect the life-cycle analysis of algal biofuels. *Environmental Research Letters*. 2012;7:014030.
- [197] Delrue F, Setier PA, Sahut C, Cournac L, Roubaud A, Peltier G, et al. An economic, sustainability, and energetic model of biodiesel production from microalgae. *Bioresource Technology*. 2012;111:191-200.
- [198] Pahl SL, Lee AK, Kalaitzidis T, Ashman PJ, Sathe S, Lewis DM. Harvesting, thickening and dewatering microalgae biomass. In: Borowitzka MA, Moheimani NR, editors. *Algae for Biofuels and Energy*: Springer Netherlands; 2013. p. 165-85.
- [199] Wileman A, Ozkan A, Berberoglu H. Rheological properties of algae slurries for minimizing harvesting energy requirements in biofuel production. *Bioresource technology*. 2012;104:432-9.
- [200] Atuonwu JC, Van Straten G, Van Deventer HC, Van Boxtel AJB. Optimizing energy efficiency in low temperature drying by zeolite adsorption and process integration. *Chemical Engineering Transactions*. 2011;25:111-6.
- [201] Bosma R, van Spronsen WA, Tramper J, Wijffels RH. Ultrasound, a new separation technique to harvest microalgae. *Journal of applied phycology*. 2003;15:143-53.

- [202] Riaño B, Molinuevo B, García-González MC. Optimization of chitosan flocculation for microalgal-bacterial biomass harvesting via response surface methodology. *Ecological Engineering*. 2012;38:110-3.
- [203] Zheng H, Gao Z, Yin J, Tang X, Ji X, Huang H. Harvesting of microalgae by flocculation with poly  $\gamma$ -glutamic acid. *Bioresource technology*. 2012;112:212-20.
- [204] Doucha J, Lívanský K. Influence of processing parameters on disintegration of *Chlorella* cells in various types of homogenizers. *Applied Microbiology and Biotechnology*. 2008;81:431-40.
- [205] Char J. JW, et al. Biodiesel production from microalgae through supercritical carbon dioxide extraction. *Journal of the Japan Institute of Energy*. 2011;90:369-73.
- [206] Rashid U, Anwar F, Ansari TM, Arif M, Ahmad M. Optimization of alkaline transesterification of rice bran oil for biodiesel production using response surface methodology. *Journal of Chemical Technology & Biotechnology*. 2009;84:1364-70.
- [207] Tran D-T, Yeh K-L, Chen C-L, Chang J-S. Enzymatic transesterification of microalgal oil from *Chlorella vulgaris* ESP-31 for biodiesel synthesis using immobilized *Burkholderia* lipase. *Bioresource technology*. 2012;108:119-27.
- [208] Patil PD, Gude VG, Mannarswamy A, Cooke P, Nirmalakhandan N, Lammers P, et al. Comparison of direct transesterification of algal biomass under supercritical methanol and microwave irradiation conditions. *Fuel*. 2012;97:822-31.
- [209] Patil PD, Gude VG, Mannarswamy A, Deng S, Cooke P, Munson-McGee S, et al. Optimization of direct conversion of wet algae to biodiesel under supercritical methanol conditions. *Bioresource technology*. 2011;102:118-22.
- [210] Patil PD, Reddy H, Muppaneni T, Mannarswamy A, Schuab T, Holguin FO, et al. Power dissipation in microwave-enhanced in situ transesterification of algal biomass to biodiesel. *Green Chemistry*. 2012;14:809-18.
- [211] Pragya N, Pandey KK, Sahoo PK. A review on harvesting, oil extraction and biofuels production technologies from microalgae. *Renewable and Sustainable Energy Reviews*. 2013;24:159-71.
- [212] Glisic S, Skala D. The problems in design and detailed analyses of energy consumption for biodiesel synthesis at supercritical conditions. *The Journal of Supercritical Fluids*. 2009;49:293-301.
- [213] Rawat I, Ranjith Kumar R, Mutanda T, Bux F. Biodiesel from microalgae: A critical evaluation from laboratory to large scale production. *Applied Energy*. 2013;103:444-67.
- [214] Weyer K, Bush D, Darzins A, Willson B. Theoretical maximum algal oil production. 2010;3:204-13.
- [215] Prommuak C, Pavasant P, Quitain AT, Goto M, Shotipruk A. Microalgal lipid extraction and evaluation of single-step biodiesel production. *Engineering Journal*. 2012;16:157-66.
- [216] Cappon H. Personal communication on ultrasound sedimentation of microalgae. 2013.
- [217] Kleinegris DM, Janssen M, Brandenburg WA, Wijffels RH. The selectivity of milking of *Dunaliella salina*. 2010;12:14-23.
- [218] Wesselingh JA, Krijgsman J. *Downstream processing in biotechnology*: Delft academic press; 2013.
- [219] Godfray HCJ, Beddington JR, Crute IR, Haddad L, Lawrence D, Muir JF, et al. Food security: The challenge of feeding 9 billion people. *Science*. 2010;327:812-8.

- [220] Tilman D, Balzer C, Hill J, Befort BL. Global food demand and the sustainable intensification of agriculture. *Proceedings of the National Academy of Sciences*. 2011;108:20260-4.
- [221] Hoekman SK, Broch A, Robbins C, Ceniceros E, Natarajan M. Review of biodiesel composition, properties, and specifications. *Renewable and Sustainable Energy Reviews*. 2012;16:143-69.
- [222] Williams PJB, Laurens LML. Microalgae as biodiesel & biomass feedstocks: Review & analysis of the biochemistry, energetics & economics. *Energy & Environmental Science*. 2010;3:554-90.
- [223] Fleurence J, Morançais M, Dumay J, Decottignies P, Turpin V, Munier M, et al. What are the prospects for using seaweed in human nutrition and for marine animals raised through aquaculture? *Trends in Food Science & Technology*. 2012;27:57-61.
- [224] Sharma N, Tiwari S, Tripathi K, Rai A. Sustainability and cyanobacteria (blue-green algae): facts and challenges. 2011;23:1059-81.
- [225] Bondioli P, Della Bella L, Rivolta G, Chini Zittelli G, Bassi N, Rodolfi L, et al. Oil production by the marine microalgae *Nannochloropsis* sp. and *Tetraselmis suecica*. *Bioresource Technology*. 2012;114:567-72.
- [226] Hu Q, Sommerfeld M, Jarvis E, Ghirardi M, Posewitz M, Seibert M, et al. Microalgal triacylglycerols as feedstocks for biofuel production: perspectives and advances. *The Plant Journal*. 2008;54:621-39.
- [227] FAOSTAT. <http://faostat.fao.org/site/345/default.aspx>.
- [228] Zayas JF. *Functionality of proteins in food*. Berlin Heidelberg New York: Springer-Verlag; 1997.
- [229] Ratledge C. Fatty acid biosynthesis in microorganisms being used for Single Cell Oil production. *Biochimie*. 2004;86:807-15.
- [230] Griffiths M, Harrison SL. Lipid productivity as a key characteristic for choosing algal species for biodiesel production. 2009;21:493-507.
- [231] Rodolfi L, Zittelli GC, Bassi N, Padovani G, Biondi N, Bonini G, et al. Microalgae for oil: Strain selection, induction of lipid synthesis and outdoor mass cultivation in a low-cost photobioreactor. *Biotechnol Bioeng*. 2009;102:100-12.
- [232] Breuer G, Lamers PP, Martens DE, Draaisma RB, Wijffels RH. The impact of nitrogen starvation on the dynamics of triacylglycerol accumulation in nine microalgae strains. *Bioresource Technology*. 2012;124:217-26.
- [233] Lamers PP, van de Laak CCW, Kaasenbrood PS, Lorier J, Janssen M, De Vos RCH, et al. Carotenoid and fatty acid metabolism in light-stressed *Dunaliella salina*. *Biotechnol Bioeng*. 2010;106:638-48.
- [234] Pal D, Khozin-Goldberg I, Cohen Z, Boussiba S. The effect of light, salinity, and nitrogen availability on lipid production by *Nannochloropsis* sp. 2011;90:1429-41.
- [235] Santos AM, Janssen M, Lamers PP, Evers WAC, Wijffels RH. Growth of oil accumulating microalga *Neochloris oleoabundans* under alkaline-saline conditions. *Bioresource Technology*. 2012;104:593-9.
- [236] Stephenson AL, Dennis JS, Howe CJ, Scott SA, Smith AG. Influence of nitrogen-limitation regime on the production by *Chlorella vulgaris* of lipids for biodiesel feedstocks. *Biofuels*. 2009;1:47-58.

- [237] Yu E, Zendejas F, Lane P, Gaucher S, Simmons B, Lane T. Triacylglycerol accumulation and profiling in the model diatoms *Thalassiosira pseudonana* and *Phaeodactylum tricornutum* (Baccillariophyceae) during starvation. 2009;21:669-81.
- [238] Harris W, Kris-Etherton P, Harris K. Intakes of long-chain omega-3 fatty acid associated with reduced risk for death from coronary heart disease in healthy adults. 2008;10:503-9.
- [239] Mozaffarian D REB. Fish intake, contaminants, and human health: Evaluating the risks and the benefits. *JAMA*. 2006;296:1885-99.
- [240] Chen JE, Smith AG. A look at diacylglycerol acyltransferases (DGATs) in algae. *Journal of Biotechnology*. 2012;162:28-39.
- [241] Guarnieri MT, Nag A, Smolinski SL, Darzins A, Seibert M, Pienkos PT. Examination of triacylglycerol biosynthetic pathways via de novo transcriptomic and proteomic analyses in an unsequenced microalga. *PLoS ONE*. 2011;6:e25851.
- [242] Radakovits R, Jinkerson RE, Darzins A, Posewitz MC. Genetic engineering of algae for enhanced biofuel production. *Eukaryotic Cell*. 2010;9:486-501.
- [243] Wang D, Lu Y, Huang H, Xu J. Establishing oleaginous microalgae research models for consolidated bioprocessing of solar energy. *Adv Biochem Eng Biotechnol*. 2012;128:69-84.
- [244] Nakano S, Takekoshi H, Nakano M. *Chlorella pyrenoidosa* supplementation reduces the risk of anemia, proteinuria and edema in pregnant women. 2010;65:25-30.
- [245] Zendejas FJ, Benke PI, Lane PD, Simmons BA, Lane TW. Characterization of the acylglycerols and resulting biodiesel derived from vegetable oil and microalgae (*Thalassiosira pseudonana* and *Phaeodactylum tricornutum*). *Biotechnol Bioeng*. 2012;109:1146-54.
- [246] Knothe G, Van Gerpen J. *The biodiesel handbook*. Champaign, IL: AOCS Press; 2010.
- [247] Chacón-Lee TL, González-Mariño GE. Microalgae for “healthy” foods—Possibilities and challenges. *Comprehensive Reviews in Food Science and Food Safety*. 2010;9:655-75.
- [248] Schwenzfeier A, Wierenga PA, Gruppen H. Isolation and characterization of soluble protein from the green microalgae *Tetraselmis* sp. *Bioresource Technology*. 2011;102:9121-7.
- [249] Izumo A, Fujiwara S, Sakurai T, Ball SG, Ishii Y, Ono H, et al. Effects of granule-bound starch synthase I-defective mutation on the morphology and structure of pyrenoidal starch in *Chlamydomonas*. *Plant Science*. 2011;180:238-45.
- [250] Cheng Y-S, Zheng Y, Labavitch JM, VanderGheynst JS. The impact of cell wall carbohydrate composition on the chitosan flocculation of *Chlorella*. *Process Biochemistry*. 2011;46:1927-33.
- [251] Ho S-H, Chen C-Y, Chang J-S. Effect of light intensity and nitrogen starvation on CO<sub>2</sub> fixation and lipid/carbohydrate production of an indigenous microalga *Scenedesmus obliquus* CNW-N. *Bioresource Technology*. 2012;113:244-52.
- [252] Krienitz L, Takeda H, Hepperle D. Ultrastructure, cell wall composition, and phylogenetic position of *Pseudodictyosphaerium jurisii* (Chlorococcales, Chlorophyta) including a comparison with other picoplanktonic green algae. *Phycologia*. 1999;38:100-7.
- [253] USDA. <http://www.fas.usda.gov/oilseeds/Current/default.asp>.

- [254] Ryan AS, Zeller S, Nelson EB. Safety evaluation of single cell oils and the regulatory requirements for use as food ingredients. In: Cohen Z, Ratledge C, editors. *Single cell oils*. 2nd edition ed. Champaign, IL: AOCS Press; 2010. p. 317-50.
- [255] Constable A, Jonas D, Cockburn A, Davi A, Edwards G, Hepburn P, et al. History of safe use as applied to the safety assessment of novel foods and foods derived from genetically modified organisms. *Food and Chemical Toxicology*. 2007;45:2513-25.
- [256] Day AG, Brinkmann D, Franklin S, Espina K, Rudenko G, Roberts A, et al. Safety evaluation of a high-lipid algal biomass from *Chlorella protothecoides*. *Regulatory Toxicology and Pharmacology*. 2009;55:166-80.
- [257] Klok AJ, Martens DE, Wijffels RH, Lamers PP. Simultaneous growth and neutral lipid accumulation in microalgae. *Bioresource Technology*. 2013;134:233-43.
- [258] Geider RJ, Macintyre HL, Kana TM. Dynamic model of phytoplankton growth and acclimation: responses of the balanced growth rate and the chlorophyll a: carbon ratio to light, nutrient-limitation and temperature. *Marine Ecology Progress Series*. 1997;148:187-200.
- [259] de Winter L, Klok AJ, Cuaresma Franco M, Barbosa MJ, Wijffels RH. The synchronized cell cycle of *Neochloris oleoabundans* and its influence on biomass composition under constant light conditions. *Algal Research*. 2013;2:313-20.
- [260] Franz A, Lehr F, Posten C, Schaub G. Modeling microalgae cultivation productivities in different geographic locations – estimation method for idealized photobioreactors. *Biotechnology Journal*. 2012;7:546-57.
- [261] Saltelli A. Making best use of model evaluations to compute sensitivity indices. *Computer Physics Communications*. 2002;145:280-97.
- [262] Cuaresma M, Janssen M, van den End EJ, Vilchez C, Wijffels RH. Luminostat operation: A tool to maximize microalgae photosynthetic efficiency in photobioreactors during the daily light cycle? *Bioresource Technology*. 2011;102:7871-8.
- [263] Bosma R, Vermuë MH, Tramper J, Wijffels RH. Towards increased microalgal productivity in photobioreactors. *International Sugar Journal*. 2010;112:74-85.
- [264] Stephens E, Ross IL, Mussgnug JH, Wagner LD, Borowitzka MA, Posten C, et al. Future prospects of microalgal biofuel production systems. *Trends in plant science*. 2010;15:554-64.
- [265] Klok AJ, Verbaanderd JA, Lamers PP, Martens DE, Rinzema A, Wijffels RH. A model for customising biomass composition in continuous microalgae production. *Bioresource Technology*. 2013;146:89-100.
- [266] Amer L, Adhikari B, Pellegrino J. Technoeconomic analysis of five microalgae-to-biofuels processes of varying complexity. *Bioresource Technology*. 2011;102:9350-9.
- [267] Agusdinata DB, Zhao F, Ileleji K, DeLaurentis D. Life Cycle Assessment of potential biojet fuel production in the United States. *Environmental Science & Technology*. 2011;45:9133-43.
- [268] Schenk P, Thomas-Hall S, Stephens E, Marx U, Mussgnug J, Posten C, et al. Second generation biofuels: High-efficiency microalgae for biodiesel production. *BioEnergy Research*. 2008;1:20-43.
- [269] Liu X, Clarens AF, Colosi LM. Algae biodiesel has potential despite inconclusive results to date. *Bioresource Technology*. 2012;104:803-6.
- [270] Sacramento-Rivero JC. A methodology for evaluating the sustainability of biorefineries: framework and indicators. *Biofuels, Bioprod Bioref*. 2012;6:32-44.



## SUMMARY

Microalgae are a promising biomass for the biobased economy to produce food, feed, fuel, chemicals and materials. So far, large-scale production of algae is limited and as a result estimates on the performance of such large systems are scarce. There is a need to estimate large-scale biomass productivity and energy consumption, while considering the uncertainty and complexity in such large-scale systems.

In this thesis frameworks are developed to assess 1) the productivity during algae cultivation, 2) energy consumption during the transport of resources and processing biomass to biodiesel, and 3) the frameworks are applied to estimate the impact of algae cultivation in the production of algae-based food commodities. Design, location and future scenario are applied to deal with the complexity and uncertainty arising in the various data and models used.

The first part of this thesis focuses on the development of a productivity framework for biomass production for flat panels (**Chapter 2**), horizontal and vertical tubular photobioreactors (**Chapter 3**) and raceway ponds (**Chapter 4**). The framework uses bio-physics-based models to simulate the light input on the reactor surface and the light gradient inside the reactor systems. The internal light gradient depends on the reactor geometry and dimensions, and the penetration of diffuse light between parallel reactors, which includes the canyon effect, and the reflection of light from the ground surface to the reactors are incorporated as well. Specific growth rates are derived from this internal light gradient based on species-specific growth characteristics. In raceway ponds the effect of the dynamic water temperature on the specific growth rate is included.

The productivity framework enables to study cultivation under a wide range of process conditions and reactor designs, even those which have not been yet developed or tested under outdoor conditions. The results show that regional weather conditions, solar angles and algae species are key factors in making the best choice for the specific reactor design. The productivity framework allows to optimise the reactor design (e.g. geometry, light path, distances between parallel units and height) to the regional light conditions and growth characteristics of the algae species of interest. The best biomass concentration for cultivation varies between the reactor design, location and algae species. We recommend to select species suited to growth well at the regional light angles and weather conditions. An initial global sensitivity analysis shows that the absorption coefficient, maximum specific growth rate and functional cross section of the photosynthetic apparatus are the essential parameters of the model for single flat panels. An important next step is to validate and calibrate the productivity framework using data from outdoor experiments in various reactor designs, at different locations and with several algae species.

Algae production is strongly connected to regional weather conditions, but also to the infrastructure for resource supply and to the processing of biomass. The energy consumption for resource supply has not been quantified yet and the energy consumption of biomass processing is mostly based on fixed values. These elements are tackled in part 2 of this thesis.

In **Chapter 5** the productivity framework is combined with logistic models to optimise the supply network for algae cultivation. The results show that the availability, supply and demand of resources has a dominant effect on the feasibility of regions for algae cultivation. Not all locations achieve a positive energy balance for transport and the supply logistics is essential for planning algae cultivation locations. In the Benelux many locations are feasible for algae production due to the availability of large amounts of resources, while the limited supply of CO<sub>2</sub> in southern France and the Sahara demands for plants which are scattered over the regions. For the Sahara the distance for water transport should be minimal. Still, the average transport distances are higher than commonly assumed and algae cultivation does not necessarily need to take place in proximity of CO<sub>2</sub> supply. The transport energy consumption is found to be low compared to the energy contained in algae biomass (mostly below 3%).

**Chapter 6** describes a model-based combinatorial optimisation approach for the energy-efficient processing of algae biomass. In this approach, mass and energy balances and additional relations are used to relate the product yield and energy consumption of process units and process routes to the processing conditions. Process routes with the highest net energy ratios are derived by optimising the process conditions of each process unit in a given superstructure. This optimisation leads to 5-38% improvement of the net energy ratio compared to fixed process conditions. The approach moreover allows a bottleneck analysis for each process route. The results show that process design should be tailor-made. The model-based approach proves to be a versatile tool for the design of efficient microalgae processing systems.

The developed frameworks combined with scenario studies are a powerful tool to assess algae production. The presented approaches help to reduce the uncertainty in the interpretation of data and are thereby an appropriate basis to use in impact analysis. In **Chapter 7** this is illustrated for the production of algae protein and oil as food commodities. The design scenarios show the implications of various reactor designs, two algae species and at two locations on biomass productivity, production cost and environmental life cycle indicators.

The achievements of this work and the new horizons from this work are discussed in **Chapter 8**. The results of the developed frameworks demonstrate the power of the scenario approach and show that sensible predictions and projections of biomass productivity and energy consumption for logistics and biomass processing follow from the models.

## SAMENVATTING

Microalgen zijn een veelbelovende grondstof voor de productie van voedsel, veevoeder, brandstoffen, chemicaliën en materialen. Op het moment is grootschalige algenproductie gelimiteerd en als gevolg zijn er amper schattingen van de prestatie van deze algensystemen. Er is een behoefte om de grootschalige biomassa-productiviteit en het bijbehorende energieverbruik te schatten, waarbij de onzekerheid en complexiteit in deze grootschalige systemen worden beschouwd.

In dit proefschrift zijn raamwerken ontwikkeld voor het bepalen van: 1) biomassa-productiviteit, 2) energieverbruik gedurende de toevoer van grondstoffen en tijdens het verwerken van biomassa naar biodiesel, en 3) de impact van algencultivatie voor de productie van bulkvoedsel met algen. Ontwerp, locatie en toekomstscenario's zijn toegepast om om te gaan met de complexiteit en onzekerheid in de gebruikte data en modellen.

Het eerste gedeelte van dit proefschrift is gericht op de ontwikkeling van een productiviteitsraamwerk voor biomassa-productie in vlakke panelen (**Hoofdstuk 2**), horizontale en verticale buizenreactoren (**Hoofdstuk 3**) en vijvers (**Hoofdstuk 4**). In het raamwerk worden biofysicagebaseerde rekenmodellen gebruikt om de lichtinval op de reactoren te simuleren en de lichtgradiënt in de systemen te bepalen. Deze gradiënt hangt af van de reactorgeometrie en dimensies, en van de indringing van diffuus licht tussen parallelle systemen. Dit omvat het tunneleffect van licht en de reflectie van licht op de bodem. Specifieke groeisnelheden worden afgeleid uit deze gradiënt. Voor vijvers wordt het effect van de watertemperatuur op de groeisnelheid meegenomen. Het productiviteitsraamwerk maakt het mogelijk om algencultivatie voor uiteenlopende procescondities en reactorontwerpen te onderzoeken, zelfs als deze nog niet zijn ontwikkeld of niet zijn getest voor buitencondities. De resultaten laten zien dat de regionale weersomstandigheden, lichthoeken en eigenschappen van de alg sleutelementen zijn in de beste keuze voor reactorontwerp. Het raamwerk kan worden gebruikt om het reactorontwerp te optimaliseren (o.a. geometrie, lichtpad, afstand tussen parallelle systemen en de hoogte) op basis van regionale lichtomstandigheden en groei-eigenschappen van de gewenste alg. De beste biomassa-concentratie is een samenspel van het reactorontwerp, de locatie en algensoort. We adviseren om een algensoort te kiezen die goed groeit bij de lichthoeken en weerscondities van de beoogde productielocatie. Een initiële globale gevoeligheidsanalyse toont aan dat de absorptiecoëfficiënt, maximale specifieke groeisnelheid en de functionele doorsnede van het fotosynthetisch apparaat essentiële parameters zijn in het rekenmodel voor vrijstaande panelen. Een belangrijke volgende stap is het valideren en kalibreren van

het productiviteitsraamwerk aan de hand van experimentele data van verschillende lichtcondities, reactor ontwerpen en algensoorten.

Algenproductie is sterk gecorreleerd met de regionale weersomstandigheden, maar ook met de aanwezige infrastructuur voor grondstoffen. Daarnaast is er een sterke samenhang met het verwerken van de biomassa. Het energieverbruik voor grondstoftoevoer is nog niet gekwantificeerd en het energieverbruik voor biomassaverwerking is merendeels gebaseerd op vaste waarden. Deze twee elementen worden in deel 2 van het proefschrift behandeld.

In **Hoofdstuk 5** is het productiviteitsraamwerk gecombineerd met logistieke modellen om het toevoernetwerk voor algencultivatie te optimaliseren. De resultaten laten zien dat de beschikbaarheid, toevoer en vraag van grondstoffen dominant zijn in de haalbaarheid van regio's voor algenproductie. Niet alle locaties behalen een positieve energiebalans voor grondstoftransport. Toevoerlogistiek is essentieel voor het plannen van locaties voor algenproductie. In de Benelux zijn veel plekken geschikt voor algenproductie door de beschikbaarheid van grote hoeveelheden grondstoffen. In Zuid-Frankrijk en de Sahara zorgt gelimiteerde beschikbaarheid van CO<sub>2</sub> voor een verstrooiing van de ideale locaties in de regio. In de Sahara is het belangrijk om de afstand voor watertransport te beperken. Niettemin zijn de gemiddelde transportafstanden hoger dan voorheen gedacht en algencultivatie hoeft niet noodzakelijkerwijs in de nabijheid van de CO<sub>2</sub>toevoer plaats te vinden. Het energieverbruik voor transport is laag ten opzichte van de aanwezige energie in algen (meestal onder de 3%).

**Hoofdstuk 6** beschrijft een op rekenmodellen gebaseerde optimalisatiemethode voor het energie-efficiënt verwerken van algenbiomassa. De methode gebruikt massa, energiebalansen en verdere relaties om de productopbrengst, energieconsumptie te relateren aan de procescondities. Dit wordt gedaan voor iedere processtap en voor de gehele procesroute. De procesroutes met de hoogste Netto Energie Ratio (NER) worden bepaald door optimalisatie van de procescondities, van elke processtap, in een gegeven superstructuur. Deze optimalisatie leidt tot een 5-38% verbetering van de NER ten opzichte van het gebruik van vaste procescondities. Daarnaast kunnen knelpunten in de procesroutes worden bepaald met de rekenmodel gebaseerde methode. Deze methode is een veelzijdig instrument voor het ontwerpen van efficiënte verwerking van microalgen.

De ontwikkelde raamwerken zijn een krachtig en flexibel hulpmiddel om algenproductie te analyseren met behulp van scenario's. De gepresenteerde methoden helpen om de onzekerheid in datainterpretatie te verminderen en zijn daardoor een geschikte basis

om te gebruiken in impactanalyse van nieuwe en in ontwikkeling zijnde technologieën zoals algenproductie. In **Hoofdstuk 7** wordt dit geïllustreerd voor de productie van bulkeiwitten en oliën uit algen. De ontwerpscenario's laten de consequenties zien van verschillende reactorontwerpen in combinatie met twee algensoorten en twee locaties, op de productiviteit, productiekosten en milieueffecten.

De resultaten van dit werk, nieuwe inzichten en volgende onderzoeksstappen worden besproken in **Hoofdstuk 8**. De scenariomethode is krachtig en leidt in combinatie met de rekenmodellen tot schappelijke uitkomsten.



## DANKWOORD

Gerrit en René, bedankt voor jullie inzet in én voor mijn project. We hebben veel constructieve overleggen gehad en het was fijn om jullie input (uit de verschillende richtingen) te krijgen. Gerrit, zonder enige ervaring in het SCO-vakgebied begon ik als aio. Inmiddels ben ik een stuk wijzer over systeemtheorie en ‘state-space’. Ik waardeer je bijdrage aan mijn werk enorm, het was erg fijn om je tot het eind als promotor te hebben ondanks je pensioen. Bij ieder manuscript wist ik dat ik veel gekrabbel in de kantlijn van je kon verwachten, maar dat maakte de stukken iedere keer weer beter. René, ik ben blij dat ik de uitdagingen in dit project ben aangegaan, ik heb zeker geen spijt van het kiezen voor een promotieplek en het was erg fijn om je steun te hebben op de momenten dat er erg kritisch naar het onderzoek werd gekeken. Ton, bedankt voor al je adviezen en de samenwerking. Het begon allemaal met mijn stage naar Finland en eigenlijk is dat project nooit opgehouden. Je deur staat altijd open en dat is erg aangenaam. Ik moest erg lachen toen mijn gele lijstjes langzaam een begrip werden in onze overleggen of beter gezegd onze wekelijkse gesprekken.

In mijn promotieonderzoek heb ik veel samengewerkt en veel nieuwe mensen leren kennen. Ik wil iedereen van het Wetsus “Algen”-thema bedanken voor de samenwerking en voor de interesse in het ‘algen scenario studies’ project. Alle collega’s van “Biobased science and technology” bedankt voor de gezellige en roerige tijd samen. In het bijzonder wil ik Marja bedanken, wie heeft een hoogleraar nodig als er zulke sterke secretaresse is? Bedankt voor je luisterend oor en de gemoedelijkheid. Also thanks to all my fellow PhD students at BRD and BCH. It was great to share my PhD time with all you guys, even if it was only during short periods during the PhD. James, Xin, Jimmy and Jan we started our PhD within one year and it was very nice to share the PhD period with you. Jimmy it’s great to finish this important period with you by side as paranymp. Xin, thanks for the wonderful company in the office. We have seen many work places and luckily we could keep on sharing our thoughts, frustration and holiday plans (Yunnan here we come). Good luck with your position at Suzhou University. Special thanks to all my students: Martin L., Peter, Randy, Mark, Bart, Martin. S, Rick, Susanne, Timo, you were a diverse group with many different backgrounds and personalities. I enjoyed supervising you, discussing the results and in some cases even published your work. Thanks for being there, I also learned from you! Jan-Eise, bedankt voor je bijdrage aan de gebruikersinterface voor de algenmodellen en het toevoegen van verschillende regelsystemen. Uiteindelijk is het toch gelukt je iets met algen te laten doen.

Ook dank aan alle stafleden en aio's van Bioprocess Engineering voor de discussies over algengroei, modellen en onze poging om de Academische Jaarprijs te winnen. Lenneke, het is gelukt om met onze drukke agenda's en je experimenten om regelmatig samen te lunchen. Je was een luisterend oor, het is fijn om onze ideeën en mening eerlijk te kunnen delen. Also thanks to my fellow Wetsus PhD's Sina, Anja, Claudia, Ana, Lenneke, Anne and Zlatica. I have enjoyed our time together, the trips in the car to Leeuwarden were always fun, now it's time for the next step in our life and career. Nadine, we komen elkaar steeds weer tegen, wie weet ook in de rest van onze carrières. During my PhD I had the honour to start a special collaboration with Sylvain Leduc and Michael Obersteiner from IIASA in Laxenburg. Thanks for this, especially Sylvain for all the work in Beaver. The initial three-month project was more work than expected, but I'm very happy with the result and it was great to discuss it with the BeWhere family in October last year.

Laura, thanks for your input on the DSP modelling work. Our collaboration started off really well when you were almost leaving the Netherlands. It was surprising to find that we have similar research ideas, and I'm looking forward to finish our project on geographical and seasonal LCA. Maria, bedankt voor de interesse in mijn project vanaf dag één. De wisselwerking tussen mijn onderzoek en de praktijk op AlgaePARC is uitdagend en spannend. Jeroen, ook jij bedankt voor de leuke en gezellige samenwerking. Je begon als 'modelleergroentje', maar stiekem kun je dat computerwerk verrassend goed. René Draaisma, bedankt voor het vertrouwen en de samenwerking tot een bijzonder stuk in Current Opinion in Biotechnology. Het is een erg mooi verhaal geworden en een eer om een bijdrage te mogen leveren. Michiel, Niels-Hendrik, Packo and Ilse, thanks for the collaboration in the 'side-projects'. It was great to share our ideas and to work on publishing the results.

I want to thank everyone in the organising committee of YoungAFSG and the participants of activities for the 'social collaboration'. We managed to successfully start the networking group, we had many interesting activities and my Wageningen world has broadened thanks to you.

Het was erg fijn om buiten het werk terug te kunnen vallen op mijn vrienden en familie. Leonie en Marcel, we kennen elkaar nu al jaren. Vriendschap is elkaar begrijpen zonder iets te zeggen en ook als je ver weg bent van elkaar. Bedankt voor jullie vriendschap, het aanhoren van mijn frustraties en het samen lachen. Judith, wie had aan het begin van onze tijd in Wageningen kunnen denken dat we zo op onze plek terecht zouden komen. Ons dispuut Scotia heeft ons dichterbij elkaar gebracht en ik ben heel blij dat

we nog steeds een paar keer per jaar bij elkaar komen, met onze mannen en ook Lucy, om gezellig te theeleuten. Marinka, samen pauzeren zoals 15 jaar geleden doen we al lang niet meer. Gelukkig kunnen we ook zonder dat nog steeds gezellig kletsen over allerlei dingen, maar niet te veel over werk! I believe that friendship is not only about being together often, it's about sharing a connection. Thanks to all my friends abroad for the time we have shared together, special thanks to Niclas and Riikka for your warm friendship in a cold country.

Ook dank aan mijn grote familie, voor al jullie interesse in mijn onderzoek, mijn leven in Wageningen en de zuidelijke gemoedelijkheid als we samen zijn. Ook dank natuurlijk aan de uitbreiding van mijn familie: familie Puylaert en familie van der Wolf, erg fijn dat jullie ook altijd geïnteresseerd zijn. Ben en Mariëlle, bedankt voor jullie gastvrijheid en Ben we gaan een manier verzinnen om van die algen in je vijver af te komen. Pap en mam, ik wil jullie heel erg bedanken voor al jullie wijze lessen, de nooit ophoudende interesse en al het andere wat jullie voor mij hebben gedaan. Jullie stimulans heeft me zo ver gebracht, dus dit boekje is ook van jullie. Straks heb ik er een titel bij, maar ik blijf natuurlijk altijd jullie Elleke. Sanne, sis! Wat ben ik blij met jou als mijn zus – ik zou je niet in willen ruilen. Ik kan ongelofelijk met en om je lachen en ben heel dankbaar voor onze goede band. En wat fijn dat jij bij mij op het podium zit als paranimf; je past prima tussen al die andere slimmeriken! Ik ben heel trots dat het je zo snel is gelukt om een opleidingsplek in het ziekenhuis te krijgen. Zullen we ooit stoppen met studeren? Ik ben erg benieuwd wat de toekomst ons tweeën nog meer gaat brengen.

Last but not least, Philippe. Dit proefschrift is er ook mede door jou. Want het promoveren was vast nog lastiger geweest zonder je schaterende lach als ik een uitdrukking verkeerd gebruik, je super-relativerende vermogen of onze wandelingen samen. Op de juiste momenten zorgde je voor nieuwe energie. Je bent een geduchte discussiepartner, met een beetje tegengas op z'n tijd. Bedankt dat je me al deze tijd hebt gesteund! Het was niet altijd even gemakkelijk voor je, maar ik waardeer alles wat je hebt gedaan of hebt gelaten voor mij: bedankt voor het aanhoren van al mijn frustraties, het 'er zijn' voor mij.

*Ellen*

## ABOUT THE AUTHOR

Petronella Margaretha (Ellen) Puylaert-Slegers was born in Deurne, the Netherlands on 16 June 1986. She followed her secondary education at the Bouwens van der Boijecollege in Panningen (Netherlands) where she graduated at the Gymnasium. She studied the Bachelor and Master in Biotechnology at Wageningen University (the Netherlands), where she graduated cum laude in 2009. She specialised in bioprocess technology, fermentation and operations research and logistics. Her first MSc thesis “*Adaptive evolution of mixed yoghurt cultures*” was done at the Dutch Institute for Dairy Research (NIZO). For the second MSc thesis “*Applying Operations Research methods to the automatic generation of Food Frequency Questionnaires*” she received the thesis award “Wageningen University Fund Scriptieprijs” in 2009. She finished her studies with an internship at Neste Oil in Finland.



In 2009 she started her PhD research at the Systems and Control group of Wageningen University. As part of her research program she participated in the interdisciplinary Young Scientist Summer Program of IIASA (Austria) in 2011. The results of her PhD research are described in this thesis.

She is currently working as a post-doc researcher at Wageningen University where she is involved in the development and teaching of the course “Sustainability Analysis”, and working in several research projects that focus on integrated sustainable biorefineries. This work includes modelling the processing of algae biomass into various products and logistics.

## PUBLICATIONS

**P.M. Slegers**, B.J. Koetzier, F. Fasaei, R.H. Wijffels, G. van Straten, A.J.B. van Boxtel. A model-based combinatorial optimisation approach for energy-efficient processing of microalgae. *Submitted*.

**P.M. Slegers**, S. Leduc, R.H. Wijffels, G. van Straten, A.J.B. van Boxtel. Analysis of algae cultivation supply logistics. *Submitted*.

M.H.A. Michels, **P.M. Slegers**, M.H. Vermuë, R.H. Wijffels. Effect of biomass concentration on the productivity of *Tetraselmis suecica* in a pilot-scale tubular photobioreactor using natural sunlight. *Algal Research* (in press)

**P.M. Slegers**, M.B. Lösing, R.H. Wijffels, G. van Straten, A.J.B. van Boxtel (2013). Scenario evaluation of open pond microalgae production. *Algal Research* 2(4, Special issue: Mass cultivation): 258-368

**P.M. Slegers**, P.J.M. van Beveren, R.H. Wijffels, G. van Straten, A.J.B. van Boxtel (2013). Scenario analysis of large scale algae production in tubular photobioreactors. *Applied Energy* 105(5): 395-406.

R.B. Draaisma, R.H. Wijffels, **P.M. Slegers**, L.B. Brentner, A. Roy, M.J. Barbosa (2013). Food commodities from microalgae. *Current Opinion in Biotechnology* 24 (Special issue: Food Biotechnology):169-177.

J.C. Gerdessen, **P.M. Slegers**, O.W. Souverein & J.H.M. De Vries (2012). Use of OR to design food frequency questionnaires in nutritional epidemiology. *Operations Research for Health Care* 1(2-3):30-33.

**P.M. Slegers**, R.H. Wijffels, G. van Straten, A.J.B. van Boxtel (2011). Design scenarios for flat panel photobioreactors. *Applied Energy* 88(10, Special issue: Energy from algae - Current status and future trends): 3342-3353.

G. van Straten, **P.M. Slegers**, L.G. van Willigenburg, R. Bosma, A.J.B. van Boxtel, R.H. Wijffels (2010). Towards optimal control of flat plate photobioreactors: the greenhouse analogy? *IFAC Proceedings Volumes – Agricontrol Kyoto Japan* 3(1).



## OVERVIEW OF COMPLETED TRAINING ACTIVITIES

### Discipline specific activities

System and control theory (WageningenUR, 2010)

Sustainable process, product and system design (OSPT, 2010)

gPROMS software course; basics and optimisation (PSE, 2010)

30<sup>th</sup> Benelux meeting on Systems and Control (DISC, 2010)

IIASA Young Scientists Summer Programme in Laxenburg, Austria (2011)

2<sup>nd</sup> European biorefining training school (WageningenUR, 2012)

Minisymposium “Towards high productivities of microalgae in photobioreactors” (2010)

Minisymposium “Photosynthetic cell factories” (2010)

NBC13: biotechnology for a sustainable society in Ede, Netherlands<sup>2</sup> (2010)

8<sup>th</sup> algae workshop in Nuthetal, Germany<sup>1</sup> (IGV, 2010)

1<sup>st</sup> European Congress on Applied Biotechnology in Berlin, Germany<sup>1</sup> (2011)

Algae Biomass Summit in Minneapolis, USA<sup>1</sup> (2011)

NBC14: biotechnology, delivering value in Ede, Netherlands<sup>2</sup> (2012)

European Science Foundation 3<sup>rd</sup> Marine Board Meeting in Brussels, Belgium<sup>1</sup> (2012)

Young Algaeneers Symposium in Wageningen, Netherlands<sup>1</sup> (2012)

Biorefinery for food, fuel and materials in Wageningen, Netherlands<sup>1</sup> (2013)

### General

Scientific writing (Language center, 2009)

Project and time management (WageningenUR, 2010)

Guide to scientific artwork (WageningenUR, 2010)

Presentation skills (Language center, 2010)

Teaching methodology and skills for PhD students (WageningenUR, 2011)

Supervising thesis students (WageningenUR, 2011)

Career perspectives (WageningenUR, 2012)

### Optional

Updating PhD project proposal

Wetsus 3-monthly meetings (2009-2013)

VLAG PhD student week (2009)

Brainstorm days and PhD days Bioprocess Engineering (2009- 2012)

YoungAFSG meetings (2009- 2012)

PhD visit to IGV in Nuthetal, Germany (2009)

PhD foreign excursion to USA<sup>1,2</sup> (2010)

PhD visit to KIT in Karlsruhe, Germany<sup>1</sup> (2011)

### Teaching

Proceskunde voor Technologen (2009, 2010)

Mathematics for Time-dependent Systems (2011-2013)

Biorefinery, computer practical development and teaching (2013)

Supervision of 2 BSc and 5 MSc thesis students (2010-2013)

<sup>1</sup> oral presentation

<sup>2</sup> poster presentation





This work was performed at Wageningen University within the chair groups 'Biomass refinery and process dynamics' and 'Bioprocess engineering'. The research has been financially by Wetsus, centre of excellence for sustainable water technology ([www.wetsus.nl](http://www.wetsus.nl)).

Cover design: Ocelot design, Wageningen

Lay-out: GildePrint, Enschede

Printed by: GildePrint, Enschede



